

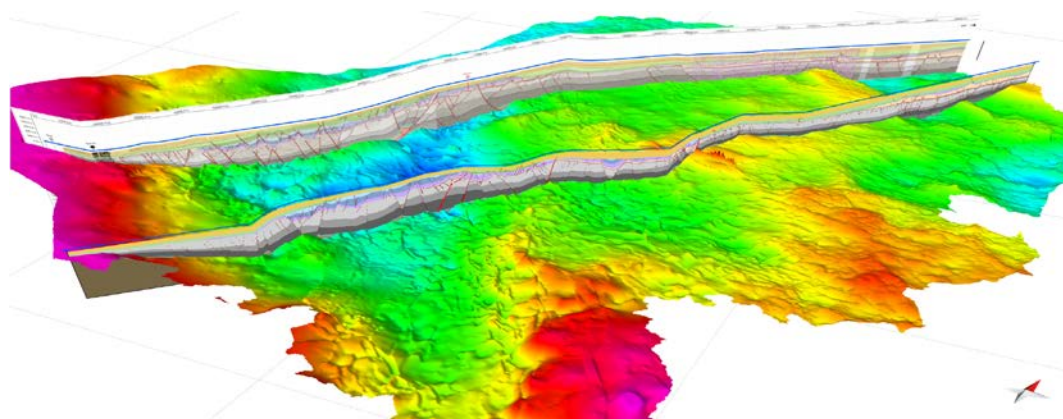


# **Burial and Structural Analysis of the Dinantian Carbonates in the Dutch Subsurface**

Report by SCAN

September 2019

# Burial and Structural Analysis of the Dinantian Carbonates in the Dutch Subsurface



Report written by  
Renaud Bouroullec<sup>1</sup>, Susanne Nelskamp<sup>1</sup>, Armelle  
Kloppenburger<sup>2</sup>, Rader Abdul Fattah<sup>1</sup>, Jurgen Foeken<sup>1</sup>,  
Johan ten Veen<sup>1</sup>, Kees Geel<sup>1</sup>, Tim Debacker<sup>3</sup> and Jeroen  
Smit<sup>4</sup>

1. Applied Geoscience Group, Netherlands Organisation for Applied Scientific Research TNO, Princetonlaan 6, 3584 CB, Utrecht
2. 4DGeo / Applied Structural Geology, Daal en Bergselaan 80, 2565 AH The Hague, The Netherlands
3. TiBA ScConsulting, Hofmeierstraat 7, 9000 Gent, Belgium
4. Department of Earth Sciences, Utrecht University, PO Box 80.021, 3508 TA, Utrecht, The Netherlands

September 2019

*Dit rapport is een product van het SCAN-programma en wordt mogelijk gemaakt door het Ministerie van Economische Zaken en Klimaat*





**Acknowledgements:** We would like to thank Werner Schoeler, Nico Holleman, Pieter van Heiningen, Geert de Bruin, Alberto Riva, Bastiaan Jaarsma, Mahtab Mozafari, Marten ter Borgh, Henk van Lochem, Douwe Leverink for the fruitful discussions throughout the project. We would also like to thank Harald de Haan and Andreas Kruisselbrink for their help with the depth conversations of the seismic sections restored. Thanks to Alexander Houben for new biostratigraphic insights.

## Table of Contents

List of figures, tables and appendices .....	7
1. Samenvatting .....	11
1.1. Doelstellingen .....	11
1.2. Conclusies .....	11
1.2.1. 2D structurele restauraties .....	11
1.2.2. 1D begraving en maturiteit modellering .....	12
1.3. Aanbevelingen .....	12
2. Executive summary .....	15
2.1. Aims and Objectives .....	15
2.2. Conclusions .....	15
2.2.1. 2D structural restorations .....	15
2.2.2. 1D burial and maturity modeling .....	16
2.3. Recommendations .....	16
3. Introduction .....	18
3.1. Background and rationale .....	18
3.2. Objectives .....	19
3.3. Plan .....	19
3.4. Deliverables .....	21
4. State of knowledge and literature review on the geological setting and evolution of the Dutch onshore .....	22
4.1. Late Caledonian to Early Variscan structural evolution of the Netherlands and neighbouring countries .....	22
4.2. A southern perspective on the structuration of the Dinantian: Constrains from the Brabant Massif and the Campine Basin .....	28
4.3. The post-Devonian structural evolution in the Dutch onshore .....	30
5. Database .....	39
5.1. Seismic Data .....	39
5.2. Non-Seismic Data .....	41
5.3. Well data .....	41
5.4. Other relevant data and information .....	41
6. Methodologies and workflows applied in the project .....	43
6.1. 2D Structural restoration methodology .....	43
6.1.1. Section selection .....	44
6.1.2. Data selection, loading and Move project set up .....	45
6.1.3. Interpretation and validation of horizons and faults .....	52
6.2. Methodology for the burial and maturity modeling for wells (1D-plots) .....	56
6.2.1. Input stratigraphy .....	57

6.2.2.	Boundary conditions .....	57
6.2.3.	Source rocks properties .....	58
7.	Results .....	63
7.1.	Structural restoration results .....	63
7.1.1.	Assumptions and uncertainties .....	63
7.1.1.1.	Western Section .....	65
7.1.1.2.	Central Section .....	72
7.1.3.3.	Structural elements .....	97
7.2.	Burial and maturity modeling for wells (1D-plots) .....	102
	London Brabant Massif/ Zeeland High area .....	131
8.	Discussion and integration .....	143
8.1.	2D structural restorations .....	143
8.2.	1D Basin Modelling .....	147
9.	Recommendations for future work .....	149
10.	References .....	151
11.	Appendices .....	159

## List of figures, tables and appendices

### Figures

Figure 1: Extent of Avalonia across the Atlantic Ocean (dashed domains) after Mesozoic opening of the Atlantic Ocean.	23
Figure 2: Palinspastic restoration of allochthonous units in the Rhenish Massif.	25
Figure 3: Paleogeography at end of early Carboniferous rifting including basement structures as far as known.	26
Figure 4: Map view of the restoration of early Variscan, Lower Carboniferous extension of Avalonia.	27
Figure 5: Simplified map of the Campine Basin.	28
Figure 6: Geological map based on the stratpiller analysis.	34
Figure 7: Late Jurassic - Early Cretaceous structural elements of the Netherlands.	35
Figure 8: Simplified stratigraphic diagram of the Netherlands.	36
Figure 9: Deep seismic section showing an overview of the main structural domains and main unconformities of the Dutch onshore.	37
Figure 10: This NNE-SSW-oriented deep seismic section displaying the tectonic structure of the central and southern Netherlands onshore.	38
Figure 11: Overview of all the available and consulted 2D and 3D seismic data.	40
Figure 12: Map of the Dutch onshore showing the position of the two restored sections, the Consortia sites and key wells.	45
Figure 13: Composite seismic line used for the Central Section.	46
Figure 14: Coordinate system used in the Move project.	47
Figure 15: The Drill hole import functionality from Move.	48
Figure 16: Stratigraphic framework used in the structural restoration.	51
Figure 17: Seismic interpretation and model building for the Western Section.	52
Figure 18: Scenario showing the main modelling variables relevant for each restoration step and the various modelling options.	53
Figure 19: Stratigraphy and rock properties used in Move for each of the stratigraphic unit selected.	54
Figure 20: Source rock summary.	59
Figure 21: Sensitivity test for well SWD-01 between an assumed Type II vs Type III source rock.	60
Figure 22: . Sensitivity test for well BHG-01 between an assumed Type II vs Type III source rock.	61
Figure 23: Base map showing the position of the two restored sections.	63
Figure 24: Western Section - Present-day situation.	65
Figure 25: Western Section-North Sea Group removed and Top Cretaceous restored to 0.	65
Figure 26: Western Section - Upper Chalk (CKEK) removed and Subhercynian inversion and erosion reconstructed and restored to 0.	66
Figure 27: Western Section - Lower Chalk removed, Rijnland Group restored to 0.	66
Figure 28: Western Section - Rijnland Group removed, and Upper Jurassic restored to 0.	67
Figure 29: Western Section - Upper Jurassic removed and Mid Kimmerian Unconformity restored to 0.	67
Figure 30: Western Section - Lower Jurassic removed, and Triassic restored to 0.	69
Figure 31: Western Section - Triassic and Permian removed and Base Permian Unconformity restored to 0.	69
Figure 32: Subcrop maps used to estimate the amount of Westphalian eroded by the BPU along the restored sections, plotted on the depth map of the Dinantian.	70
Figure 33: Western Section - Westphalian removed, Upper Namurian restored.	70

Figure 34: Western Section-Upper Namurian removed, Lower Namurian restored to 0 m.	70
Figure 35: Western Section-Lower Namurian removed and Dinantian restored to a paleo topography.	71
Figure 36: Central Section - Present-day geometry.	72
Figure 37: Central Section - North Sea Group removed and Top Cretaceous restored to 0.	72
Figure 38: Central Section - Upper Chalk removed and Subhercynian inversion and erosion reconstructed and restored to 0.	73
Figure 39: Central Section - Lower Chalk removed, Rijnland Group restored to 0.	74
Figure 40: Central Section - Rijnland Group removed, and Upper Jurassic restored to 0.	74
Figure 41: Central Section - Upper Jurassic removed, Mid Kimmerian Unconformity restored to 0, eroded Lower Jurassic, Triassic and Permian reconstructed and restored to 0.	75
Figure 42: Central Section - Lower Jurassic removed, and Triassic restored to 0.	76
Figure 43: Central Section - Triassic and Permian removed, Base Permian Unconformity restored to 0, Westphalian erosion reconstructed and restored to 0.	77
Figure 44: Central Section - Westphalian removed, Upper Namurian restored.	78
Figure 45: Central Section - Upper Namurian removed, Lower Namurian restored to 0 m, Intra-Namurian erosion reconstructed and restored.	77
Figure 46: Central Section - Lower Namurian removed and Dinantian restored to a paleo topography.	80
Figure 47: Present-Day configuration of the Western Section showing the named faults analysed in term of kinematics.	83
Figure 48: Present-Day configuration of the Central Section showing the named faults analysed in term of kinematics.	84
Figure 49: Fault kinematic summary chart showing the growth history for all the 65 main faults present on the Western Section.	87
Figure 50: Fault kinematic summary chart showing the growth history for all the 65 main faults present on the Central section.	88
Figure 51: Western Section restoration results.	94
Figure 52: Central Section restoration results.	101
Figure 53: Modelled present day maturity (%Ro) in well UHM-02 compared to measured Vitrinite reflectance (Vr%).	105
Figure 54: Well LWS-01. A. Modelled present day temperature compared to measured BHT. B. Burial history with the modelled maturity (%Ro). C. Transformation Ration (TR %) of the main source rocks.	107
Figure 55: Well SWD-01. A. Modelled present day temperature compared to BHT. B. Burial history with the modelled maturity (%Ro). C. Transformation Ration (TR %) of the main source rocks.	110
Figure 56: Well BAC-01. A. Present day modelled versus well BHT. B. Modelled present day maturity (%Ro) compared to measured Vitrinite reflectance (Vr%). C. Burial history with the modelled maturity (%Ro). D. Transformation Ration (TR %) of the main source rocks.	113
Figure 57: Well EMO-01. A. Present day modelled versus well BHT. B. Modelled present day maturity (%Ro) compared to measured Vitrinite reflectance (Vr%). C. Burial history with the modelled maturity (%Ro). D. Transformation Ration (TR %) of the main source rocks.	115
Figure 58: Well NAG-01. A. Present day modelled versus well BHT. B. Modelled present day maturity (%Ro) compared to measured Vitrinite reflectance (Vr%). C. Burial history with the modelled maturity (%Ro). D. Transformation Ration (TR %) of the main source rocks.	118

Figure 59: Well Ext-01. A. Burial history with the modelled maturity (%Ro). B. Transformation Ration (TR %) of the main source rocks.	120
Figure 60: Well Ext-02. A. Burial history with the modelled maturity (%Ro). B. Transformation Ration (TR %) of the main source rocks.	122
Figure 61: Interpreted seismic section of along which well EXT-03 was extracted	123
Figure 62: Well Ext-03. A. Burial history with the modelled maturity (%Ro). B. Transformation Ration (TR %) of the main source rocks.	125
Figure 63: Well AST-01-ext. A. Burial history with the modelled maturity (%Ro). B. Transformation Ration (TR %) of the main source rocks.	128
Figure 64: Well HVS-01. A. Present day modelled versus well BHT. B. Modelled present day maturity (%Ro) compared to measured Vitrinite reflectance (Vr%). C. Burial history with the modelled maturity (%Ro). D. Transformation Ration (TR %) of the main source rocks.	130
Figure 65: Apatite Fission Track (AFT) thermal models from which the subsidence/uplift history is derived for the 1D basin modelling of the London Brabant Massif wells.	132
Figure 66: Well BHG-01. A. Present day modelled versus well BHT. B. Modelled present day maturity (%Ro) compared to measured Vitrinite reflectance (Vr%). C. Burial history with the modelled maturity (%Ro). D. Transformation Ration (TR %) of the main source rocks.	136
Figure 67: Well S02-02. A. Present day modelled versus well BHT. B. Modelled present day maturity (%Ro) compared to measured Vitrinite reflectance (Vr%). C. Burial history with the modelled maturity (%Ro). D. Transformation Ration (TR %) of the main source rocks.	139
Figure 68: Well WDR-01. A. Present day modelled versus well BHT. B. Modelled present day maturity (%Ro) compared to measured Vitrinite reflectance (Vr%). C. Burial history with the modelled maturity (%Ro). D. Transformation Ration (TR %) of the main source rocks.	142
Figure 69: Dinantian summary burial graph for the Western Section.	145
Figure 70: Dinantian summary burial graph for Central Section.	146
Figure 71: Summary of main phases of Westphalian source rock maturation and hydrocarbon generation.	148
Figure 72: Location of proposed additional 2D structural restorations for follow up geothermal exploration research projects.	150

## Tables

Table 1: List of wells used in this study.	41
Table 2: list the seismic lines used to construct the composite seismic lines that was used for the two restorations.	46
Table 3: Coordinate system used in the Move project.	47
Table 4: List of key wells imported to the Move project.	48
Table 5: List of modelled wells.	57
Table 6: Average source rock parameters used for simulating source rock maturity and hydrocarbon generation.	62
Table 7: Central Section fault characteristics.	85
Table 8: Western Section fault characteristics.	86

## Appendices

Appendix 1A: Present-Day uninterpreted (A and C) and interpreted (B and D) depth migrated sections used for the 2D structural restorations.	160
---	-----

Appendix 1B: Present-Day interpreted depth migrated sections used for the restoration. See location map in Figures 11 and 19.	161
Appendix 2: Summary chart of the structural evolution of the 19 recognized structural elements identified in the study area.	162
Appendix 3A: Central Section fault throw values for each time steps.	163
Appendix 3B: Western Section fault throw values for each time steps.	163
Appendix 4A: Structural restoration of the Western Section at one to one scale (part 1).	164
Appendix 4A: Structural restoration of the Western Section at one to one scale (part 2).	165
Appendix 4B: Structural restoration of the Central Section at one to one scale (part 1).	166
Appendix 4B: Structural restoration of the Central Section at one to one scale (part 2).	167
Appendix 5: Updated summary chart of the structural evolution of the 19 recognized structural elements identified in the study area.	168



# 1. Samenvatting

## 1.1. Doelstellingen

Kennis van de structurele ontwikkeling en de begravings-/opheffingsgeschiedenis van het onder Carboon Dinantien in de Nederlandse onshore was voorafgaand aan deze studie beperkt, voornamelijk als gevolg van het gebrek aan systematisch en gestructureerd onderzoek en kennis over de verbreiding en architectuur van dit stratigrafisch interval. Om de onzekerheden in de structurele ontwikkeling van de Dinantien carbonaten te verkleinen, is een tweeledige studie uitgevoerd bestaand uit twee 2D structurele reconstructies en een 1D maturiteit modelleer studie. Ook is voor deze studie een nieuw overzicht van gepubliceerde artikelen en recente kennis van specialisten op het gebied van de structurele ontwikkeling van het Dinantien gecompileerd. Dit bevat ook lessen over de Dinantien carbonaat systemen uit België en het Noordzee gebied.

Het voornaamste doel van deze studie is het ontwikkelen van een structureel geologisch solide analyse van de begravings-/opheffingsgeschiedenis van de potentiële Dinantien carbonaat geothermische doelen, door rekening te houden met de nieuwste kennis van de afzettingssystemen, hun huidige geografische verbreiding en diepte, en de structurele ontwikkeling van een aantal belangrijke breuken die de Dinantien carbonaten beïnvloed kunnen hebben sinds het vroeg Carboon. De inzichten die verkregen zijn in deze studie kunnen worden gebruikt om concepten te ondersteunen over de ontwikkeling van carbonaatplatformen gedurende het Dinantien en daaropvolgende episoden van diagenese en breukbewegingen.

## 1.2. Conclusies

### 1.2.1. 2D structurele restauraties

- De twee structurele restauraties die in deze studie zijn uitgevoerd geven een nieuw perspectief op de mogelijke begravings-/opheffingsgeschiedenis van de Dinantien gesteentelagen.
- Om de impact te bepalen die tal van belangrijke tektonische gebeurtenissen (orogeen vorming, spreiding) en bijbehorende erosies hadden op de evolutie van het Dinantien, is een reconstructieprocedure opgezet die 16 opeenvolgende stappen omvat.
- De Dinantien begraving/opheffing werd sterk beïnvloed door laat Carboon samentrekking, Midden-Jura opheffing/*dome*-vorming en Laat-Jura spreiding.
- De invloed van de Alpine samentrekking gedurende het Laat-Krijt is verwaarloosbaar; de belangrijkste ontwikkeling tijdens het Kenozoïcum was een gestage en continue begraving van het Dinantien, gemiddeld met zo'n 1 tot 1,5 km.
- Het Dinantien bereikte zijn maximale begravingsdiepte op verschillende tijden, afhankelijk van zijn positie binnen de verschillende structurele eenheden. Langs het N-Z lopende gerestaureerde profiel in het centrale deel van de Nederlandse onshore, bereikte het Dinantien in het noordelijke twee-derde deel van de Nederlandse onshore (noordwaarts vanaf het Peel-Maasbommel Complex) de maximale begraving gedurende het Onder-Jura. In andere delen bereikte het Dinantien maximale begraving gedurende het Westfalien, Vroeg-Krijt, Laat-Krijt of huidige tijd.
- Van het Vroeg- tot Laat-Jura werden alle gebieden, met uitzondering van het West-Nederlands Bekken, opgeheven (gemiddeld van 2 tot 2.5 km) als gevolg van een combinatie van opheffing gerelateerd aan *doming* in de Noordzee en de opheffing van de riftschouders tijdens de Jura spreiding.

- Een paar breuken waren actief tijdens en voorafgaand aan de afzetting van de Dinantien carbonaten. Deze structuren hebben waarschijnlijk de positie en groeigeschiedenis van deze carbonaatplatformen bepaald.

### 1.2.2. 1D begraving en maturiteit modellering

- De verschillende 1D bekkenmodellen voor de bestudeerde boorgaten suggereren dat op een bepaald moment in de geologische geschiedenis, de moedergesteenten diep genoeg begraven werden om olie- en gas te kunne vormen. Voor de meeste boorgaten suggereert de gemodelleerde data dat de initiële en voornaamste fase van maturatie van de Westfalien moedergesteenten en vorming van koolwaterstoffen plaatsvond gedurende het laat Carboon tot vroeg Perm. Voor boorgaten uit het West-Nederlands Bekken suggereren de modellen dat dit gevolgd werd door een tweede fase van maturatie gedurende het Laat-Krijt tot Neogeen.
- De gemodelleerde Transformatie Ratio (TR%, een mate voor het percentage van het voltallig in moedergesteente aanwezige gehalte aan organisch materiaal dat naar koolwaterstoffen is omgezet), suggereert dat voor de meeste Westfalien moedergesteenten, tenminste de helft tot al het aanwezige organisch materiaal omgezet is naar olie en/of gas.
- De voornaamste fase van olie/gas vorming vond plaats in het Perm, met uitzondering van het West-Nederlands Bekken en boorgat BAC-01 waarin de koolwaterstoffen in het Laat-Krijt tot Neogeen ontstaan zijn volgens de gemodelleerde data.
- 1D bekkenmodellen voor potentiële Namurien en Dinantien moedergesteenten suggereren dat in de meeste boorgaten de moedergesteenten over-rijp zijn sinds het Perm, en eventuele koolwaterstof vorming moet daardoor eerder hebben plaatsgevonden.
- Hoewel de 1D bekken modellen informatie verschaffen over het tijdstip waarop koolwaterstoffen gevormd zijn, geven ze geen informatie over volumes of de paden waarlangs de koolwaterstoffen bewogen hebben. Er kan daarom niet geconcludeerd worden dat koolwaterstoffen (nog) aanwezig zijn. Om de eventuele aanwezigheid van koolwaterstoffen in de bestudeerde boorgaten beter te kunnen inschatten zijn (lokale) gedetailleerde 3D bekkenmodellen nodig.
- De 1D bekkenmodellen zijn gekalibreerd aan onafhankelijke metingen zoals vitriniet reflectie en boorgattemperaturen. Voor de boorgaten op het Londen-Brabant Massief/Zeeland Hoog zijn een aantal test modellen gemaakt, om te bepalen welke warmte-gradiënt nodig is om de modellen te kalibreren aan de gemeten data. Uit deze testen is gebleken dat een hogere dan verwachte warmte-gradiënt nodig is voor deze boorgaten. Gelijke observaties werden gedaan in bijvoorbeeld boorgat UHM-02, waar een vitriniet meting aangaf dat een hogere warmte-gradiënt nodig was om de om deze hogere vitriniet waarde te verklaren. In de huidige studie worden geen specifieke verklaringen gegeven voor de hogere warmte-gradiënten. Vervolg onderzoek is nodig om verder te bouwen op deze en andere SCAN Dinantien projecten; in het bijzonder de petrofysische studie van Carlson (2019).

### 1.3. Aanbevelingen

Dit project omvat veel informatie uit eerder werk, andere SCAN Dinantien projecten en van verschillende soorten data. Dit rapport is een robuuste verbetering van de Pre-Zechstein structurele ontwikkeling in de Nederlandse onshore, en voegt veel waardevolle nieuwe

informatie toe aan deze complexe geschiedenis. Hieronder stellen we een serie aanbevelingen voor omtrent toekomstig werk en wat verdere substantiële kennis kan leveren voor het minimaliseren van de risico's van het Dinantien geothermische doelen.

- Seismische kartering van een aantal nieuwe Carboon lagen is nodig om de structurele ontwikkeling van de Nederlandse onshore en de en begravingsgeschiedenis van de Dinantien carbonaten beter te kunnen begrijpen. Wij denken dat 3D regionale kartering van drie of vier extra lagen (twee intra-Namurien en een of twee intra-Westfalien lagen) tot een beter begrip van de Carboon architectuur zal leiden.
- Gedetailleerde kartering en 3D kinematische analyse van de Dinantien breuksystemen gevormd voorafgaand en tijdens de afzetting, zou moeten worden uitgevoerd ter evaluatie van bekende en mogelijk onontdekte carbonaatplatformen die aanwezig zijn op de breukblokken van deze structuren. Stratigrafisch modeleren met inbegrip van breukactiviteit kan op lokale schaal ook licht werpen op de locatie, groei en behoud van deze carbonaat afzettingssystemen.
- De nieuw verworven, of binnenkort te verwerven seismische data in de Nederlandse onshore zou gebruikt moeten worden, naast de bestaande seismische database, om de bestaande interpretatie en nieuwe lagen te valideren en om nieuwe lagen te karteren. Met het hieruit ontwikkelde nieuwe geologisch model, zou een revisie van de structurele restauratie geproduceerd in dit project ook opnieuw geprobeerd kunnen worden. Ook kunnen dan nieuwe secties worden toegevoegd ter restauratie. Ook de onlangs verwerkte 3D seismische dataset moet worden opgenomen.
- Nieuwe biostratigrafische analyse van Paleozoïsche boorgaten (CAL-GT-01 tot -05, UHM-02, WSK-01, O18-01 en LTG-01) en ontsluitingen in Nederland, België en Duitsland zijn nodig om verdere onzekerheden in de aanwezigheid en behoud van pre- en post-Dinantien gesteentelagen te verminderen. De nieuwe informatie moet daarna toegevoegd worden aan de database met huidige kennis opgebouwd uit het SCAN Dinantien Programma en zou, na voltooiing, als addendum moeten worden toegevoegd.
- Kortere secties met structurele restauraties met verschillende oriëntatie zouden een beter begrip van de laterale begraving geschiedenis van specifieke Dinantien carbonaatplatformen kunnen geven, en kan op lokale schaal zorgen voor het verkleinen van risico's met betrekking tot toekomstige geothermische exploratie. Kleinschaligere restauraties (20-50km lang) kunnen ook van belang zijn om ideeën te testen in specifieke locaties, inclusief consortium locaties.
- Uit de 1D bekkenmodellen komt duidelijk naar voren dat in bepaalde boorgaten, in het bijzonder die op het Londen Brabant Massief maar bijvoorbeeld ook in UHM-02, de warmte-gradiënt die nodig is om de gemodelleerde temperaturen en/of maturiteit data te koppelen aan de gemeten kalibratie data, significant hoger is dan wat verwacht wordt gebaseerd op regionale warmte-gradiënt modellen. Aanvullend werk is nodig om de redenen hiervoor te achterhalen omdat dit de (gemodelleerde) diagenetische geschiedenis in de Dinantien carbonaatgesteenten kan beïnvloeden. Dit zou uitgevoerd moeten worden door gebruik te maken van, en het integreren van resultaten van andere SCAN studies, inclusief deze alsmede de Carlson (2019) en Mozafari *et al* (2019) studies.
- Verkrijg een beter begrip van de begravings- en opheffingsgeschiedenis van het Nederlands deel van het Londen-Brabant Massief/ Zeeland Hoog. De grote discordantie tussen het Carboon en de Krijt eenheden bemoeilijken het begrip van een significant deel van de Meozoïsche geologische ontwikkeling van het Zeeland Hoog gebied. Lage temperatuur thermochronologische studies (bijvoorbeeld (U-Th)/He en/of splijtspoor analyses) zouden onderdeel moeten uitmaken van dit werk. Extra

geochronologische analyses langs de noordelijke flank van het Londen-Brabant Massief (Zeeland Hoog, Kempen Bekken en Limburg Hoog) zouden ook zeer waardevol zijn om de Paleozoïsche evolutie van dit gebied beter te kunnen begrijpen.

## 2. Executive summary

### 2.1. Aims and Objectives

Knowledge of the structuration and burial/uplift history of the Lower Carboniferous Dinantian in the Dutch onshore was limited prior to this study due to the lack of systematic research and knowledge on the distribution and architecture of this stratigraphic interval. To decrease uncertainties in the structural evolution of the Dinantian carbonates, a two part study that includes two 2D structural restorations and 1D maturity modeling is undertaken. A new review of published papers and recent knowledge from specialists on the structural evolution of the Dinantian was also compiled for this study and includes learnings of the Dinantian carbonate systems from Belgium and the North Sea area. The main goal of this study is to develop a structurally sound analysis of the burial/uplift history of the potential Dinantian carbonate geothermal targets by taking into account state-of-the-art knowledge of the depositional environments, their present day geographic extent and depths, and the structural evolution of key faults that may have impacted the Dinantian carbonates since the Early Carboniferous. The insights from this study could be used to support concepts of development of carbonate platforms during the Dinantian and subsequent diagenetic and fracturing events.

### 2.2. Conclusions

#### 2.2.1. 2D structural restorations

- The two structural restorations that were carried out in this study give a good new perspective on the possible burial/uplift history of the Dinantian strata.
- To capture the impact that numerous key tectonic events (orogen, rifting) and their associated erosions had on the evolution of the Dinantian a 16 steps sequential restoration procedure was required.
- The Dinantian burial/uplift was heavily impacted by Late Carboniferous contraction, Mid Jurassic doming/uplift and Late Jurassic rifting.
- The impact of the Alpine contraction during the Late Cretaceous is negligible with the main evolution during the Cenozoic being a steady continued burial of the Dinantian by an average of 1 to 1,5 km.
- The Dinantian reached its maximum burial depth at different times, depending on its position within different structural elements. Along the restored section located in the central part of the Dutch onshore and trending NS, the northern two third part of the Dutch onshore (from Peel-Massbommel Complex northward) the Dinantian reached maximum burial during the Early Jurassic. In other locations, the Dinantian reached maximum burial during the Westphalian, Early Cretaceous, Late Cretaceous or at present day.
- From the Early to Late Jurassic, all areas, except the West Netherlands Basin, were uplifted by an average of 2 to 2.5 km due to a combination of uplift related to the Mid-North Sea doming and the uplift of the rift shoulder during the Jurassic rifting.
- A few faults were active during and prior to the deposition of the Dinantian Carbonate. These structures likely influenced the localization and growth histories of these carbonates platforms.

### 2.2.2. 1D burial and maturity modeling

- The various 1D basin models for the studied wells suggest that at some stage in the geological history, the source rocks have matured sufficiently to reach the oil and/or gas generation window. For most wells, modelled data suggests that the initial, and main phase of Westphalian source rock maturation and hydrocarbon generation occurred during the Late Carboniferous – Early Permian. For wells from the West Netherlands Basin, modelling suggests that this was followed by a second maturation phase in the Late Cretaceous to Neogene.
- Modelled Transformation Ratio's (TR%, a proxy for the percentage of the total organic material present in the source rocks that has been converted into hydrocarbons), suggest that for most Westphalian source rocks, at least half to all of the available organic material was converted into oil and/or gas.
- Main phase of oil/gas generation occurred in the Permian, with the exception of the wells in the West Netherlands Basin and well BAC-01 which have been generating hydrocarbons in the Late Cretaceous to Neogene according to modelling results.
- 1D basin model results for the potential Namurian and Dinantian source rocks suggest that in most wells, the source rocks are overmature since the Permian, and any hydrocarbon expulsion must have occurred prior.
- Although 1D basin modelling provides indications for (the timing of) hydrocarbon generation, it does not quantify volumes or reconstruct migration pathways. Therefore, it cannot be concluded that hydrocarbons will (still) be present. In order to understand the likelihood of the presence of hydrocarbons at the studied well locations, (local) detailed 3D basin models are required.
- The 1D basin models are calibrated against independent measurements such as vitrinite reflectance and bore hole temperatures. For the London Brabant Massif/Zeeland High wells, sensitivity tests were conducted to constrain the heat flow required to calibrate the modelled data to the measured data. From these tests it was apparent that a higher than expected heat flow was needed for these wells. Similar observations were made in for example UHM-02, where one vitrinite measurement indicated that a high heat flow was required in order to explain the high vitrinite measurement. In the current study, we do not propose any specific explanations for the higher heat flow gradients. Further work is required to build on the observations obtained by the other SCAN Dinantien projects, and especially the petrophysical study of Carlson (2019).

### 2.3. Recommendations

This project encapsulated numerous information from previous work, from other SCAN Dinantien projects and from a variety of data types. This is a robust structural update on the Pre-Zechstein structural evolution of the Dutch onshore and adds valuable new insights on this complex history. Below we propose a series of recommendations for future work that would add substantial knowledge for de-risking the Dinantian carbonate geothermal play further.

- Seismic mapping of additional Carboniferous horizons is required to better understand the structural evolution of the Dutch onshore and the burial history of the Dinantian carbonates. We believe that 3D regional mapping of three to four more horizons (two intra Namurian horizons and one to two intra-Westphalian horizons) would allow to capture more precisely the Carboniferous architecture.
- Detailed mapping and 3D kinematic analysis of the Dinantian pre- and syn-depositional faults should be undertaken to evaluate the known and potentially

undiscovered carbonate platforms that are located on the footwall of these structures. Modern stratigraphic modeling that takes into account the fault activity can also shed some lights on the location, growth and preservation of these carbonate depositional systems on a local scale.

- The newly acquired, or soon to be acquired seismic data in the Dutch onshore should be used, in addition to the existing seismic database, to further validate the existing interpretation and to map new horizons. With such a new geological model, a revision of the structural restorations produced in this project could be attempted as well as add other sections to be restored. Recently re-processed and depth-imaged 3D seismic datasets should be included as well.
- New biostratigraphic analysis of Paleozoic wells (CAL-GT-01 to -05, UHM-02, WSK-01, O18-01 and LTG-01) and outcrops in the Netherlands, Belgium and Germany is also required to decrease uncertainties in the presence and preservation of pre- and post- Dinantian strata. The new information should then be added to the knowledge base constructed from the SCAN Dinantien Program and be presented as an addendum when completed.
- Shorter structural restoration sections with different orientations would also allow to better understand the lateral burial evolution of specific Dinantian carbonate platforms and allow to further de-risk those targets for future geothermal exploration on a local scale. Smaller scale restorations (20-50 km long) could also be valuable to test some ideas on specific sites, including consortia sites.
- From the 1D basin models it has been apparent that in certain wells, notably those on the London Brabant Massif, but also in for example UHM-02, the heat flow required to match the modelled temperature and/or maturity data to the measured calibration data is significantly higher than what would be expected based on the regional heat flow models. Future work should investigate the reasons for the required higher heat flows as this may impact the (modelled) diagenetic events in the Dinantian carbonate rocks. This should be carried out using and integrating the results of several other SCAN Dinantien studies including the present study as well as Carlson (2019) and Mozafari *et al.* (2019).
- Gain better understanding of the burial and uplift history of the Dutch segment of the London Brabant Massif/ Zeeland High. The large unconformity between the Carboniferous and Cretaceous units hampers understanding of a significant part of the Mesozoic geological evolution of the Zeeland High area. Low temperature thermochronological studies (e.g., apatite (U-Th)/He and or Fission Track) work should be conducted as part of this work.

Additional geochronological analysis along the northern flank of the London Brabant Massif (Zeeland High, Campine Basin, Limburg High) would also be valuable to better calibrate the evolution of the Paleozoic strata in this area.

### 3. Introduction

“Geothermal energy systems have been considered as a potential alternative for the fossil fuel heating. Currently, there are geothermal projects already functioning in the Netherlands. However, the application of geothermal energy in existing projects is not adequate for the provision of high-temperature heat for, as an example, the process industry. It is anticipated that Ultra Deep Geothermal (UDG) energy could potentially make a substantial contribution to the transition towards a sustainable heat supply. To reach sufficiently high temperatures in the Netherlands, geothermal reservoirs at depths over 4 km are required. The Dutch subsurface at these depths has not been explored extensively until now and is therefore relatively unknown. Based on the limited amount of subsurface data, the Lower Carboniferous Dinantian Carbonates were identified by Boxem *et al.*, 2016 as the most promising target matching the initial requirements for UDG.

The burial and structuration analysis reported in this document is a result of SCAN, a government funded, program to scope out the potential of geothermal energy, including from the Dinantian Carbonates. This program includes a range of subsurface studies of the Dinantian Carbonates. The results of the SCAN studies will be released and become available via [www.nlog.nl](http://www.nlog.nl).”

Understanding the structural evolution of the Dinantian in the Dutch onshore is an important topic for future deep geothermal exploration. This report concerns the work package 2.1.3: Burial and Structuration of the UDG-EWP / SCAN Dinantien Program that focuses on the structural evolution of the Dinantian via 1D maturity modeling and 2D structural restoration techniques. This study was carried out by a team of geoscientists from TNO, 4DGeo, TiBA ScConsulting and the University of Utrecht. This project was also closely linked to several other UDG-EWP / SCAN Dinantien studies such as the seismic interpretation and depth conversion study presented in Ten Veen *et al.* (2019), the facies analysis and diagenetic evolution study presented in Mozafari *et al.* (2019), and the petrophysical study presented in Carlson (2019). Results from all those work packages were used in this study to build a more robust geological model of the deep Dutch onshore and to better characterize the Dinantian Carbonate platforms in regard of their growth history, distribution, paleogeographic positioning, diagenetic history, petrography and their relationship to syn- and post-depositional structuration. In this chapter, we will discuss the background, rationales, objectives, scope and deliverables of this study.

#### 3.1. Background and rationale

Having hot water targets at a depth of 4 km is a double-edged sword: the depth provides the heat, but burial causes compaction, diagenesis and a related decrease in porosity and permeability, making it more difficult for water to flow through the rocks. Processes related to uplift, such as faulting and fracturing, erosion and the forming of karsts and caves may have a favourable effect. Uplift may mask how deep the rocks once were, which may lead to over-estimation of permeability potential.

The burial/uplift history of Dinantian carbonate platforms has clearly impacted the diagenesis and heat history and potential of these deep geothermal targets. The Dutch subsurface has gone through multiple phases of structuration since the Devonian to Early Carboniferous when the Dinantian carbonate platform developed. The impact of two major compressional phases (Variscan and Alpine), two rifting phases (Late Devonian to Early Brigantian and Jurassic) and several major erosional events, on the Dinantian burial/uplift has to be assessed in light of new knowledge regarding the present-day configuration and the geological evolution of the Dutch subsurface. This study aims at assessing the structural history of this



interval by using state-of-the-art methods and software, namely 1D maturity modeling using PetroMod software from Schlumberger and 2D structural restoration in a 3D modelling context using 2D Move software from Midland Valley/Petex. Structural restoration has been a well-established technique for petroleum exploration related studies in compressional settings since the '60s and was first applied to extensional structures in the North Sea (Gibbs, 1983). In this study, these techniques are deployed to get a better understanding of the structural evolution as well as including the drowning depositional environment, subsidence and uplift, karstification, and erosion events that affected the Dinantian carbonates. These research techniques incorporated new information and knowledge regarding the Dinantian carbonate platforms obtained from several other SCAN Dinantien WPs, specifically their 1) present-day distribution, 2) facies, 3) petrography, 4) diagenetic evolution, 5) paleogeography, and 6) physiography (e.g. paleo-water depth).

### 3.2. Objectives

The goal of this study is to reconstruct the structural history and associated burial/uplift history of the Dinantian strata in the Dutch onshore subsurface. The goal is to better understand the overall structural history of the Dutch onshore subsurface via the structural restoration of two regional panels and 1D maturity/thermal history at well and pseudo well locations. The structural restorations allow to reconstruct unravel, investigate and quantify precisely the timing, the structural geometry and in particular vertical position at several geological stages. By backstripping and decompacting multiple geological layers, geologists can take out the effects of faulting, folding and compaction, and replace restore relevant geological structures in space and time to better understand their burial and/or uplift history and therefore their possible diagenetic and thermal history, information that is critical for de-risking geothermal targets. The goal of the 1D modeling phase is to get a better understanding of the thermal history of the Dinantian. In addition, it investigates unfavourable maturity of potential oil and gas source rocks at well and pseudo well locations, to predict possible oil or gas generation that could negatively impact geothermal doublet planning. These 1D models also give better constraints on the thermal history of the Dinantian at those specific locations.

### 3.3. Plan

The project was set up as a structurally focused study setting the stage for a new integrated tectono-stratigraphic model of the Dinantian in the Dutch onshore. The study consisted of four phases: a literature review, two complementary analytical studies and an integration/reporting phase. The first phase of the project consisted of a literature review and a series of discussion meetings with experts from the core team and externals to set the stage for the technical part of the study. This allowed for a reassessment of the geological history of the Dutch onshore using recently acquired knowledge from the Dutch offshore, the UK, Germany and Belgium (see Chapter 3). The second phase consisted of two new 2D structural restoration models and aimed at decreasing uncertainties on the Dinantian's burial and uplift history. The third phase consisted of fourteen 1D maturity models that were carried out to better evaluate local burial and maturity history at well or pseudo well locations and to evaluate the risk of hydrocarbon generation at critical location (e.g. consortia locations) and to better evaluate local burial and maturity history at well or pseudo well locations. The final phase of the project consisted on the integration and reporting of all the results.

#### Phase 1: Setting up the project and evaluating the state of geological knowledge

A comprehensive review of key literature was performed, including recent knowledge gathered and developed in neighbouring countries where Dinantian Carbonates are also encountered. New geological results from other SCAN Dinantien studies were also discussed

and integrated in this study, such as new seismic interpretation, facies information, gravity modeling and diagenetic information. The geoscientific project team discussed the goals and the state of knowledge regarding the structural evolution of the Dinantian and younger stratigraphic units with representatives of other SCAN Dinantien work packages, specifically: 1) Johan Ten Veen, Nico Holleman, Wegner Schoeler, Pieter van Heiningen, Geert de Bruin, Harald de Haan and Andrea Kruisselbrink (Ten Veen *et al.*, 2019) and 2) Mathab Mozafari, Kees Geel and Alberto Riva (Mozafari *et al.*, 2019)

#### Phase 2: 2D structural restoration

Structural restoration helps to investigate the geological history, and quantify the change of shape, at key moments in geological time. Structural restoration and analysis software Move uses a set of algorithms to quantify the geometrical effects of faulting, folding and (differential) compaction. This way, structural restoration helps to produce repeatable results, it allows to compare and contrast multiple scenarios, and as such decreases the subjectivity in the interpretation process.

Selection of the SCAN trajectories for the 2D restoration negotiated a trade-off between optimum angle with respect to the key structural elements, and interception or proximity to the limited amount of constraining wells, useful seismic data, and location of consortia sites of interest.

Existing horizon and fault interpretation grids – after depth conversion - were integrated in Move in 3D modelling space and tested for internal consistency in the 2D sections. In total seventeen horizons were included. Input came from the recent 3D seismic interpretation study (work package 2.1.1) as well as from the published 3D horizons from the Dutch Geological Survey (especially for the younger, overburden intervals). The fault interpretation was fine-tuned and expanded. First and, smaller, second-order faults were identified, and (re-)interpreted aiming at internal consistency with local horizon shapes. Growth faults were marked, as well as faults with a significant strike-slip component.

Uncertainty in the description of the present-day geometry of the Dinantien is caused by the quality of the available seismic that was not designed to image such deep horizons, and by the lack of well-penetration. Testing the present-day geometry of the Dinantien and other horizons in the 2D section would – in normal structural analysis procedure – be done using line-length balancing techniques. These techniques build on the principle that there is no loss or gain of material in the section during deformation (apart from geological reasons).

Unfortunately, the significant amount of strike-slip deformation in the Netherlands limit these techniques and they were not applied.

Structural restoration parameters were identified, and optimum settings discussed. Parameters include rock type, decompaction parameters (initial porosity and change of porosity with depth), stratal age, amount of erosion, and estimated fault timing (based on tectonic context, observed growth stratigraphy and stratal terminations). The range of parameter values were identified, and the optimum - and alternative - restoration scenario discussed.

Sixteen steps of sequential restoration were required to capture the complexity of the structural and burial/uplift history of the study area. This first-pass effort is designed to form the basis for future iterations as and when additional data come in and forms a context that allows fine-tuning in particular areas of interest.

Methods based on structural geometry and structural principles such as structural restoration methods (palinspastic restoration) provide additional constraints for capturing the geological evolution of complex areas such as the Dutch subsurface. Such approaches allow to decrease the subjective limited interpretation that low quality/quantity data often triggers. Structural restoration techniques provide also the opportunity to test multiple scenarios while restoring geological sections and therefore provide educated new kinematic models. The 2D

restorations were carried out on two selected seismic transects oriented SSW-NNE and positioned to: 1) highlight key structural elements that impacted the burial/uplift history of the Dinantian at key locations, 2) intercept or be close to key wells, 3) be close to consortia sites, and 4) capture the best quality seismic data available that allow imaging the Paleozoic interval with the greater constrain and confidence. These 2D seismic sections were interpreted using mapping results from the seismic interpretation study (work package 2.1.1) as well as previously interpreted horizon from the Dutch Geological Survey (especially for the overburden intervals). In total seventeen horizons and numerous faults were interpreted, depth converted and uploaded to 2D Move software for the structural restoration phase. Key parameters were gathered and included as input for the restorations, such as lithologies, facies, decompaction factors, stratal age, amount of erosion, paleo-water depth estimations and estimated fault activity based on growth stratigraphy and stratal terminations. The restoration proper were then carried out with sixteen steps being modelled to capture the complex structural and burial/uplift history of the study area.

#### Phase 3: Burial and maturity 1D modelling

This part of the study consisted of the reconstruction of the burial and temperature history of the Dinantian carbonates. The main objectives of the study are to reconstruct and better understand the burial history (burial/uplift) of the Dinantian carbonates; and to provide predictions on the potential of Carboniferous source rocks to generate and expel hydrocarbons. This work does not provide predictions or risk assessment on the possible occurrences and/or accumulations of hydrocarbons in the well sections. Although the 1D basin models provide some first order indications on the potential of the source rocks to have expelled hydrocarbons they do not quantify volumes or reconstruct migration pathways. For this purpose, detailed 3D basin models are required. In total fourteen 1D basin models of selected wells have been constructed. Modelled wells are close to several regional seismic lines studied in the structural restoration work-package.

#### Phase 4: Integration and reporting

The integration and reporting of the new results regarding the structuration and burial/uplift of the Dinantian represent the final phase of this study. The implication toward other relevant topics such as carbonate facies mapping, seismic interpretation, fractures and diagenesis are discussed, but further integration between the SCAN Dinantien Program will be required as follow up. It is important to note that this project is initiating the first steps for integrations of multiple WPs of the SCAN Dinantien Program, but the real integration will be carried out after the completion of this WP through a more thorough approach and with a dedicated team of experts.

### **3.4. Deliverables**

The deliverables of this study are presented in the form of a report (pdf format) where all the results obtained from the different project phases are presented, such as the high-resolution structural restoration models (graphics), new constraints for uncertainties and assumptions regarding the structuration and burial of the Dinantian, burial/uplift curves, maturity/heat charts and a new structural evolution chart.

- 1) A literature review of the structural evolution of the Dutch onshore and relevant neighbouring areas (London Brabant Massif and North Sea)
- 2) Two detailed structural restoration models, including 16 steps of the study area's evolution, which bring new evaluation of the burial, uplift and erosional events that impacted the Dinantian since its deposition. The evolution of individual basins, faults,

fault blocks, folds and carbonate platforms are discussed in detail for each incremental step of the structural restorations,

- 3) Specific assumptions and uncertainties are listed, discussed in regards of their impact on the restorations of the Dinantian. This information is important for future work, to build even more robust models by better calibrating key parameters such as amount of erosion and its spatial variability, syn-sedimentary growth history of individual faults or paleo-physiography of the Devonian, Dinantian and Namurian basins and structural highs
- 4) Two interpreted transects in depth (ascii)
- 5) Fourteen 1D models with new burial and maturity curves
- 6) A new composite summary structural evolution chart, incorporating new information from this and other SCAN Dinantien WPs.

## 4. State of knowledge and literature review on the geological setting and evolution of the Dutch onshore.

The geology of the Dutch subsurface is a vast topic that spawned a multitude of studies, reports, papers, book and atlases over the last 40 years. This chapter will succinctly summarise the state of knowledge of the key geological structures, events and parameters that are pertinent to the story of the Dinantian in the Dutch onshore. Attention is paid toward lessons learned from neighbouring countries (UK, Germany and Belgium) as well as from the Dutch offshore where often good quality data (seismic and wells), and/or outcrop exposures allow to evaluate the Dinantian in more details. The recent published work of Tim Debacker (Debacker, 2012; Debacker *et al.* 2004, 2005, in prep) and Jeroen Smit (Smit *et al.* 2016 and 2018) regarding Belgium and North Sea regions were for example instrumental in understanding the basement and crustal configuration and their impact on the Dinantian geometry and evolution. Both Tim Debacker and Jeroen Smit were part of the core team of this project as advisors/experts and were consulted on regular basis during the course of the project. Below is a series of relevant geological summaries from key areas within the study and in neighbouring regions to the study area. A list of key structural elements is also discussed in regards of their possible impact on the local evolution of the Dinantian carbonates. These structural elements are revisited in Chapter 7 in light of the new results obtain in this study.

### 4.1. Late Caledonian to Early Variscan structural evolution of the Netherlands and neighbouring countries

Recent work by Smit *et al.* (2016 and 2018) and Yudistira *et al.* (2017) give new insights into the characteristics and evolution of the Dutch onshore crust and its evolution since the Early Carboniferous. Below is a short description of the larger scale plate tectonic and crustal evolution of the study area. Like the Brabant Massif, the Netherlands are located on the East Avalonia micro-continent, one of the peri-Gondwana terranes, as parts of Mexico, North America, Armorica, Adria, Iberia and Saxothuringia (Torsvik and Cocks, 2013; Smit *et al.*, 2018; Figure 1). Avalonia was part of the Gondwana active margin until around the Cambro-Ordovician boundary (ca. 490 Ma) when rifting and opening of the Rheic Ocean caused Avalonia to drift northward toward Baltica and Laurentia, closing the Iapetus Ocean (e.g. Ziegler, 1990; Torsvik and Cocks, 2013; Domeier, 2016). The dominant northwest-southeast trending basement grain and fault network of the southern North Sea and the Netherlands is inherited from the times that Avalonia was part of Gondwana's active margin during the late Proterozoic and earliest Paleozoic (e.g. Holdsworth *et al.*, 2012).

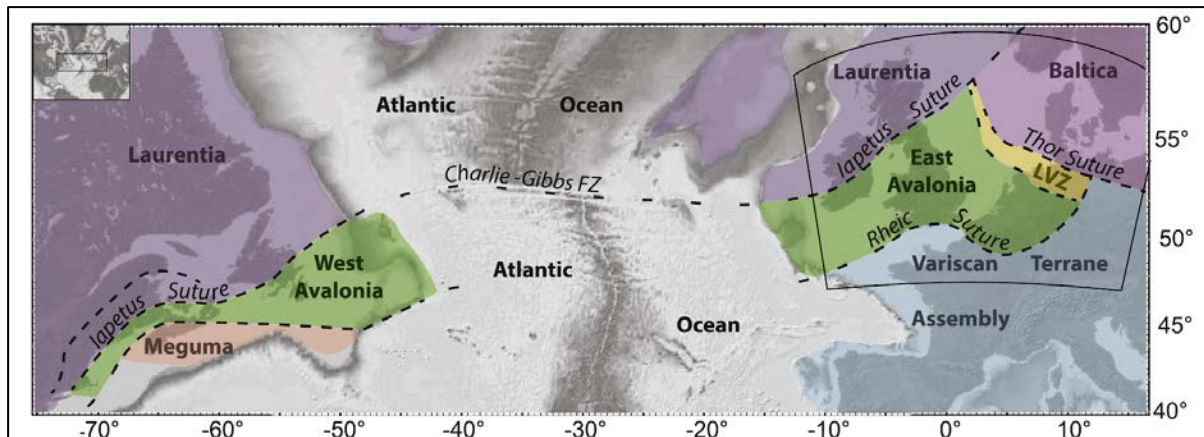


Figure 1: Extent of Avalonia across the Atlantic Ocean (dashed domains) after Mesozoic opening of the Atlantic Ocean. West Avalonia includes parts of the East Coast of the US and Canada. East Avalonia covers the area of NW Europe between the Caledonian Iapetus and Thor and the Variscan Rhenic suture. From Smit *et al.*, 2018

The Caledonian (Silurian) Thor Suture with Baltica forms Avalonia's north-eastern margin e.g. Ziegler, 1990; Torsvik and Cocks, 2013). This margin runs across the Dutch northern offshore (Smit *et al.*, 2016), from the North Sea Triple junction between the Moray-Firth, Viking Graben and Central Graben to the Variscan Rhenic suture in North Germany. The Terschelling basin and the southern termination of the Central Graben are located on the edge of Avalonia (Smit *et al.*, 2016). During most of the Ordovician, this north-eastern margin was the location of active subduction of oceanic lithosphere of the Thor Ocean (or Tornquist Sea) until the docking with Baltic (e.g. Torsvik and Cocks, 2013), as witnessed by subduction-related magmatism found on the British Isles, Ireland and the Brabant Massif.

The oldest geology of Avalonia is known from a few places where it is complicated by later tectonic overprinting (for a review see Holdsworth *et al.*, 2012). Nevertheless, outcrop studies in the UK and Ireland yield that Avalonia itself is an amalgamation of cratonic lithosphere in the south and one or more volcanic arcs to the north of the Brabant Massif (e.g. Pharaoh, 1999, Holdsworth *et al.*, 2012). It follows that the northern boundary of the London-Brabant massif, the NW-SE oriented Dowsing-South Hewett Fault Zone (DSHFZ) and its south-eastern extension, may coincide with a suture (e.g. Pharaoh, 1999, Guterch *et al.*, 2010) between cratonic lithosphere and such pre-Cambrian arc. The dominant northwest-southeast trending basement grain and fault network of the southern North Sea and the Netherlands is inherited from the times that Avalonia was part of Gondwana's active margin during the late Proterozoic and earliest Paleozoic (e.g. Holdsworth *et al.*, 2012). In analogy with other peri-Gondwanan terrains, the Avalonian crystalline basement probably consists of rocks with protolith ages of ca. 1.0–1.3 Ga and igneous rocks with depleted mantle model ages (TDM) of 1.35–1.77 Ga (Keppie *et al.*, 2012).

In absence of outcrops or well data from the Netherlands' territory, the LISPB profiles (e.g. Maguire *et al.*, 2011) and Irish Varnet profiles (Landes *et al.*, 2000) image the Precambrian basement at a depth of ca. 10–12 km and a Moho depth, which is comparable to that in the Netherlands. This leaves space for at the most a few kilometres of early Paleozoic sediments on the Avalonian plate north of the Welsh-Brabant Massif. Such early Paleozoic sediments are known from a few places in Ireland and England including the Leinster and Lake District Basins and on the Isle of Man (Woodcock, 2012 and references herein), they mainly consist of Cambrian to Ordovician deep water turbidites. The oldest sediments found in the Netherlands so far were retrieved from offshore well O18-1 located on the northern margin of the Brabant Massif. These siliciclastics are Early Devonian or older than (Lochkovian) and



younger than the Caradocian (Late Ordovician) (Swennen and Muchez, 1991). Based on the presence of spores and black spheres that resemble Leiospheres, these authors conclude that these sediments most likely date from the late Silurian (Ludlovian-Wenlockian).

The Late Caledonian phase must have had an impact on potentially present basins in the Netherlands deep subsurface during the early Devonian. A strong pulse of extension had already started during Early Devonian times and led to the formation of a rift basin on the Rheno-Hercynian Shelf filled with a considerable thickness (up to 14 km) of marine Lower Devonian sediments (Oncken *et al.*, 2000). Early Devonian extension also occurs around the Ardennes inliers (Belgium, France) and the Krefeld high but not in the Brabant Massif; there, extension only started from Mid Devonian onwards. The extension continued during Mid- and Late Devonian and caused rapid subsidence of the shelf with often no angular unconformities within the Devonian successions observed except in eastern England, Wales and northern England, where Lower Devonian strata are slightly deformed and unconformably overlain by very Late Devonian (Famennian) age strata. This regionally important unconformity is related to the Acadian phase, the final Caledonian deformation episode that took place (McKerrow, 1988) during the Early to or Mid-Devonian interval (Verniers *et al.*, 2002). Late Devonian-Early Carboniferous extension has been recognized in UK (Fraser and Gawthorpe, 2003), Norway (Fossen and Dunlap, 1998), Germany (Oncken *et al.*, 2000; Franke, 2000, see Figure 2), Belgium (Muchez & Langenaeker, 1993; Deckers *et al.*, 2019; Debacker *et al.* in prep), Poland (Szulczewski *et al.*, 1996) and the Dutch Northern offshore (e.g. Ter Borgh *et al.*, 2018). However, this extension phase is best known in the Netherlands from the Dinantian, when limestone build ups covered the margins of the Brabant Massif, the Groningen block and locally, other highs. The Devonian and Early Carboniferous basins in the Netherlands developed in response to back-arc extension in the Rhenohercynian Basin to the south-east of the Netherlands (Ziegler, 1990). The result was a series of WNW-ESE trending, fault-bounded, half-grabens in the southern North Sea, similar to the basins described in the English onshore (Leeder, 1988; Fraser & Gawthorpe, 1990; Chadwick, 1993, Hollywood & Whorlow, 1993). Devonian rocks in the Netherlands have been encountered in a few deep offshore wells but no Lower Devonian has been documented. In the western part of the Dutch offshore sector on the flanks of the Brabant Massif, wells S02-2, S05-1 and O18-1 have penetrated the marine mudstone and fine-grained sandstones of the Famennian Bosscheveld Formation (Banjaard Group). Kastanjelaan-2 Well in Limburg has also penetrated 120 m of late Frasnian to early Famennian Bollen Claystone (Banjaard Group) and shows sporadic carbonate streaks. The group reaches thicknesses of 300 to 700 m in the southern Netherlands but is thinner in the eastern Netherlands where it is up to 500 m thick (NITG, 1999). Devonian extensional movements along the northern margin of the London-Brabant Massif were frequently reported (e.g. Muchez & Langenaeker, 1993; Geluk *et al.*, 2007; Vandenberghe *et al.*, 2014).

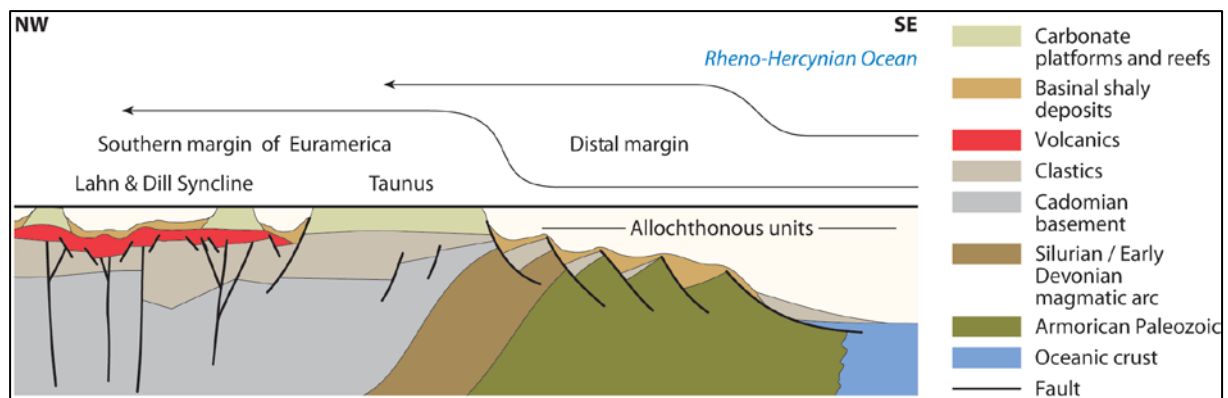


Figure 2: Palinspastic restoration of allochthonous units in the Rhenish Massif (from Franke, 2000).

During late Viséan/early Namurian (ca. 330 Ma), the onset of the Variscan orogeny marked the end of extension in Avalonia and the onset of post-rift thermal subsidence (e.g. Kombrink *et al.*, 2008) causing deepening and drowning of the Dinantian basin and the onset of clastic sedimentation along its southern and eastern margin (Leeder and Hardman, 1990; Kombrink *et al.*, 2008). This late Carboniferous Variscan orogeny caused the final closure of the Rheic Ocean by addition of the remaining peri-Gondwana terranes to Laurussia (e.g. Zwart and Dornsiepen, 1978; Ziegler, 1989, 1990; Ballèvre *et al.*, 2009). Variscan shortening of Avalonia was mainly concentrated in the formation of the Ardennes along its southern margin. Nevertheless, Late Devonian-Dinantian basins were inverted as far north as the Midland Valley. The northwest directed shortening predominantly inverted the orthogonal NE-SW trending basins of Ireland and England, together with the Mid North Sea High (e.g. Corfield *et al.*, 1996). At least some of the numerous NW-SE trending basement faults of the Netherlands and the southern North Sea must have acted as transfer faults during this time, accommodating dextral strike-slip motion between the suture and the closing foreland basins and the Mid-North Sea High. Folding of the crust and lithosphere under influence of the horizontal stresses induced by the orogeny may have caused differential subsidence and local uplift. The end of the Variscan orogeny in the latest Westphalian (ca. 305 Ma) coincided with the rise of an asthenospheric plume under large parts of the northern and southern Permian basins including the Netherlands, causing regional magmatism, pervasive heat flow in the Netherlands (Bonté *et al.*, subm.) as well the base Permian unconformity.

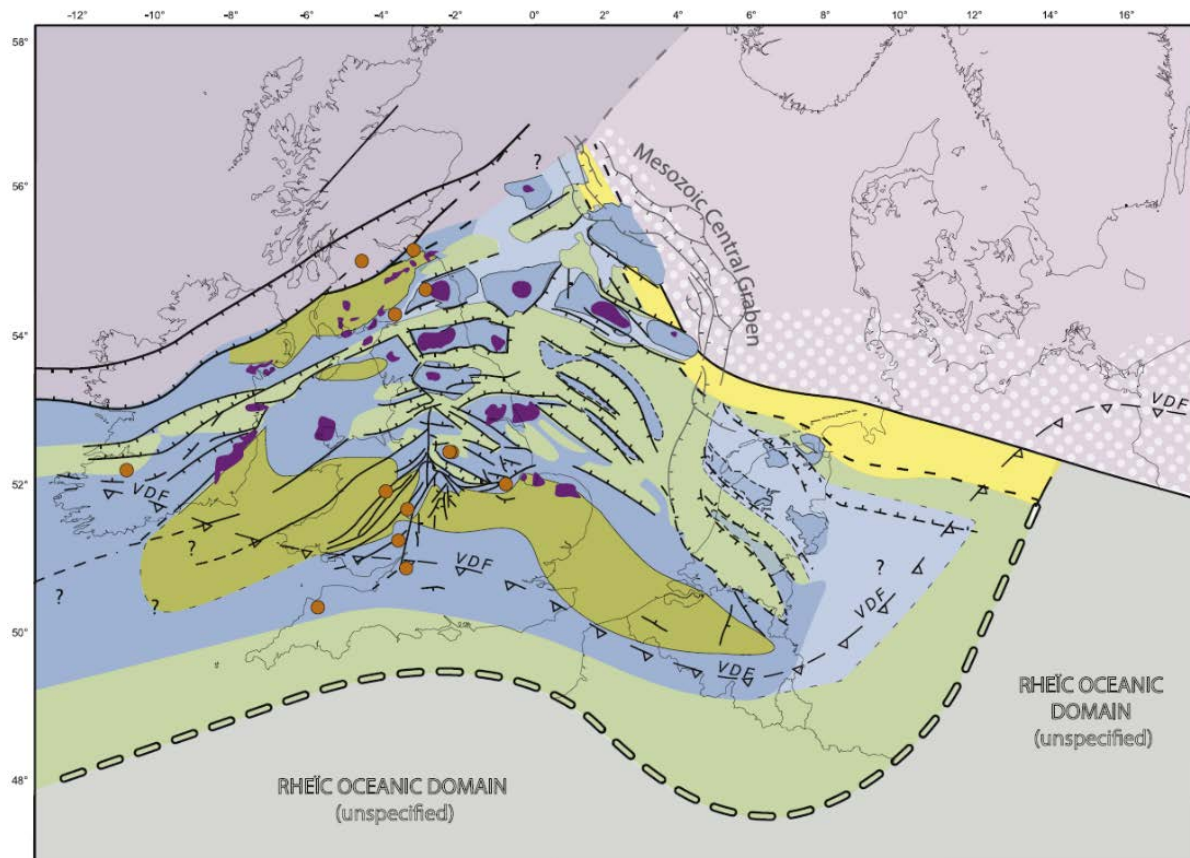


Figure 3: Paleogeography at end of early Carboniferous rifting including basement structures as far as known (horsts-and-grabens, blue). Purple: late Caledonian intrusive, in North Sea area inferred from gravity anomalies. Orange dots: Locations of Dinantian (syn-extension) magmatic activity. Thin black lines, early Carboniferous faults; thin black dashed lines, possible early Carboniferous faults; thin grey lines, post-Carboniferous North Sea Central Graben. From Smit *et al.*, 2018.



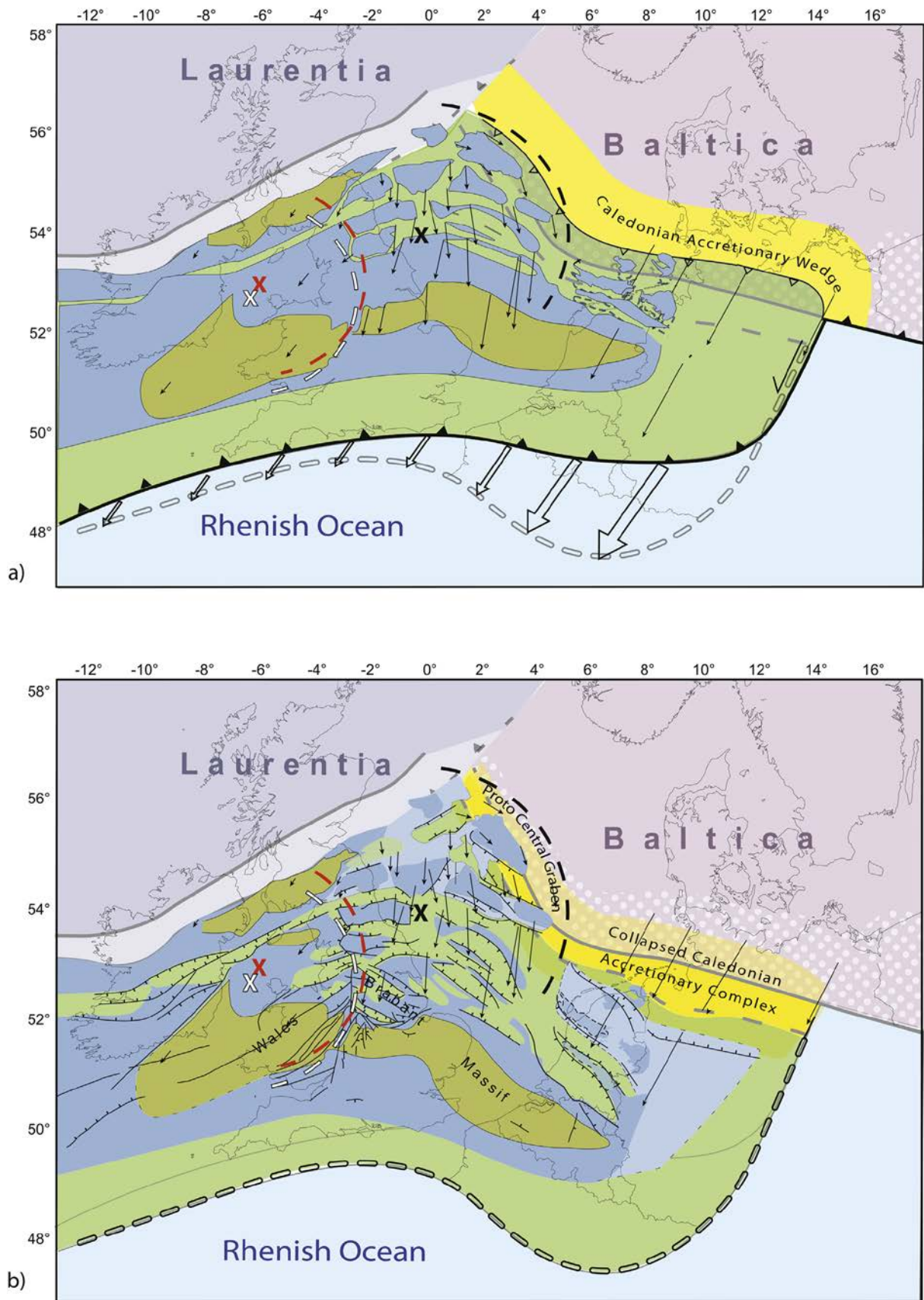


Figure 4: Map view restoration of early Variscan, Early Carboniferous extension of Avalonia. a) Initial late Caledonian, pre-extension configuration as deduced from restoration. b) Configuration at end of extension. From Smit *et al.*, 2018.

#### 4.2. A southern perspective on the structuration of the Dinantian: Constrains from the Brabant Massif and the Campine Basin

The Brabant Massif is a very low-grade Lower Palaeozoic massif in the subsurface of N-Belgium. It forms the south-eastern and best exposed part of the Anglo-Brabant Deformation Belt, a slate belt composed of lowermost Cambrian to upper Silurian, mainly siliciclastic deposits. Outcrops are restricted to river valleys that cut through the overlying Cretaceous and Cenozoic deposits, and because of the NNE-dipping erosion surface most outcrops are encountered along the southern part of the massif. To the south, the Brabant Massif is overlain via an (exposed) angular unconformity by Middle Devonian and younger deposits of the Namur Basin. To the NE, in subcrop, it is overlain, also via angular unconformity, by Middle Devonian and younger deposits of the Campine Basin (Figure 4). To the east, below the Vise-Puth Basin and the southern Roer Valley Graben, the Anglo-Brabant Deformation belt is considered to continue to the Krefeld High (Verniers *et al.*, 2002).

The Brabant Massif formed because of the progressive inversion of the Brabant Basin during NNE-SSW directed shortening. This progressive inversion is called the Brabantian Deformation event and is considered to have taken place from the late Llandovery until the Middle Devonian (~30 my; Debacker, 2001; Debacker *et al.*, 2005). This mainly resulted in the formation of folds and a moderately to well-developed cleavage.

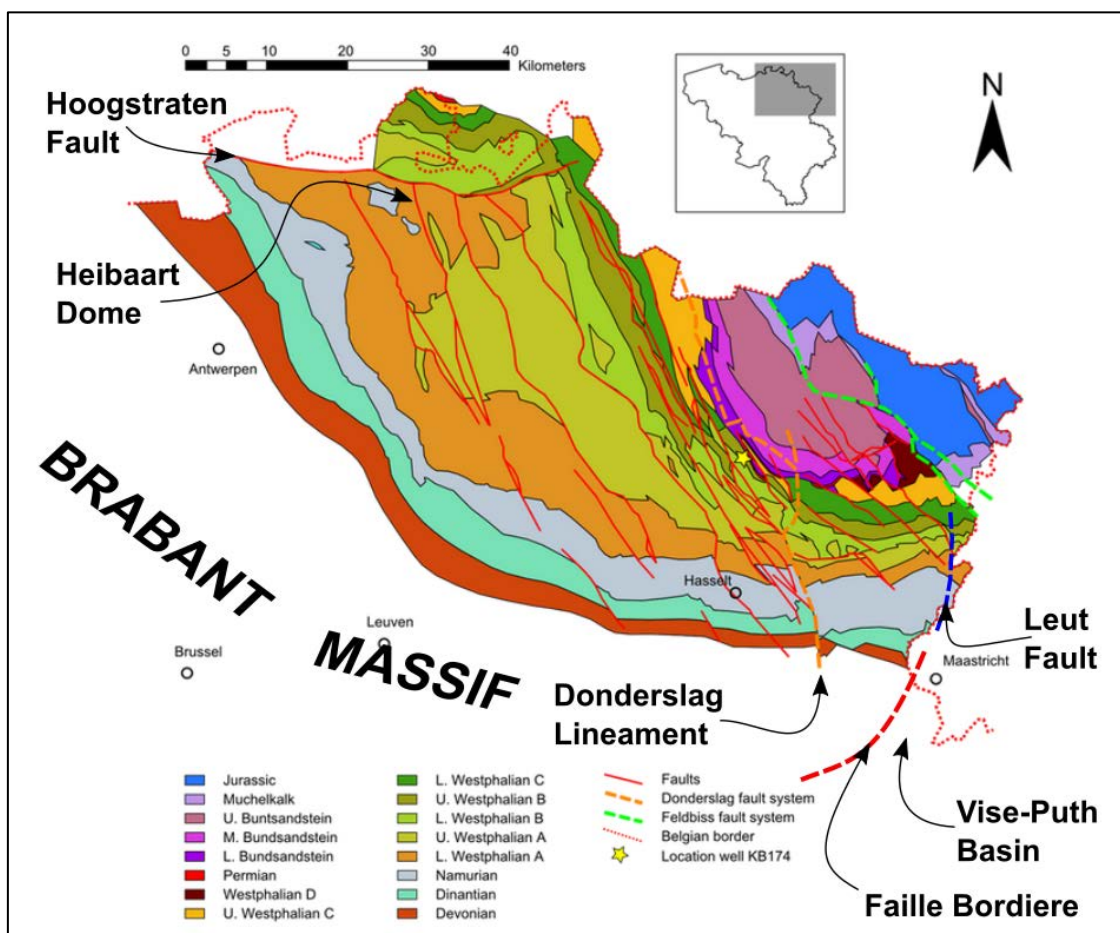


Figure 5: Simplified map of the Campine Basin, taken from Vandewijngaarde *et al.* (2016), with added positions of the E-W trending Hoogstraten Fault, the Heibaart dome, the N-S trending Donderslag Lineament, the N-S trending Leut Fault, the Vise-Puth Basin, and the Faille Bordiere, the latter separating the eastern part of the Brabant Massif from the Vise-Puth Basin.

The Brabantian Deformation event can be regarded as the build-up of a compressional wedge, due to progressive shortening of a pre-existing Cambrian basin, surrounded by cratonic basement blocks and overlain by a relatively thin sequence of Ordovician and early Silurian units (Sintubin & Everaerts, 2002). As the compressional wedge was building up, from the late Llandovery onwards the lithosphere started flexing down, causing the development of Silurian foreland basins along either side of the inverting Cambrian core (Sintubin & Everaerts, 2002; Verniers *et al.*, 2002; Debacker *et al.*, 2005). During the middle and late Silurian, deformation spread outwards, resulting in Ordovician units experiencing cleavage development whereas only few kilometres away middle to late Silurian turbidites were still being deposited (Debacker, 2001; Debacker *et al.*, 2005). As observed in the southern part of the Brabant Massif, southward propagating progressive deformation was influenced by pre-existing basin architecture. There, a series of deep (>1-2 km depth), low-density bodies, visible as negative Bouguer gravity anomalies, behaved as competent blocks during shortening (De Vos, 1997; Sintubin, 1999; Debacker 2001; Debacker *et al.*, 2005, 2012). Because of the modelled relative density and the occurrence of Late Ordovician – early Silurian magmatic rocks above these gravity anomalies, the low-density bodies usually have been interpreted as Late Ordovician batholiths (Everaerts *et al.*, 1996; cf. Sintubin & Everaerts, 2002). Similar, but more deeply buried, low-density bodies may be interpreted also along the NE-side of the Brabant Massif, below the Campine Basin (Debacker *et al.*, in prep.). The angular unconformity between deformed anchizonal to epizonal cleaved Silurian units, and overlying, relatively undeformed diagenetic Middle Devonian and younger deposits, implies the former presence of a Silurian to Early Devonian sedimentary load, of minimum four kilometres thick, that was eroded during the Early to Middle Devonian (see overview in Debacker *et al.*, 2005). Along the southern rim of the Brabant Massif paleovalleys contain locally very thick Givetian conglomerates, and normal WNW-ESE trending post-cleavage faults occur that were active during and after the Givetian (Legrand, 1967; Debacker *et al.*, 2004). Along the unexposed N-side of the Brabant Massif, the very large thickness (~400 m) of Givetian to Upper Devonian conglomerates in the Booischot well points to a similar scenario, with local depocenters bounded by ~NW-SE trending faults (Muechez & Langenaeker, 1993; Deckers *et al.*, 2019; Debacker *et al.* in prep). Hence, normal faulting took place during the Middle and Late Devonian, both along the N- and S-side of the Brabant Massif.

During the Late Devonian, carbonate growth around the Brabant Massif had to compete with detrital material shedding from the eroding massif(s) (Dusar *et al.*, 2015). During the Early Carboniferous (Dinantian) significant carbonates developed around the Brabant Massif: Viséan carbonate platforms grew along the edges of the massif, but lateral facies changes within the Campine Basin indicate that the Brabant Massif was still a high (Dusar *et al.*, 2015). The thick Viséan build-up at Heibaart (N Campine Basin, Figure 5) contrasts with the clay-rich late Viséan deeper facies to the north of the E-W trending Hoogstraten fault (Dusar *et al.*, 2015) and may suggest Viséan carbonate growth at the edge of a (fault-controlled) Viséan escarpment/basement high, along which the listric Hoogstraten fault (Figure 5) developed between Westphalian and Early Cretaceous during the Late Carboniferous (Deckers *et al.*, 2019).

At the end of the Viséan emersion took place, resulting in wide-spread karstification. This resulted in a secondary (fracture-controlled?) porosity, which mainly affected local highs (island karst model), such as the Heibaart dome now used for gas storage (N Campine basin; Dusar *et al.*, 2015; Figure 5).

From the late Tournaisian, the Visé-Puth Basin, situated at the eastern termination of the Brabant Massif, got separated from southern basins and became part of the Campine Basin as



a result of the uplift of the ~WSW-ENE trending Booze – Val Dieu Ridge (Poty and Delculée, 2011; Dusaar *et al.*, 2015; Poty, 2016). During the Viséan, the Visé-Puth Basin (Figure 5) was a deep basin, that got infilled by calcareous turbidites, sourced from the south (Dusaar *et al.*, 2015). Poty & Delculée (2011) refer to the Visé-Puth Basin as a graben, but the geometry and the continuation to the north are unknown. The western edge of the Visé-Puth Basin coincides with the Faille Bordière (Legrand, 1968; Figure 5), which continues to the NNE towards the Leut Fault (Deckers *et al.*, 2019; Figure 5). Even though Faille Bordière's activity is placed between Westphalian (Pennsylvanian) and Triassic (Legrand, 1968), and also the Leut Fault is regarded as a Late Carboniferous structure, the presence of the Visé-Puth Basin at the eastern termination of the Brabant Massif necessitates a western bounding fault, with a downthrow to the east. As such, earlier, Early Carboniferous activity of the Faille Bordière – Leut Fault system is likely (Debacker *et al.*, in prep.). At present, the top Dinantian in the Visé-Puth area is very shallow, with NNE-trending antiformal structures (Kimpe *et al.*, 1978), even though it represented one of the deepest parts of the broader Dinantian Campine Basin. This suggests post-Dinantian relative uplift with respect to the surrounding areas. Likely candidates are the Faille Bordière – Leut Fault system (Figure 5) and similar structures to the east (Debacker *et al.*, in prep.).

Even though the most significant pre-Cenozoic faulting in the Campine Basin is now attributed to Jurassic extension (Cimmerian; Deckers *et al.*, 2019), also Carboniferous and older fault activity took place. Most of the Campine Basin faults appear normal on seismic data and are NNW-SSE and NW-SE trending but also older NNE-SSW structures can be recognised in gravity data (Deckers *et al.*, 2019; Debacker *et al.*, in prep.). The Carboniferous (?) Faille Bordière – Leut Fault system and the Late Carboniferous Donderslag Lineament (Figure 5) belong to the latter group. As the top Dinantian forms the main density contrast within the Campine Basin, most of the faults affecting the top Dinantian can be recognised in high-resolution gravity data (Debacker *et al.*, in prep.).

Apatite fission track data from igneous rocks along the S-side of the Brabant Massif point to a rapid and steady cooling between 195-165 Ma (Van Den Haute & Vercoutere, 1989; cf. Barbarand *et al.*, 2018). This suggests the presence of an overburden on top of the Brabant Massif prior to the Middle Jurassic of at least 3 km, which was eroded during the Cimmerian phase. This overburden has been attributed to the late Carboniferous and confirms earlier suggestions made by (Patijn, 1963; Van Den Haute & Vercoutere, 1989; Barbarand *et al.*, 2018). It should be mentioned here that all samples are from igneous rocks situated along the broad Nieuwpoort-Asquempont Fault zone, which was active not only prior to and during the Givetian, but also at younger times (see Debacker, 2001, 2012; Debacker *et al.*, 2004).

During the Cretaceous, widespread karstification of the Dinantian carbonates took place, in particular in the Visé-Puth Basin, intensive Cretaceous weathering resulted in karstification, silicification and paleosol development (Dusaar *et al.*, 2015). In many if not most cases, however, it is difficult to tell at what time(s) weathering and dissolution of the Dinantian limestones occurred in the Campine Basin.

#### 4.3. The post-Devonian structural evolution in the Dutch onshore

Setting up the stage in a report format for the complex Carboniferous to Present day structural evolution of the Dutch onshore is a daunting task due to the vast amount of publications on the subject. To address this, we present the structural evolution of the Dutch onshore over the last 358 Ma in the format of a compilation table (Table 1) that summarises the state of the art regarding the structural evolution of the 19 structural elements (Figures 5 and 6), including their similarities and specificities regarding major tectonic and erosional phases affecting the Dutch subsurface since the beginning of the Carboniferous (Figure 8).

The term ‘structural element’ is assigned to regional structures with a uniform deformation history in terms of subsidence, faulting, uplift and erosion during a specific time interval (Kombrink *et al.*, 2012). This classification of structural elements in the Netherlands originated from Heybroek (1974), with subsequent work by NAM & RGD (1980) and Van Wijhe (1987). Revision of this map were made by van Adrichem Boogaert and Kouwe (1993) and then by Duin *et al.* (2006). Kombrink *et al.* (2012) presented the latest updated version of the structural element map of the Netherlands, which is used in the present study as the structural framework. It is important to note that most of those structural elements were formed during Late Jurassic and Early Cretaceous Late Kimmerian rifting (De Jager, 2007), often as a result of the reactivation of Paleozoic fault systems (Kombrink *et al.*, 2012). In this classification, 1) a high is defined as an area with significant non-deposition and erosion down to Carboniferous or Permian strata (Rotliegend and/or Zechstein). 2) A platform is characterised by the absence of Lower and Upper Jurassic strata due to Late Jurassic erosion down to the Triassic, and 3) the term graben is used for a fault-bounded basin and where, in general, Jurassic sediments are preserved.

Below is a short description of each of the nineteen structural elements present in the Dutch onshore (modified from Kombrink *et al.*, 2012, see Figures 6 to 8):

- 1) **London-Brabant Massif (LBM):** According to the definition of Legrand (1968) the London- Brabant Massif is the area where Upper Cretaceous or younger sediments overlie Cambro-Silurian rocks. In the Netherlands, only the southernmost part of the province of Zeeland and a small area in the southwest of Limburg are therefore part of the LBM (Figure 9). Further north, the Devonian and Carboniferous overlie the Cambro-Silurian folded succession, which is in this paper attributed to the Zeeland High.
- 2) **Zeeland High (ZH):** The Zeeland High represents the area where Upper Cretaceous sediments directly overlie Devonian and Carboniferous rocks (Figures 7 and 9). It forms a transitional area in between the London-Brabant Massif in the south, where Late Cretaceous sediments directly overlie Cambro-Silurian rocks, and the platform areas further north where Permian up to Late Cretaceous rocks are found (Oosterhout Platform, Roer Valley Graben and West Netherlands Basin). The Zeeland High is equivalent to the Limburg High further to the southeast.
- 3) **Limburg High (LH):** The Limburg High is the southeasternmost extension of the Zeeland High. In this area, Upper Cretaceous deposits directly overlie Carboniferous rocks. It is bounded in the north by the Oosterhout Platform, where Triassic rocks are found. In the south, east and west, the Limburg High gives way to the adjacent fault blocks in Germany and Belgium Campine Basin).
- 4) **Oosterhout Platform (OP):** The area south of the Roer Valley Graben forms a transitional area between the Roer Valley Graben in the north and the Zeeland High in the south. Here, Triassic rock can be found overlain by Upper Cretaceous. The southern boundary of the Oosterhout Platform is defined as the area where Triassic rocks pinch out.
- 5) **Roer Valley Graben (RVG):** The Roer Valley Graben is a distinct fault-bounded graben. Like the Dutch Central Graben and the West Netherlands Basin, the RVG existed as a structural feature in Paleozoic times, but the main differential subsidence clearly started In the Jurassic (Figures 7 and 10). Since the sediments of the Rijnland Groups (Early Cretaceous) are missing in the RVG, it is not clear which tectonic regime the RVG experienced in those times. Subsidence returned during the Oligocene times and continues to the present day. Apart from the northwest, where the RVG passes into the West Netherlands Basin (WNB), it is surrounded by platform

areas such as the Limburg High and the Oosterhout Platform to the south and the Peel-Maasbommel Complex (PMC) to the north. The boundary to the WNB has been taken at the pinch-out line of Upper Cretaceous sediments.

- 6) **West Netherlands Basin (WNB):** The West Netherlands Basin is a Jurassic Basin which was mildly to strongly inverted in Late Cretaceous and Paleogene times (Figures 7 and 9). The southern boundary to the Roer Valley Graben corresponds to the area where the Chalk has been completely eroded due to inversion. In the southwest, a clear fault zone marks the boundary to the London Brabant Massif or Oosterhout Platform. In the northeast, the boundary with the Broad Fourteens and Central Netherlands basins consists of a fault zone, known as the Zandvoort Ridge, which extends offshore to the IJmuiden Platform.
- 7) **IJmuiden Platform (IJP):** The IJmuiden Platform is part of the transition zone between the Central Netherlands, Broad Fourteens and West-Netherlands Basin, where several upthrown blocks can be found. The IJP is part of the Mid-Netherlands Fault Zone (van Adrichem Boogaert & Kouwe, 1993) which runs from the IJP towards the southern boundary of the Peel-Maasbommel Complex (Figure 6) and encompass the Zandvoort Ridge.
- 8) **Broad Fourteens Basin (BFB):** The Broad Fourteens Basin is a strongly inverted Jurassic basin that probably had a connection to the Central Graben in the main rifting period (Late Jurassic - Early Cretaceous times), although minor faulting occurred already in Permian and Triassic times (Hooper *et al.*, 1995; Verweij & Simmelink, 2002). Due to Late Cretaceous inversion, the Upper Cretaceous Chalk has been entirely removed in the greatest part of the basin (Figures 7 and 9). This applies to the Lower Cretaceous to a lesser extent. In the southwest, the transition into the West-Netherlands Basin runs across a fault system that also comprises the IJmuiden Platform. The boundary to the Central Netherlands Basin is gradual and has therefore been defined at the coast.
- 9) **Peel-Maasbommel Complex (PMC):** Due to the presence of numerous important faults in this area and the associated names of individual fault blocks, it was decided to lump these together in the new element Peel-Maasbommel Complex. In this way, the PMC represents the complex of NW-SE striking fault blocks that separate the Roer Valley Graben along its southwestern boundary and the Central Netherlands Basin in the northeast (Figures 7 and 10). Towards the southeast (Germany), the PMC passes into the Krefeld and Erkelenz Highs in Germany.
- 10) **Zandvoort Ridge (ZR, new):** The upthrown block forms the southwestern boundary of the Central Netherlands Basin and is linked toward the northwest to the IJmuiden Platform and to the to the Peel-Maasbommel Complex to the southeast (Figure 9).
- 11) **Central Netherlands Basin (CNB):** The Central Netherlands Basin does not entirely fit the classification scheme. In the area now indicated as CNB only some patches of Jurassic rocks are preserved (Figures 7 to 10). However, it is likely that Jurassic sediments had a wider distribution. These have been eroded by Late Jurassic erosion (evidenced by the presence of Upper Jurassic and Lower Cretaceous rocks in places (dark green in Figure 6) and strong Late Cretaceous inversion (Nelskamp, 2011). The outline of the CNB represents the area where the Upper Cretaceous is missing. In previous papers and maps, the southwestern boundary of the CNB has been formed by the Zandvoort Ridge (ZR). In the current map, the ZR is not defined because it does not stand out in stratigraphic sense. The former ZR is acknowledged in such a way that it forms the boundary zone of reverse faulting between the CNB and the WNB and is part of the Mid-Netherlands Fault Zone (Nelskamp, 2011). In the east, the CNB continues into Germany. To the east, the Gronau Fault Zone separates it from the

Lower Saxony Basin. To the west, the coast marks the transition into the Broad Fourteens Basin.

- 12) **Noord-Holland Platform (NHP):** The North Holland Platform is to be found just south of the Texel-IJsselmeer High, in the province of North Holland (Figures 7 and 9). It is characterised by a heavily faulted Triassic succession, overlain by Cretaceous rocks. Towards the south, the NHP is bounded by the inverted Central Netherlands Basin via a complex fault system.
- 13) **Texel-IJsselmeer High (TIJH):** The Texel-IJsselmeer High is a NW-SE striking tilted fault block of which the southern boundary is made up of a steep fault system while the northern margin gradually passes into the Friesland Platform. It has been a high since Carboniferous times (Rijkers & Geluk, 1996), but most of the erosion took place in Jurassic - Early Cretaceous times.
- 14) **Vlieland Basin (VB):** The Vlieland Basin has been a Late Jurassic and Early Cretaceous depocenter, which probably had a connection to the Terschelling Basin. The thickness of the Upper Jurassic - Lower Cretaceous succession is less than the other rift basins, which is explained by the buoyancy caused by the magmatic event related to the Zuidwal volcano (De Jager, 2007). Herngreen *et al.* (1991) suggest that the Vlieland Basin formed a pull-apart basin in between the Dutch Central Graben and the Lower Saxony Basin. Although there are many faults in the area (mainly NW-SW trend), the Vlieland Basin is not bounded by major faults similar to the other Late Jurassic basins.
- 15) **Friesland Platform (FP):** The Friesland Platform represents a large and geologically diverse area. The platform experienced Middle to Late Jurassic erosion (Mid and Late Kimmerian unconformity). In the north - eastern and southern part of the Friesland Platform, the Triassic can reach a thickness up to 800 m. In the northeast, the Friesland Platform is fault-bounded by the Lauwerszee Trough. Towards the southwest, the Texel-IJsselmeer High forms the boundary. In the northwest, the Friesland Platform passes into the Late Jurassic - Early Cretaceous Vlieland Basin and in the southeast towards the Lower Saxony Basin.
- 16) **Dalfsen High (DH):** The Dalfsen High is a relatively small isolated high on the Friesland Platform that is characterised by Cretaceous sediments on top Carboniferous rocks. In the area surrounding the DH, the Triassic has been eroded (Figures 7 and 9), which points to a Jurassic or more recent phase of uplift.
- 17) **Lower Saxony Basin (LSB):** The LSB is a strongly inverted Jurassic basin. Since its depocenter was situated in NW Germany, the Dutch part of the basin forms a marginal area only. The Friesland and Groningen Platform border the LSB to the northwest. The Gronau Fault Zone separates the LSB from the Central Netherlands Basin in the southwest. The LSB was not strongly inverted during the Late Cretaceous.
- 18) **Lauwerszee Trough (LT):** The Lauwerszee Trough already formed a basin in Early Carboniferous times when carbonate deposition occurred on both the Friesland and Groningen Platforms while the LT was probably a site of (distal) turbiditic and fine-grained sedimentation (Kombrink *et al.*, 2010). It is bounded by two major fault systems in the west and east. The Mesozoic and Cenozoic successions of the LT do not differ markedly in thickness from the adjacent Friesland and Groningen Platforms; i.e. the bounding faults have not been extensively reactivated. However, the normal fault movement that took place created sealing faults, which caused the Rotliegend to be gas-bearing with an independent GWC with respect to the Groningen Platform (De Jager & Geluk, 2007).
- 19) **Groningen Platform (GP):** Although the former Groningen High is a well-known element because of the presence of the Groningen gas field, it should classify as a

platform according to the scheme used here (absence of Jurassic rocks, presence of Triassic and Lower Cretaceous rocks). The Lauwerszee Trough in the west is a marked element and the bounding faults played an important role throughout geological history. The outlines of the Groningen Platform are comparable with the outlines of the Groningen High as published before (Van Adrichem Boogaert & Kouwe, 1993). In the west, it is bounded by the Hantum Fault Zone that marks the transition into the Lauwerszee Trough. In the south, the GP borders the Lower Saxony Basin. To the north and east, the depth of the base of the Zechstein most clearly delineates the boundary of the GP.

A literature review of the structural evolution of each of these 19 structural elements is summarized in a compilation chart (Appendix 2).

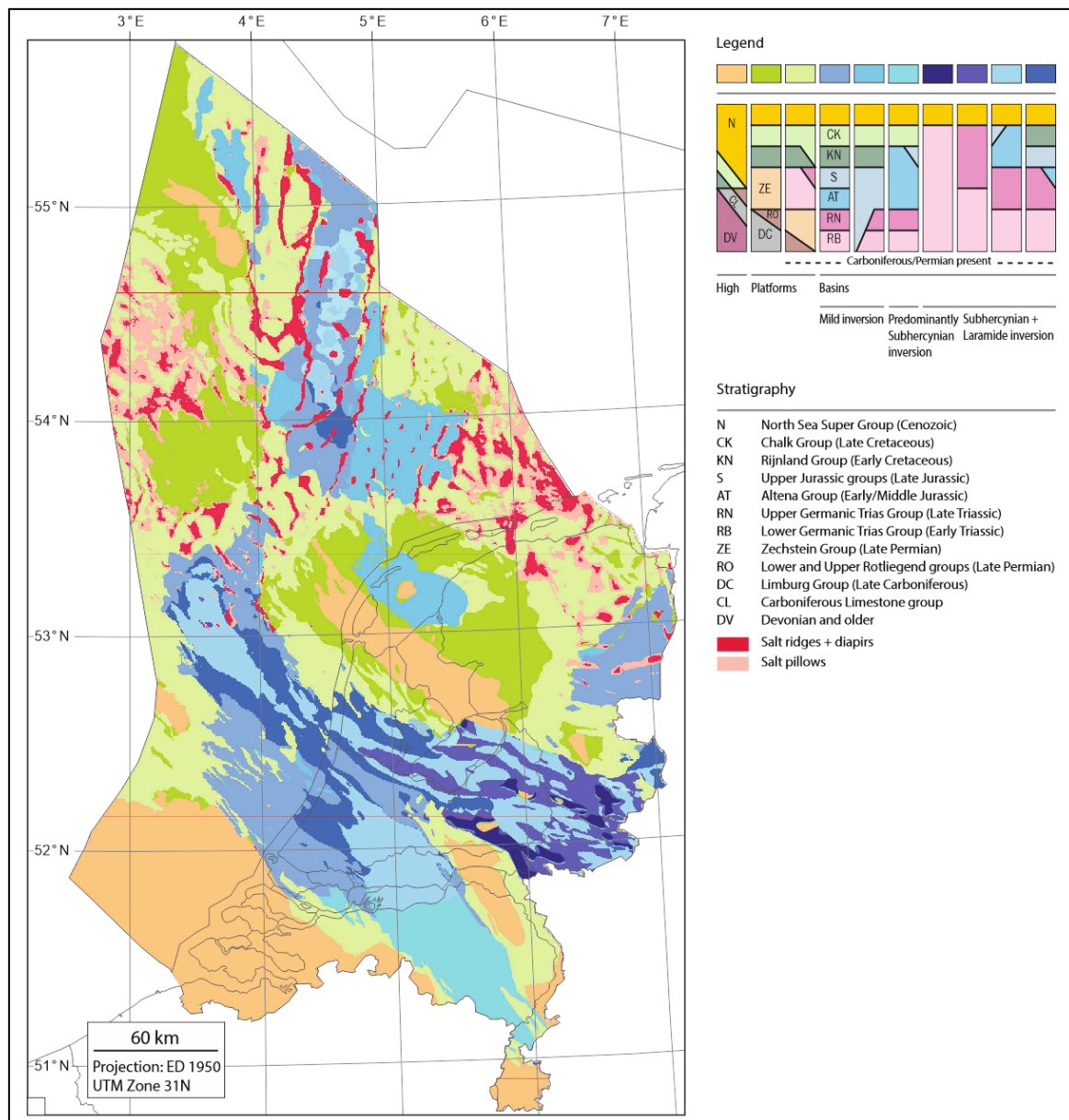


Figure 6: Geological map based on the stratpiller analysis, showing the degree of inversion that took place in Late Cretaceous - Paleogene times and the presence of salt pillows and diapirs (from Kombrink *et al.*, 2012).



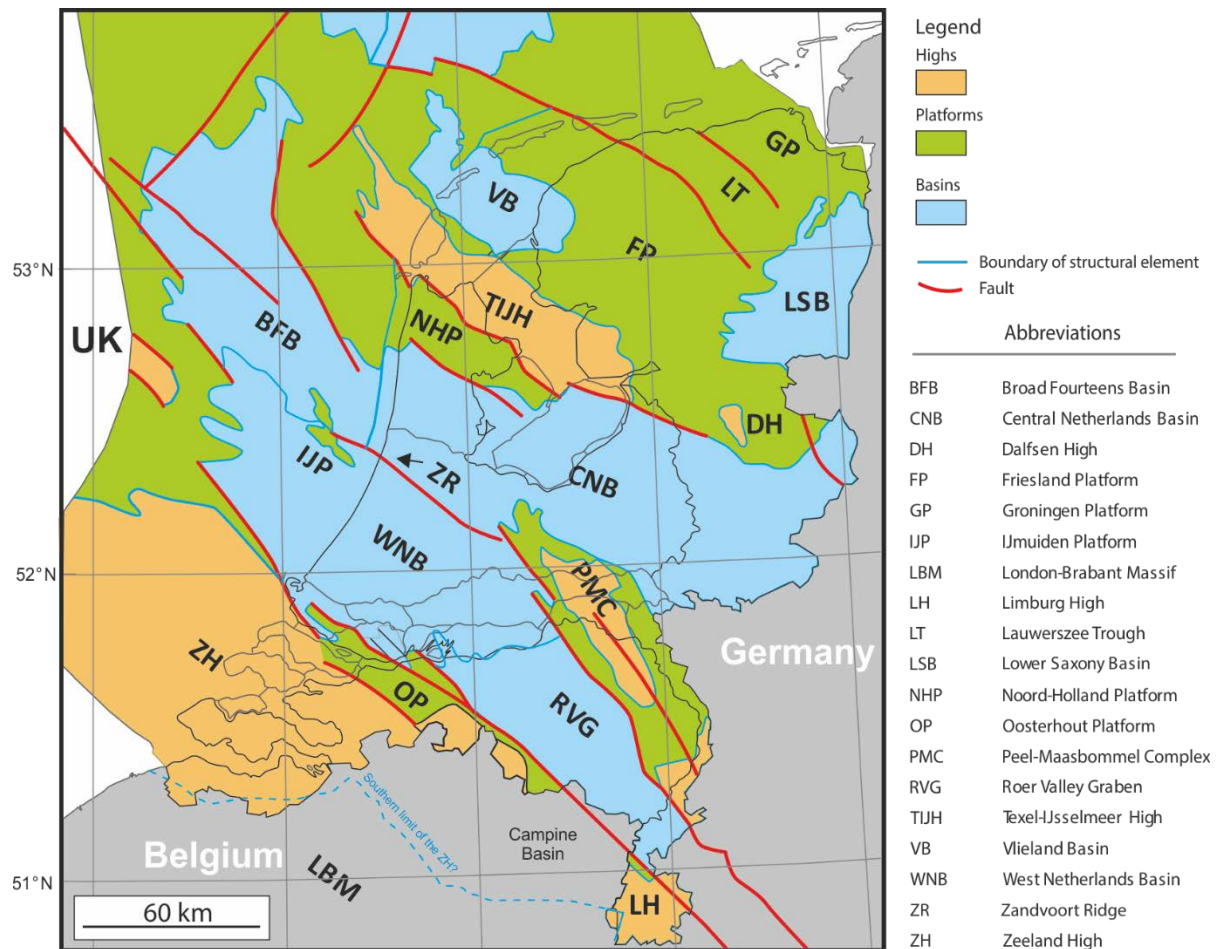


Figure 7: Late Jurassic - Early Cretaceous structural elements of the Netherlands. Faults that terminate at the border may well continue but have not been mapped within the project (from Kombrink *et al.*, 2012).

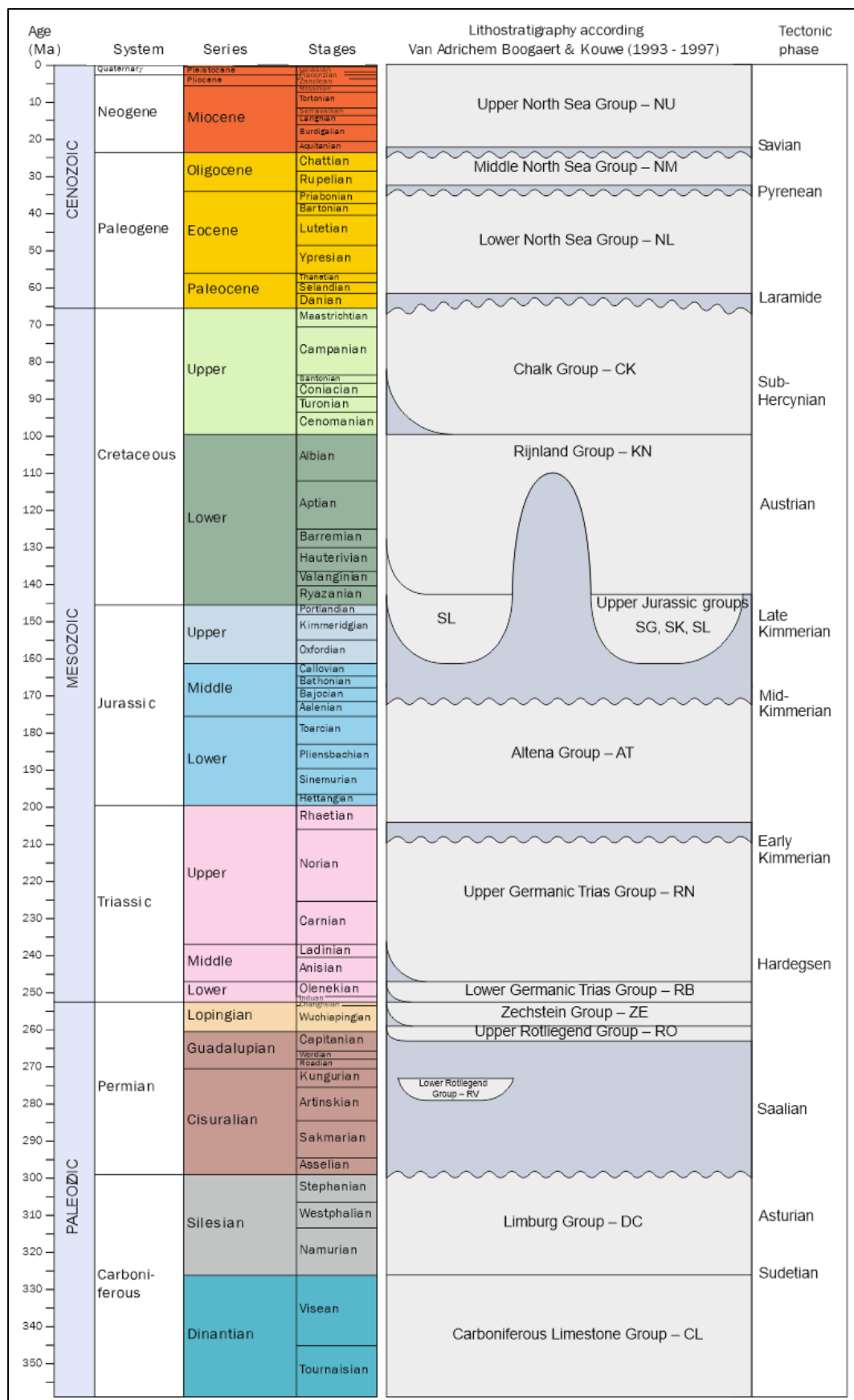


Figure 8: Simplified stratigraphic diagram of the Netherlands showing the age and names of the main intervals of which the base has been mapped in the available seismic data. From Kombrink *et al.* (2012)

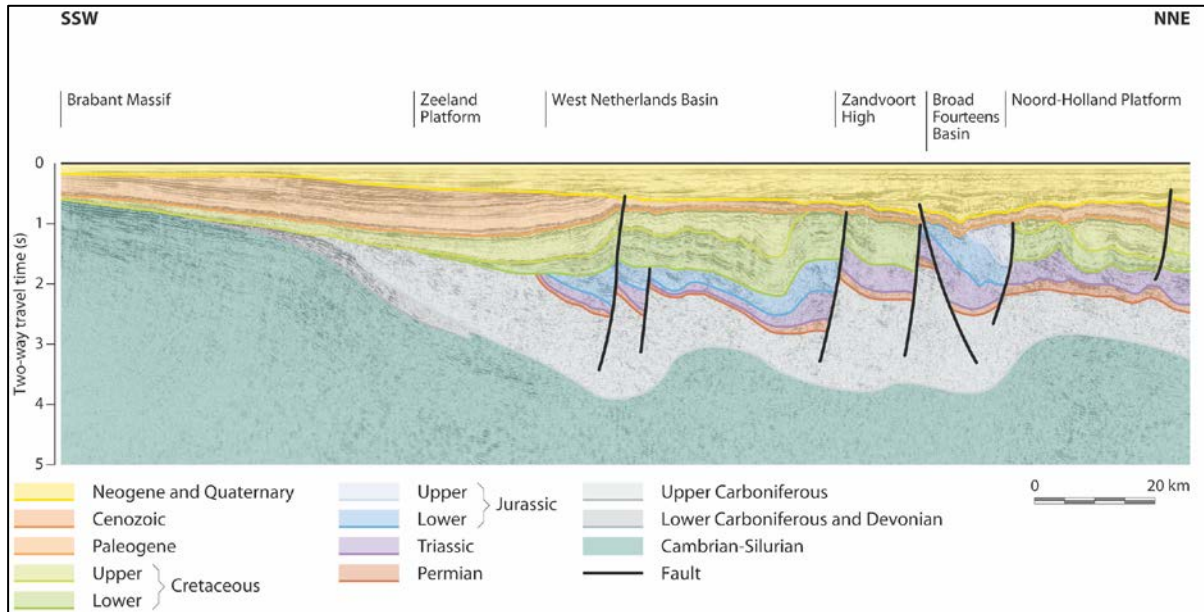


Figure 9: Deep seismic section showing an overview of the main structural domains (referred as structural elements in this report) and main unconformities of the Dutch onshore: the Brabant Massif, the Zeeland Platform/High (with a northward-thickening Carboniferous succession), the inverted West Netherlands and Broad Fourteens basins and the bordering Zandvoort High and Noord-Holland Platform. The section illustrates the relatively shallow position of Carboniferous and pre-Carboniferous rocks in the southern Netherlands and their deep burial below the Mesozoic basins. In the south-westernmost part of the section, only a thin Chalk Group and Cenozoic succession rests unconformably on Caledonian deformed Cambro-Silurian deposits (as encountered in the Belgian wells Knokke, Knokke-Heist and Eeklo (Legrand, 1968; De Vos *et al.*, 1993)). Northwards, a rapidly expanding wedge of Devonian and Carboniferous deposits marking the Variscan Foreland Basin infill north of the Variscan Mountains, are situated below the Chalk Group and Cenozoic on the Zeeland Platform/High. Thick Carboniferous deposits, often in excess of 5000 m, are present below the West Netherlands and Broad Fourteens basins. Permian to Middle Jurassic deposits were deposited in almost the entire area. From Pharaoh *et al.*, 2010. See Figure 10 for location of the seismic profile.

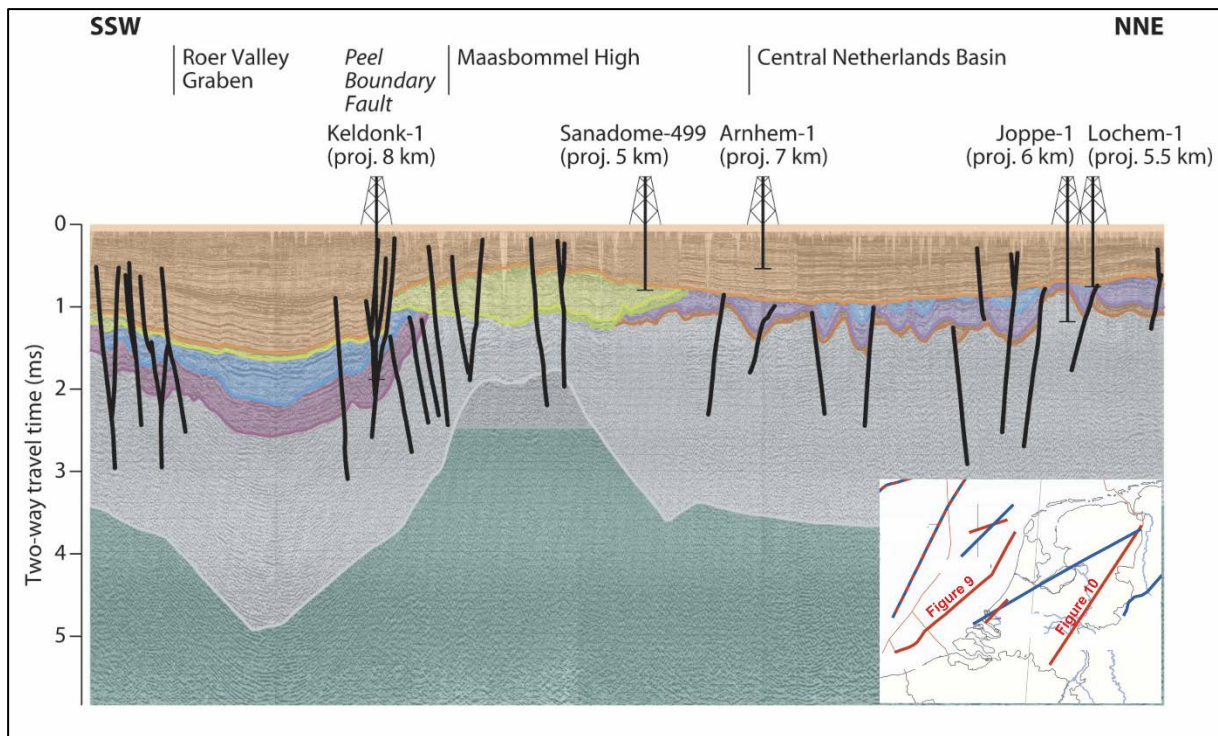


Figure 10: This NNE-SSW-oriented deep seismic section displaying the tectonic structure of the central and southern Netherlands onshore. It shows two Late Paleozoic-Mesozoic basins, the Roer Valley Graben and the Central Netherlands Basin, characterised by a thick succession of Permian to Jurassic sediments and a general absence of Cretaceous sediments due to Late Cretaceous inversion tectonics. Four main tectonic events are responsible for the current structure: Early Permian uplift and wrenching, Late Jurassic – Early Cretaceous extension, Late Cretaceous compression and Neogene rifting. Pronounced Early Permian uplift of the Maasbommel High/Complex resulted in erosion of the Namurian-Westphalian succession, as shown by well data and an angular unconformity at the base of the Permian in the NW of the Roer Valley Graben (NITG, 2001). Strong uplift of the Maasbommel High/Complex took place during the Late Jurassic – Early Cretaceous, removing most of the Permian to Middle Jurassic sediments. Differential subsidence of the basins continued until Santonian times, after which compressional tectonics resulted in the inversion of the Roer Valley Graben and Central Netherlands Basin. At the same time, the Maasbommel High started to subside rapidly and erosional products from the inverted basins were deposited on the high (Gras & Geluk, 1999). The Roer Valley Graben, the NW branch of the Rhine Graben rift system underwent strong Late Oligocene and Neogene subsidence (Geluk *et al.*, 1994). The Peel Boundary Fault Zone separates the Roer Valley Graben from the Peel Horst. The Roer Valley Graben and Central Netherlands Basin display quite different structures. The Roer Valley Graben is essentially a relatively simple faulted synclinal structure with mainly normal faults, and only some indications of small reversal movements. The Carboniferous depocenter underlying the Mesozoic/Cenozoic basin is slightly offset, with its axis on the SW flank of the Cenozoic graben. Lower Jurassic sediments are preserved locally in lows. Relatively thin Zechstein salt has created minor salt pillows and local detachment zones. The Permian shows local thickness variations across faults, probably reflecting mainly early salt flow in salt-filled half-grabens. Reverse faults and low-angle thrusts have resulted in much more shortening than in the Roer Valley Graben. From Pharaoh *et al.* 2010. See insert map for location of the seismic profile.



## 5. Database

Several types of data and results from other studies (including other SCAN Dinantian Projects) were used in this project for the 2D restoration and the 1D modeling. This includes well, seismic, core, vitrinite reflectance data as well as seismic horizons from the Dutch geological survey (GDN) and from recent mapping within the SCAN Dinantien Program (Ten Veen *et al.*, 2019). Below is the list of the data used in this project.

### 5.1. Seismic Data

The seismic database used in the project includes the database used for the Seismic Interpretation carried out in the SCAN Dinantien WP 2.1.1 (Ten Veen *et al.*, 2019). See Ten Veen *et al.* (2019) for a complete list and description of the seismic database, including data coverage, penetration depth, seismic reflection quality and seismic resolution (Appendix 1). A Master Petrel Project was compiled by Ten Veen *et al.* (2019) and was used in this project to identify and select the best seismic transects for the 2D structural restorations. This master Petrel Project (referred as UDG\_Masterproject\_RD) includes all the 3D seismic data available, most of the pre-existing interpretation and grids from TNO/NLOG, all public domain wells with composite logs and cultural data (Figure 11). The Petrel project contains the DGM V4.0 grids from 2014, with TVT-time, TVD, TWT and thickness grids. Besides the DGM grids the project has nationwide interpretations for the top of the Dinantian. The base of the Dinantian was previously only interpreted in the southern part of the Netherlands (Reijmer *et al.*, 2017).

Seismic horizons (time and depth grids) from the Dutch Geological Survey and from Ten Veen *et al.* (2019) were used as an interpretation framework for the two structural restorations. Key horizons for the overburden (until Base Rotliegend) were provided by TNO (NLOG/GDN, DGM 5) as well as new depth grids for several Pre-Permian horizons, including the Base Devonian, Base Dinantian (Top Devonian), Top Dinantian, Intra Namurian (transparent basin) fill, Intra-Namurian, Base Westphalian, Base Permian unconformity, Base Salt, Top Salt (from Ten Veen *et al.*, 2019). Some new fault interpretation from Ten Veen *et al.* (2019) for the Devonian/Dinantian interval were added to the structural restorations, especially in the southern part of the Dutch onshore where there were more systematically identified.

Fault maps from publications and from NLOG were used in the Move models. Some new fault interpretation from Ten Veen *et al.* (2019) for the Devonian/Dinantian interval were added to the structural restorations, especially in the southern part of the Dutch onshore where they were identified.

Depth converted seismic data was provided by TNO for the restoration panels (Ten Veen *et al.*, 2019) (see Appendix 1 with depth seismic panels).

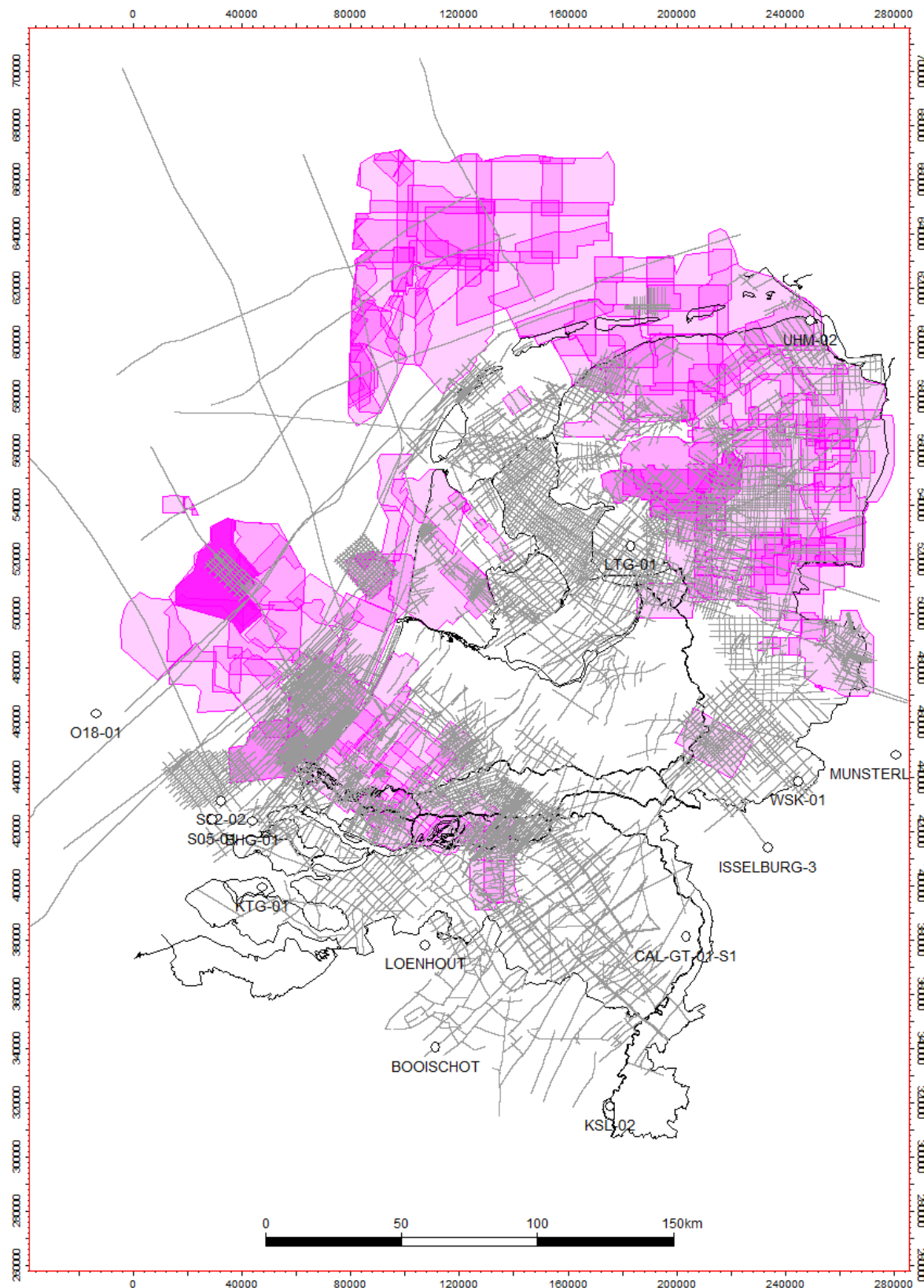


Figure 11: Overview of all the available and consulted 2D (grey lines) and 3D (pink polygons) seismic data (from Ten Veen *et al.*, 2019).

## 5.2. Non-Seismic Data

Ten Veen *et al.* (2019) used publicly available Dutch gravity and magnetic datasets as well as German and Belgian data. Selected gravity and magnetic data and maps produced by Ten Veen *et al.* (2019), as well as extracted fault interpretation and magmatic intrusion maps (including geochronological information), were used in this project to better constrain the deep onshore Dutch subsurface. The information and discussion with geoscientists active in those projects provided additional constraints for the seismic interpretation done in the present project.

## 5.3. Well data

Wells data including location, trajectory and well top were provided by TNO/NLOG. A list of wells used for each restoration as well as for the 1D modelling (Table 1).

Table 1: List of wells used in this study

Well name	Section	Structural element	Target	Used for
S02-02	Western	ZH	OBGZ	Restoration and 1D modelling
BHG-01	Western	ZH	OBGZ	Restoration and 1D modelling
WDR-01	Central	ZH	CLZL	Restoration and 1D modelling
NAG-01	Central	TIJH	DCGE	Restoration and 1D modelling
EMO-01	Central	TIJH	DCGE	Restoration and 1D modelling
SWD-01	Central	FP	DCGE	Restoration and 1D modelling
UHM-02	Central	GP	OB	Restoration and 1D modelling
LTG-01	Central	TIJH	OB	Restoration
RSB-01	Central	OP	DCGE	Restoration
EGZ-01	Western	CNB	DCCR	Restoration
LWS-01	Western	FP	ZEZ3	1D modelling
BAC-01		CNB	DC	1D modelling
HVS-01		OP	DCCR	1D modelling
AST-01 EXT		RVG	RBSHN	1D modelling
TJM-02-S2		GP	DCGE	Reference
ESG-01		FP	DCCB	Reference
MGT-01	Western	LT	DCCB	Reference
DWL-01		DH	DCCB	Reference
OZN-01		CNB	DCCB	Reference
SPL-01		WNB	DCCB	Reference
WOB-01-S1		WNB	DCCB	Reference
BRG-01	Western	TIJH	DCCR	Reference
BLA-01-S1	Central	CNB	DCCU	Reference
DRO-01	Central	CNB	DCCR	Reference
BFD-14		PMC	DCGE	Reference
CAL-GT-01		PMC	CLZL	Reference
APN-01		CNB	DCCU	Reference
WSK-01		CNB	OB	Reference
S05-01	Western	ZH	OBGC	Reference
KTG-01		ZH	OS	Reference
KRD-01	Central	CNB	DCCR	Reference

## 5.4. Other relevant data and information

Other type of information and data was use in this project:

1. Depth information for several ultra-deep horizons: Moho, Base upper crust from Yudistira *et al.* (2017).

2. Decompaction parameters (initial porosity, c-factor, change of porosity with depth) from TNO from previous studies.
3. Regional tectonic history, structural events information from previous publications and compiled for this project (Appendix 2).
4. Petrographic information as provided by TNO/NLOG as well as from other SCAN Dinantien Projects.
5. Facies and paleo-water depth information as provided by other SCAN Dinantien Projects.
6. Vitrinite reflectance data as compiled from literature and TNO database. Some additional VR data were provided by EBN.



## 6. Methodologies and workflows applied in the project

The methodology specific to the two analytical studies is described below, specifically, the 2D structural restoration and the 1D burial/maturity modelling, are described below.

### 6.1. 2D Structural restoration methodology

Structural restoration was undertaken using software Move by Midland Valley/Petex. This first study has focussed on two 2D sections only, rather than a full 3D restoration study, to identify and test key parameters, and investigate initial outcomes.

The restoration was done in 2D, but in 3D context. Existing horizon and fault interpretation 3D grids – after depth conversion - were integrated in Move 3D modelling space and tested for internal consistency. In total sixteen horizons were included. Some came from the recent 3D seismic interpretation study (work package 2.1.1), and some from the published 3D horizons from the Dutch Geological Survey (especially for the younger, overburden intervals).

The 2D sections in Move were constructed by slicing through the above 3D grids. The sections contain line-work (top and/or base of stratigraphic units, and faults), as well as seismic panels (bitmap format) and vertical polygons that govern the stratigraphic units and that are required to carry the seismic image in the restoration. Horizon and fault interpretation was fine-tuned and expanded. First-order and, smaller, second-order faults were identified, and (re-)interpreted aiming at internal consistency with local horizon shapes. Growth faults were identified and marked, as well as faults with a significant strike-slip component (as identified on the 3D grids). Offsets along larger first-order faults was restored but offset on smaller second-order faults was not. The latter were drawn to indicate deformation style and dominant shear angles.

Uncertainty in the present-day geometry of the Dinantian is due to the uneven quality of the seismic data available, and by the lack information from well-penetration. Testing the present-day geometry of the Dutch subsurface on the 2D sections would – in normal structural analysis procedure – be done using line-length balancing techniques. These techniques are based on the principle that there is no loss or gain of material in the section during deformation (apart from geological reasons, such as erosion, intrusion, or out of plane movement due to a strike-slip component of deformation). Unfortunately, the significant component of strike-slip deformation in the Netherlands during inversion limit the usefulness of these techniques and they were not applied at this stage.

Structural restoration parameters were identified and gathered. They include rock type, decompaction parameters (initial porosity and change of porosity with depth), stratal age, amount of erosion and the geometry of the structures that were eroded (in particular the Cretaceous, the Jurassic and the Base Permian erosional phases), and estimated fault timing (based on tectonic context, observed growth stratigraphy and stratal terminations). The range of parameter values were identified, and the optimum - and alternative - restoration scenario discussed.

Sixteen steps of sequential restoration were required to capture the essence of the structural and burial/uplift history of the study area. This first-pass effort is designed to form the basis

for future iterations to be undertaken as and when additional data come in, and forms a context that allows fine-tuning of particular areas of interest.

The sequence of restoration steps was defined in tectonic context following a series of initial workshops with the entire project team as well as external experts discussing the complex geological evolution of the Dutch sector as well as surrounding areas such as the London-Brabant Massif and the North Sea, especially in regards of the Devonian and Carboniferous intervals. Key geological moments and a preferred number of restoration steps were identified and discussed prior to the restoration. A thorough literature review was also undertaken to gather as much information on the geological evolution of the structural elements crossed by the two sections restored. Discussions with seismic interpreters active in the SCAN Dinantien WP 2.1 were also critical to understand the assumption and the results of the seismic mapping of the Dinantian and Devonian. The results from the WP 2.2 (Non-seismic Methods) helped to get a better grip on magnetic basement and to better constraints the basement depth and composition.

Below we describe the methodology process followed in this study, from 1) the selection of the sections to be restored, 2) the data selection and loading, 3) the interpretation and fine-tuning of horizons and faults, 4) selecting settings for key modelling variables, including the decompaction parameters, and 5) sequential restoration of the two selected sections, which is the most important step and the most time consuming.

#### 6.1.1. Section selection

The selection of the section positions and trends was based on several factors:

The known structural grain of the study area is a primary factor since sections represent structures most realistically when they are at right-angle. Also, restoring structures in 2D is optimum when the tectonic transport is parallel to the section, and no rocks move in or out of the section plane. To avoid as much as possible those geometrical challenges, the sections were selected perpendicular to major bounding structures (e.g. basin bounding fault zones, major thrusts and fold axis). Therefore, the sections that were selected for this study are both oriented SSW-NNE to be as perpendicular to major basin and high axis that are mainly NNW-SSE (e.g. LBM, WNB, CNB, LT).

The consortia locations were also taken into account: selected sections were located as close as possible to possible future geothermal exploration site (see green dashed circles and ovals in Figure 12).

The position of key wells was also a factor in the selection of the two sections, especially wells that penetrate the Dinantian, Namurian and Westphalian. Figure 12 shows the wells that penetrate the Dinantian in the Dutch onshore and shows that four out of six consortia sites are on or close to the two sections selected.

The selection of the two sections was highly based on the availability of seismic data and on their depth of imaging and quality/resolution.

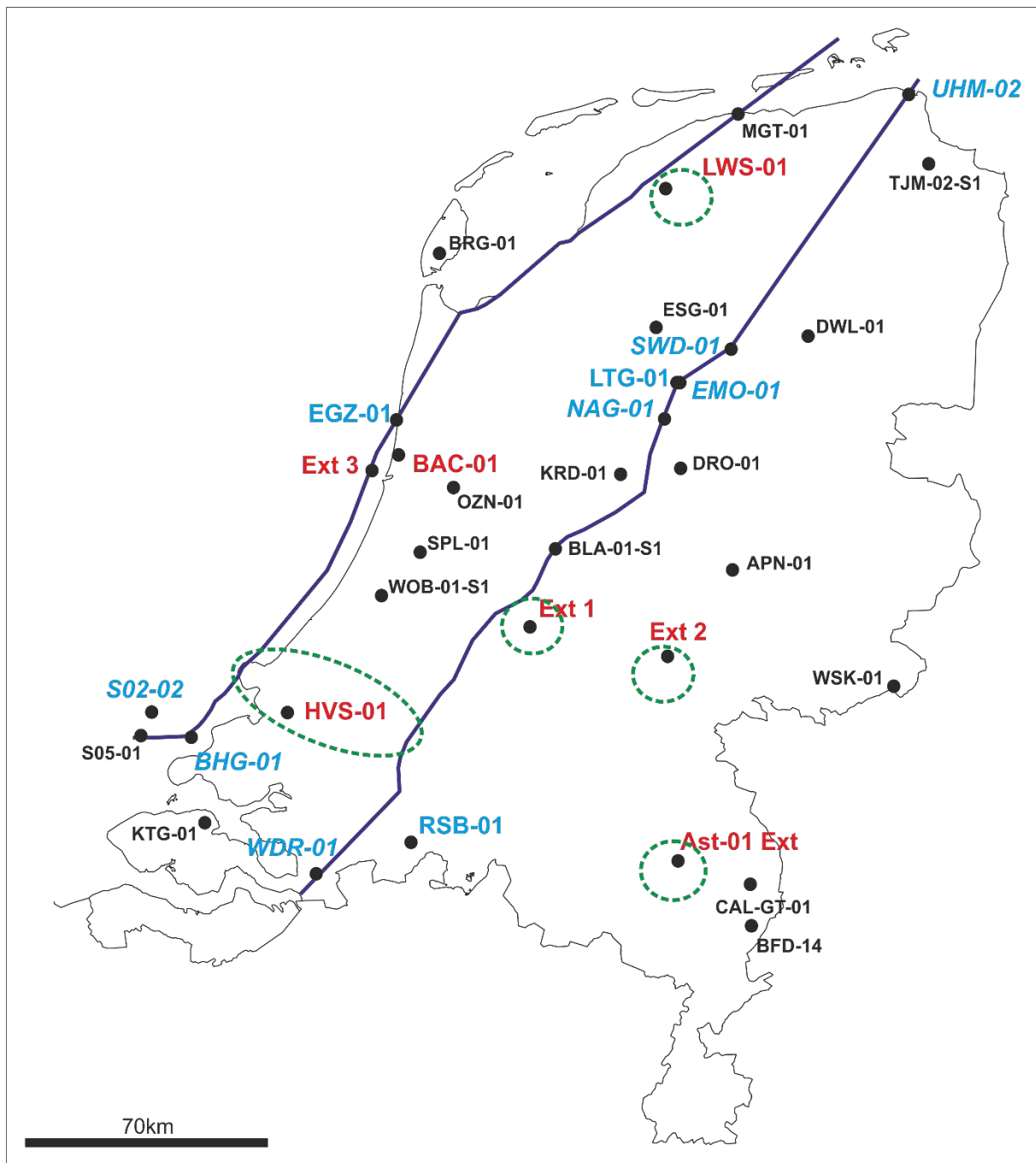


Figure 12: Map of the Dutch onshore showing the position of the two restored sections (Western and Central Sections show as dark blue lines), the Consortia sites (dark green dashed ovals and circles), and the key wells used for the 2D restoration (light blue text), for 1D maturity modelling (red and italicic blue texts). Other wells used to gather additional information for the study are shown in black text.

### 6.1.2. Data selection, loading and Move project set up

The number of useful seismic lines for this project was limited, especially in the southern part of the Dutch onshore where only 2D seismic surveys, often of limited vertical extent, are available. We evaluated all possible seismic data to be used for each section and created two composite lines in Petrel from the individual 2D and 3D seismic lines selected (Table 2).

Table 2: List the seismic lines used to construct the composite seismic lines that were used for the two restorations. The list of additional seismic lines listed refers to seismic lines that were used for the updated fine-tuning of the seismic interpretation carried out for each composite seismic transect.

Seismic line used				Additional seismic lines			
Section	Survey	Line	Max depth	Section	Survey	Line	Max depth
West	Offshore NAM 85H	85H499_2_mig160001		West	Offshore NAM 85H	85H499_2_mig160001	4000ms
West	Offshore NAM AO	AO1W_mig160001	4000ms	West	Offshore NAM UNSNS	UNSNS7533_mig160001	
West	Offshore NAM NSW	NSW-1_mig160001		Central	NAM1988B	19950102-1-62_0006.sgy	
West	3D extract	West line WNB	4000ms	Central	Onshore NAM 84	843005_mig160001	
West	Offshore NAM NSW	NSW-1A_mig160001		Central	Onshore NAM 84	843026_mig160001	
West	3D extract	West line Nholland	6000ms	Central	NAM 82	826041_mig160001	
West	L2DGP1988B	8704CD	6000ms	Central	Onshore NAM 84	843010R_mig160001	
West	L2DGP1988B	8704AB		Central	L2NAM1987	872206_mig160001	
West	3D extract	West line Groningen		Central	NAM1988B	19950102-1-62_0005.sgy	
Central	Onshore NAM 84	846012_mig160001		Central	NAM 82	826042_mig160001	
Central	NAM82	821005R_mig000001		Central	Onshore NAM 84	843013_mig160001	
Central	NAM82	823416R_mig160001		Central	NAM 82	826043_mig160001	
Central	Onshore NAM 84	843009_mig160001	4000ms	Central	NAM73	731139_mig160001	
Central	NAM 1980C	803012_h.segy		Central	NAM 82	826040_mig160001	
Central	NAM1980C	803007_h.segy	4000ms	Central	Onshore NAM 84	846003_mig160001	
Central	L2NAM1987	872204_mig160001	4000ms	Central	Onshore NAM 84	846014_mig160001	
Central	3D extract	Central line Groningen		Central	Onshore NAM 84	846012_mig160001	

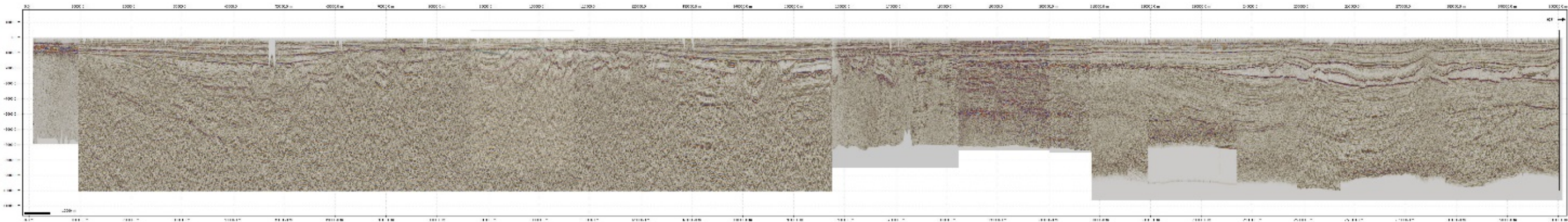


Figure 13: Composite seismic line used for the Central Section. This composite line showing the variable depth of penetration of each contributing seismic line used to construct this composite, as well as . It also shows the variable seismic resolution and quality of the variable surveys used. See Appendix 1 for high resolution versions of both composite seismic transects for restoration used for the two structural restorations



The composite lines were depth converted using the latest knowledge of the velocity fields in the Dutch onshore (see SCAN Dinantian 2.3.1 report, ten Veen *et al.*, 2019). Adjustments were made in locations where the depth conversion created artefacts, especially around large faults. The composite lines were then imported to Move 3D space along with key georeferenced maps used for this study, such as structural element maps, paleo structure maps, paleogeographic maps and subcrop maps.

The setting up the Move project was then carried out in the depth domain.

a) Coordinate system

The coordinate system selected in Move was the ‘Amersfoort’ (EPSG = 4289) option plus Manual projection parameters as specified in Petrel (see Table 3 and Figure 14). The coordinate system was saved as a “.prj” file format for future use.

Table 3: Coordinate system used in the Move project.

Petrel: Amersfoort * EPSG-Nld / RD New [28992,1672] (Petrel Code 502617)	
PROJCS	RD_New
	28992
AUTHORITY	EPSG
PROJECTION	Double_Stereographic
False_Easting	155000
False_Northing	463000
Central_Meridian	5.387638889
Scale_Factor	0.9999079
Latitude_Of_Origin	52.15616056
UNIT	Meter 1.0
GEOGCS	GCS_Amersfoort
UNIT	Degree 0.0174532925199433
PRIMEM	Greenwich 0.0
DATUM	D_Amersfoort
SPHEROID	Bessel_1841,
	6377397.155
	299.1528128

Figure 14: Coordinate system used in the Move project.

## Data loading in Move

A total of 19 wells (Figure 15 and Table 4), and 17 stratigraphic horizon grids were imported in the Move project. Below is a description of the selected stratigraphic units.

ASCII Drill Hole Import Options

Column Separators: ☐ Tab ☐ Space ☐ Treat multiple as one ☒ Comma ☐ Semicolon

Units: XY: Metres Z: Metres Depth

Start Import at: Worksheet: Sheet1 Line 1

Vertical drill hole defined as: ☒ Zero degrees ☐ -90 degrees ☐ +90 degrees

☒ Null values in file: Value: 1.0E37 Drill Hole Curve Calculation Method: Tangential

Column Specification and Preview

Well Name	MD	Deviation	Direction			
short_nm	Diepte	Deviatie	Azimuth	Verticale diepte	X Offset	Y Offset
BHG-01	50.0	0.37	40.2	50.00	0.10	0.13
BHG-01	75.0	0.25	50.9	75.00	0.19	0.23
BHG-01	100.0	0.15	49.0	100.00	0.26	0.28
BHG-01	125.0	0.15	48.2	125.00	0.30	0.33
BHG-01	150.0	0.27	10.6	150.00	0.34	0.41
BHC-01	175.0	0.27	250.7	175.00	0.27	0.44

Help ☒ Show import summary Cancel Previous Load

Figure 15: The Drill hole import functionality from Move

Table 4: List of key wells imported to the Move project.

Drill Holes (19)	
<input checked="" type="checkbox"/>	BFD-14 [38]
<input checked="" type="checkbox"/>	BHG-01 [39]
<input checked="" type="checkbox"/>	CAL-GT-01 [43]
<input checked="" type="checkbox"/>	CAL-GT-01-S1 [44]
<input checked="" type="checkbox"/>	CAL-GT-02 [45]
<input checked="" type="checkbox"/>	CAL-GT-03 [46]
<input checked="" type="checkbox"/>	EMO-01 [86]
<input checked="" type="checkbox"/>	KTG-01 [96]
<input checked="" type="checkbox"/>	LTG-01 [98]
<input checked="" type="checkbox"/>	NAG-01 [103]
<input checked="" type="checkbox"/>	RSB-01 [111]
<input checked="" type="checkbox"/>	S02-02 [113]
<input checked="" type="checkbox"/>	S05-01 [114]
<input checked="" type="checkbox"/>	SWD-01 [120]
<input checked="" type="checkbox"/>	TJM-02 [124]
<input checked="" type="checkbox"/>	TJM-02-S1 [125]
<input checked="" type="checkbox"/>	UHM-02 [128]
<input checked="" type="checkbox"/>	WDR-01 [130]
<input checked="" type="checkbox"/>	WSK-01 [133]

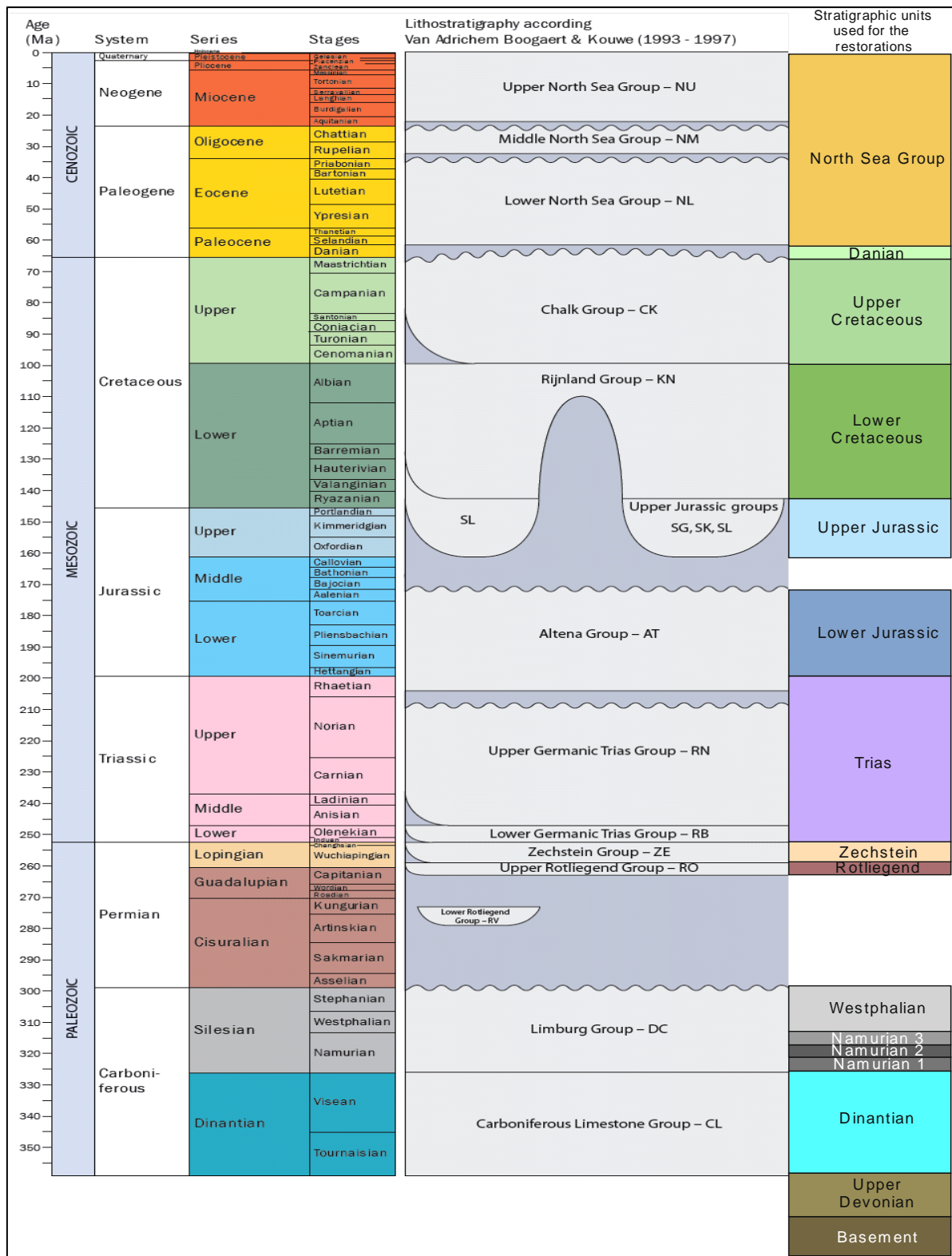
b) Stratigraphic unit selection.

For an optimum and meaningful restoration, the stratigraphic record needs to be subdivided into meaningful units that recorded key events of the structural evolution of the study area. The selection of key intervals was based on the review of the structural evolution of the study area (Chapter 3). A total of sixteen units were selected (Figure 16). Below is a description of the units used in this study:

- 1) **Basement:** For the structural restoration, the “basement” unit refers to the stratigraphic interval older than late Devonian, that are separated from Devonian extensional units by a regional intra-Devonian (to even Silurian in Ardennes) unconformity. The top of the unit is often seen as an intra-Devonian erosional surface (See Chapter 3). The base of this unit is unknown and for the sake of the modelling a straight line at 10 km depth was used.
- 2) **Upper Devonian:** This unit was mapped by Ten Veen *et al* (2019) in the northern part of the Dutch onshore. It was extended in this project to the southern and central parts of the study area. The thickness variation of this unit is highly interpretative in the central part of the two sections restored, due to seismic limitations (depth and resolution).
- 3) **Dinantian:** The Dinantian unit was mapped by Ten Veen *et al.* (2019) and their interpretation was used for the identification of this unit throughout the two sections. The geometry of this unit was further discussed and updated during a series of discussions with colleagues from EBN and from TNO. In the Dutch nomenclature, this interval is referred to as the Carboniferous Limestone Group (CL).
- 4) **Namurian 1:** This unit refers to a seismically transparent unit recognized in the northern part of the Dutch onshore (Ten Veen *et al.*, 2019). The exact age of this unit is still debated and could be partly or entirely of Viséan age. For the purpose of this study, it is referred to as Namurian 1 unit.
- 5) **Namurian 2:** The Namurian 2 unit is defined as the interval located either above the Namurian 1 unit or above the Dinantian unit. It is believed that it is composed of Pendleian to early Arnsbergian age strata (329.06 to 327.78 Ma) based on the palynological information of well UHM-02. The top of this unit was interpreted in this study based on the recognition of some high amplitude horizons intra Namurian that can be traced across most of the sections, even across large bounding faults. The interpretation is locally uncertain however due to the low seismic resolution in a few zones (especially below the WNB) and the fact that some of those high amplitude reflectors could locally be related to magmatic intrusions rather than a regionally significant stratigraphic marker.
- 6) **Namurian 3:** The Namurian 3 unit is defined as the Namurian unit located between the Namurian 2 and the Westphalian unit. Based on the biostratigraphic information of the well UHM-02, this unit is composed of upper Arnsbergian to Yeadonian age strata (327.78 to 318.65 Ma).
- 7) **Westphalian:** The base of the Westphalian unit was based on the Dutch Geological Survey grid (DGM 5 version) and was adjusted in a few locations (e.g. WNB) to better match the structural architecture used in the present study. The top of this unit is defined as the Base Permian Unconformity (BPU) or the Saliaan Unconformity (see Chapter 3). The amount of erosion at the top of this unit is highly variable due to the inherited geometry of the intra-Westphalian units (Westphalian A, B, C, D) related to the Variscan Orogen, and due to the absence of Stephanian in the Dutch sector (De Bruin *et al.*, 2015).



- 8) **Rotliegend:** The Rotliegend Unit was obtained from the Dutch Geological Survey grid (DGM 5 version). In the Dutch nomenclature, this interval is referred to as the Lower and Upper Rotliegend Group (RV + RO).
- 9) **Zechstein:** The Zechstein Unit was obtained from the Dutch Geological Survey grid (DGM 5 version). In the Dutch nomenclature, this interval is referred to as the Zechstein Group (ZE).
- 10) **Triassic:** The Triassic Unit was obtained from the Dutch Geological Survey grid (DGM 5 version). It is composed of strata of Induan to Norian age. After discussion with colleagues from EBN and TNO, the decision was taken mid-restoration procedure to merge the Rotliegend, Zechstein and Triassic intervals into one unit for Permo-Triassic restoration step rather than three individual steps. This was decided since the structural evolution of this interval was relatively homogenous and simple over the study area. This was also permitted by the fact that Zechstein salt tectonics is limited in the restored sections. In the Dutch nomenclature, this interval is referred to as the Lower and Upper Germanic Trias Groups (RB + RN).
- 11) **Lower Jurassic;** The Lower Jurassic unit is composed of strata of Late Triassic (Rhaetian), Early Jurassic and earliest Middle Jurassic (Aalenian/Bajocian) age. The name Lower Jurassic was selected for simplification. The top of this unit corresponds to the Mid-Cimmerian Unconformity related to the mid-North Sea doming (see Chapter 3). In the Dutch nomenclature, this interval is referred to as the Altena Group (AT).
- 12) **Upper Jurassic:** The Upper Jurassic Unit is composed of strata of latest Middle Jurassic (Bathonian to Callovian) to earliest Early Cretaceous (Ryazanian) age. The name Lower Jurassic was selected for simplification. The top of this unit corresponds to the Late Cimmerian Unconformity. In the Dutch nomenclature, this interval is referred to as the Upper Jurassic Groups (SL, SG and SK)).
- 13) **Lower Cretaceous:** The Lower Cretaceous unit is composed of Lower Cretaceous strata of Valanginian to Albian age. In the Dutch nomenclature, this interval is referred to as the Rijnland Group (KN).
- 14) **Upper Cretaceous:** The Upper Cretaceous Unit is composed of Upper Cretaceous strata referred to in the Dutch nomenclature as the Chalk Group (CK). The next unit (Danian) is also part of the Chalk Group but is located above an important intra-Chalk Group unconformity.
- 15) **Danian:** The base of the Danian Unit is an important intra-Chalk Group unconformity which was mapped along the sections for this study.
- 16) **North Sea Group:** The North Sea Group is the younger unit defined for this project. It is composed of strata of Selandian to Present age. It is referred to in the Dutch Nomenclator as the Lower, Middle and Upper North Sea Groups (NL, NM and NU)



### 6.1.3. Interpretation and validation of horizons and faults

The horizon grids from the Dutch Geological Survey and the work carried out in the SCAN Dinantian Program (Ten Veen *et al.*, 2019) was used to interpret key horizons in Western and Central sections. Because of the many erosional stratigraphic tops, most stratigraphic levels are stratigraphic “bases”. Key faults recognized from previous studies were also added to the seismic interpretation carried out in the present study. More faults were interpreted for each section and adjustments/revisions of the horizons were made aiming for internal consistency matching the structural configuration for example of the dip of growth faults and tilt of the infilling strata (Figure 17 and Appendix 1). Therefore, such fine-tuning of the interpretation, with emphasis on first-order faults (including extensional, compressional, strike-slip), and with illustrative smaller structures were made and discussed with the core team and external colleagues. Line-length balancing techniques were of limited use because of the known component of strike-slip displacement(s).

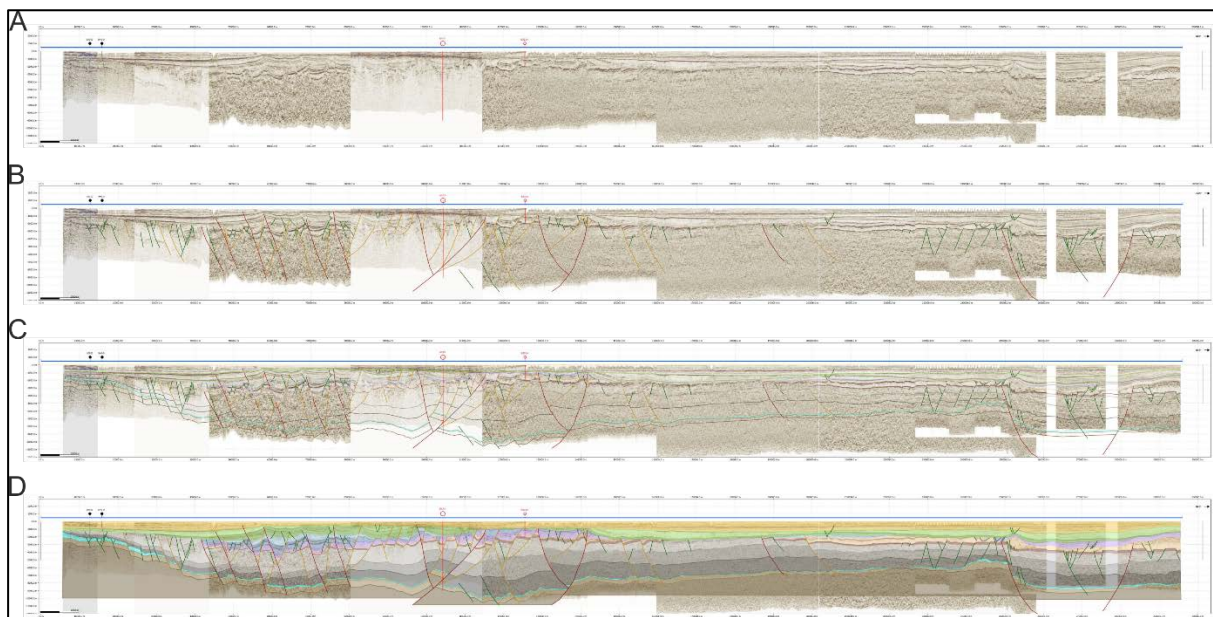


Figure 17: Seismic interpretation and model building for the Western Section. A) Composite seismic section without any interpretation. B) Main faults (red lines), secondary faults (orange lines) and minor faults (green lines) were interpreted based on previously known geometry (e.g. presence of basins and highs) as well as on recent interpretation (Ten Veen *et al.*, 2019). C) Devonian to Cenozoic horizons are added and are adjusted to match the new structural configuration. D) The stratigraphic units (shown in Figure 16) are added and further adjusted and fine-tuned based on discussion with colleagues from the core team and external advisors.

### 6.1.4. Modelling variables, optimum and alternative restoration scenarios

The restoration procedure involved a number of variables. The general variables are listed in Figure 18 and options in black or grey text. The modelling scenario chosen for this study follows the options in black text.

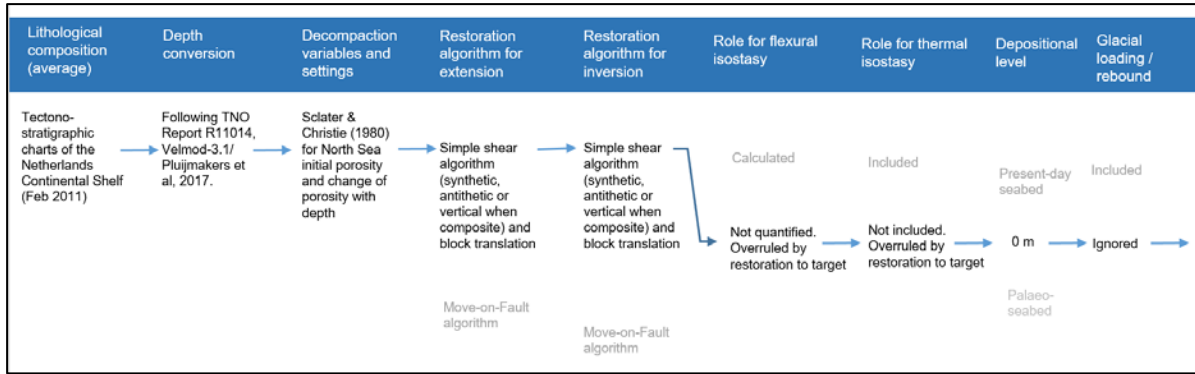


Figure 18: Scenario showing the main modelling variables relevant for each restoration step, and the various modelling options, selected option for this scenario in black. The sensitivity of the resulting geometry to these variables is briefly discussed below. An additional modelling variable that has a strong effect on the geometry and the vertical position of the Dinantian through time, but is only relevant for selected restoration steps, is the amount of reconstructed erosion, and the geometry and thickness of the units that were eroded. For this, overall, Occam's Razor principles were followed, applying a least complicated solution. The options and choices for this variable are discussed at each individual restoration steps.

Effects of compaction were restored using a decompaction algorithm. Input parameters per stratigraphic unit include 'initial porosity', which is the porosity at surface, and the 'c-factor', which is the change of porosity with depth. The initial porosity and c-factor were specified in a list, the Stratigraphic Database, in Move. Salt is considered to be incompressible and was assigned an incompressible depth coefficient (zero porosity).

The selected relationship between burial and compaction was that described by Sclater and Christie (1980), a negative exponential curve with greatest porosity loss occurring at shallow depths, most appropriate for sandstones and mixed sedimentary sequences.

$$f = f_0 (e^{-cy})$$


Where:

- $f$  is the present-day porosity at depth
- $f_0$  is the porosity at the surface
- $c$  is the porosity-depth coefficient ( $\text{km}^{-1}$ )
- $y$  is depth (m)

An average lithology was assumed for each unit based on published information as well as previous studies carried out at TNO. For mixed clastic intervals, percentages of sandstones, shale and limestone were used. For example, the North Sea Group was given a 50% sandstone and 50% shale content reflective of its mixed grain-size, while the Namurian was given a 25% sandstone and 75% shale content due to its predominantly deep-water setting in distal basin configuration (see Figure 19).

Stratigraphy & Rock Properties [v5 seismic cropped Move2017.1]

File Edit Table



Stratigraphy Rock Properties Strat. Column Compaction Curves

	1: Rock Type	2: Rock Group	3: Background_colour	4: pattern	5: Sandstone(%)	6: Shale(%)	7: Limestone(%)	8: Porosity	9: DepthCoefficient	10: Compaction Curve
	Sandstone	Sand			100	0	0	0.49	0.27	Sclater-Christie
	Shale	Shale			0	100	0	0.63	0.51	Sclater-Christie
	Limestone	Limestone			0	0	100	0.41	0.40	Sclater-Christie
Unit					%	%	%		km <sup>-1</sup>	
1	Default	Sand						0.56	0.39	Sclater-Christie
2	ShalySand	Silt						0.56	0.39	Sclater-Christie
3	Salt	Salt						0.00	0.00	Sclater-Christie
4	Chalk	Limestone						0.70	0.71	Sclater-Christie
5	North Sea NU	Sand			50	50	0	0.56	0.39	Sclater-Christie
6	Shale Rijnland KN	Shale				100		0.63	0.51	Sclater-Christie
7	Upper Jr Schieland SL	Sand			50	50	0	0.56	0.39	Sclater-Christie
8	Shale Altana AT	Shale			25	50	25	0.54	0.42	Sclater-Christie
9	Shale Upper Trias RN	Shale			25	50	25	0.54	0.42	Sclater-Christie
10	Shale Lwr Trias RB	Shale				100		0.63	0.51	Sclater-Christie
11	Upper Rotliegend RO	Sand			85	15		0.51	0.31	Sclater-Christie
12	Westphalien DC	Shale			50	50	0	0.56	0.39	Sclater-Christie
13	Namurian Epen DC	Shale			25	75	0	0.59	0.45	Sclater-Christie
14	Basement	Basement						0.00	0.00	Sclater-Christie

Figure 19: Stratigraphy and rock properties used in Move for each of the stratigraphic unit selected. The “Porosity” and “Depth Coefficients” are used for the decompaction step of each of the restoration step (back stripping)

For the restoration algorithms, for both extension and inversion, two groups are available in Move. One group are Move-on-fault algorithms, which perform the restoration by movement along fault planes (restoring fault offsets and related hanging wall deformation). A second group are Unfolding algorithms, which can be used without knowing underlying fault shapes. In this study, because of the high uncertainty of the fault shapes with depth, which is further complicated by the significant component of transcurrent out-of-section displacement, the algorithm used is Simple Shear Unfolding. Simple Shear is used to model penetrative deformation that occurs throughout the hanging wall at high angle to the beds rather than discrete slip between bedding planes (i.e. flexural slip). The shear angle was either vertical or inclined, the latter at either synthetic or antithetic shear angles or a weighted average angle that was specified per fault block and was different for each restoration step. Unfolding can be done to any vertical level, or to a target of any shape, but ideally is to palaeo-seabed. However, in this study, with the palaeo-seabed mostly unconstrained, restoration for most steps was to a horizontal level at 0 m altitude. For the Namurian and Dinantian, however, palaeo-water depth information was included in the restoration step, based on recent information from other SCAN Dinantian studies, especially the work carried out on Dinantian sedimentary facies and paleogeographic evaluation.

Restoration of the Zechstein salt domes in the far NE of the Central Section was done using the Simple Shear Unfolding algorithm with a vertical shear angle (to 0 m elevation), detaching the overlying units from the ones below the salt, allowing the salt volume to accommodate the difference, i.e. salt could flow in/out of the section.

#### 6.1.5. Restoration sequence, and fine-tuning of settings

The restoration steps followed the scenario of the general variables as specified in Figure 18. For individual steps, detailed decisions on the restoration required taking into account local geometrical parameters (e.g. shape of faults at that specific time, geometry of a fault block,

dominant shear angle, and the shape and thickness of reconstructed (added) stratigraphic thickness after the effects of erosion were restored.

Below is a list of the general actions taken at each restoration step carried out for the two sections. More detailed considerations, assumption and uncertainties are described for each individual step as part of the results chapter (Chapter 6):

1. Present-day geometry;
2. Remove the North Sea Group Unit and decompact the fifteen older units (based on specific decompactions factors and lithologies);
3. Flatten the top of the Danian Unit back to surface (0 m) and restore fault offsets;
4. Adjust geometry to remove artefacts and clean up section.
5. Remove Danian Unit and decompact the fourteen older units;
6. Reconstruct eroded Upper Cretaceous and other stratigraphic units that were affected by Subhercynian inversion and associated erosion;
7. Flatten on the new top surface of the Upper Cretaceous Unit and restore the effects of inversion on faults;
8. Adjust geometry to remove artefacts and clean up section.
9. Remove the Lower Cretaceous Unit and decompact the thirteen older units;
10. Flatten the Top of the Rijnland to sea-level (0 m) and restore fault offsets;
11. Adjust geometry to remove artefacts and clean up section.
12. Remove the Lower Cretaceous Unit and decompact the twelve older units;
13. Flatten the Top of the Upper Jurassic Unit to sea-level (0 m) and restore fault offsets;
14. Adjust geometry to remove artefacts and clean up section.
15. Remove the Upper Jurassic Unit and decompact the eleven older units;
16. Reconstruct the units that were eroded during the Mid-Cimmerian phase, including Lower Jurassic, Triassic and Permian units;
17. Flatten the Top of the newly restored Lower Jurassic Unit to sea-level (0 m) and restore fault offsets;
18. Adjust geometry to remove artefacts and clean up section.
19. Remove the Lower Jurassic Unit and decompact the ten older units;
20. Flatten the top of the Triassic Unit to sea-level (0 m) and restore fault offsets;
21. Adjust geometry to remove artefacts and clean up section.
22. Remove the Triassic/Zechstein/Rotliegend Units and decompact the seven older units;
23. Reconstruct the Westphalian Unit that was eroded during the Variscan Phase (BPU) by taking into account the BPU subcrop maps published;
24. Flatten the top of the newly restored Westphalian Unit to sea-level (0 m) and restore fault offsets;
25. Adjust geometry to remove artefacts and clean up section.
26. Remove the Westphalian Unit and decompact the six older units;
27. Flatten the top of the Namurian 3 Unit to sea-level (0 m) and restore fault offsets;
28. Adjust geometry to remove artefacts and clean up section.



29. Remove the Namurian 3 Unit and decompact the five older units;
30. Flatten at the top of the Namurian 2 Unit;
31. Add Namurian 2 Unit and thin Dinantian strata above the Dinantian in the south to correct from the intra-Namurian erosion/Karstification along the London Brabant Massif and Zeeland High;
32. Flatten the top of the Namurian 2 Unit to sea-level (0 m) along the London Brabant Massif/ZH and 400 m of water depth in the rest of the sections. Then restore the fault offsets;
33. Adjust geometry to remove artefacts and clean up section.
34. Remove the Namurian 2 and 1 Units and decompact the three older units;
35. Flatten the top of the Dinantian Carbonate Platforms Unit to 50 m water depth, restore palaeo water depth between the platforms and restore fault offsets;
36. Adjust geometry to remove artefacts and clean up section.

Limitations, uncertainty and assumptions in the work include:

- The existing horizon interpretation (TNO/EBN grids) were taken at face value, only minor changes were made along the cross-sections during the structural interpretation;
- The structural interpretation is assumed to be correct. Yet, uncertainty of the fault and horizon interpretation with depth is significant due to the lack of quality of the seismic imagery.
- No well-ties were checked but we assumed they were honoured by the TNO/EBN grids.
- It is assumed that depth conversion of the seismic was consistent with the depth converted stratigraphic grids.
- Decompaction was done using average values for initial porosity and change of porosity with depth for individual modelled stratigraphic units.
- The structural restoration steps were done using techniques including block-restoration and unfolding. Move-on-fault restorations were considered not useful in 2D because of significant strike-slip components to most deformation phases and - at this stage - due of the uncertainty of the fault geometry interpretation with depth.
- By using the unfolding algorithms, restoration targets can include paleo-seabed. However, without constraints, and rather than making estimates for each individual step, a target of 0 m level is taken for all apart from the last restoration steps. For these last steps, the restoration of Namurian and Dinantian, we optimise it with facies and paleo water depth constrains from other SCAN Dinantien studies (Mozafari *et al.*, 2019).
- The sections in this study were chosen at high angle to the main structural trend. This is expected to be an old (Devonian or older) inherited trend and is not expected to be parallel to the subsequent transport directions during inversion and Jurassic extension. Therefore, balancing techniques were of limited use. Consistency between fault dip and fault block tilt was taken into account in the fine-tuning of the seismic interpretation.

More specific information is provided in Chapter 6 regarding the assumptions made and the relevant uncertainties for each time steps.

## 6.2. Methodology for the burial and maturity modeling for wells (1D-plots)

The main input for basin modelling consists of the stratigraphy of the well and the conditions for the model. Well stratigraphy represents the main formations encountered in the well as well as their ages and lithologies. Boundary condition consist of the Paleo-Water Depth



(PWD), Sediment-Water-Interface-Temperature (SWIT) and basal heat flow HF). In addition to that, erosion thicknesses during main erosion events are also required inputs for the models. Finally, calibration data, such as measured (borehole) temperatures and vitrinite reflectance maturity data (%Ro) are needed to calibrate and verify the models.

A total number of 14 wells are modelled (Table 4 and Figure 12) using Schlumberger PetroMod software following well-established and tested TNO in-house workflows. Ten 1D basin models are constructed for existing drilled wells. Four models are built from pseudo-wells (i.e. wells constructed from existing TNO regional basin models). Modelled wells have been selected based on their proximity to the regional sections and being in the consortia areas. For most wells, maturity (vitrinite reflectance measurements) and temperature (borehole temperature) calibration data are available.

Table 5: List of modelled wells

Well	Description
<u><i>Northern Netherlands</i></u>	
UHM-02	Drilled well
LWS-01	Drilled well
SWD-01	Drilled well
<u><i>Central Netherlands</i></u>	
NAG-01	Drilled well
EMO-01	Drilled well
BAC-01	Drilled well
Ext-1	Pseudo well (Extracted from TNO regional models)
Ext-2	Pseudo well (Extracted from TNO regional models)
Ext-3	Pseudo well (Extracted from regional 3D TNO models)
<u><i>West Netherlands Basin</i></u>	
HVS-01	Drilled well
AST-01-Ext	Pseudo well (Extracted from regional thickness maps at the location of well AST-01)
<u><i>Zeeland High</i></u>	
S02-02	Drilled well
WDR-01	Drilled well
BHG-01	Drilled well

### 6.2.1. Input stratigraphy

The input stratigraphy of the modelled wells depends on the well. For drilled wells, the stratigraphy is based on the drilled formations (available from the NLOG website). For pseudo wells (extractions), the stratigraphy is based on 3D regional TNO models which are based on the regional mapping programs. In pseudo wells close to the regional seismic lines, the stratigraphy is updated by the intersection of these lines.

For all the wells where deeper Paleozoic sections are not drilled, the stratigraphy of the Paleozoic is annexed based on the interpretation of the regional seismic lines in the structural restoration work-package.

Erosion thicknesses during the major erosion events (such as the Permian Saalian, the Upper Jurassic Late-Mid Kimmerian and the Upper Cretaceous Laramide events) are mainly estimated following TNO regional 3D basin models where these thicknesses are estimated and calibrated with various types of data. The applied erosion thicknesses are modified during the modelling in case new insights are available or if new calibration is needed. Moreover, the estimated erosion thicknesses are cross-checked with the outcome of the structural restoration work-package along the regional lines whenever needed.

### 6.2.2. Boundary conditions

Time dependent paleo water depths (PWDs) and sediment-water interface temperatures (SWITs) are introduced into the model. The PWD curve was based on detailed investigation by the Geobiology department at TNO for some intervals. The SWITs were calculated using the integrated PetroMod tool based on Wygrala (1989). A more detailed temperature curve was used for the Tertiary and Quaternary (Abdul Fattah *et al.*, 2012; Verweij *et al.*, 2012).

Basal heat flow curves used in the models are derived from previous studies carried out by TNO. The heat flow models have been used in TNO calibrated regional basin models. In general, a tectonic based heat flow modelling approach is applied to calculate heat flow variations throughout the geological history (Van Wees *et al.* 2009). Although different heat flow models are applied to different wells, a thermal peak (in the form of an elevated heat flow) is introduced in all the models during the Saalian Permian uplift (Abdul Fattah *et al.*, 2012; Bonté *et al.*, submitted; Van Wees *et al.*, 2009).

### 6.2.3. Source rocks properties

Source rock kinetics and properties, such as Type, Total Organic Carbon (TOC) and Hydrogen Index (HI) values, are estimated from measured data from surrounding areas and published sources (e.g., Abdul Fattah *et al.*, 2012; Gerling *et al.*, 1999; Pletsch *et al.*, 2010; Schroot *et al.* 2006; Van Balen *et al.*, 2000). Source rock properties for the Westphalian, Namurian and Dinantian are shown in Table 6 and discussed below.

#### 5.2.3.1 Westphalian and Namurian source rocks

Westphalian coal-seams are considered to be one of the principal sources of gas that charged the reservoirs in the onshore and offshore Netherlands (De Jager and Geluk, 2007; Gerling *et al.*, 1999; Kombrink *et al.*, 2012). Westphalian coal bearing formations, such as the Baarlo, Ruurlo and Maurits Formations form a source rock of kerogen type III. Additional charging of the reservoirs from older sources cannot be excluded (Abdul Fattah *et al.* 2012; De Jager and Geluk, 2007; Kombrink *et al.*, 2012).

Knowledge on the occurrence of potential pre-Westphalian source rocks is mainly based on regional correlations and paleogeographic models (Abbink *et al.*, 2007; Gerling *et al.*, 1999; Pagnier *et al.*, 2002; Schroot *et al.*, 2006). The lower part of the Namurian generally consists of a thin layer of deep marine shale (Geverik Member) that could make a good source rock of type II (Gerling *et al.*, 1999; Pagnier *et al.*, 2002; Schroot *et al.*, 2006).

#### 5.2.3.2 Dinantian source rocks

The distribution and existence of potential Dinantian source rocks is not well understood. In the central onshore Netherlands, the Dinantian is of shallow marine and deltaic origin suggesting a type III to II source rock (e.g., Gerling *et al.*, 1999; Pagnier *et al.*, 2002; Schroot *et al.*, 2006).

In order to assess source rocks potential, a thin portion of the Dinantian units (either Zeeland Formation, or its separate members (Goeree, Schouwen and Beveland Members) were assigned as source rock. These source rocks may not be present, but if they are, they provide some insights if hydrocarbon expulsion from Dinantian rocks may have occurred.

Schroot *et al.* (2016, Petroplay Project) conducted a review of the source rock types (Figure 20). Based on this report, Dinantian source rocks in the southern part of the Netherlands are considered a mixture between terrestrial and marine organic matter (Type III and Type II respectively, Figure 20). Source rock data from the easternmost part of the Netherlands is comparable to source rocks encountered the Dinantian units in Germany, and mainly composed of carbonates with intercalated shale deposits. Owing to the marine character of these units a source rock Type II is expected (Schroot *et al.*, 2016).

For the present basin modeling study, a Type III is assumed for all Dinantian source rocks (Table 6). A sensitivity test was carried out on two wells (SWD-01 in the centre-north, and BHG-01 in the south, see Figure 12 for well location) to determine if the assumption of a Type II vs. Type II source rock is significant for the modelled maturity and/or the transformation ratio (see Section 6.2 for details on the basin model input and assumptions).

Figures 20 and 21 show the modelled Transformation Ratio (proxy for the amount of converted organic to hydrocarbons) and the Vitrinite Reflectance for wells SWD-01 and BHG-01 respectively. A Type II or III source does not have an effect on the modelled Vitrinite Reflectance data for either wells (Figures 20A and 21A).

A Type II or III source rock does have an effect on the modelled Transformation Ratio (Figures 21B and 22B). In well SWD-01, this mainly affects the timing when most of the organic matter has been converted to hydrocarbons. Onset of hydrocarbon expulsion is comparable in the two scenarios, but for a Type II source rock nearly 90% of organic matter was converted in the middle Carboniferous, whereas for a Type III source rock all the organic matter was converted to hydrocarbons by the beginning of the Permian. From the Permian onwards, all organic matter in the source rock has been converted irrespective of the type of source rock (Figure 21B).

For well BHG-01, the assumed source rock type has a more significant effect (Figure 22B). Although the timing for the onset of hydrocarbon expulsion is roughly similar (late Carboniferous), for a Type II source rock the model suggests that only some 95% of available organic matter is converted to hydrocarbons, whereas for a Type III this amounts to roughly 75%. A lower present day Transformation Ratio may suggest that the Dinantian units in well BHG-01 have more organic matter left that potentially could be expelling hydrocarbons. For well BHG-01 (and other wells on the LBM), there is, however uncertainty on the erosion/uplift history, given the large hiatus between the Carboniferous units and the overlying Cretaceous Chalk units. Those uncertainties also contribute to the probability that Dinantian source rocks may or may not be expelling hydrocarbons. Within the uncertainties, we postulate that a Type III source rock can be assumed for the Dinantian units.

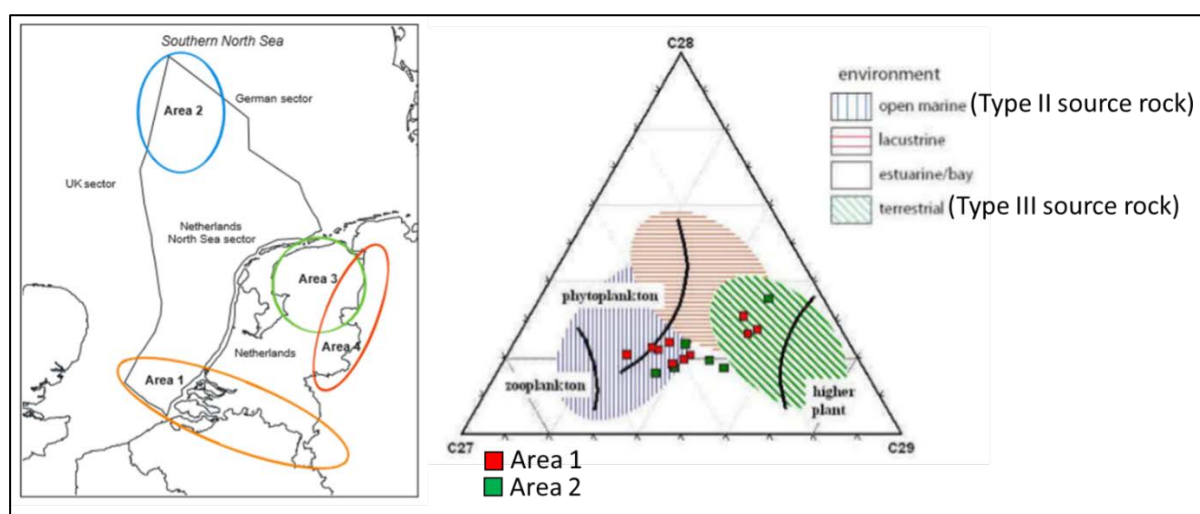


Figure 20: Source rock summary. A (left). Dinantian source rocks investigated in the Petroplay Project, figure adopted from Schroot *et al.* (2016). B (right). Biomarker analysis (GCMS, C27-C28-C29 steranes) on Dinantian facies in the Petroplay Project (Schroot *et al.*, 2016). Analyses suggests that Dinantian source rocks in the London Brabant Massif (Area 1 in Schroot *et al.*, 2016) are a mixture between terrestrial (Type III) and marine (Type II) facies. For the Central Netherlands (Area 3 & 4, Petroplay Project), a Type II source rock may be expected based on the marine character of the Dinantian and regional correlation to studied German source rocks here (Schroot *et al.*, 2016).

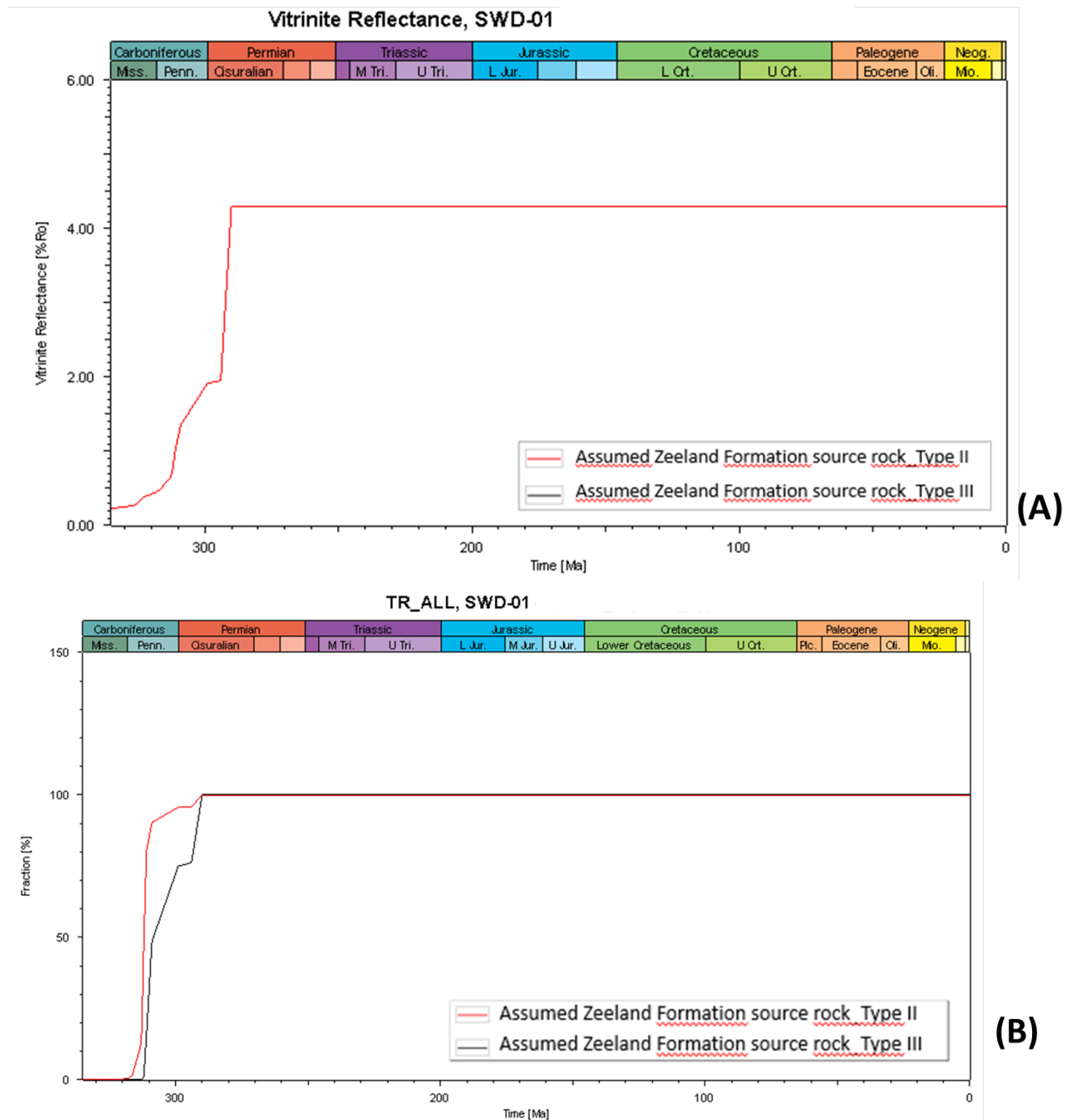


Figure 21: Sensitivity test for well SWD-01 between an assumed Type II vs Type III source rock for (a portion of) the Dinantian Zeeland Formation. A. Modelled Vitrinite Reflectance show no difference between a Type II or a Type III source rock. B. Modelled Transformation Ratio (proxy for the amount of organic material converted to hydrocarbons) suggests that the type of source rock mainly affects the timing when most of the organic matter has been converted to hydrocarbons: for a Type II source rock, most of organic matter is converted in the middle Carboniferous, whereas for a Type III source rock this is reached at the beginning of the Permian.

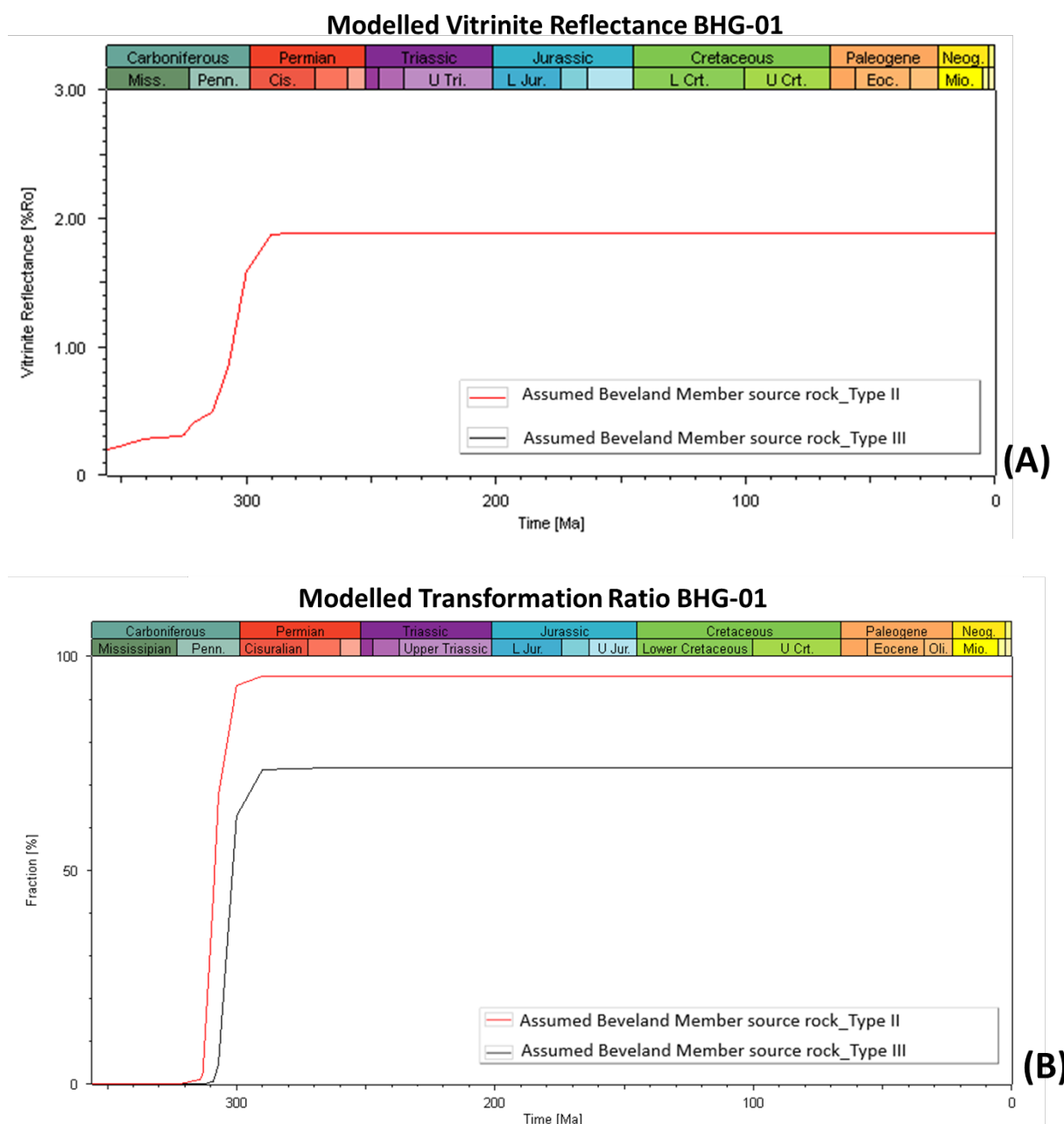


Figure 22. Sensitivity test for well BHG-01 between an assumed Type II vs Type III source rock for (a portion of) the Dinantian Beveland Member (Zeeland Formation). A. Modelled Vitrinite Reflectance show no difference between a Type II or a Type III source rock. B. Modelled Transformation Ratio (proxy for the amount of organic material converted to hydrocarbons) suggests that the type of source rock predominantly affects the amount of organic matter converted to hydrocarbons, with a Type II source rock suggesting that some 95% of organic matter has been converted, compared to some 75% for a Type III source rock. Main phase of hydrocarbon expulsion is roughly similar for both cases at the end of the Carboniferous.

Table 6: Average source rock parameters used for simulating source rock maturity and hydrocarbon generation.

Source Rock	TOC (wt %)	HI (mg HC/g TOC)	Kerogen type
<u>Westphalian:</u>			
Maurits Fm	4-5	200	III
Ruurlo Fm	1-3	100	III
Baarlo Fm	1-3	100	III
<u>Namurian</u>			
Geverik Mb	2-5	200-500	II
<u>Dinantian</u>			
Zeeland (Goeree, Schouwen, Beveland Mbs)	2	200	III (II)

## 7. Results

The results of both sub studies (2D structural restoration and 1D maturity modeling) are presented below and then integrated in Chapter 7.

### 7.1. Structural restoration results

The results of the structural restoration of the Western and Central sections are presented below. The first part consists of a description of the action taken for each time steps as well as the assumptions and uncertainties associated with each individual time step. The second part relates to the geologically significant results that are presented in the form of an updated summary chart that lists the new information for each or the structural elements for each key period. Finally, a summary of the kinematics of key faults is presented.

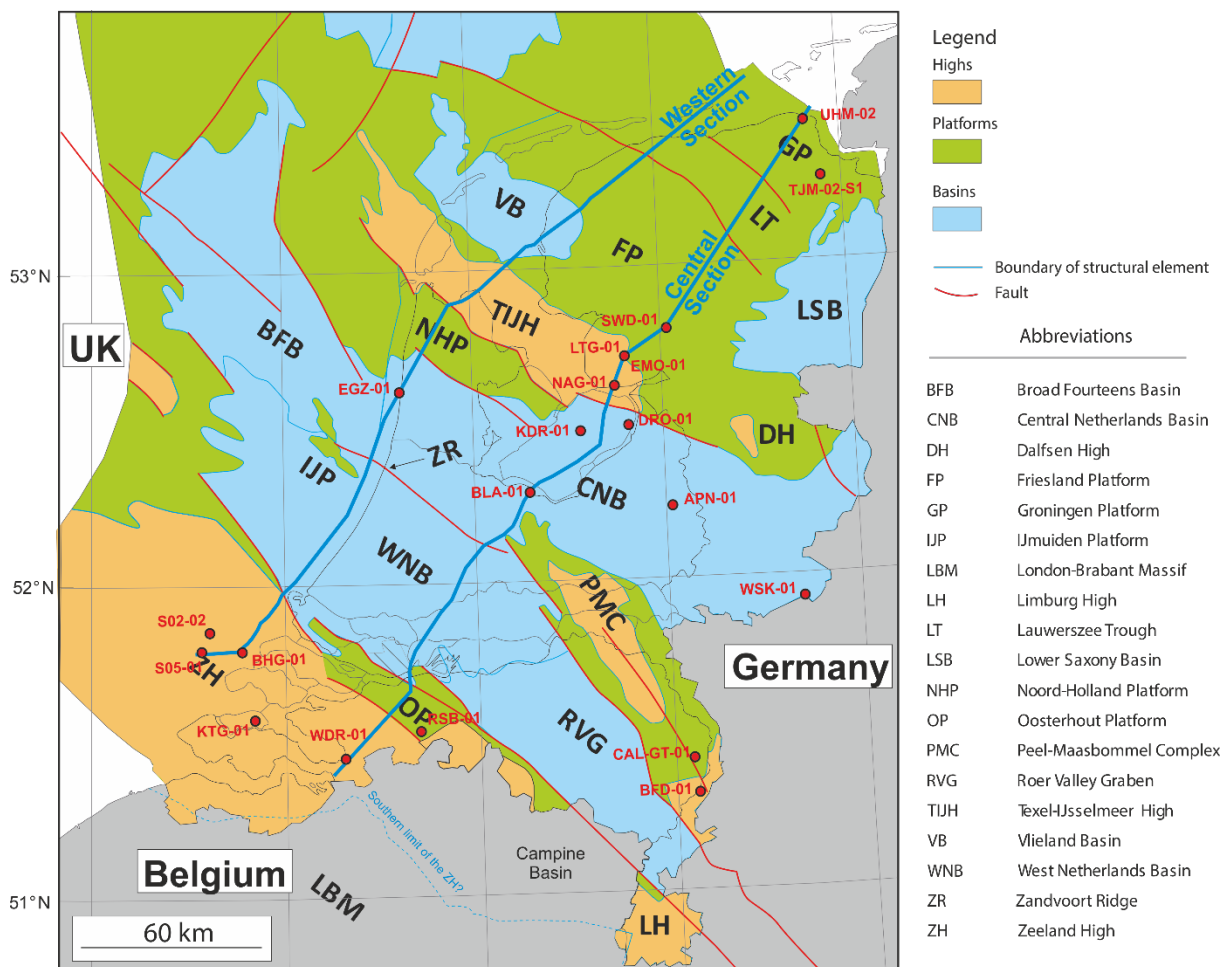


Figure 23: Base map showing the position of the two restored sections (Western and Central) as blue lines, key wells (red dots) and structural elements (colour polygons)

#### 7.1.1. Assumptions and uncertainties

Structural restoration techniques requires some assumptions and a good understanding of the uncertainties related to the data used, geological knowledge of the restored geological cross section, and the understanding of structural dynamics that affected the area throughout the time period considered. Below is a list of specific assumptions made during the restoration process, allowing the reader to better understand the decision process followed during this analysis.



During the restoration the fault throw restoration was only done for the main fault lines (bright red faults). In some cases, smaller faults were also separately restored when the geometry was too complex. A simplified approach was used to approximate movement along smaller faults; however, this can lead to errors in the geometry of the underlying layers when the fault direction was different to the main structural trend. Most of these errors were removed during or after the reconstruction in a cleaning step. In some cases, this could not be fixed and will be mentioned in the description of the sections.

An important step in structural reconstructions can be the geological reinterpretation of an area based on results during the restoration (e.g. fault geometries or eroded thickness assumptions) and subsequent redoing of the reconstruction using the new interpretation. Due to time constraints in this reconstruction this method was applied very rarely, and most assumptions were discussed beforehand to avoid time consuming reinterpretations.

### 7.1.1.1. Western Section

During the reconstruction of the Western line some reinterpretation of the central structure was necessary. To speed up the reconstruction only the reinterpreted part of the section was redone and later inserted into the previously finished sections. Because of this only the restored sections are available for display and not the intermediate results such as the decompaction steps.

#### Present day

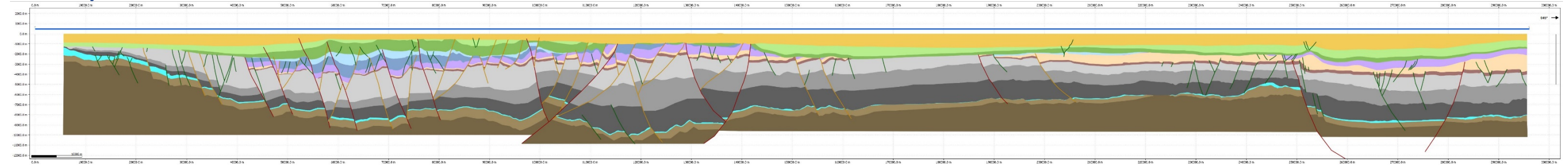


Figure 24: Western Section - Present-day situation. Two time vertical exaggeration.

- Interpretation based on DGM 5 for available horizons (Base N, CK, KN, S, AT, RB, ZE, RO) as well as depth converted Base DCC from DGM 5. From the SCAN project the depth converted merged top Dinantian as well as the “intra-Namurian”, “top transparent Namurian”, “Top Devonian” and “Top Basement” interpretations from the northern area were used.
  - The depth conversion is based on the Time-Depth conversion for the Dinantian from the SCAN project as well as velocity maps created for the overlying intervals based on the latest velocity model.
- The available horizon interpretation was refined along the identified faults and the “Intra-Namurian”, “Top Devonian” and “Top Basement” horizons were interpreted along the whole length of the section.
- For the updated interpretation of the Carboniferous intervals the subcrop map from Kombrink *et al.* (2010) was taken into account to assess the remaining thickness trends.
  - For the updated structural interpretations and identification of the main faults the structural maps from Kombrink *et al.* (2012) as well as Duin *et al.* (2006) were used.

#### End of Danian

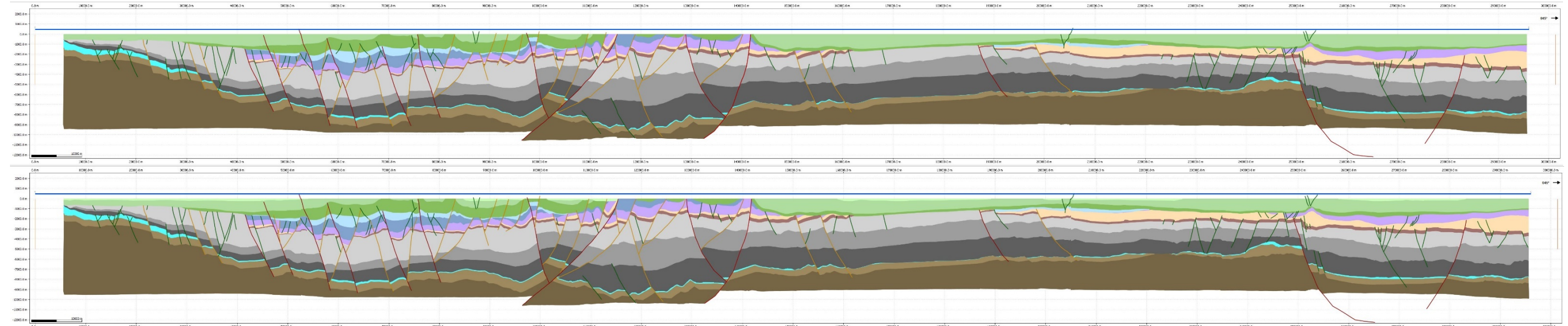


Figure 25: Western Section - North Sea Group removed and Top Cretaceous restored to 0. Two time vertical exaggeration.

For this step an Intra-Chalk horizon was introduced to better reconstruct geometry during the main phase of inversion during the Campanian. This Intra-Chalk unconformity was identified on seismic if possible (mainly in the south and north of the section) and inferred from well information, structural interpretation and local sedimentological information (EBN – personal comment).



## End of Late Cretaceous

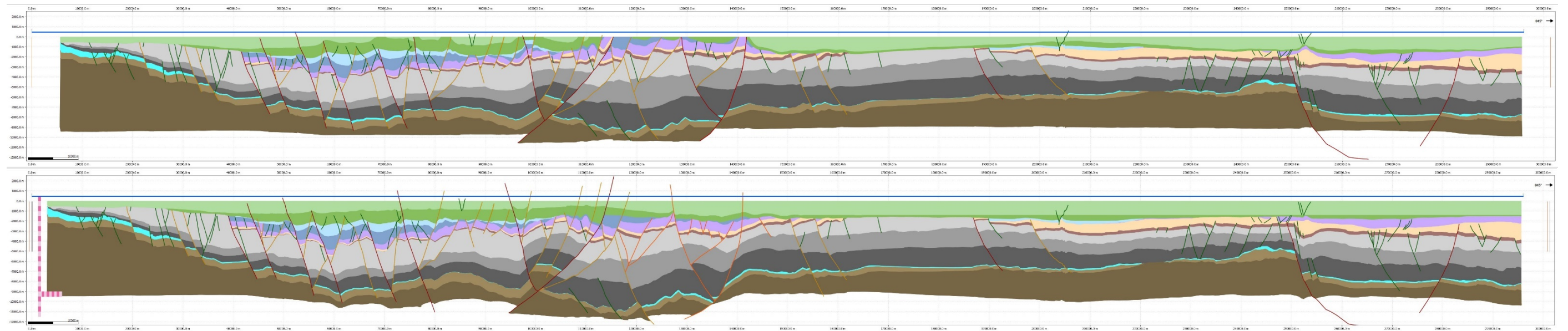


Figure 26: Western Section - Upper Chalk (CKEK) removed (1) and Subhercynian inversion and erosion reconstructed and restored to 0 (2). Two time vertical exaggeration.

- Zeeland High: Very little to no erosion, present-day thickness is depositional thickness, thinning towards the London Brabant Massif.
- West Netherlands Basin: Maximum thickness of the Chalk Group close to the ZH and thinning towards the NE. Less Chalk was reconstructed at the main inversion fault in the NE towards the CNB.
- Central Netherlands Basin: Thickness of the reconstructed Chalk Group increases towards the NHP in the NE. The reconstructed thickness of the Rijnland Group is taken from the maximum thickness of the remaining sediments in the CNB in the section. The Altena Group was reconstructed along the main inversion fault in the NE based on the geometry of the remaining sediments. No Upper Jurassic was reconstructed, as for the reconstruction of the eroded thickness it was assumed that the main deposition was focussed in local grabens and half grabens.
- Noord-Holland Platform, Texel-IJsselmeer High, Friesland Platform, Vlieland Basin, Lauwerszee Trough and Groningen Platform: A constant thickness of 1350 m was assumed for the Chalk Group for this area based on the maximum preserved thickness. Only minor erosion occurred along the fault in the SW, in the Vlieland Basin and on top of the salt structures in the NE.

## End of Early Cretaceous

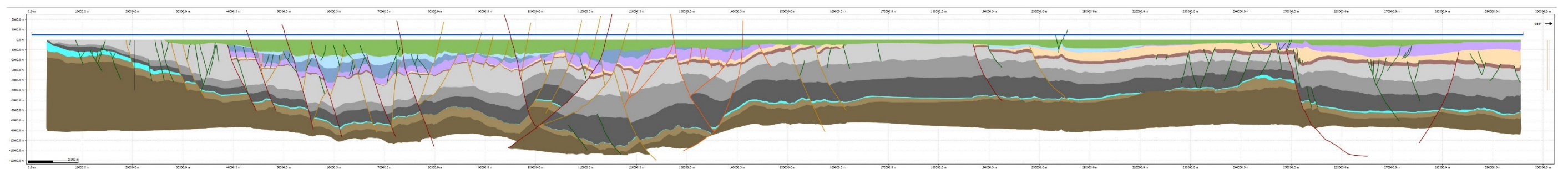


Figure 27: Western Section - Lower Chalk removed, Rijnland Group restored to 0. Two time vertical exaggeration.

- No unconformity at the base of the Chalk Group, the distribution of the Rijnland Group is therefore as present-day plus the sheet-like reconstruction in the inverted basins. No Lower Cretaceous sediments are recorded on the LBM which was probably exposed and subjected to erosion at the time. This is in agreement with exhumation ages from fission track analyses further south (e.g., Vercoutere and van den Haute, 1993) as well as the diagenesis and karstification analyses from the SCAN project.



## End of Ryazanian

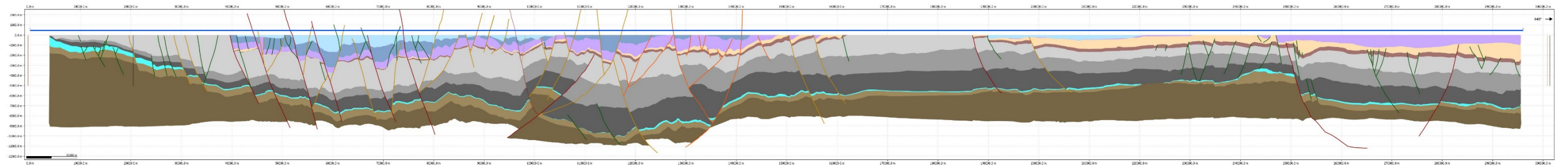


Figure 28: Rijnland Group removed, and Upper Jurassic (S) restored to 0. Two time vertical exaggeration.

- During the Late Kimmerian pulse only minor erosion has been reported mainly from the basin margins and platforms in the offshore (e.g., Bouroullec *et al.* 2015, 2016). Sedimentation was continuous in the WNB, in the CNB the transition is unknown due to the erosion during the Late Cretaceous. It is possible that some Late Jurassic sediments were initially deposited on the Friesland Platform or in the Lauwerszee Trough which were eroded at this stage. However, the theoretical thickness of these sediments is not expected to have a significant influence on the compaction and thermal history of these areas.

## End of Callovian (Mid-Jurassic)

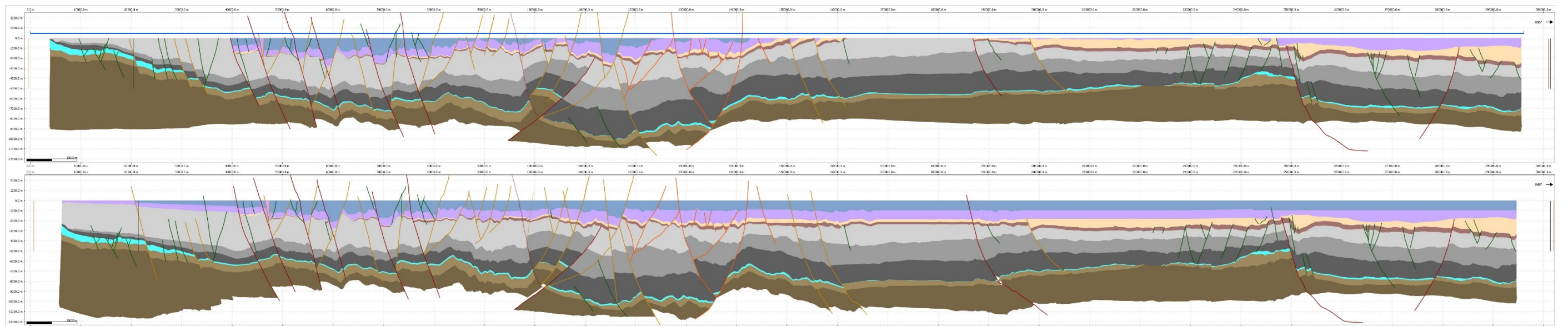


Figure 29: Western Section - Upper Jurassic (S) removed and Mid Kimmerian Unconformity restored to 0 (1), eroded Lower Jurassic, Triassic and Permian reconstructed and restored to 0 (2). Two time vertical exaggeration.

- The Mid Kimmerian tectonic pulse caused widespread erosion in most areas of the Netherlands. The only areas with continuous sedimentation throughout the Jurassic are the Roer Valley Graben, West Netherlands Basin and the southern part of the offshore Broad Fourteens Basin (Wong 2004). The main process for the erosion was the thermal uplift of the Central North Sea due to rifting as well as relative sea level drop. The main assumptions for the reconstruction of the eroded thickness were:
  - LBM: The depositional patterns of the Jurassic at the southern margin of the West Netherlands Basin suggest that the LBM was a source for coarser sediments and subjected to erosion already during the Early Jurassic. Therefore, the reconstructed thickness of the Lower Jurassic thins towards the centre of the LBM to represent its uplifted state. On the southern margin of the LBM in Belgium Triassic sediments were found in isolated small basins or grabens. However, the sedimentary pattern of the remaining Triassic sediments on the Platform between the LBM and the WNB suggest a marginal setting. It was, therefore, also decided to reconstruct the Triassic as thinning towards the centre of the LBM. Permian sediments in the WNB already show a clear basin margin setting. No Permian sediments were restored on the LBM in the section. Fission track analyses further south as well as thermal maturity indicators (e.g., Vitrinite reflectance) suggest deep burial and subsequent uplift of the LBM. The fission track results show that the last phase of major uplift was during the Middle to Late Jurassic, bringing the sediments to temperatures below 60°C (zone of partial annealing of Apatite fission tracks, e.g. Vercoutere & v.d. Houste, 1993). It is, however, possible that earlier tectonic events, such also the late-Variscan thrusting, caused uplift and erosion on the LBM that can no longer be seen in the samples due to overprinting during later phases. It was therefore decided to subdivide the total potential depositional thickness of the Westphalian between the two erosion phases. For the Mid

Kimmerian phase the remaining thickness of the Westphalian at the base of the remaining Triassic was used (~3 km), again thinning towards the centre of the LBM, resulting in 1.5 to 2 km of total erosion at the southernmost end of the section during this phase.

- WNB: Sedimentation in the WNB was continuous during the Jurassic, no sediments were reconstructed. The geometry of the Triassic in a fault block at the SW margin of the WNB is atypical for the Triassic evolution in the Netherlands, which is characterized by very little tectonic activity. It was therefore decided not to restore the Jurassic on top of that fault block as that might have significant influences on the reconstructed geometry of the lower layers.
- Rest of the section: The sedimentary pattern of the Lower Jurassic is very homogeneous. In a study from TNO well logs signatures for the Toarcian could easily be correlated across all major sedimentary basins and well into Germany (Nelskamp *et al.* 2015). This suggests a very quiet continuous deposition without any elevated elements. Based on this it was decided to reconstruct the Lower Jurassic with an overall sheet like geometry but slightly thicker in the basins. The Permian and Lower Triassic is also described as a tectonically quiet phase. Deposition occurred mainly in one big basin (Southern Permian Basin), with the centre of the basin in the present-day German offshore, to the NE of the section. The reconstructed thickness is based on the preserved thickness that already shows a thickening towards the NE. In both cases it was assumed that sedimentation also occurred on the ZR and FP during the Triassic and Jurassic, however, the Rotliegend and Zechstein Groups were reconstructed with reduced thickness there, based on present-day thickness and distribution of these groups.
- Some of the salt structures in the NE of the section were flattened during this reconstruction step.



## End of Norian (Late Triassic)

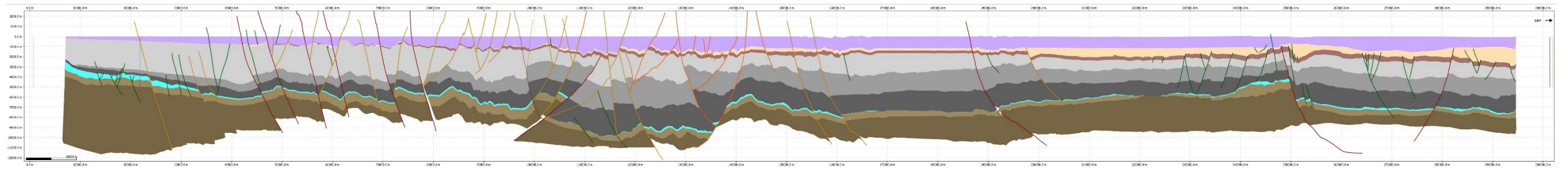


Figure 30: Western Section - Lower Jurassic removed, and Triassic restored to 0. Two time vertical exaggeration.

- Smaller fault displacements were restored in the WNB, otherwise it is assumed that no significant fault activity has occurred at this step.
- Because of the large basin scale geometry and relative tectonic quiescence it was decided to combine the Triassic and Permian in one reconstruction step.
- Some of the thickness variations (general but also across faults) of the Triassic interval in the WNB and CNB are probably related to simplifications from previous reconstruction steps instead of actual tectonic processes (see section 6.1.1).

## End of Westphalian

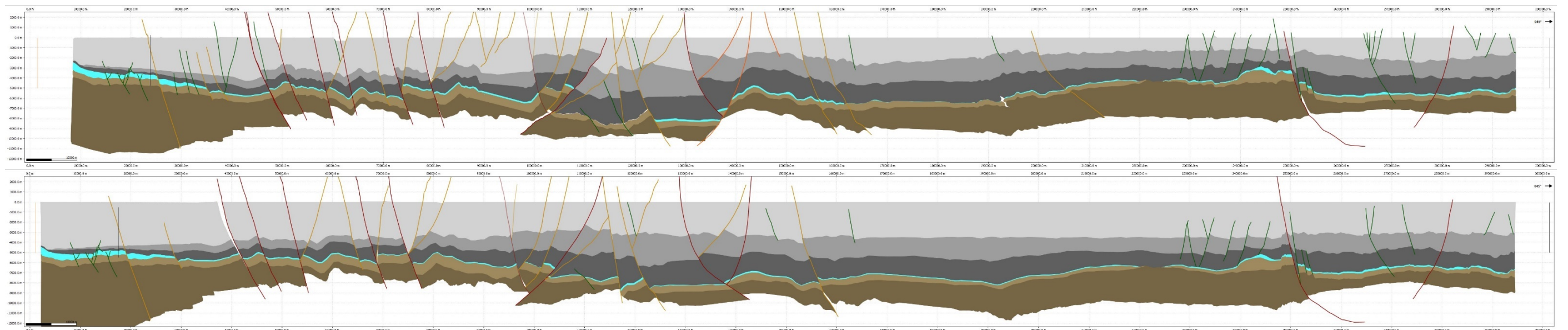


Figure 31: Western Section - Triassic and Permian removed and Base Permian Unconformity restored to 0 (1), Westphalian erosion reconstructed and restored to 0 (2) Two time vertical exaggeration.

- The Base Permian Unconformity was restored to 0 m. This includes the restored thicknesses of the Carboniferous on the LMB from the Jurassic erosion. The subcrop along the other parts of the section was checked against the published Base Permian subcrop maps (Mijnlieff, 2002; Kombrink *et al.*, 2010 and van Buggenum & den Hartog Jager, 2007).
- The thickness trends published from the PetroPlay project (Schoot *et al.*, 2006) were taken into account as well as updated well picks from the deep wells in the study area.
- These thickness trends of the Intra-Westphalian intervals show thickness differences between the north and the south. These trends were interpolated across the central parts of the section. However, the total thickness of the Westphalian along the section shows only minor thickness changes and can be modelled with an average total thickness of 3500 m. This overall thickness fits well with the total decompacted thickness of the preserved Westphalian on the Zeeland Platform and the SW part of the WNB.
- According to general structural understanding it was decided to reduce the reconstructed thickness on the strongly inverted areas in the centre of the section. Based on discussions with the expert group it was also decided to slightly increase the reconstructed thickness towards LBM.
- In order to restore the pre-erosion setting, the main focus of the reconstruction was along main faults, restoring compressional movements and pop up structures.
- The geometry of the restored top Westphalian was simplified, minor faults trends observed at the top Namurian were not taken into account in the reconstruction. It is therefore possible that smaller faults still show compressive movements at the top of the Namurian that should have been restored during the Westphalian.



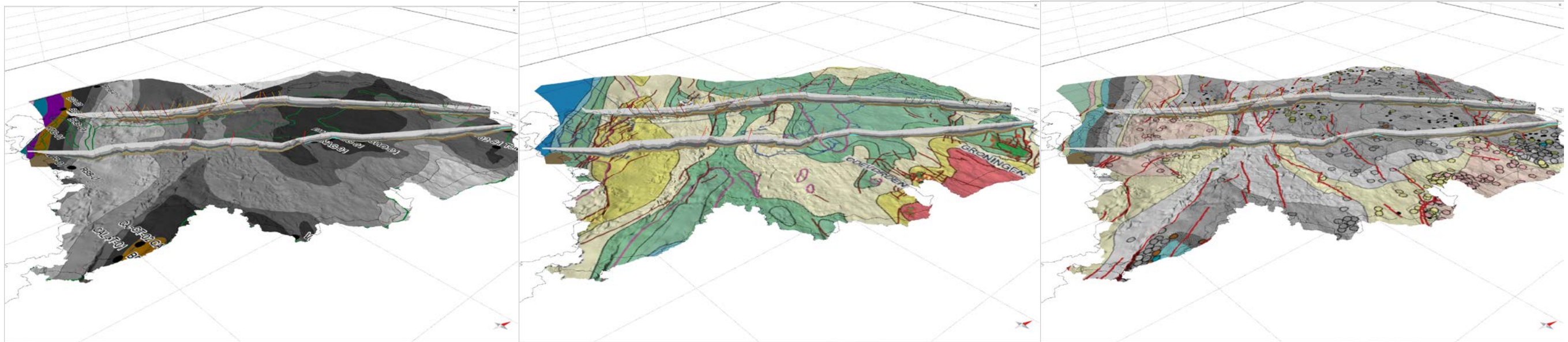


Figure 32: Subcrop maps used to estimate the amount of Westphalian eroded by the BPU along the restored sections, plotted on the depth map of the Dinantian. (left) Subcrop map published by Kombrink *et al.* (2010), (centre) van Buggenum & den Hartog Jager (2007) and (right) Mijndieff, (2002).

## End of Namurian

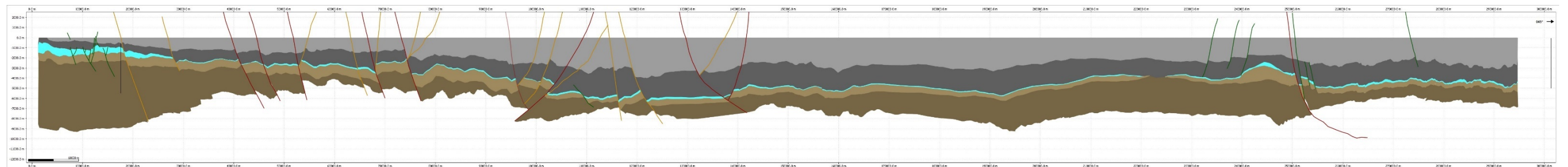


Figure 33: Western Section - Westphalian removed, upper Namurian restored. Two time vertical exaggeration.

- According to regional knowledge there is no major unconformity at the base of the Westphalian.
- The top of the Namurian was restored to 0 m, based on the assumption that the Namurian basin was completely filled at the beginning of the Westphalian.

## Mid-Namurian

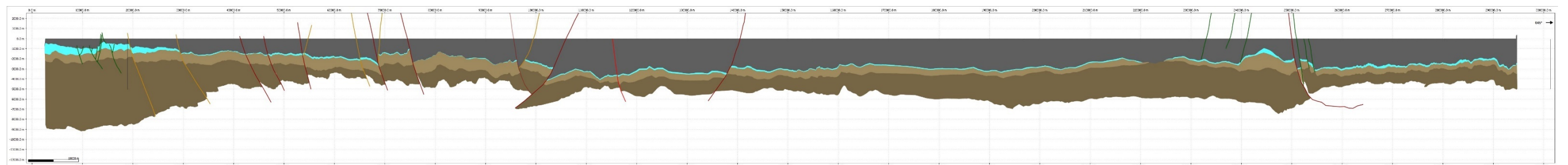


Figure 34: Western Section - upper Namurian removed, lower Namurian restored to 0 m. Two time vertical exaggeration.

- The general structural trend during the Namurian is extensional. Some structures show uncharacteristic compressional trends that are assumed to be related to the uncertainties of the interpretation.

- No erosion was reconstructed in this section as there is still lower Namurian interpreted on the ZH. According to the diagenetic analyses however, this area has also experienced significant karstification. It is possible that this occurred before the deposition of the Namurian rather than intra-Namurian and that the reduced thickness of the lower Namurian is related to later onset of deposition on the ZH.
- No significant paleotopography was reconstructed in this section, compared to the Central Section (see fig. 41) and the top of the section was restored to 0 m. To be comparable to the Central Section the whole section should be situated at a depth of 400 m below sea level. This was included in the cleaned up version of this section.

### End of Dinantian

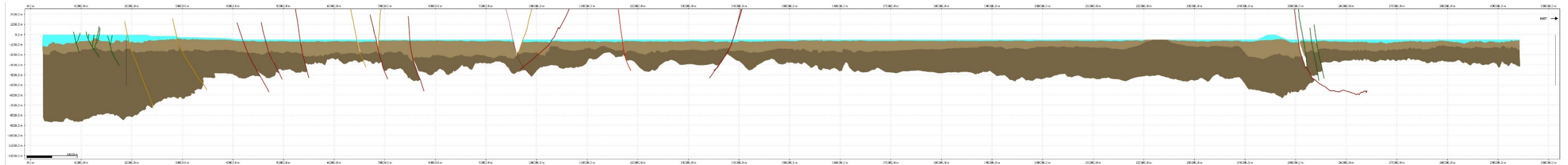


Figure 35: Western Section - lower Namurian removed and Dinantian restored to a paleo topography. Two time vertical exaggeration.

- The reconstruction of the paleo topography for the Dinantian was based on several different assumptions. (1) The tectonic activity during the Dinantian is difficult to assess because of the seismic resolution, especially in the deep basins. For the paleotopographic reconstruction it was therefore decided to keep the base of the Dinantian relatively flat. (2) The tops of the identified platforms should be at a water depth of maximum 20-30 m (because of the scale of the reconstruction the depth was set to 50 m). (3) The thickness of the platforms determines the minimum water depth between the platforms if there is no movement along the bounding faults during the Dinantian (resulting in a minimum water depth of 500 m between platforms at the end of the Dinantian). This is especially relevant for the Fryslan platform as no bounding faults could be identified. (4) The Dinantian on the ZH developed on a shallow slope rather than as a platform which would be slowly deepening towards to NE.



### 7.1.1.2. Central Section

Present day

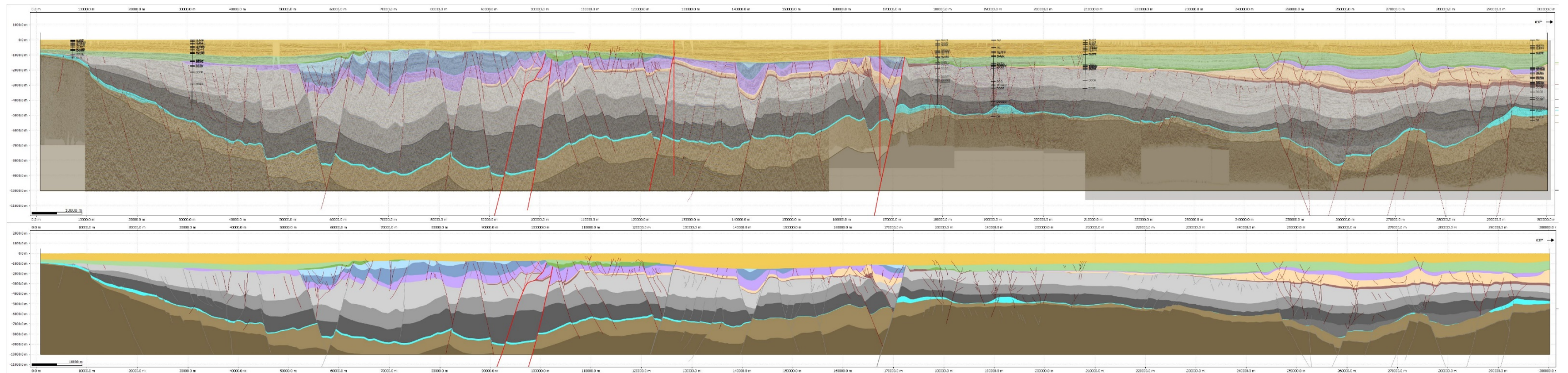


Figure 36: Central Section - Present-day geometry. Upper section shows the present day geometry with the seismic data displayed behind the transparent intervals, with a three time vertical exaggeration. The lower section is the same present day section with two time vertical exaggeration.

- Interpretation based on DGM 5 for available horizons (Base N, CK, KN, S, AT, RB, ZE, RO) as well as depth converted Base DCC from DGM 5. From the SCAN project the depth converted merged top Dinantian as well as the “intra-Namurian”, “top transparent Namurian”, “Top Devonian” and “Top Basement” interpretations from the northern area were used.
- The depth conversion is based on the Time-Depth conversion for the Dinantian from the SCAN project as well as velocity maps created for the overlying intervals based on the latest velocity model.
- The available horizon interpretation was refined along the identified faults and the “Intra-Namurian”, “Top Devonian” and “Top Basement” horizons were interpreted along the whole length of the section.
- For the updated interpretation of the Carboniferous intervals the subcrop map from Kombrink *et al.* (2010) was taken into account to assess the remaining thickness trends.
- For the updated structural interpretations and identification of the main faults the structural maps from Kombrink *et al.* (2012) as well as Duin *et al.* (2006) were used.

End of Danian

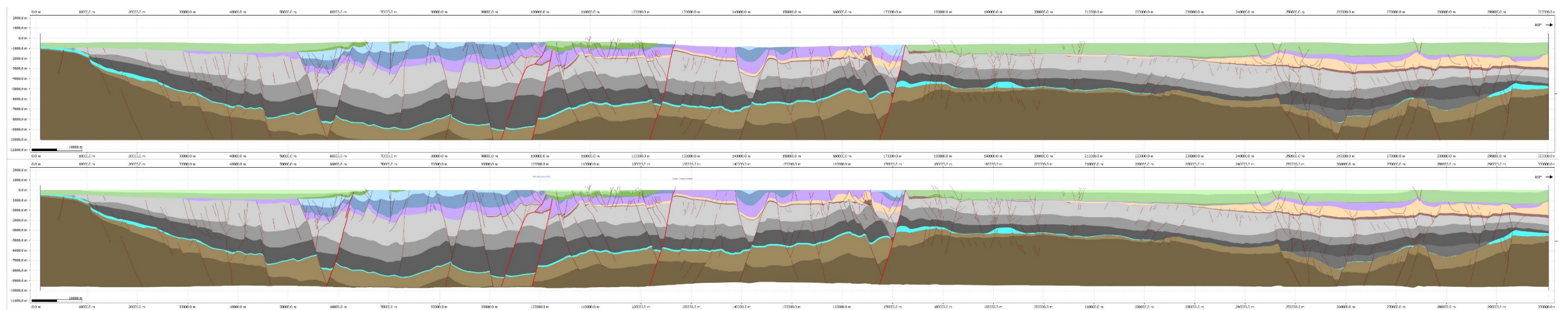


Figure 37: Central Section - North Sea Group removed (1) and Top Cretaceous restored to 0 (2). Two time vertical exaggeration.



- The North Sea Group was removed in one step even though some unconformities have been reported (de Jager, 2007) for the Eocene-Oligocene and Oligocene-Miocene which could also be seen on the seismic sections. Previous studies have shown that these unconformities can be considered minor and the estimated eroded thickness has not exceeded the present-day burial. However, it might have an influence on the exact timing of late hydrocarbon generation.
- For this step an Intra-Chalk horizon was introduced to better reconstruct geometry during the main phase of inversion during the Campanian. This Intra-Chalk unconformity was identified on seismic if possible (mainly in the south and north of the section) and inferred from well information, structural interpretation and local sedimentological information (EBN – personal comment).

## End of Late Cretaceous

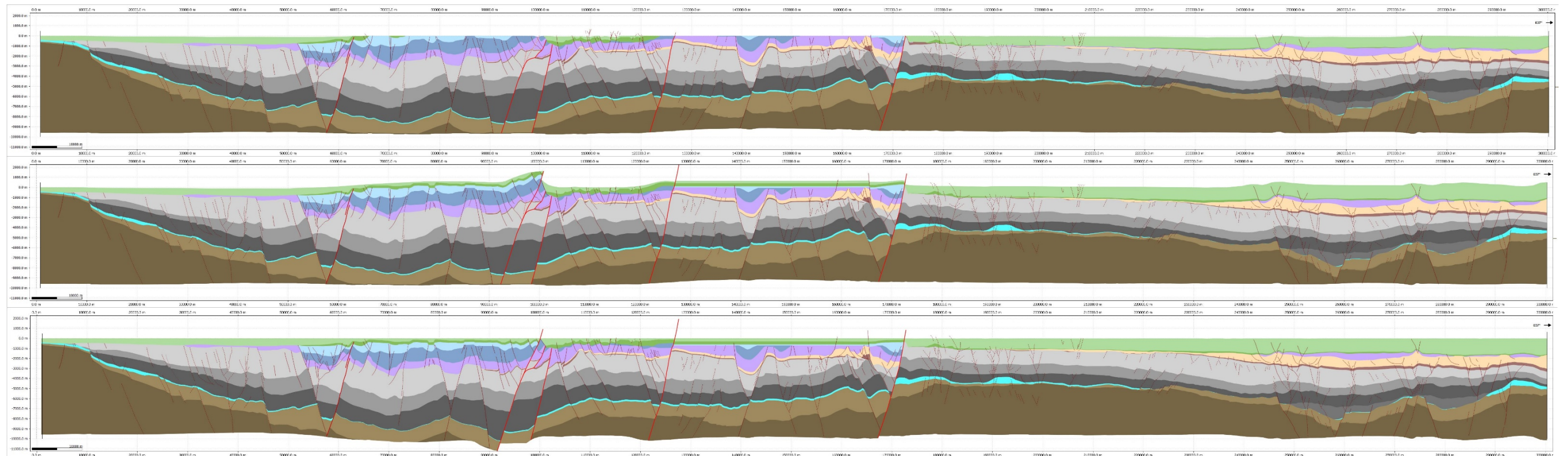


Figure 38: Central Section - upper Chalk (CKEK) removed (1) and Subhercynian inversion and erosion reconstructed (2) and restored to 0 (3). Two time vertical exaggeration.

- Zeeland High: Very little to no erosion, present-day thickness is depositional thickness, thinning towards the London Brabant Massif.
- West Netherlands Basin/Roer Valley Graben: Maximum thickness of the Chalk Group close to the ZH and thinning towards the NE. No/very little Chalk reconstructed at the main inversion fault in the NE towards the Peel-Maasbommel Complex, based on known sedimentary facies on the PMC (clastic sediments instead of classic chalk facies). The Rijnland Group was reconstructed with the sheet like depositional pattern based on the description of e.g., Van Adrichem Boogaert, H.A. & Kouwe, W.F.P., 1993-1997 and a maximum thickness of 250 m based on the preserved thickness of the KN Group in the SW of the WNB. For reconstruction of the S, AT and RN/RB Groups the depositional and structural trend within the basin was continued until the main bounding fault.
- Peel-Maasbommel Complex: Minor erosion was reconstructed at the SW and NE boundary of the structural element based on preserved thickness and structural setting. Again, a thinning of the depositional thickness of the Chalk group towards the main inversion fault (NE) was assumed.
- Central Netherlands Basin: A thin layer of Chalk with a maximum of 300 m was reconstructed for the CNB, again thinning towards in the NE towards the main inversion fault. The Rijnland Group was again reconstructed with a sheet like depositional style and a maximum thickness of 300 m. The Schieland Group in the CNB at present-day is very patchy and restricted to local grabens and half-grabens. The depositional environment is described as a muddy coastal plain with repeated intercalations of marine units as well as lagoonal carbonates (Van Adrichem Boogaert, H.A. & Kouwe, W.F.P., 1993-1997). For the reconstruction of the eroded thickness it was assumed that the main deposition was focussed in these local grabens and half grabens at the beginning and only later, with rising sea level during the Ryazanian overstepped the margins of the grabens and deposited a thin layer of Lowermost Cretaceous sediments in the CNB. No AT or RN/RB was restored at this point as (based on well stratigraphic data as well as 1D basin modelling) these intervals were most likely eroded during the Mid-Kimmerian erosion phase.
- Texel-IJsselmeer High, Friesland Platform, Lauwerszee Trough and Groningen Platform: A constant thickness of 1350 m was assumed for the Chalk Group for this area based on the maximum preserved thickness. Only minor erosion therefore occurred along the fault in the SW and on top of the salt diapirs in the NE.



- Other possible scenarios for the reconstruction of the erosion: (1) no Chalk sedimentation in the inverted basins, (2) more Chalk deposition in the inverted basins, (3) thicker Upper Jurassic sediments in the CNB, (4) also Lower Jurassic and Triassic sediments eroded during the Subhercynian.

## End of Early Cretaceous

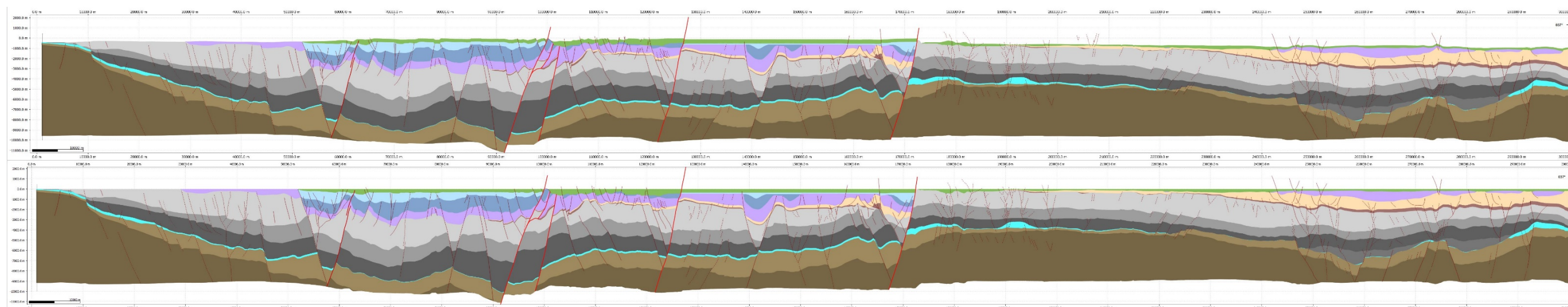


Figure 39: Central Section - Lower Chalk removed, Rijnland Group restored to 0. Two time vertical exaggeration.

- No unconformity at the base of the Chalk Group, the distribution of the Rijnland Group is therefore as present-day plus the sheet-like reconstruction in the inverted basins. No Lower Cretaceous sediments are recorded on the LBM which was probably exposed and subjected to erosion at the time. This is in agreement with exhumation ages from fission track analyses further south (e.g., Vercoutere and van den Haute, 1993) as well as the diagenesis and karstification analyses from the SCAN project.

## End of Ryazanian

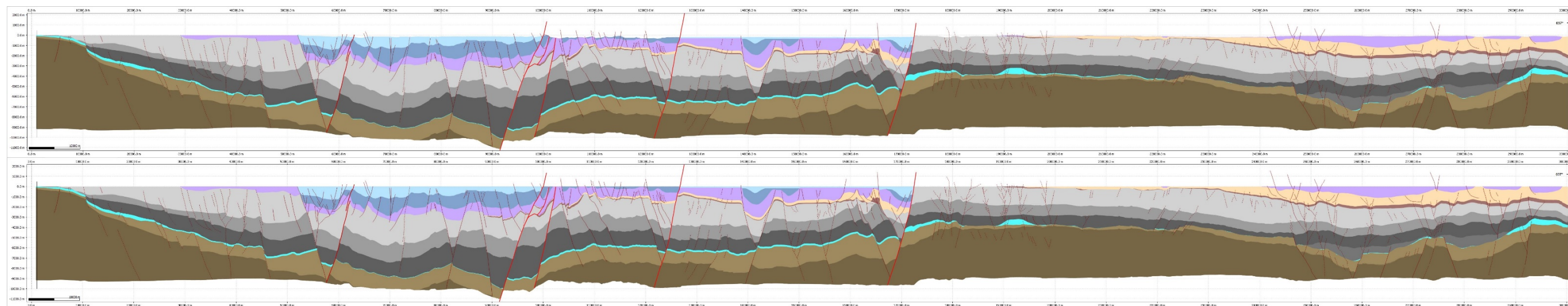


Figure 40: Central Section - Rijnland Group removed, and Upper Jurassic (S) restored to 0. Two time vertical exaggeration.

- During the Late Kimmerian pulse only minor erosion has been reported mainly from the basin margins and platforms in the offshore (e.g., Bouroullec *et al.* 2015, 2016). Sedimentation was continuous in the WNB, in the CNB the transition is unknown due to the erosion during the Late Cretaceous. It is possible that some Late Jurassic sediments were initially deposited on the Friesland Platform or in the Lauwerszee Trough which were eroded at this stage. However, the theoretical thickness of these sediments is not expected to have a significant influence on the compaction and thermal history of these areas.



## End of Callovian (Mid-Jurassic)

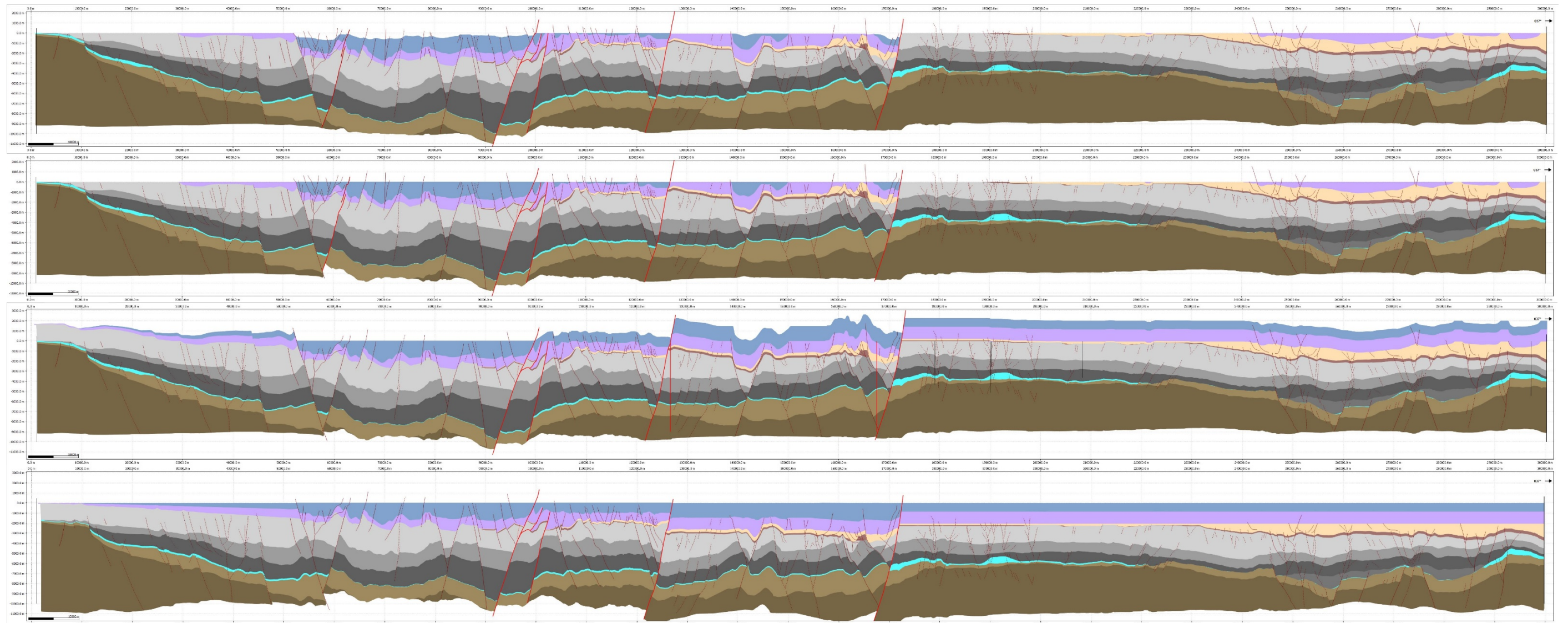


Figure 41: Central Section - Upper Jurassic (S) removed (1), Mid Kimmerian Unconformity restored to 0 (2), eroded Lower Jurassic, Triassic and Permian reconstructed (3) and restored to 0 (4). Two time vertical exaggeration.

- Restoration of the grabens and half-grabens in the CNB showed that with the current fault and horizon geometry the Mid Kimmerian Unconformity could not be restored to sea level without significant geometry mismatch in the deeper parts of the section. This can be a result of either wrong fault and horizon interpretation or of lateral movements perpendicular to the 2D restoration. Previous studies (e.g., de Jager, 2004) have mentioned that the faults in the CNB especially show lateral movements, which might explain the geometry mismatch.
- The Mid Kimmerian tectonic pulse caused widespread erosion in most areas of the Netherlands. The only areas with continuous sedimentation throughout the Jurassic are the Roer Valley Graben, West Netherlands Basin and the southern part of the offshore Broad Fourteens Basin (Wong 2004). The main process for the erosion was the thermal uplift of the Central North Sea due to rifting as well as relative sea level drop. The main assumptions for the reconstruction of the eroded thickness were:
  - LBM: The depositional patterns of the Jurassic at the southern margin of the West Netherlands Basin suggest that the LBM was a source for coarser sediments and subjected to erosion already during the Early Jurassic. Therefore, the reconstructed thickness of the Lower Jurassic thins towards the centre of the LBM to represent its uplifted state. On the southern margin of the LBM in Belgium Triassic sediments were found in isolated small basins or grabens. However, the sedimentary pattern of the remaining Triassic sediments on the Platform between the LBM and the WNB suggest a marginal setting. It was, therefore, also decided to reconstruct the Triassic as thinning towards the centre of the LBM. Permian sediments in the WNB already show a clear basin margin setting. No Permian sediments were restored on the LBM in the section. Fission track analyses further south as well as thermal maturity indicators (e.g., Vitrinite reflectance) suggest deep burial and subsequent uplift of the LBM. The fission track results show that the last phase of major uplift was during the Middle to Late Jurassic, bringing the sediments to temperatures below 60°C (zone of partial annealing of Apatite fission tracks, e.g. Vercoutere & v.d. Houte, 1993). It is, however, possible that earlier tectonic events, such as the late-Variscan thrusting, caused uplift and erosion on the LBM that can no longer be seen in the samples due to overprinting during later phases. It was therefore decided to subdivide the total potential depositional thickness of the Westphalian between the two



erosion phases. For the Mid Kimmerian phase the remaining thickness of the Westphalian at the base of the remaining Triassic was used (~3 km), again thinning towards the centre of the LBM, resulting in 1.5 to 2 km of total erosion at the southernmost end of the section during this phase.

- WNB: Sedimentation in the WNB was continuous during the Jurassic, no sediments were reconstructed.
- Rest of the section: The sedimentary pattern of the Lower Jurassic is very homogeneous. In a study from TNO well logs signatures for the Toarcian could easily be correlated across all major sedimentary basins and well into Germany (Nelskamp *et al.* 2015). This suggests a very quiet continuous deposition without any elevated elements. Based on this it was decided to reconstruct the Lower Jurassic with an overall sheet like geometry but slightly thicker in the basins. The Permian and Lower Triassic is also described as a tectonically quiet phase. Deposition occurred mainly in one big basin (Southern Permian Basin), with the centre of the basin in the present-day German offshore, to the NE of the section. The reconstructed thickness is based on the preserved thickness that already shows a thickening towards the NE. In both cases it was assumed that sedimentation also occurred on the ZR and FP during the Triassic and Jurassic, however, the Rotliegend and Zechstein Groups were reconstructed with reduced thickness there, based on present-day thickness and distribution of these groups.
- LT and GP: During the restoration of the Jurassic to 0 the salt structures were also flattened.

### End of Norian (Late Triassic)

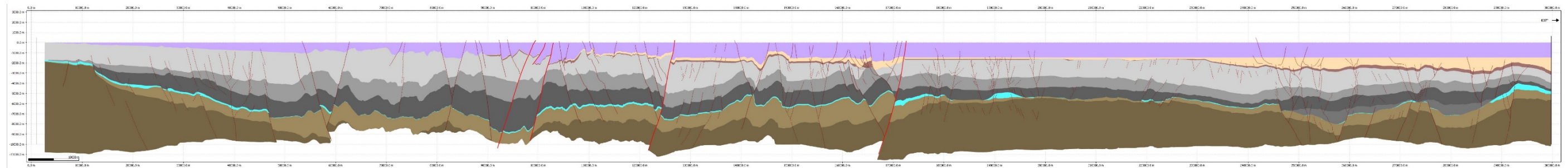


Figure 42: Central Section - Lower Jurassic removed, and Triassic restored to 0. Two time vertical exaggeration.

- Smaller fault displacements were restored in the WNB, otherwise it is assumed that no significant fault activity has occurred at this step.
- Because of the large basin scale geometry and relative tectonic quiescence, it was decided to combine the Triassic and Permian in one reconstruction step.
- Some of the thickness variations (general but also across faults) of the Triassic interval in the WNB and CNB are probably related to simplifications from previous reconstruction steps instead of actual tectonic processes (see section 6.1.1).

## End of Westphalian

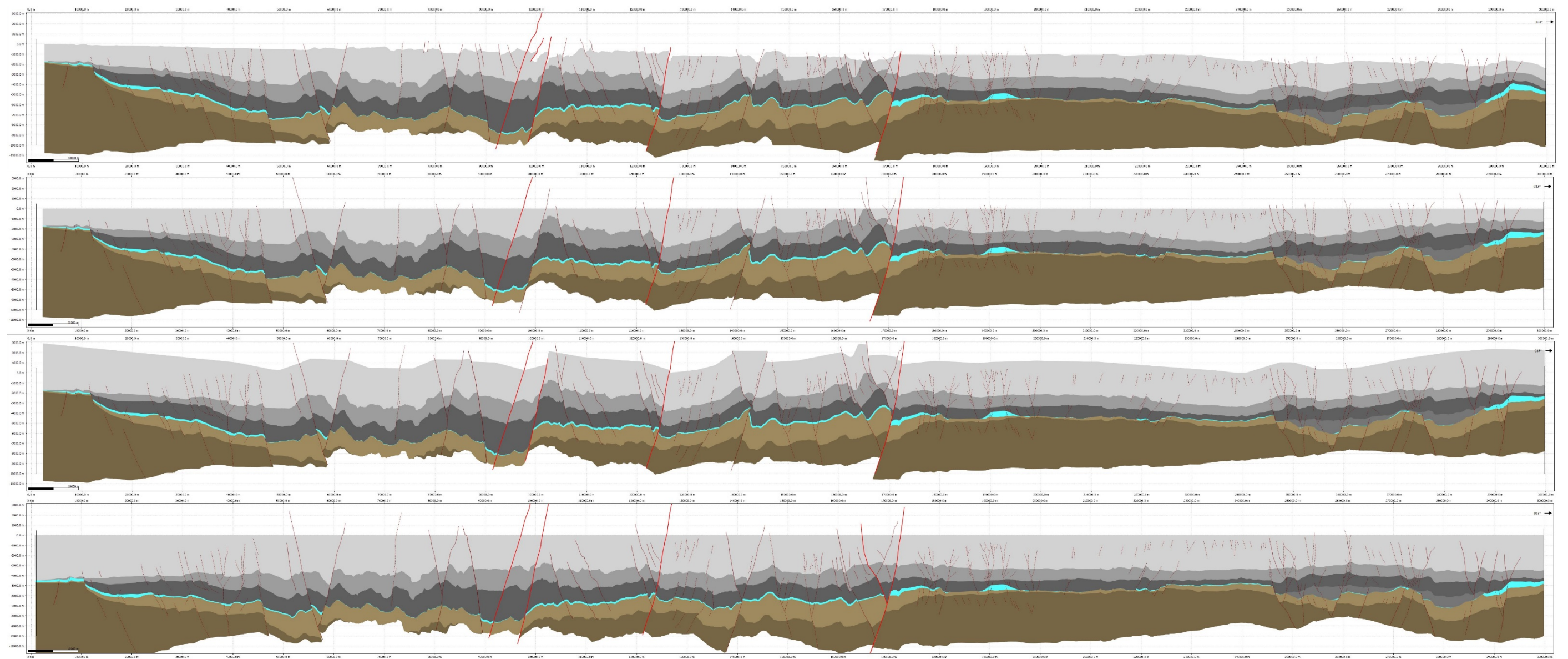


Figure 43: Central Section - Triassic and Permian removed (1), Base Permian Unconformity restored to 0 (2), Westphalian erosion reconstructed (3) and restored to 0 (4). Two time vertical exaggeration.

- The Base Permian Unconformity was restored to 0 m. This includes the restored thicknesses of the Carboniferous on the LMB from the Jurassic erosion. The subcrop along the other parts of the section was checked against the published Base Permian subcrop maps (Mijnlieff, 2002; Kombrink *et al.*, 2010 and van Buggenum & den Hartog Jager, 2007).
- The thickness trends published from the PetroPlay project (Schroot *et al.*, 2006) were taken into account as well as updated well picks from the deep wells in the study area.
- These thickness trends of the Intra-Westphalian intervals show thickness differences between the north and the south. These trends were interpolated across the central parts of the section. However, the total thickness of the Westphalian along the section shows only minor thickness changes and can be modelled with an average total thickness of 3500 m. This overall thickness fits well with the total decompacted thickness of the preserved Westphalian on the Zeeland High and the SW part of the WNB.
- According to general structural understanding it was decided to reduce the reconstructed thickness on the strongly inverted areas in the centre of the section. Based on discussions with the expert group it was also decided to slightly increase the reconstructed thickness towards to LBM.
- In order to restore the pre-erosion setting, the main focus of the reconstruction was along main faults, restoring compressional movements and pop up structures.
- The geometry of the restored top Westphalian was simplified, minor faults trends observed at the top Namurian were not taken into account in the reconstruction. It is therefore possible that smaller faults still show compressive movements at the top of the Namurian that should have been restored during the Westphalian.



## End of Namurian

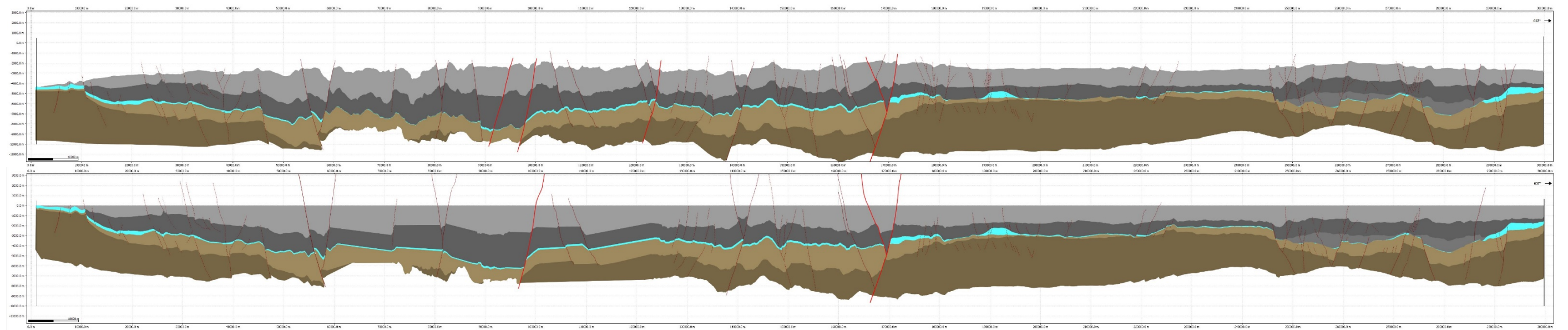


Figure 44: Central Section - Westphalian removed, upper Namurian restored. Two time vertical exaggeration.

- According to regional knowledge there is no major unconformity at the base of the Westphalian.
- The interpretation of the Namurian, especially south of the Texel-Ijsselmeer High is not very well constrained. In addition, a lot of noise was introduced into the interpretation due to smaller and not restored fault movement. It was therefore decided to simplify the Namurian and Dinantian at this step.
- The top of the Namurian was restored to 0 m, based on the assumption that the Namurian basin was completely filled at the beginning of the Westphalian.

## Mid-Namurian

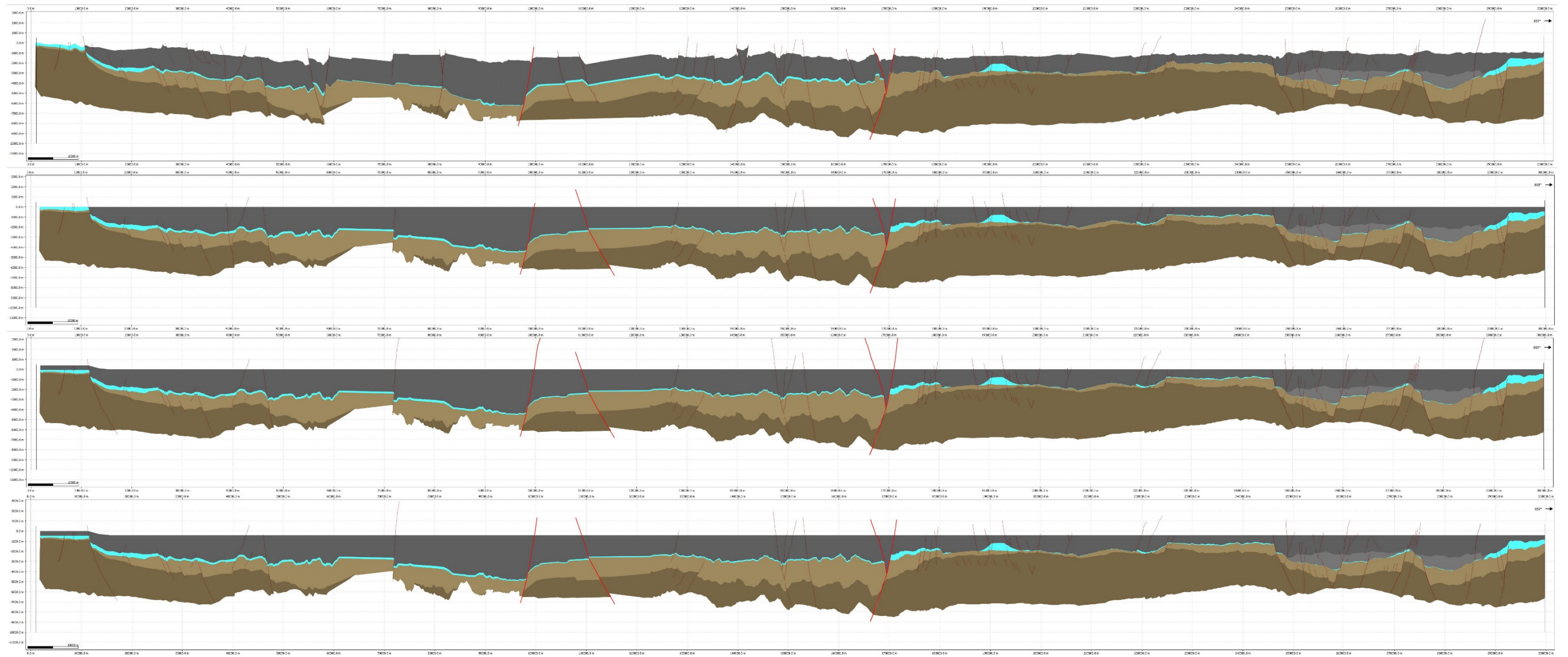


Figure 45: Central Section - upper Namurian removed, lower Namurian restored to 0 m, Intra-Namurian erosion reconstructed and restored. Two time vertical exaggeration.

- Only a minor unconformity Intra-Namurian on LBM is assumed. The reconstructed total eroded thickness is 300 m.
- The general structural trend during the Namurian is extensional. Some structures show uncharacteristic compressional trends that are assumed to be related to the uncertainties of the interpretation. These atypical features were removed from the reconstruction.
- According to the general understanding the Namurian sediments were deposited in a deep water setting. The reconstruction of the situation before the erosion therefore includes a simple paleo water depth trend of 400 m for the whole section with the exception of the eroded part on the LBM.
- As the lowermost part of the Namurian was only interpreted in the NE of the section it was decided to remove both intervals at the same time.

### Suggestions:

- More in-detail interpretation of the Namurian including more intra-Namurian intervals and looking at e.g., onlap configurations of the lowermost Namurian for a better understanding of the basin evolution.
- Better stratigraphic age control of the individual Namurian intervals to identify potentially elevated area during the early Namurian.



## End of Dinantian

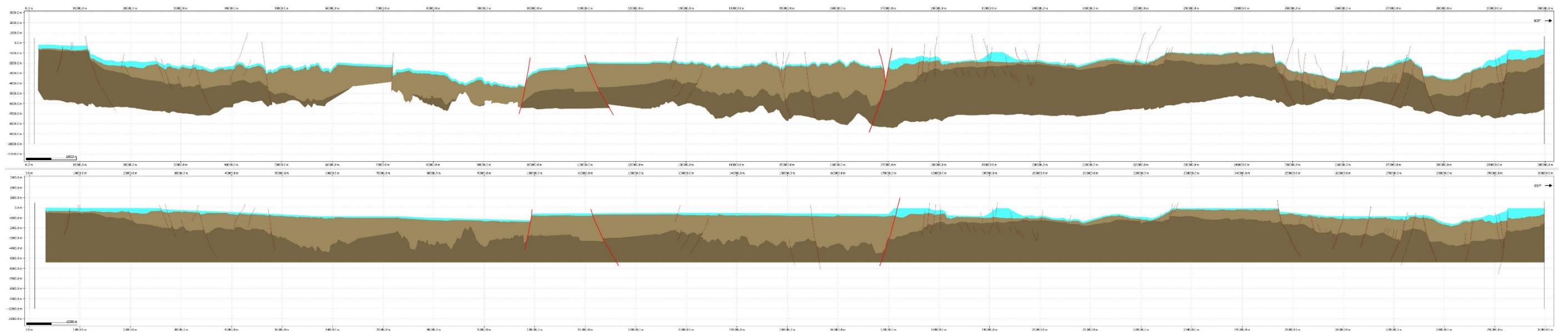


Figure 46: Central Section - lower Namurian removed and Dinantian restored to a paleo topography. Two time vertical exaggeration.

- The reconstruction of the paleo topography for the Dinantian was based on several different assumptions. (1) The tectonic activity during the Dinantian is difficult to assess because of the seismic resolution, especially in the deep basins. For the paleotopographic reconstruction it was therefore decided to keep the base of the Dinantian relatively flat. (2) The tops of the identified platforms should be at a paleo water depth of maximum 20-30 m (because of the scale of the reconstruction the depth was set to 50 m). (3) The thickness of the platforms determines the minimum paleo water depth between the platforms if there is no movement along the bounding faults during the Dinantian (resulting in a minimum paleo water depth of 800 m between platforms at the end of the Dinantian). This is especially relevant for the LTG platform as no bounding faults could be identified. (4) The Dinantian along the LBM developed on a shallow slope rather than as a platform which would be slowly deepening towards to NE. (5) Along some of the major structures (LT and NE boundary of the WNB) some Intra-Dinantian extensional fault movement can be envisioned, based on the depositional thickness of the Namurian.
- Three potential scenarios were discussed for the Frysland Platform. According to the seismic interpretation the Platform is mainly developed further W of the Central section and this is discussed in more detail in the Western section. However, the reconstruction suggests that the area was also a structural high during the Early Namurian in this section. The lack of platform carbonates in this area can be explained by either too high (> 50 m) or too low paleo water depth (top of the block remains at/close to the surface of the water and no space for platform growth is created). It is also possible that the Frysland Platform developed in a similar fashion as the other platforms. The three suggested scenarios are presented in the results section.

### 7.1.2. Fault kinematics

A total of 130 faults have been identified and restored along the Western (65) and Central (65) Sections. Figures 47 and 48 shows the location of these faults that have been named in reference to the structural elements that they belong to (e.g. F-WNB1 for the 1<sup>st</sup> fault in the south within the West Netherlands Basin). The kinematic analysis of these fault was carried out using a vertical fault throw technique developed by Cartwright *et al.* (1998). The numerical results of these analysis are presented in Tables 7 and 8. The graphical summary of these kinematic analysis is shown in Figures 49 and 50. The results regarding the fault activity per structural elements are presented in the updated structural chart (Appendix 5). Note that the reduced number of faults recognized as being active during the Late Devonian, Dinantian and Namurian within the WNB and CNB may be due to the limitations of seismic imaging in those deep basins.

#### Fault kinematics for the Western Section:

- Most faults throws are normal. Out of 174 fault throws measured, only 18 are reverse (Appendix 3).
- The predominance of reverse faulting occurred in the area spanning from the WNB to CNB, where 95 % of the reverse fault throws are measured (Figures 47, 49 and Appendix 3A).
- No obvious flower structures (indicative if strike slip motion) observed along this section.
- The oldest active faults, active during the Dinantian, are located on the Zeeland High and in the northern part of the WNB. This is different to the Central section that displays a few faults that are interpreted as having been active during the Devonian as well as some active Dinantian age faults present in the northern part or the Dutch onshore (LT and GP).
- The Namurian was a period of extension throughout the section (Figure 49).
- Some normal motions on several faults during the Westphalian are observed on the restored section but may be related to seismic misinterpretation of the base Westphalian horizon in area where it is poorly imaged (e.g. WNB and CNB). Some Westphalian fault movements may however be related to differential compaction of pre-existing fault blocks where variable thickness of Namurian strata were deposited.
- At the end of the Silesian (Latest Westphalian) some large reverse faults were active in the Northern part of the WNB (faults F-WNB34 and F-WNB/CNB) and in the central part of the CNB (fault F-CNB/NHP).
- A few Permian -age normal faults were active in the northern part of the section from the Vlieland Basin to the Groningen platform.
- Some early Cretaceous extension recognised in the southern part of the WNB and in the CNB (e.g. F-CNB14).
- Alpine active faults are recognized in the central and northern part of the WNB and the northern edge of the CNB.
- 35% (23 out of 65) of the faults observed have been reactivated at least once, with two faults in the WNB being reactivated at three different times (faults F-WNB27 and 34). (Figure 49).



### Fault kinematics for the Central Section:

- Most faults throws are normal. Out of 174 fault throws measured, only 17 are reverse (Appendix 3).
- The predominance of reverse faulting occurred in the area spanning from the WNB to CNB (including the PMC), where 94 % of the reverse fault throws are measured (Figures 48, 50 and Appendix 3B).
- Eight flower structures are observed and are interpreted to be mainly active during the Cretaceous (6), but a few were active during different periods such as the Permian (1) and Cenozoic (1) (Figures 48 and 50).
- The oldest active faults are predominantly located in the northern part of the sections (Lauwerszee Trough) where a thick Namurian basin fill developed in response to continued extension on the flanks and within the trough. A few late Devonian and Dinantian faults were also active in the southern part of the section in the ZH and OP.
- The Silesian (Namurian and Westphalian) was a period of extension in the area extending from the Zeeland High to the Central Netherlands Basin (Figure 50). Farther north, from the Texel-IJsselmeer High to Groningen Platform, the faulting is primarily Devonian to Namurian in age, with a few Westphalian and Permian faults active in the transitional area between the LT and GP.
- Within the West Netherlands Basin, the normal faults active during the Triassic and Jurassic are not active at the same time everywhere. The faults in the southern part of the WNB (e.g. faults F-OP/WNB or F-WNB1) are younger (Late Jurassic) than the one in the northern part of the WNB (e.g. faults F-WNB10 to 12) (see Figure 50).
- In the Lauwerszee Trough the Devonian to Late Namurian faults are getting active later from north to south, indicative of a translation of active faulting southward through time, and indicative of an overall asymmetric half graben growth dynamic.
- 38% (25 out of 65) of the faults observed have been reactivated at least once, with the Raalte Boundary Fault that separates the CNB and the TIJH that was active at five different times (Figure 50).

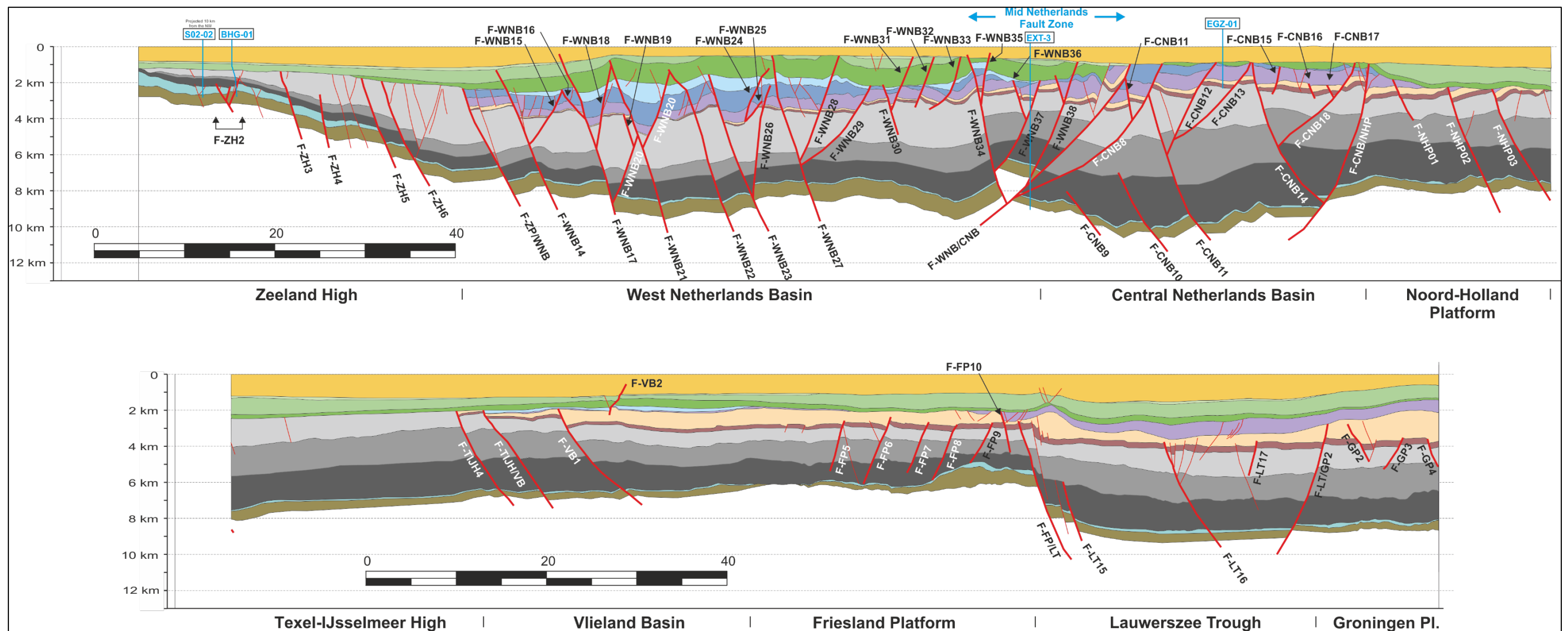


Figure 47: Present-Day configuration of the Western Section showing the named faults (shown with as thicker red lines) analysed in term of kinematics. The section is cut in two parts for easier viewing. See Table 7 and Appendix 3A for additional information regarding those faults. See Figure 49 for fault growth plots. See Figure 12 for location map.



Table 7: Western Section fault characteristics.

Faults	Type	Dip Direction	Structural Element	Stratigraphic Level	Note
F-ZH2	Normal	Variable	Zeeland Platform (ZP)	Basement to Namurian	
F-ZH3	Normal	Northeast	Zeeland Platform (ZP)	Basement to Westphalian	
F-ZH4	Normal	Northeast	Zeeland Platform (ZP)	Basement to Westphalian	
F-ZH5	Flower structure	Northeast	Zeeland Platform (ZP)	Basement to Westphalian	
F-ZH6	Normal	Northeast	Zeeland Platform (ZP)	Basement to Westphalian	
F-ZP/WNB	Normal	Northeast	Fault bounding ZP and WNB	Basement to Upper Jurassic	
F-WNB14	Normal	Northeast	West Netherlands Basin (WNB)	Basement to Upper Jurassic	
F-WNB15	Normal and reverse	Southwest	West Netherlands Basin (WNB)	Westphalian to Upper Jurassic	
F-WNB16		Northeast	West Netherlands Basin (WNB)	Westphalian to Upper Jurassic	
F-WNB17		Northeast	West Netherlands Basin (WNB)	Basement to Cenozoic	
F-WNB18		Southwest	West Netherlands Basin (WNB)	Westphalian to Lower Cretaceous	
F-WNB19		Northeast	West Netherlands Basin (WNB)	Westphalian to Permian	
F-WNB20		Southwest	West Netherlands Basin (WNB)	Basement to Lower Cretaceous	
F-WNB21		Northeast	West Netherlands Basin (WNB)	Basement to Lower Cretaceous	
F-WNB22		Northeast	West Netherlands Basin (WNB)	Basement to Lower Cretaceous	
F-WNB23		Northeast	West Netherlands Basin (WNB)	Basement to Upper Jurassic	
F-WNB24		Southwest	West Netherlands Basin (WNB)	Permian to Lower Cretaceous	
F-WNB25		Southwest	West Netherlands Basin (WNB)	Permian to Lower Jurassic	
F-WNB26		Southwest	West Netherlands Basin (WNB)	Basement to Lower Jurassic	
F-WNB27		Northeast	West Netherlands Basin (WNB)	Basement to Upper Cretaceous	
F-WNB28		Southwest	West Netherlands Basin (WNB)	Basement to Upper Cretaceous	
F-WNB29		Southwest	West Netherlands Basin (WNB)	Namurian to Upper Jurassic	
F-WNB30		Northeast	West Netherlands Basin (WNB)	Westphalian to Lower Cretaceous	
F-WNB31		Southwest	West Netherlands Basin (WNB)	Westphalian to Danian	
F-WNB32		Southwest	West Netherlands Basin (WNB)	Westphalian to Danian	
F-WNB33		Southwest	West Netherlands Basin (WNB)	Westphalian to Danian	
F-WNB34		Northeast	West Netherlands Basin (WNB)	Basement to Cenozoic	
F-WNB35		Southwest	West Netherlands Basin (WNB)	Westphalian to Cenozoic	
F-WNB36		Northeast	West Netherlands Basin (WNB)	Namurian to Lower Jurassic	
F-WNB37		Southwest	West Netherlands Basin (WNB)	Basement to Lower Jurassic	
F-WNB38		Southwest	West Netherlands Basin (WNB)	Basement to Danian	
F-WNB/CNB		Southwest	Fault bounding WNB and CNB	Basement to Danian	
F-CNB8		Southwest	Central Netherlands Basin	Basement to Lower Cretaceous	
F-CNB9		Northeast	Central Netherlands Basin	Basement to Namurian	
F-CNB10		Northeast	Central Netherlands Basin	Basement to Namurian	
F-CNB11		Northeast	Central Netherlands Basin	Basement to Lower Jurassic	
F-CNB12		Southwest	Central Netherlands Basin	Namurian to Loertt Jurassic	
F-CNB13		Southwest	Central Netherlands Basin	Namurian to Lower Cretaceous	
F-CNB14		Northeast	Central Netherlands Basin	Basement to Lower Jurassic	
F-CNB15		Southwest	Central Netherlands Basin	Westphalian to Lower Jurassic	
F-CNB16		Northeast	Central Netherlands Basin	Westphalian to Triassic	
F-CNB17		Northeast	Central Netherlands Basin	Westphalian to Triassic	
F-CNB18		Southwest	Central Netherlands Basin	Namurian to Lower Cretaceous	
F-CNB/NHP		Southwest	Fault bounding PMC and NHP	Basement to Lower Cretaceous	
F-NHP1		Northeast	Noord-Holland Ptaform	Namurian to Triassic	
F-NHP2		Northeast	Noord-Holland Ptaform	Basement to Triassic	
F-NHP3		Northeast	Noord-Holland Ptaform	Basement to Triassic	
F-TIJH4		Northeast	Texel-IJsselmeer High	Basement to Permian	
F-TIJH/VB		Northeast	Fault bounding TIJH and VB	Basement to Upper Jurassic	
F-VB1		Northeast	Vlieland Basin	Basement to Triassic	
F-VB2		Northeast	Vlieland Basin	Permian to Cenozoic	
F-FP5		Southwest	Friesland Plateform	Namurian to Permian	
F-FP6		Southwest	Friesland Plateform	Namurian to Permian	
F-FP7		Southwest	Friesland Plateform	Namurian to Permian	
F-FP8		Southwest	Friesland Plateform	Namurian to Permian	
F-FP9		Southwest	Friesland Plateform	Namurian to Permian	
F-FP10		Northeast	Friesland Plateform	Namurian to Triassic	
F-FP/LT		Northeast	Fault bounding FP and LT	Basement to Permian	
F-LT15		Northeast	Lawerszee Trough	Basement to Namurian	
F-LT16		Northeast	Lawerszee Trough	Basement to Permian	
F-LT17		Southwest	Lawerszee Trough	Westphalian to Permian	
F-LT/GP2		Southwest	Fault bounding LT and GP	Basement to Permian	
F-GP2		Northeast	Groningen Platform	Westphalian to Permian	
F-GP3		Southwest	Groningen Platform	Namurian to Permian	
F-GP4		Northeast	Groningen Platform	Namurian to Permian	



Table 8: Central Section fault characteristics.

Faults	Type	Dip Direction	Structural Element	Stratigraphic Level	Note
F-ZH1	Normal	Northeast	Zeeland Platform (ZP)	Basement to Westphalian	
F-ZH/OP	Normal	Northeast	Fault bounding ZE and OP	Namurian to Triassic	
F-OP1	Normal	Northeast	Oosterhout Platform (OP)	Basement to Dinantian	
F-OP2	Flower structure	Variable	Oosterhout Platform (OP)	Basement to Westphalian	As series of flower structures likely active during the Jurassic and /or Cretaceous
F-OP3	Normal	Northeast	Oosterhout Platform (OP)	Basement to Triassic	A fault zone with fault segment rather than a single fault plane
F-OP/WNB	Normal	Northeast	Fault bounding OP and WNB	Basement to Upper Jurassic	
F-WNB1	Normal and reverse	Southwest	West Netherlands Basin (WNB)	Namurian to Lower Cretaceous	
RF	Normal	Southwest	West Netherlands Basin (WNB)	Basement to Upper Cretaceous	Rijen Fault
F-WNB2	Normal	Southwest	West Netherlands Basin (WNB)	Westphalian to Upper Jurassic	
F-WNB3	Normal and reverse	Southwest	West Netherlands Basin (WNB)	Westphalian to Upper Jurassic	
F-WNB4	Normal	Southwest	West Netherlands Basin (WNB)	Westphalian to Lower Jurassic	
F-WNB5	Normal	Southwest	West Netherlands Basin (WNB)	Namurian to Upper Jurassic	
F-WNB6	Normal	Southwest	West Netherlands Basin (WNB)	Westphalian to Upper Jurassic	
F-WNB7	Normal and reverse	Northeast	West Netherlands Basin (WNB)	Namurian to Upper Jurassic	
F-WNB8	Normal	Southwest	West Netherlands Basin (WNB)	Basement to Lower Jurassic	
F-WNB9	Normal	Northeast	West Netherlands Basin (WNB)	Basement to Lower Jurassic	This is a fault zone rather than a single fault
F-WNB10	Normal	Northeast	West Netherlands Basin (WNB)	Westphalian to Upper Jurassic	
F-WNB11	Normal	Northeast	West Netherlands Basin (WNB)	Westphalian to Lower Jurassic	
F-WNB12	Normal	Northeast	West Netherlands Basin (WNB)	Zechstein to Lower Jurassic	
F-WNB13	Normal	Northeast	West Netherlands Basin (WNB)	Zechstein to Lower Jurassic	
PBF1/2	Normal and reverse	Southwest	West Netherlands Basin (WNB)	Basement to Upper Jurassic	The Peel Boundary Fault is a fault system that include a series of faults and duplexes.
F-WNB/PMC	Normal and reverse	Southwest	Fault bounding WNB and PMC	Basement to Triassic	
F-PMC1	Normal	Northeast	Peel-Massbommel Complex	Basement to Triassic	
F-PMC2	Normal	Northeast	Peel-Massbommel Complex	Westphalian to Upper Cretaceous	
F-PMC3	Reverse	Southwest	Peel-Massbommel Complex	Westphalian to Triassic	
F-PMC4	Normal	Northeast	Peel-Massbommel Complex	Permian to Upper Cretaceous	
F-PMC5	Normal	Northeast	Peel-Massbommel Complex	Permian to Upper Cretaceous	
F-PMC6	Normal	Northeast	Peel-Massbommel Complex	Basement to Lower Cretaceous	
F-PMC7	Normal	Northeast	Peel-Massbommel Complex	Westphalian Upper to Cretaceous	
F-PMC8	Normal	Northeast	Peel-Massbommel Complex	Permian to Upper Cretaceous	
F-PMC9	Normal	Southwest	Peel-Massbommel Complex	Permian to Upper Cretaceous	
F-PMC10	Normal	Northeast	Peel-Massbommel Complex	Permian to Upper Cretaceous	
F-PMC11	Normal	Northeast	Peel-Massbommel Complex	Namurian to Cenozoic	
TBF	Normal and reverse	Southwest	Fault bounding PMC and CNB	Basement to Cenozoic	Tegelen Boundary Fault
F-CNB1	Normal	Northeast	Central Netherlands Basin	Namurian to Triassic	
F-CNB2	Normal	Southwest	Central Netherlands Basin	Basement to Triassic	
F-CNB3	Normal	Northeast	Central Netherlands Basin	Basement to Triassic	
F-CNB4	Normal	Northeast	Central Netherlands Basin	Basement to Westphalian	
F-CNB5	Normal	Northeast	Central Netherlands Basin	Rotliegend to Triassic	
F-CNB6	Normal	Northeast	Central Netherlands Basin	Basement to Upper Jurassic	
F-CNB7	Normal and reverse	Southwest	Central Netherlands Basin	Zechstein to Upper Jurassic	
RBF	Normal and reverse	Southwest	Fault bounding CNB and TIJH	Basement to Upper Cretaceous	Raalte Boundary Fault
F-TIJH1	Flower structure	Variable	Texel-IJsselmeer High	Devonian to Cenozoic	
F-TIJH2	Flower structure	Variable	Texel-IJsselmeer High	Basement to Cenozoic	
F-TIJH3	Flower structure	Variable	Texel-IJsselmeer High	Basement to Upper Cretaceous	
F-FP1	Flower structure	Variable	Friesland Platform	Zechstein to Cenozoic	
F-FP2	Normal	Northeast	Friesland Platform	Westphalian	
F-FP3	Normal	Northeast	Friesland Platform	Zechstein to Upper Cretaceous	
F-FP4	Normal	Southwest	Friesland Platform	Zechstein to Triassic	
F-FP/LT	Normal	Northeast	Fault bounding FP and LT	Basement to Namurian	
F-LT1	Flower structure	Variable	Lauwerszee Trough	Namurian to Zechstein	
F-LT2	Flower structure	Variable	Lauwerszee Trough	Basement to Westphalian	
F-LT3	Normal	Northeast	Lauwerszee Trough	Basement to Zechstein	
F-LT4	Normal	Southwest	Lauwerszee Trough	Westphalian to Upper Cretaceous	Normal fault F-LT5 transitions upward into flower structure F-LT6, indicating that this fault system was originally a normal fault that was later reactivated as a strike slip system.
F-LT5	Normal	Southwest	Lauwerszee Trough	Basement to Namurian	
F-LT6	Flower structure	Variable	Lauwerszee Trough	Namurian to Zechstein	
F-LT7	Normal	Southwest	Lauwerszee Trough	Basement to Namurian	
F-LT8	Normal	Northeast	Lauwerszee Trough	Zechstein to Cenozoic	
F-LT9	Normal	Southwest	Lauwerszee Trough	Namurian to Zechstein	
F-LT10	Normal	Northeast	Lauwerszee Trough	Basement to Namurian	
F-LT11	Normal	Northeast	Lauwerszee Trough	Namurian to Zechstein	
F-LT12	Normal	Southwest	Lauwerszee Trough	Basement to Zechstein	
F-LT13	Normal	Southwest	Lauwerszee Trough	Namurian to Zechstein	
F-LT/GP	Normal	Southwest	Fault bounding LT and GP	Basement to Dinantian	
F-GP1	Normal	Northeast	Groningen Platform	Zechstein to Triassic	

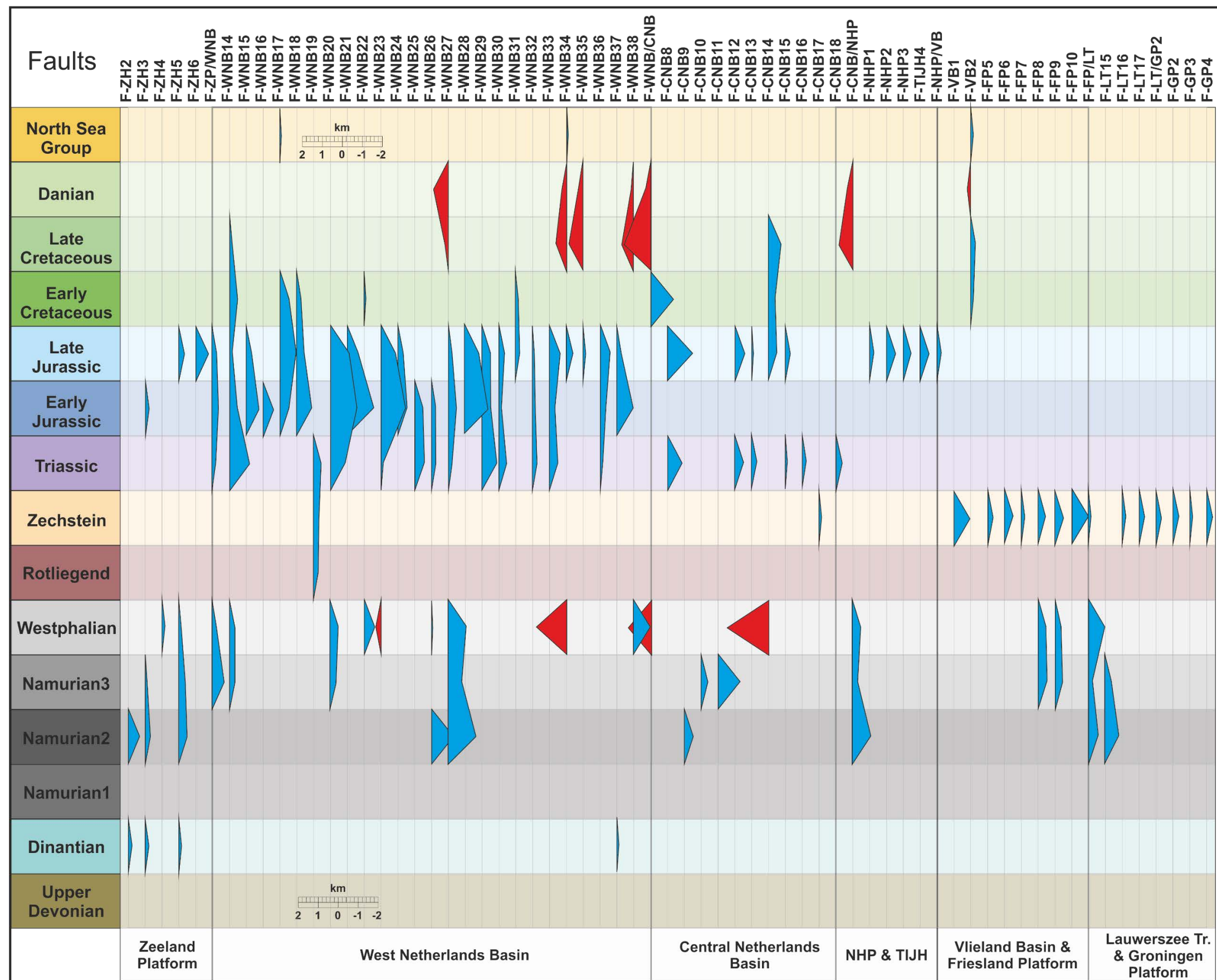


Figure 49: Fault kinematic summary chart showing the growth history for all the 65 main faults present on the Western Section. Red polygons show reverse fault throws and blue polygons show normal fault throw. The amplitude of the polygon at each time step is proportional to the throw measured for each structural restoration step. The vertical scale in km is show in the chart.



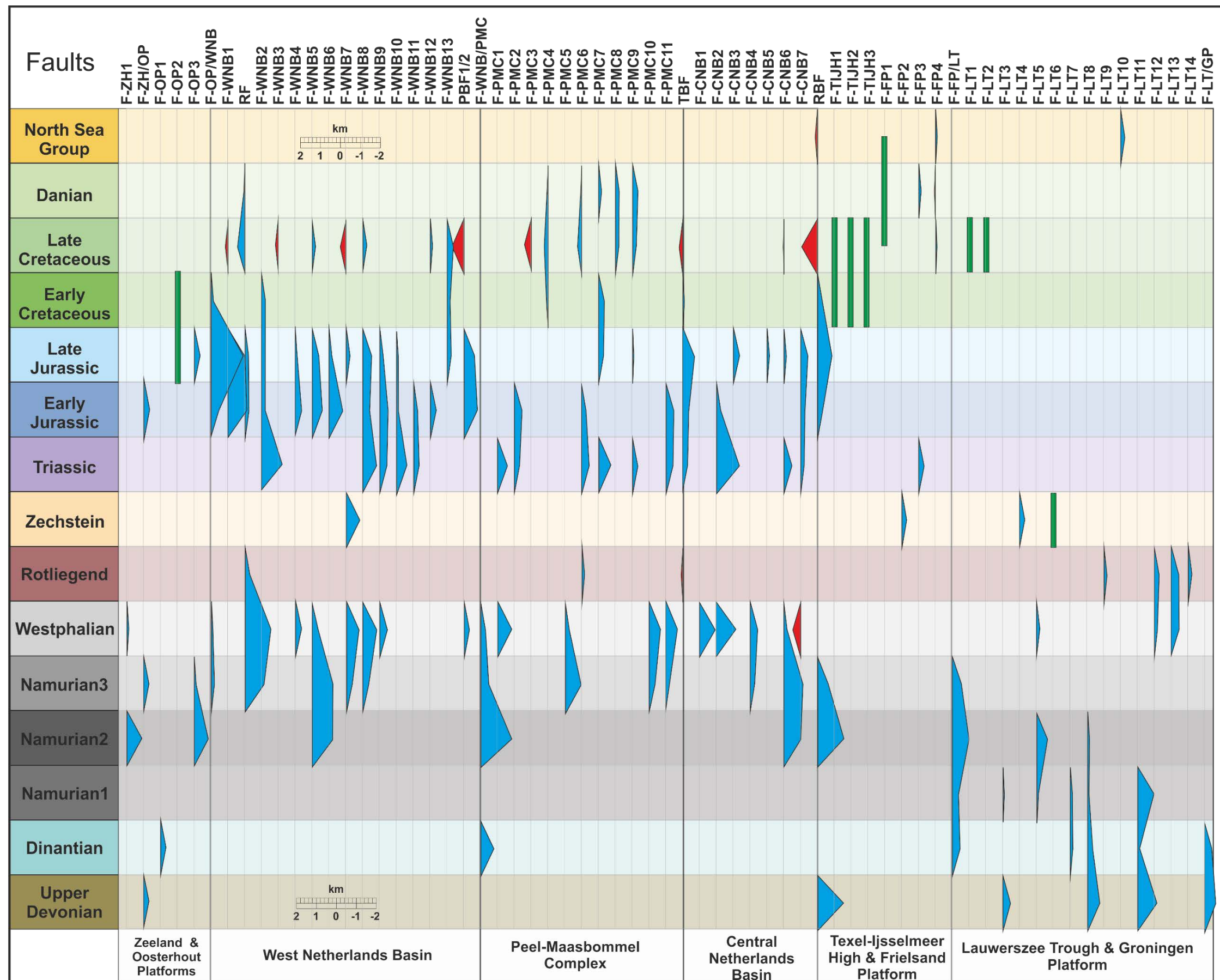


Figure 50: Fault kinematic summary chart showing the growth history for all the 65 main faults present on the Central section. Red polygons show reverse fault throws and blue polygons show normal fault throw. The amplitude of the polygon at each time step are proportional to the throw measured for each structural restoration steps. The vertical scale in km is show in the chart.

### 7.1.3. Geological results

The two structural restorations give new insights on the geological evolution of the Dutch onshore. The main results from each restoration are presented below as well as compiled in an updated version of the summary chart (Appendix 5).

#### 7.1.3.1. Western Section

All the results below are based summaries from the analytical results presented in Figures 47, 49 and 51 and in Appendix 3A.

During the **Neogene**, only minor faulting occurred, in the WNB and VB with a maximum of 100 m of normal offset.

During the **Late Cretaceous to Paleogene** the Alpine Orogen triggered uplift and inversion of pre-existing faults in the WNB (up to 850 m of reverse motion along fault F-WNB35) and in the CNB (up to 1630 m for the bounding fault between the WNB and the CNB, fault F-WNB/CNB). These reverse faults are observed in the area extending from the central part of the WNB to the northern part of the VB. This upper part of the Chalk Group (Danian) was likely not deposited above the uplifted WNB and CNB, except possibly topographically low areas located between the growth anticlines. The northern onshore area (TIJH to GP) was also subject to uplift but in the form of low amplitude folding with the anticlinal axis located above the VB and the GP.

During the **Early Cretaceous** (Rijnland Group), all active faults were normal and were present in the WNB, CNB and VB, and had a maximum offset of 1300 m in the southern part of the CNB (fault F-CNB9).

During the **Middle Jurassic to Ryazanian** (Schieland Group), all observed active faults are normal with vertical throw up to 1300 m on the southern part of the CNB (fault F-CNB8). For this period, no active faults are observed north of the TIJH. The Mid-Cimmerian unconformity that defines the base of this unit, eroded differentially the structural elements in the Dutch onshore:

- ZH had 1150 to 2450 m of Westphalian to Lower Jurassic eroded.
- WNB and CNB only had limited amount of Lower Jurassic and Triassic eroded (0 to 800 m).
- NHP and TIJH 600 m to up to 2450 m of Westphalian, Permian, Triassic to Lower Jurassic eroded.
- VB and FP had up to 2000 m of Permian, Triassic to Lower Jurassic eroded
- LT and GP had 1100 m of Triassic and Jurassic eroded.

During the **Early Jurassic** (Altena Group), all observed active faults are normal faults with vertical throw up to 1400 m in the WNB and 1300 m in the CNB. Active faults are observed exclusively in the southern and central part of the Dutch onshore (ZH to TIJH) and no active faults observed north of the TIJH.

During **Triassic**, all observed active faults are normal faults with vertical throw up to 1 km in the southern part of the WNB (fault F-WNB14). Active faults are observed exclusively in the WNB and the CNB and no Triassic fault has been identified on the highs and platforms.

During the **Permian**, a few normal faults were active. These active faults are primarily observed in the northern part of the section (VB to GP) and were active during Zechstein deposition. Only one fault active during the deposition of the Rotliegend is observed in the southern part of the WNB (fault F-WNB18). The maximum offset is observed on the bounding fault located between the CNB and the NHP (fault F-CNB/NHP) with 800 m of offset recorded. The BPU, which defined the base of this unit, erodes differentially the different structural elements:

- ZH had 0 in the north to 1.9 km in the south of Westphalian eroded.
- WNB 0 to 1500 m (in the north) of Westphalian eroded.
- CNB had up to 1200 m in the south, and up to 1500 m in the north of Westphalian eroded. The central part of the CNB was likely not uplifted and eroded but rather the northern and southern part of the basin accommodated the main uplift.
- NHP and TIJH had between 850 and 1900 m of Westphalian eroded.
- VB and FP had between 1600 and 2350 m of Westphalian eroded.
- LT and GP had between 700 m to 1900 m of Westphalian eroded.

During the **Westphalian**, a few normal faults were active in most of the structural elements, except in the TIJH and GP. The maximum normal fault throws are observed in the WNB (800 and 900 m) and on the bounding fault between the TIJH and VB (800 m). The modelled burial of the southern part of Zeeland High during the Westphalian is tremendous with up to 4400 m of burial of the platform during that period. Four reverse faults active during the Westphalian (and likely the Stephanian) have been restored. The vertical offset range from 350 m to 2200 m on the fault F-CNB14 located in the central part of the CNB.

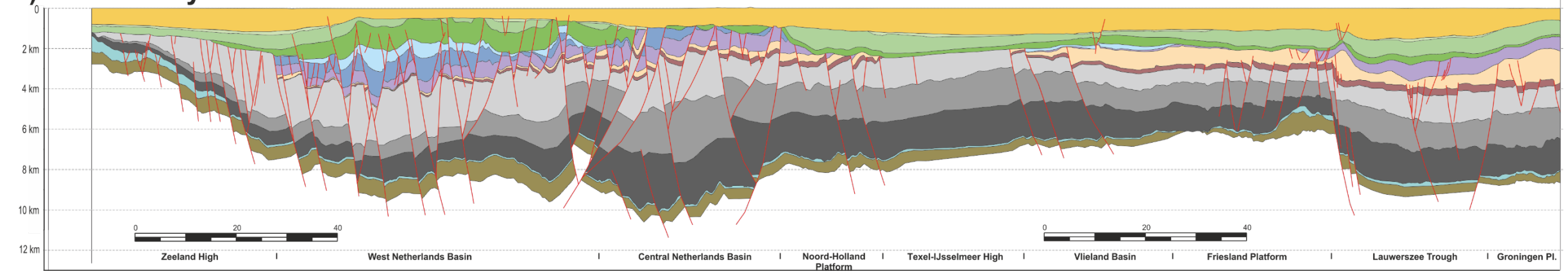
During the **Namurian** all active faults are normal, with some of them showing large vertical offset up to 2000 m on the central part of the WNB. Normal faults were active in the ZH, WNB, CNB, FP and LT. During the Namurian, the Dutch onshore basin centre was located at the location of the CNB with a possible second depocenter located below LT/GP. The two basins were separated by a structural high located in the southern part of the Friesland Platform, which possibly hosted a Dinantian carbonate platform. The exact geometry of that zone during the Devonian is unclear and no Devonian or Dinantian age faulting was observed along this section. Additional seismic mapping around this area should elucidate the relationship between this structural high during the Namurian and its possible presence prior.

During the **Dinantian**, five normal faults are interpreted as being active. They are located in the ZH and have a with maximum modelled offset of 200 m. The modelled paleo water depth varies to a few tens of meters in ZH, to around 500 m in the rest of the section, beside the carbonate platform likely present in the northern part of the FP.

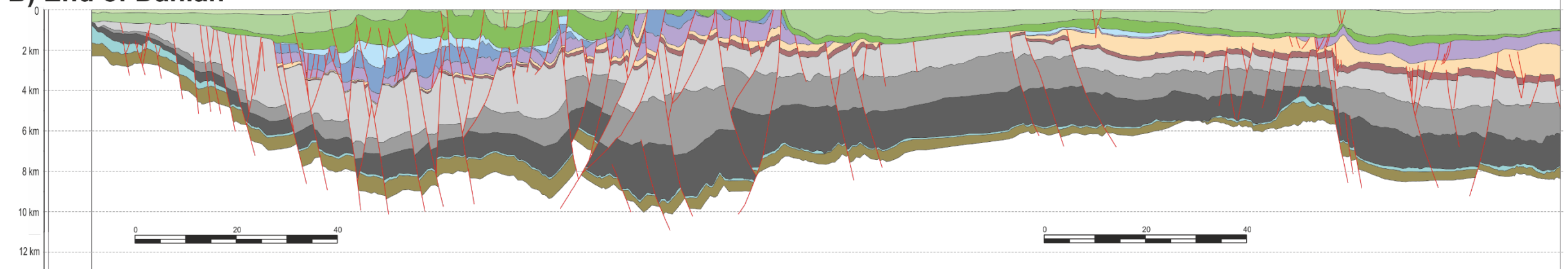
During the **Late Devonian**, only one normal fault was interpreted as being active on this section, fault F-WNB37 with 100 m of offset.

Note that the period with the largest amount of contraction measured along this section occurred (see Appendix 4A): 1) during the Middle Cretaceous to Present Day, with 0,7% (2.4 km) contraction ; and 2) during the Westphalian with 2.9 % (8.5 km) contraction. The maximum amount of extension occurred during 1) the Namurian with 0.8 % (2.5 km) of extension. and 2) during the Triassic to early Cretaceous with 2% (6 km) of extension.

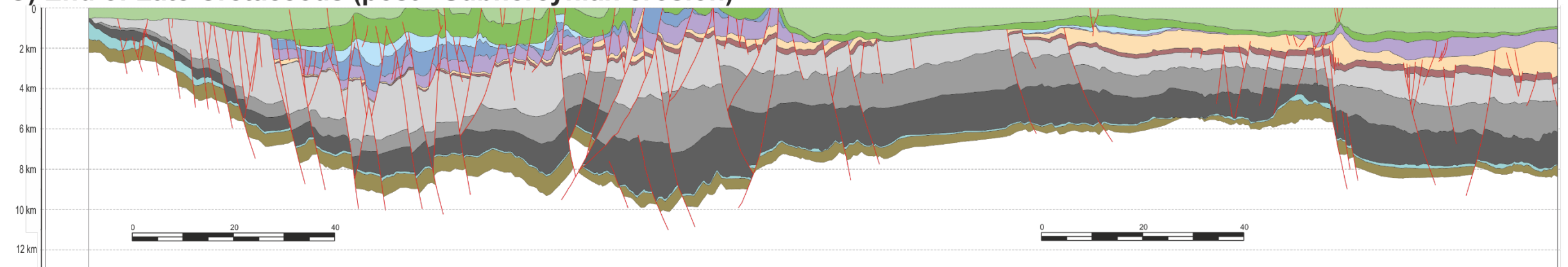
**A) Present Day**



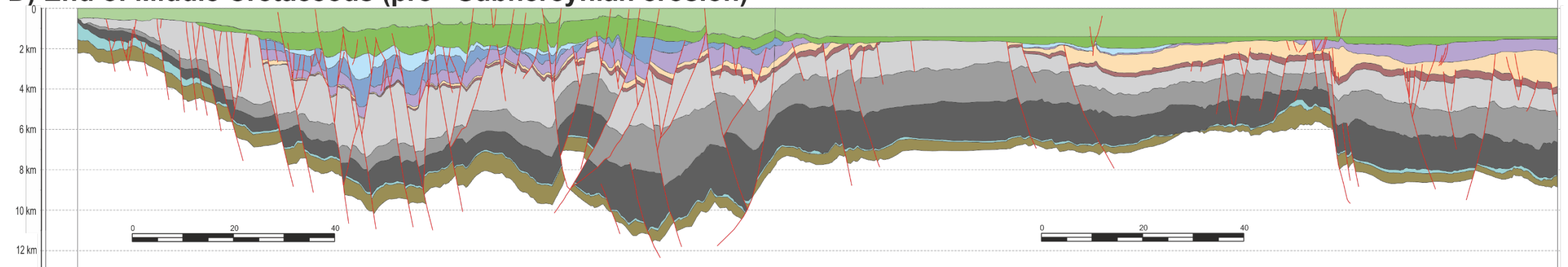
**B) End of Danian**



**C) End of Late Cretaceous (post - Subhercynian erosion)**

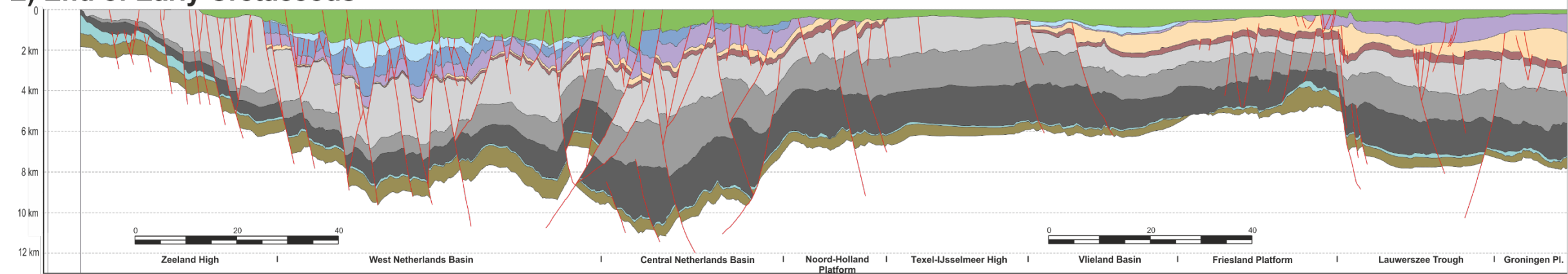


**D) End of Middle Cretaceous (pre - Subhercynian erosion)**

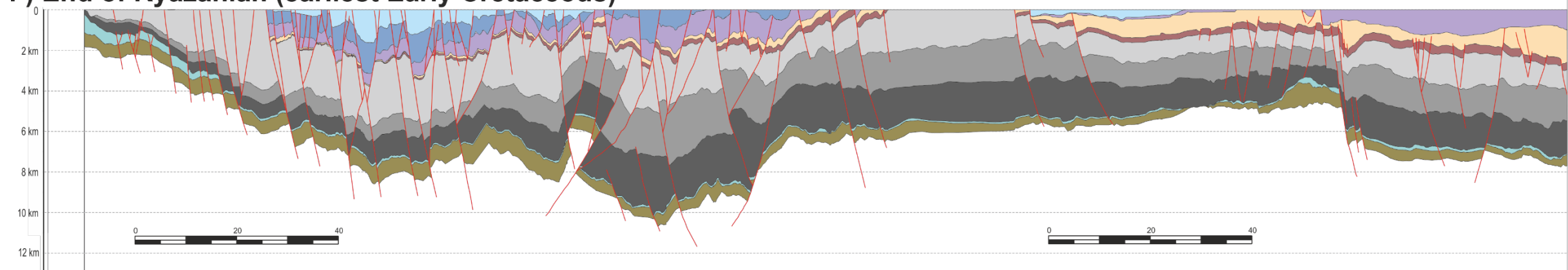




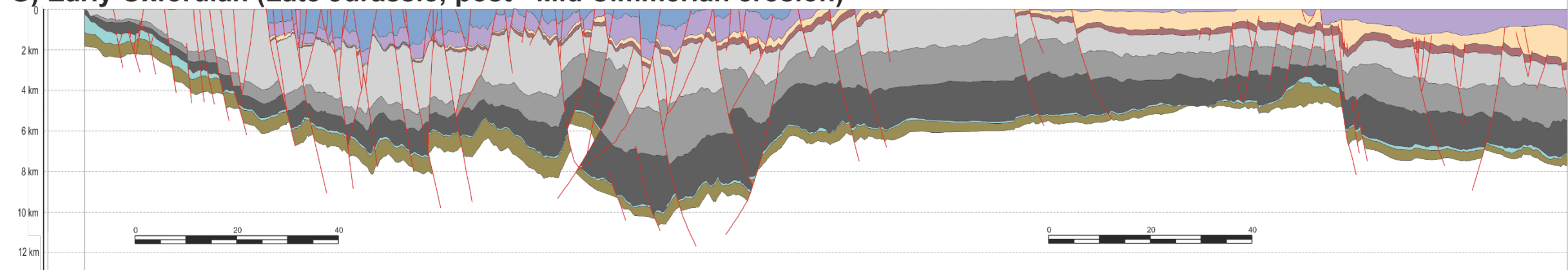
**E) End of Early Cretaceous**



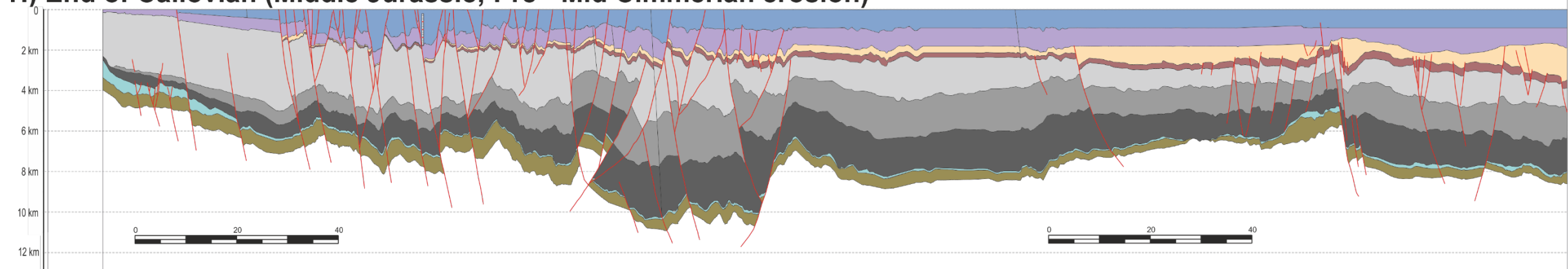
**F) End of Ryazanian (earliest Early Cretaceous)**



**G) Early Oxfordian (Late Jurassic; post - Mid Cimmerian erosion)**

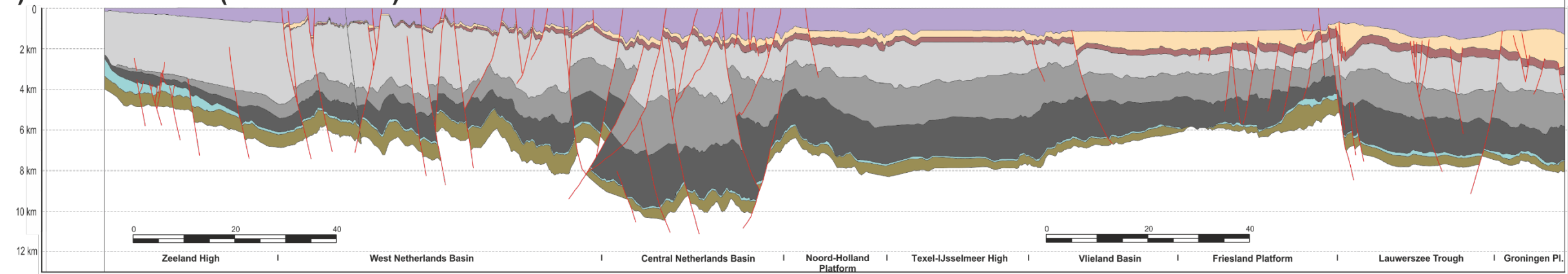


**H) End of Callovian (Middle Jurassic; Pre - Mid Cimmerian erosion)**

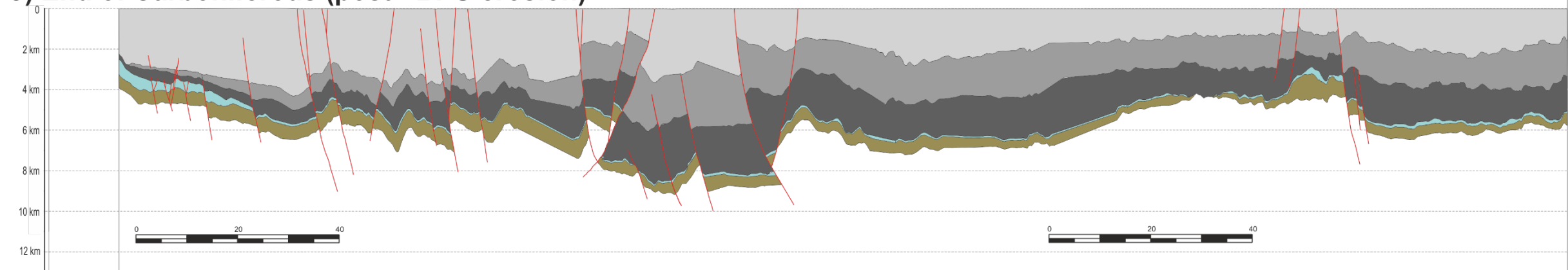




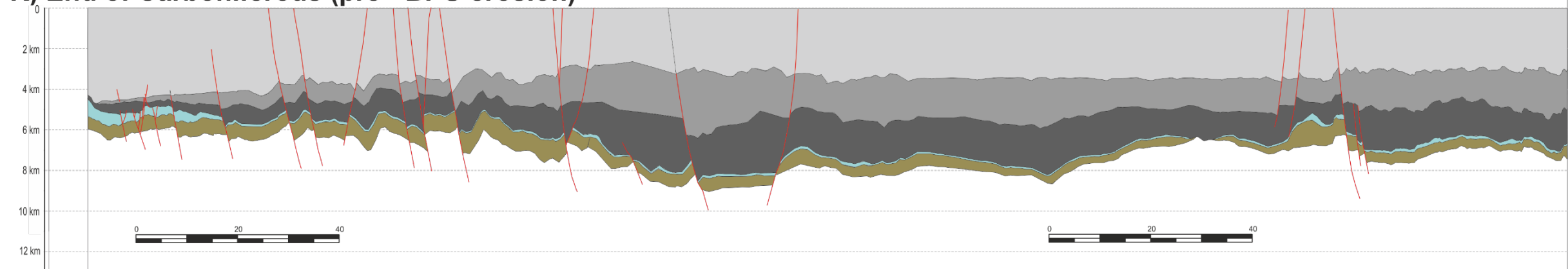
**I) End of Norian (Late Triassic)**



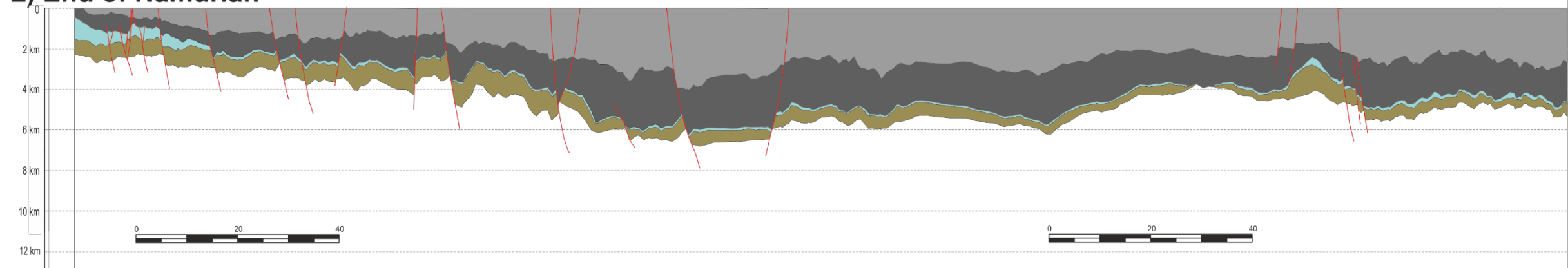
**J) End of Carboniferous (post - BPU erosion)**



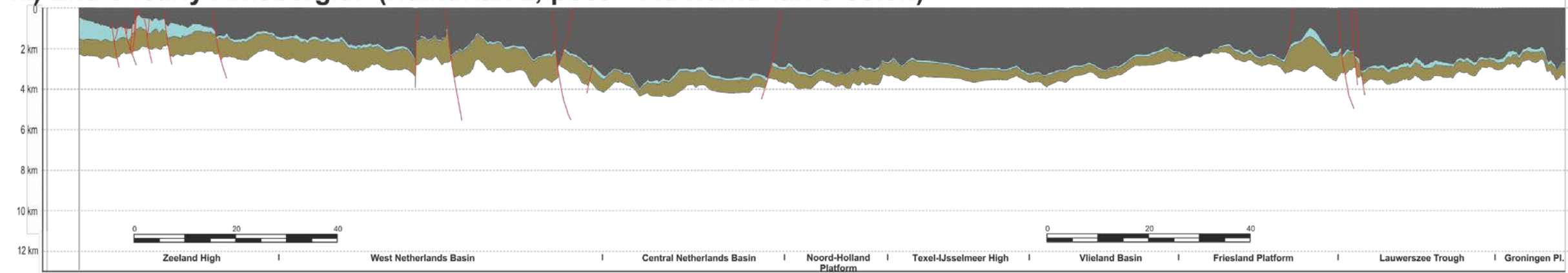
**K) End of Carboniferous (pre - BPU erosion)**



**L) End of Namurian**



**M) End of early Arnsbergian (Namurian 2; post - Mid Namurian erosion)**



**N) End of Dinantian**

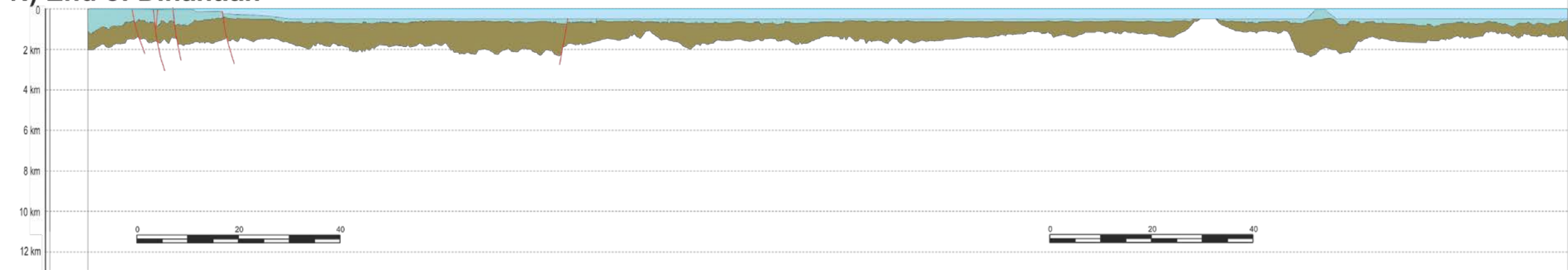


Figure 51 (this and previous three pages): Western Section restoration results. The vertical exaggeration is four times. Faults are shown in red and stratigraphic units colours are the same as shown in Figure 16. The sea level is shown for steps N.

#### 7.1.3.2. Central Section

All the results below are based summaries from the analytical results presented in Figures 48, 50 and 52, and in Appendix 3B.

During the **Neogene**, only minor faulting occurred, in CNB, TIJH and LT, with a maximum of 200 m of offset.

During the **Late Cretaceous to Paleogene** the Alpine Orogen triggered uplift in the WNB (600 m) and in the CNB (550 m) as well as predominantly (55 % of the active faults observed) compressional structures in the form of reverse faults. These reverse faults are observed in the WNB, with maximum offset of 630 m; in the PMC, with maximum offset of 60 m; in the CNB, with maximum offset of 800 m on the Raalte Boundary Fault; and in the FP, with maximum offset 40 m. During this period, several strike slip structures were also active in the TIJH, FP and LT. Normal faulting also occurred in the WNB (maximum offset of 300 m), PMC (maximum offset of 500 m), in the PF (maximum offset of 100 m) maximum offset of 300 m. This upper part of the Chalk Group (Danian) was not deposited in the northern 2/3 of the WNB (Figure 52B) and neither above the inverted CNB. During the deposition of the lower Chalk Group, the basin started to invert but a thin lower Chalk Group drape (maximum 200 m thick) covered the WNB and CNB (Figure 52D).

During the **Early Cretaceous** (Rijnland Group), most active faults were normal (95% of the faults observed) and were present in the WNB, PMC and CNB, with a maximum offset of 280 m in the PMC. A few strike slip structures were active in the OP and TIJH. The southern limit of the Rijnland Group was the southern part of the WNB with a maximum thickness deposited over the TIJH (up to 500 m, decompacted).

During the **Middle Jurassic to Ryazanian** (Schieland Group), all observed active faults are normal faults with vertical throw up to 1600 m on the southern boundary faults of the WNB (F-OP/WNB, Figure 52). Active faults are observed exclusively in the southern part of the Dutch onshore (OP to CNB). The Mid-Cimmerian unconformity that defines the base of this unit, eroded differentially the structural elements in the Dutch onshore:

- ZH had 800 to 1700 m of Westphalian to Lower Jurassic eroded.
- OP had 700 to 900 m of Triassic to Lower Jurassic eroded.
- WNB only had limited amount of Lower Jurassic eroded.
- PMC had up to 600 m of Triassic and Lower Jurassic eroded.
- CNB had up to 2100 m of Triassic to Lower Jurassic eroded.
- TIJH had up to 2300 m of Westphalian, Permian, Triassic to Lower Jurassic eroded.
- FP had up to 2000 m of Permian, Triassic to Lower Jurassic eroded.
- LT had between 900 m to 2000 m of Triassic and Jurassic eroded.
- GP had 2000 m of Permian to Lower Jurassic eroded.

During the **Early Jurassic** (Altena Group), all observed active faults are normal faults with vertical throw up to 1000 m in the WNB. Active faults are observed exclusively in the southern and central part of the Dutch offshore (OP to CNB).

During **Triassic**, all observed active faults are normal faults with vertical throw up to 1200 m in the CNB. Active faults are observed exclusively in the central part of the Dutch onshore

(northern half of the WNB to FP). Note that from the Triassic to the Late Jurassic, the main location of extension/rifting shifts southward (Figure 50).

During the **Permian**, a few faults were active, predominantly as normal faults (83%). These active faults are observed everywhere except in the south (ZH and OP). The maximum offset is in the WNB with 250 m (Rijen Fault). The BPU, which defined the base of this unit, erodes differentially the different structural elements:

- ZH had 1500 to 2400 m of Westphalian eroded.
- OP had 800 to 1600 m of Westphalian eroded.
- WNB 100 to 1500 m of Westphalian eroded.
- PMC had 1100 to 2100 m of Westphalian eroded.
- CNB had up to 1300 m of Westphalian eroded, locally even up to 2800 m in the northern part of the CNB.
- TIJH had 1600 m of Westphalian eroded.
- FP had up to 1300 of Westphalian eroded.
- LT had between 800 to 2500 m of Westphalian eroded.
- GP had 2500 m of Westphalian eroded.

During the **Westphalian**, many normal faults show as being active during the Westphalian in most of the structural elements, except in the TIJH and GP. Note, however, that the Westphalian is not known to be a major period of extension in the Dutch sector. These kinematic results may locally be due to the difficulty to identify precisely the base Westphalian on seismic beneath the WNB and the CNB, and therefore may have introduced some error in the kinematic analysis at those locations. The modelled burial of the southern part of Zeeland High during the Westphalian is tremendous with up to 4200 m of burial of the platform during that period.

During the **Namurian** all active faults are normal, with some of them showing large vertical offset up to 2000 m on the northern boundary fault of the WNB, 1800 m on the northern Boundary fault of the CNB (Raalte Boundary Fault), and 1500 m on the southern boundary fault of the LT. The modelled paleo water depth of the early part of the Namurian is estimated at around 900 m. During the early part of the Namurian, LT was still divided into two sub basins, with a fault-bounded structural high separating the two.

During the **Dinantian**, eight normal faults are interpreted as being active. They are primarily located in the LT (with maximum modelled offset of 370 m) with isolated faults in OP (250 m of offset) and at the southern limit of the WNB (650 m of offset). The modelled paleo water depth varies to a few tens of meters in ZH/OP, to around 1300 m in the southern part of WNB, to 400-800 m in PMC, CNB, TIJH and FP, and between 400 and 1300 m in LT.

During the **Late Devonian**, a few normal faults were active in the southern (ZH/OP) and northern part of the section (LT). It is possible than more faults may have been active beneath the WNB and CNB but seismic quality in those areas did not permit to identify clearly the Devonian and Dinantian intervals. The faults observed show maximum normal offsets the LT with five faults showing throws greater than 400 m, with a maximum of 1000 m (F-LT11).

Note that the limited seismic data, and locally the limited seismic interpretation, may underrepresent to number of active faults during the Dinantian and the Late Devonian. This



should be the focus of additional seismic interpretation in the near future (see recommendation chapter 8).

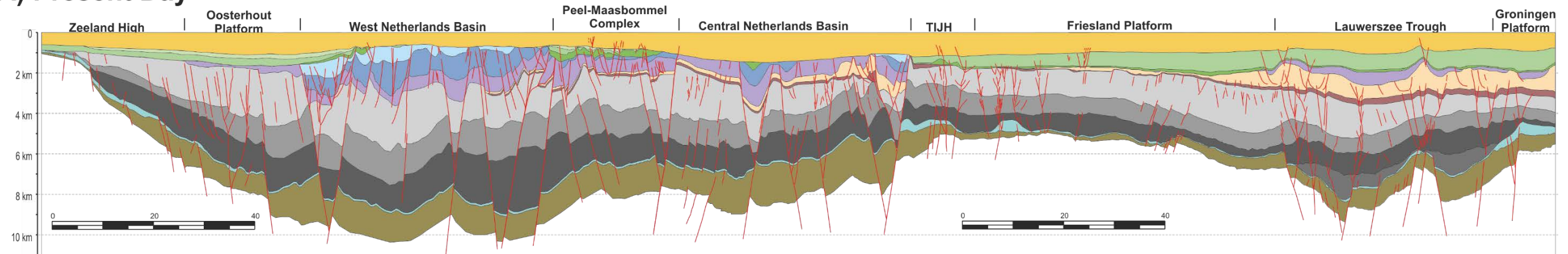
Note that the period with the largest amount of extension measured along this section is limited and occurred during the Namurian with 0.7% of extension (2.5 km) (Appendix 4B)

#### 7.1.3.3. Structural elements

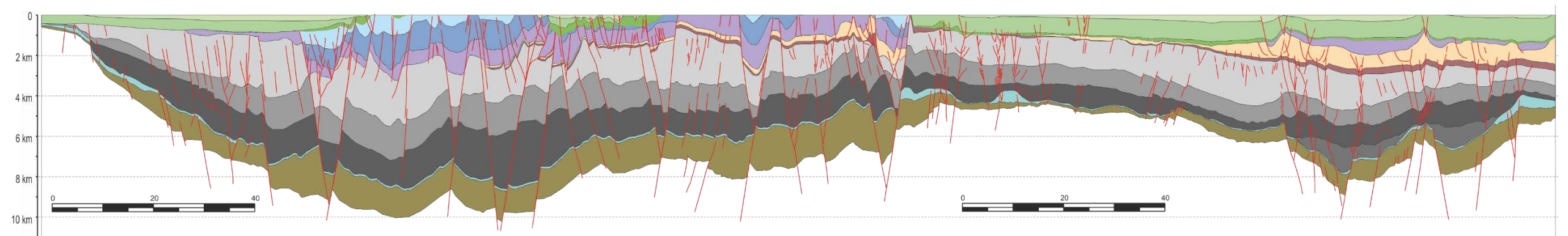
All of the results specific to the structural elements and obtained from the structural restorations are presented in the updated structural element summary chart (Appendix 5).

The amount of extension and contraction measured on each of the section restored varies from a limited amount the Central Section (0,7% contraction, no significant extension), see chapter 6.1.3.1 and Appendix 4B) to more substantial along the Western Section (2.9% contraction and 2% extension, see chapter 6.1.3.2 and Appendix 4A). This difference in the amount of contraction and extension measured can be interpreted as indicating that some of the rifting and orogen phases affecting the central part of the Dutch onshore is increasingly expressed as transtensional and transpressional movements rather than more predominantly extensional and contractional in the western part of the Dutch onshore and in the eastern part of the offshore.

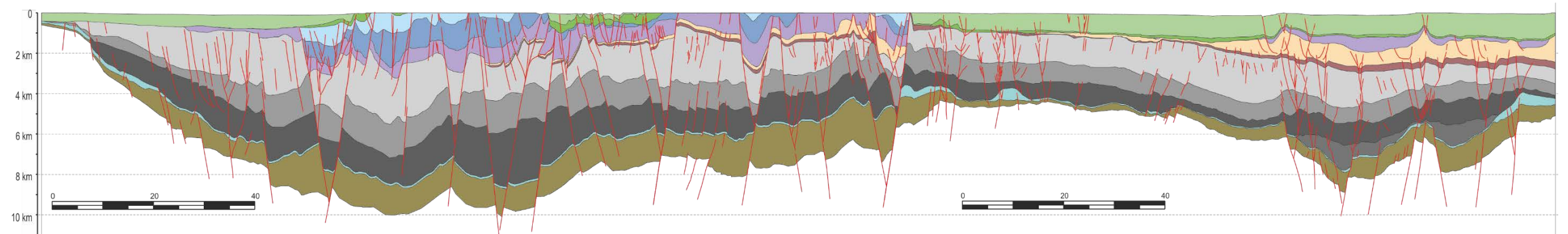
## A) Present Day



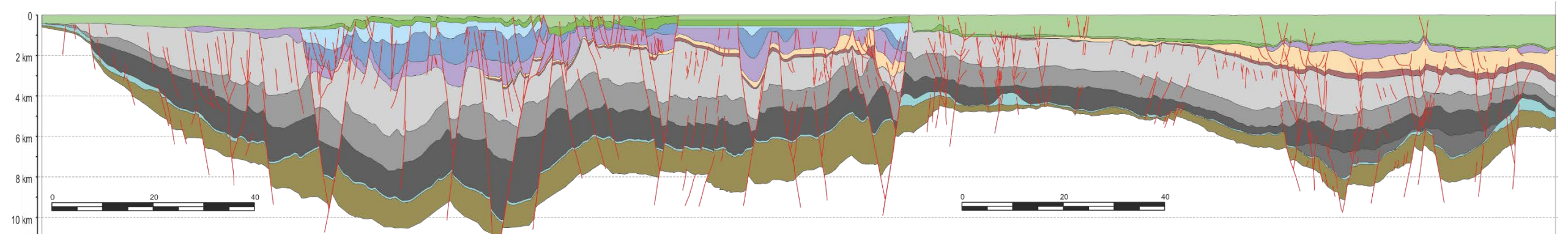
## B) End of Danian



## C) End of Late Cretaceous (post - Subhercynian erosion)

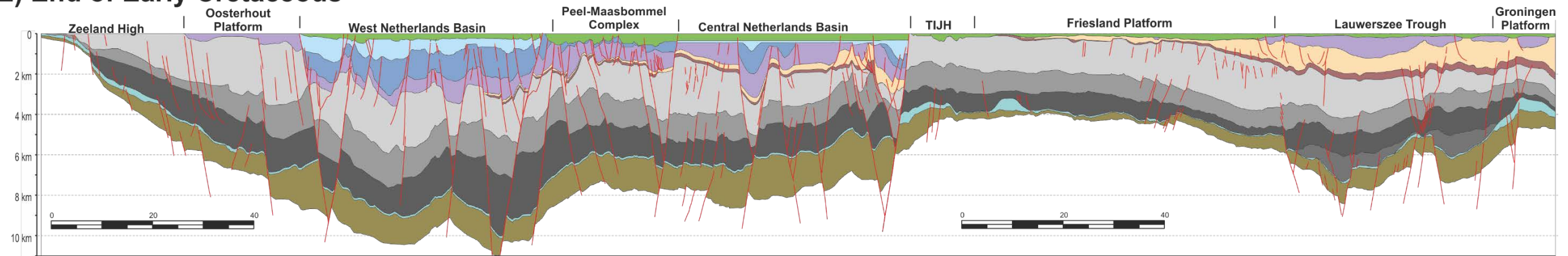


## D) End of Middle Cretaceous (pre - Subhercynian erosion)

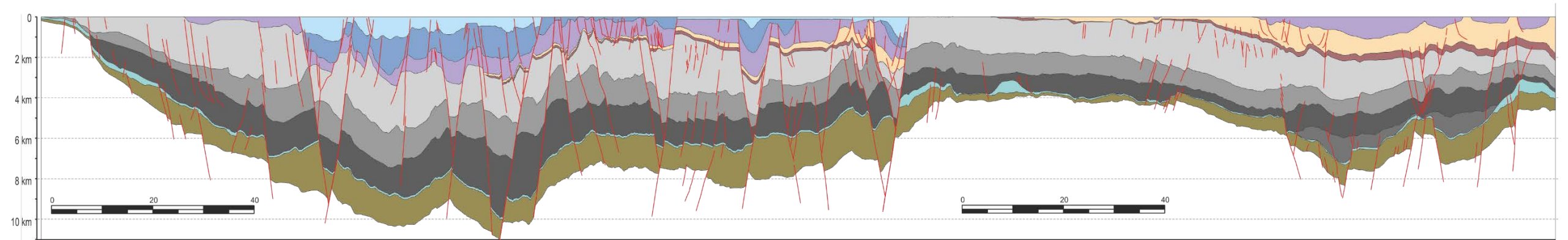




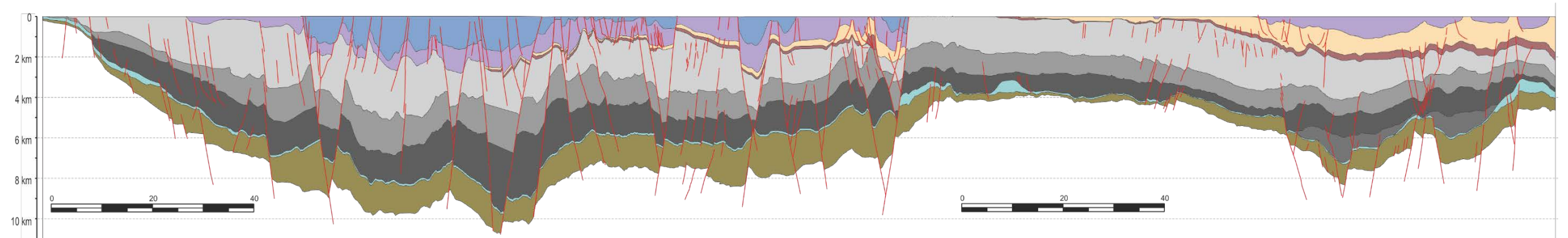
# E) End of Early Cretaceous



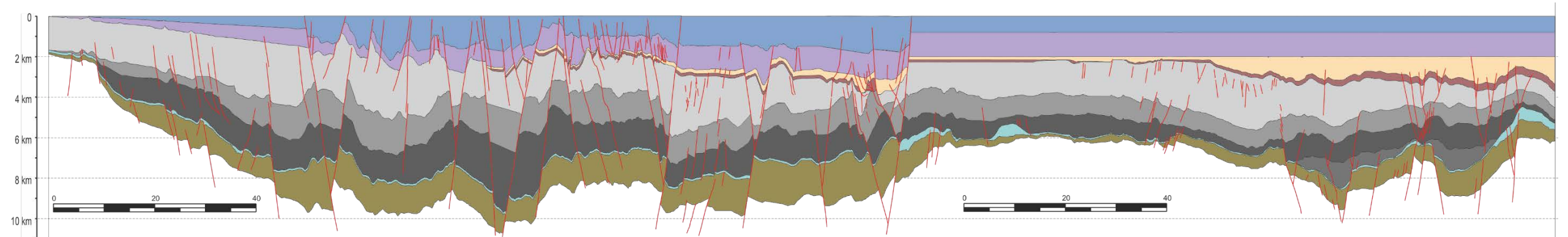
# F) End of Ryazanian (earliest Early Cretaceous)



# G) Early Oxfordian (Late Jurassic; post - Mid Cimmerian erosion)

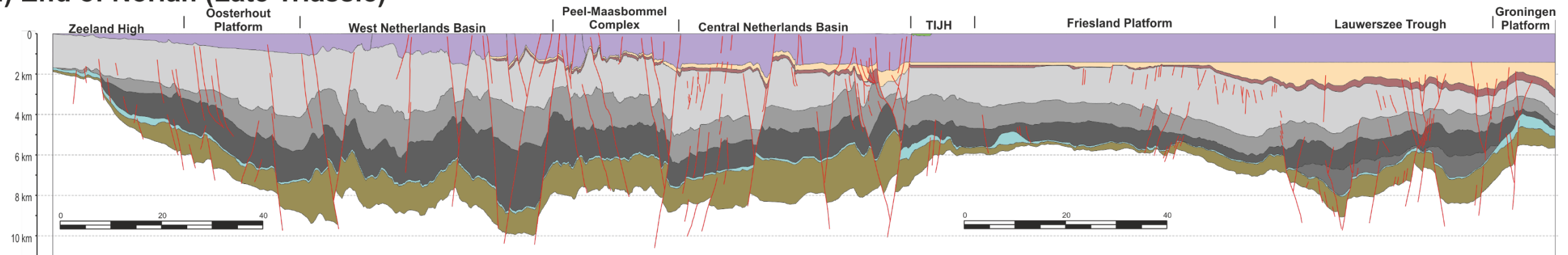


# H) End of Callovian (Middle Jurassic; Pre - Mid Cimmerian erosion)

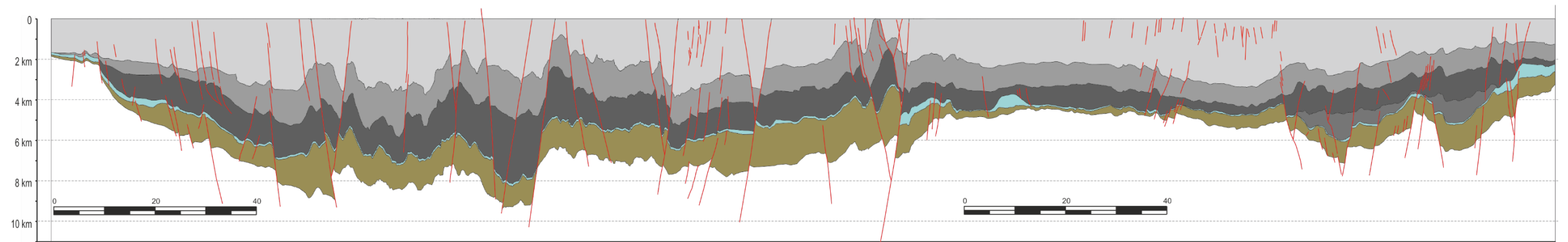




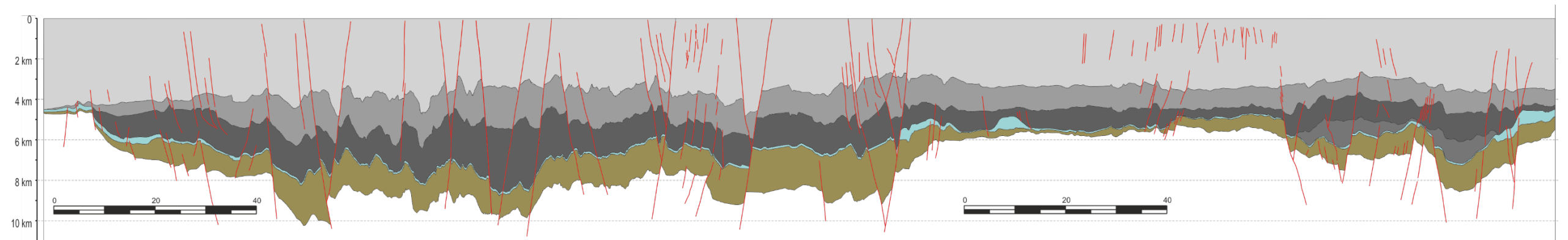
# I) End of Norian (Late Triassic)



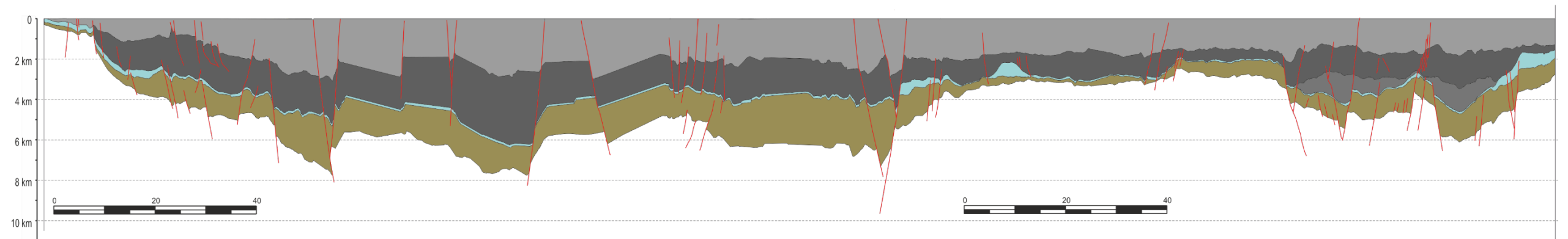
# J) End of Carboniferous (post - BPU erosion)



# K) End of Carboniferous (pre - BPU erosion)

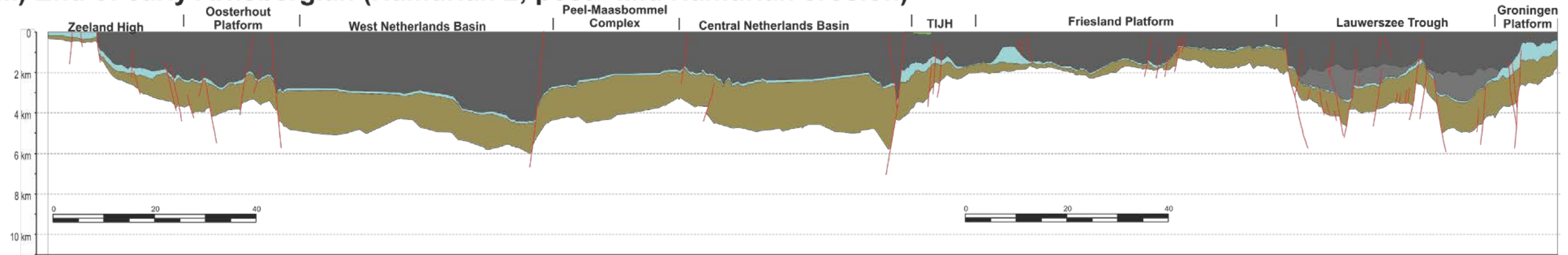


# L) End of Namurian

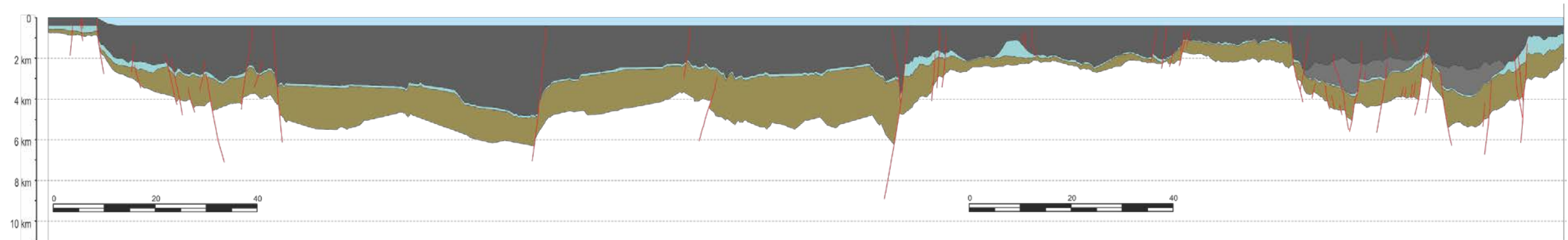




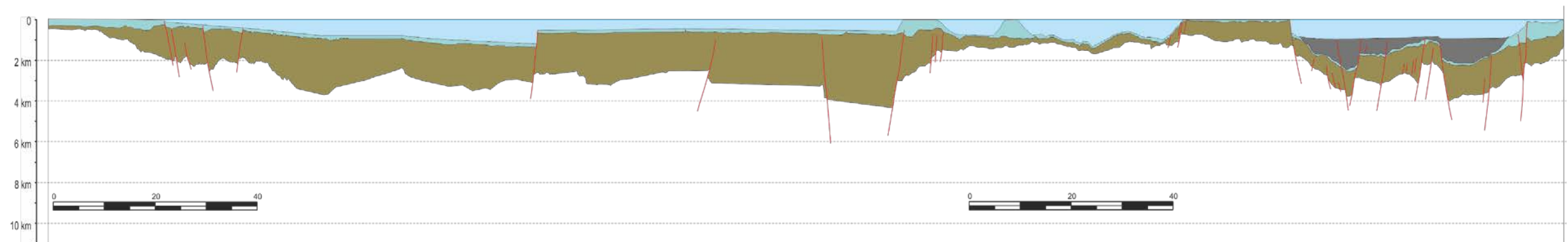
**M) End of early Arnsbergian (Namurian 2; post - Mid Namurian erosion)**



**N) End of early Arnsbergian (Namurian 2; pre - Mid Namurian erosion)**



**O) End of earliest Namurian (Namurian 1)**



**P) End of Dinantian**

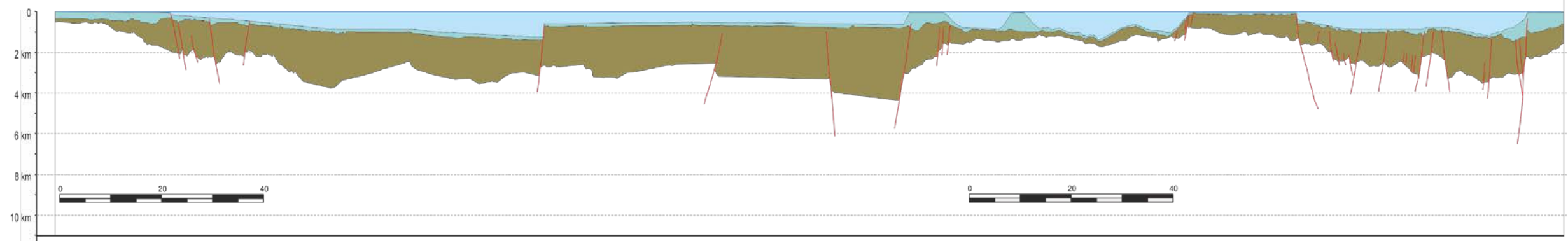


Figure 52 (previous four pages): Central Section restoration results. The vertical exaggeration is four times. Faults are shown in red and stratigraphic units colours are the same as shown in Figure 16. The sea level is shown for steps N, O and P.

## 7.2. Burial and maturity modeling for wells (1D-plots)

The burial and maturity modeling results are presented for fourteen wells and pseudo wells (referred as well extracts) that are located in various structural elements such as 1) the Groningen Platform (well UHM-02), the Friesland Platform (wells LWS-01 and SWD-01), the Texel-IJsselmeer High (Wells EMO-1, NAG-01), the Central Netherlands Basin (wells BAC-01, Ext-2 and Ext-3), West Netherlands Basin area (well HVS-1), Roer Valley Graben (wells Ext-1 and AST-01-Ext) and the Zeeland High (wells S02-02, BHG-01 and WDR-01) (see Figure 12 for well locations). The extracted wells are based on models and seismic interpretation only, the exact depth of the formations is therefore subject to uncertainty and should not be taken at face value.

Note that burial and maturity modelling is subject to some uncertainties especially in areas with large documented stratigraphic unconformities. The thermal history of a well is calibrated to present-day well temperature measurements as well as maturity indicators. In areas where the highest temperature, as recorded by the maturity indicators, occurred during an erosional event, this approach allows to assign ranges with respect to past burial/erosion and heat flow events. Depending on the length of the erosional phase, the quality of the calibration data and the additional uncertainty related to the measurements these ranges can be very high. Previous studies within the SCAN Dinantien project have shown that the maturity indicators measured on the Dinantian rocks in the study area may have experienced additional thermal events such as hydrothermal fluids or abnormal thermal conductivity (Carlson, 2019) which influence the uncertainty with respect to the results of the modelling. These processes have not been taken into account in the context of this study, it was attempted to calibrate the models using only burial and heat flow variations as parameters.

### Well UHM-02

Model stratigraphy is based on the drilled formation. The well penetrates the Devonian Banjaard Group.

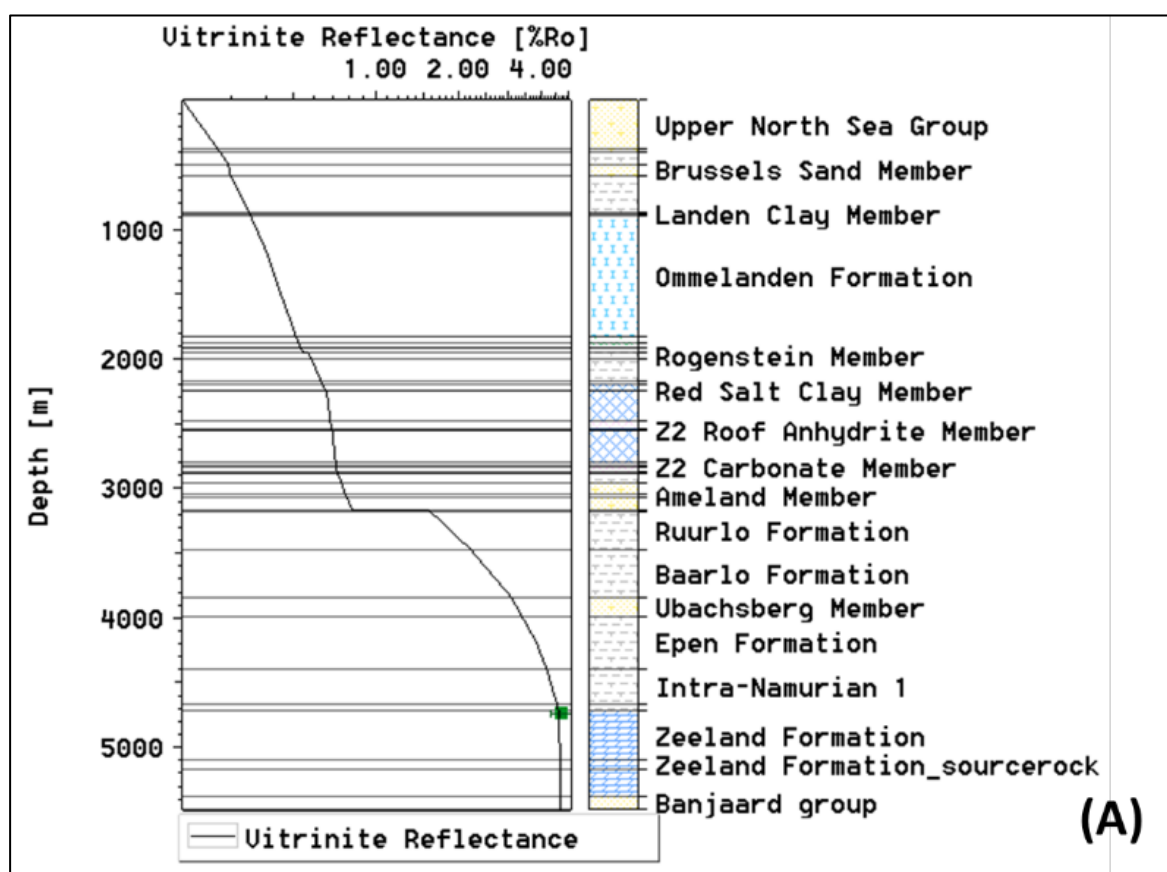
Westphalian formations as well as the Namurian Geverik Member are considered to be source rocks in the model (Table 6).

One maturity measurement (Vitrinite Reflectance %Ro) was available from the Paleozoic section indicating a relatively high value of %Ro 4.68. Assuming the measurement is correct, the model required a total erosion thickness of the Carboniferous section of ca. 2400 m as well as a heat flow peak in the Permian (Figure 53A). The introduced erosion thickness for the Jurassic/Triassic sections during the Mid Kimmerian is ca. 1500 m. This thickness is based on stratigraphic assumptions in an earlier TNO 3D basin model covering the same area and cannot be constrained in this 1D basin model.

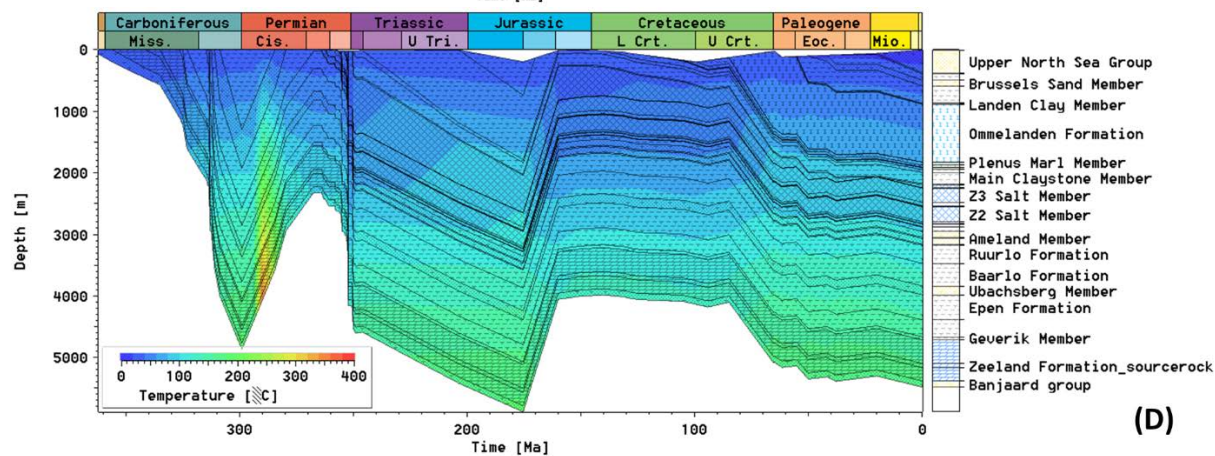
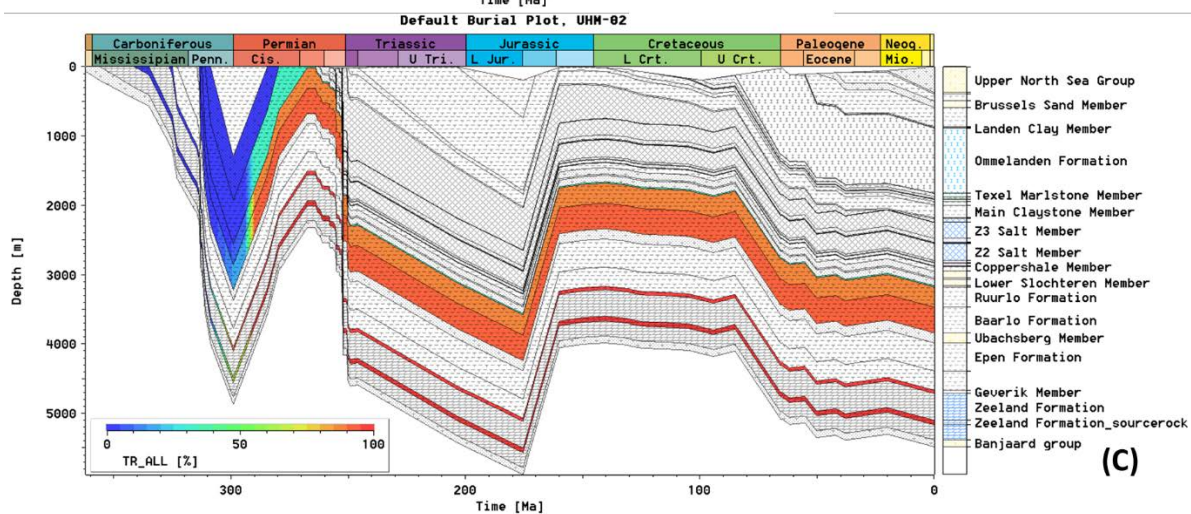
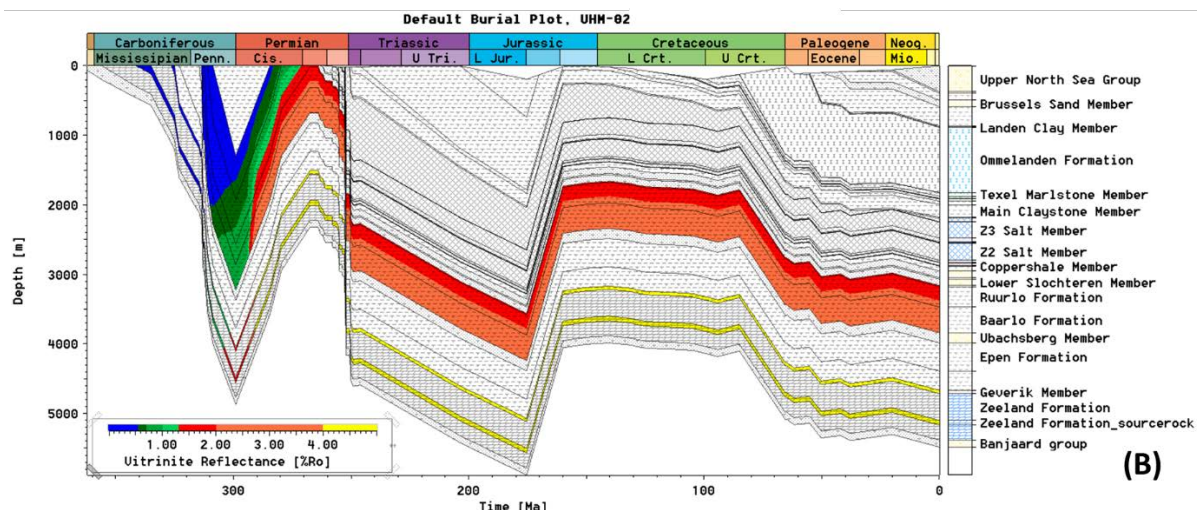
The modelled source rock maturity indicate that the main Westphalian source rocks are in the late gas equivalent window (%Ro 1.5 – 3) since the Permian. The transformation ratio (TR %) of the source rocks, which reflects the ratio of generated hydrocarbons to the generation potential of the source. The modelled transformation ratio of the Westphalian source rocks at present day indicate that 85-95 % of the convertible organic matter in the source rocks has been converted to hydrocarbons. The main generation peak took place in the Permian (Figure 53C). According to the model, Westphalian source rocks might still contain a small amount of organic matter (5-15 %) that is able of hydrocarbon generation at present day.

The modelled vitrinite reflectance and transformation ratio of the Namurian source rock indicate that the formation is in the overmature window (Figure 53). The Namurian reached this stage in the early Permian (Figure 53C). The model shows that, considering the applied thermal and burial scenario, the main source rock is either overmature or are in the late gas-equivalent window. Westphalian source rocks however, might contain small amounts of convertible organic matter that might be able to generate some hydrocarbons at present day. The temperature history of the modelled well section (Figure 53D) suggests that temperatures, apart from the Early Permian, never reached above ~250°C. During the Permian thermal peak, temperatures of the basal section could have reached 300-400°C. These high temperatures are related to a higher heat flow applied in the model, required to model the high VR data point (%Ro 4.68) measured in this well. This high heat flow peak in the early Permian is applied in various wells in the Dutch Onshore area in order to explain the higher vitrinite reflectance values and trends observed in several wells (Abdul Fattah *et al.*, 2012; Bonté *et al.*, submitted; Van Wees *et al.*, 2009).

For the Zeeland Formation this suggests that the temperatures, outside the Permian thermal peak, were for the most part of the geological history between 100 – 150°C. At present day, the modelled data suggests a temperature of ~170°C for the Zeeland Formation.









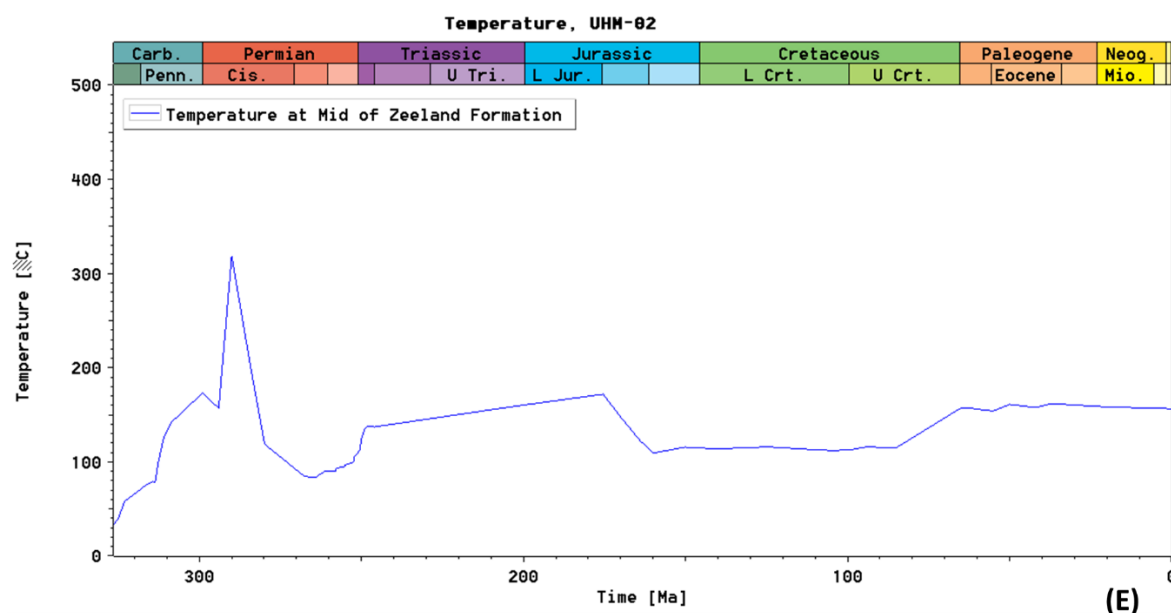


Figure 53: 1D basin model results for well UHM-02. [A]. Modelled present day maturity (%Ro) compared to measured Vitrinite reflectance (Vr%). [B] Burial history with the modelled maturity (%Ro). [C] Transformation Ratio (TR %) of the main source rocks in well UHM-02. [D] Modelled temperature history for the entire well section and [E] the modelled temperature evolution for the Zeeland Formation.

### Well LWS-01

Well stratigraphy is a composite based on the original drilled section (deepest penetrated unit the Z3 Zechstein at TD 1446 m), complemented with data from the regional 3D TNO model (base ZE, RO and erosion estimates for the DC Group, down to 3261 m) and, for the deepest part of the section, the new structural interpretation (Namurian & Dinantian, down to 5800 m).

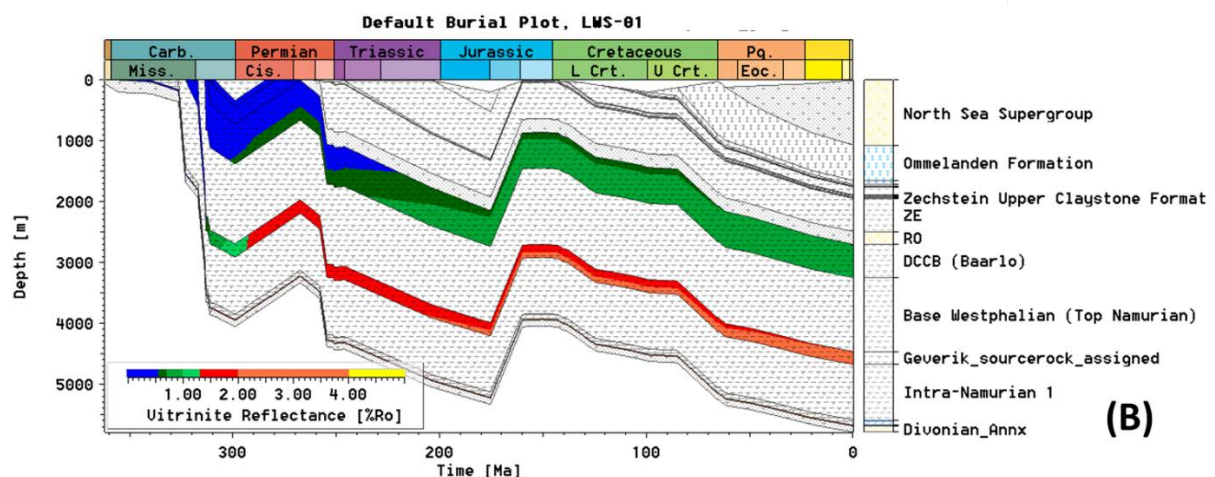
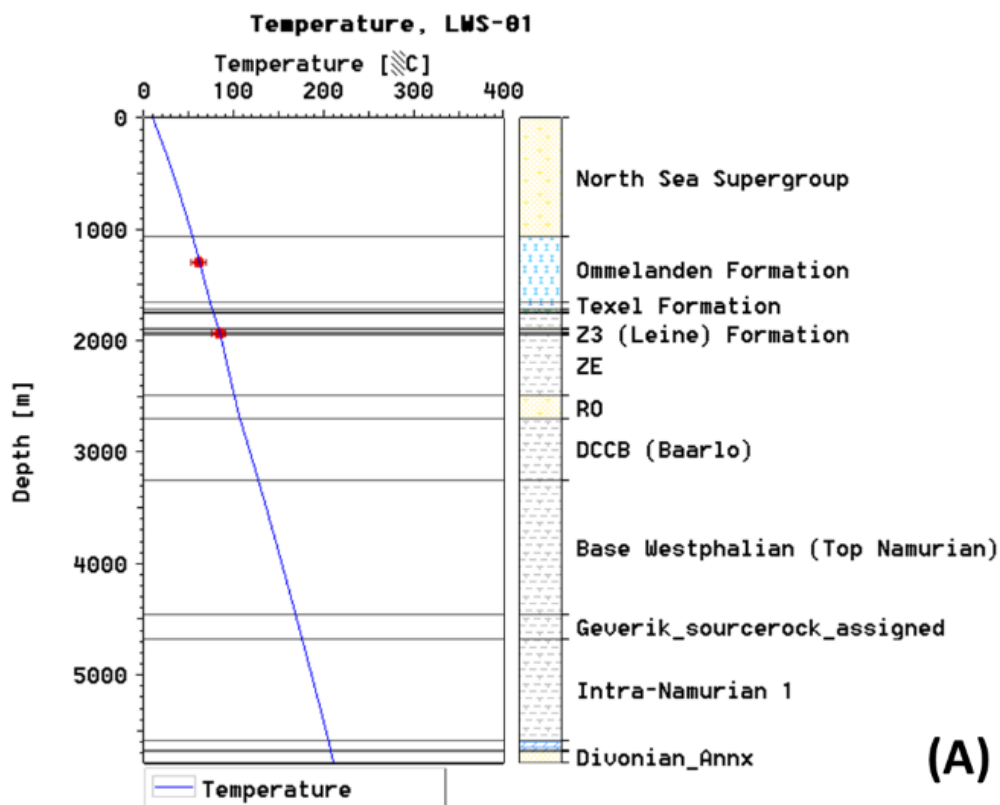
Source rock parameters for the Westphalian units are as per Table 6. In the new structural interpretation, only the Epen Formation is recognized. In order to simulate the Geverik Member, the bottom 15% of the Epen Formation is assigned as source rock (Table 6). The same is applied to the Dinantian Zeeland Formation, where the basal 15% of the formation was assigned as source rock. Both source rocks may not be present, but if they are, they provide a “what-if” scenario for the possible hydrocarbon expulsion from the Dinantian and Limburg Group units.

In the model, Jurassic/Triassic erosion is considered to be some 1000 m based on the regional 3D TNO models; Carboniferous erosion is estimated at ~650 m. Two borehole temperature (BHT) data points are available for well LWS-01; no vitrinite measurements are available. Modelled maturity data for the Westphalian source rocks suggests that from the Carboniferous, they slowly matured, reaching an initial maturity (%Ro ~0.85) in the Early Jurassic to a maximum maturity of %Ro ~1.00 in the Quaternary. Westphalian source rocks stayed mainly in the oil window (Figure 54). Modelled TR suggests that at present day they have a TR<5% suggesting that the source rocks did not expel significant amounts of hydrocarbons.

Modelled maturity data for the assumed Namurian Geverik Member source rock suggests that maturity reached Ro% ~2.00 in the Early Jurassic to Ro% ~2.17 at present day (wet to dry gas window). Modelled TR suggests that the main phase of hydrocarbon generation occurred during the Permian, with nearly 95% of its organic matter converted to hydrocarbons.

Modelling suggests that at present day from small amounts of organic matter predominantly gas may still be expelled.

The temperature history of the modelled well section (Figure 54D) suggests that temperatures, apart from the Early Permian, never reached above ~250°C. For the top of the Zeeland Formation, the modelled temperatures suggest that they were for the most part of the geological history around 200°C, with a modelled present day temperature of ~210°C.



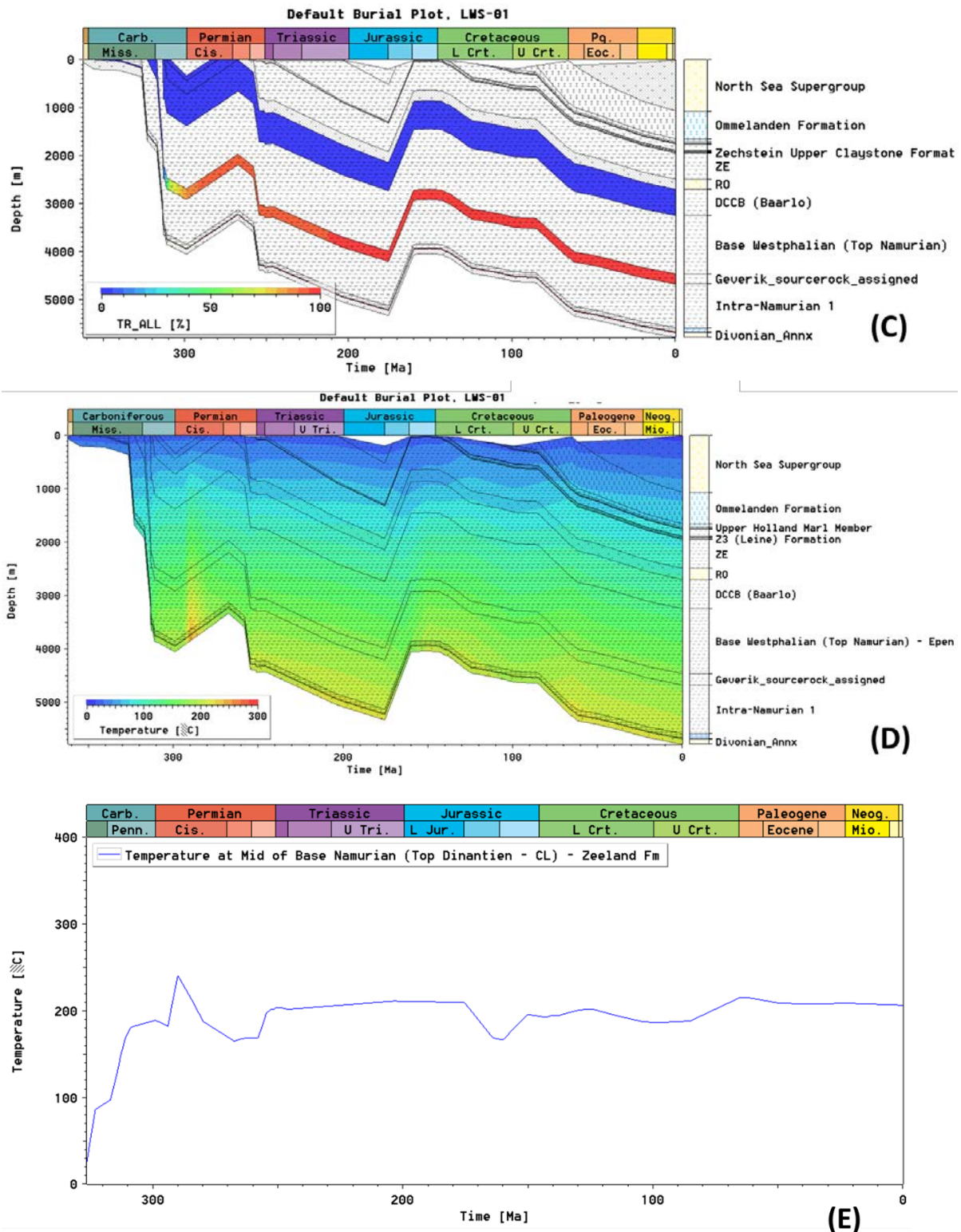


Figure 14: 1D basin model results for well LWS-01. [A]. Modelled present day maturity (%Ro) in well LWS-01 compared to measured Vitrinite reflectance (Vr%). [B] Burial history with the modelled maturity (%Ro). [C] Transformation Ratio (TR %) of the main source rocks in well LWS-01. [D] Modelled temperature history for the entire well section and [E] the modelled temperature evolution for the top of the Zeeland Formation.

## Well SWD-01

Well stratigraphy is based on a composite from the original drilled section (deepest penetrated unit is the Epen Formation at TD 3649 m) and depths derived from the new structural interpretation (Namurian & Dinantian, down to 5353 m).

Source rock parameters for the Westphalian units are as per Table 6. In the new structural interpretation, only the Epen Formation is recognized; in order to simulate the Geverik Member, the bottom 15% of the Epen Formation is assigned source rock kinetics as per Table 6. For the Dinantian Zeeland Formation, a similar exercise was conducted and the bottom 15% of the Zeeland Formation was assigned as source rock. Both source rocks may not be present, but if they are, they provide a “what-if” scenario for the possible hydrocarbon expulsion from the Dinantian and Limburg Group units.

In the model, Jurassic/Triassic erosion is considered some 600 m based on the regional 3D TNO models; Carboniferous erosion is estimated at ~650 m. Eight BHT data points are available for well SWD-01; no vitrinite measurements are available (Figure 5).

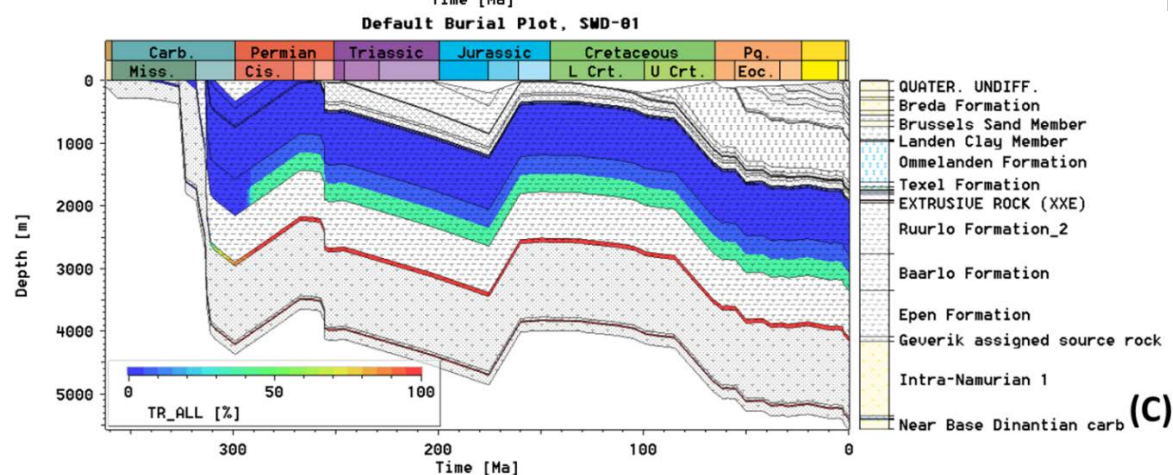
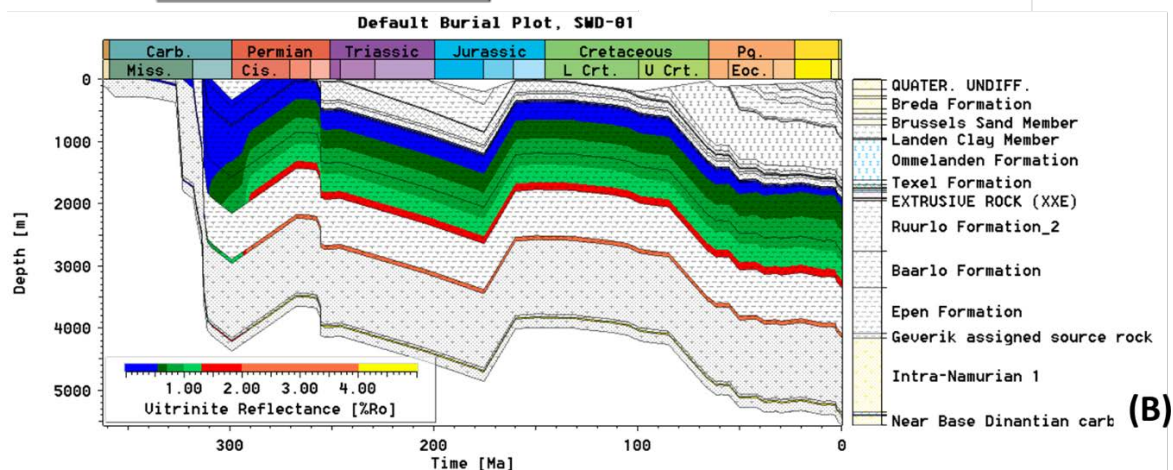
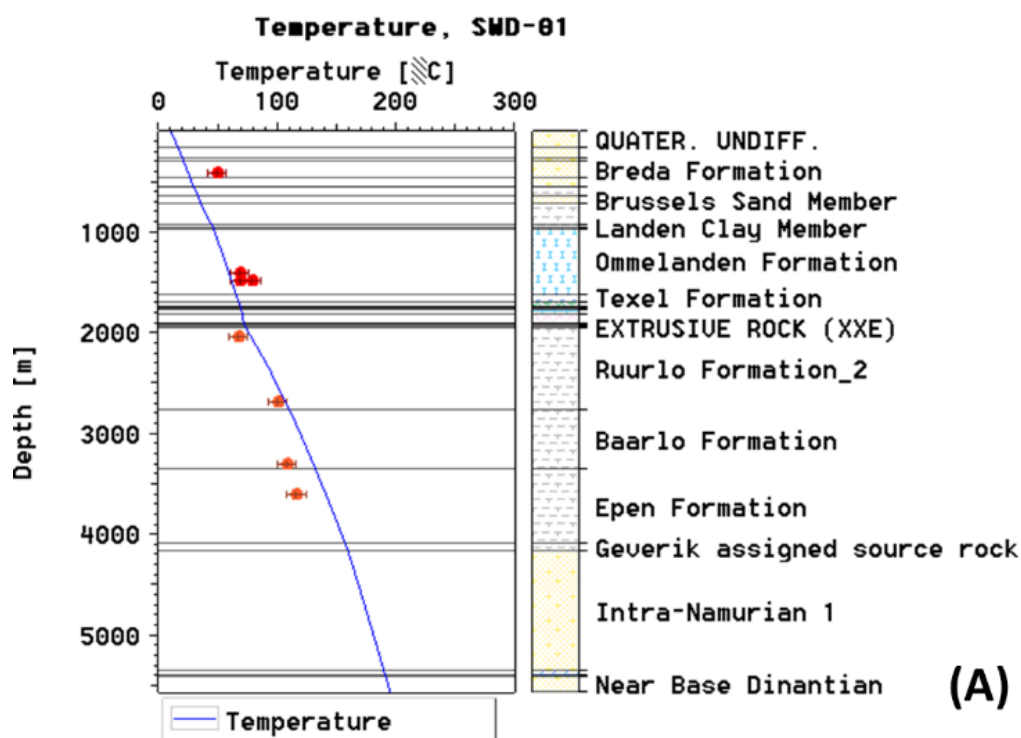
Modelled maturity suggests that the Westphalian source rocks are in the oil – wet gas equivalent window since the Permian (%Ro 0.5 – 1, Figure 5). The base of the Baarlo Formation may have reached slightly higher maturity as suggested by the modelled %Ro values of 1.00 – 1.50. Modelled TR data suggests that of the Ruurlo Formation only a small portion (<1%) of the organic matter may have been converted to hydrocarbons in the Permian. For the Baarlo Formation, modelled data suggests that a higher portion (between 7 – 38%) has been converted to hydrocarbons in the Permian; the higher TR values are modelled for the base, the lower values for the top of the formation.

The modelled maturity for the Namurian Geverik Member shows %Ro 2.00 – 2.50, suggesting it is in the dry gas window since the Permian. Continued maturation resulted in a modelled present-day maturity of Ro% ~2.65. Modelled TR suggests that most of the organic matter (~99%) has been converted to hydrocarbons in the Permian. Modelled data for the Dinantian source rocks suggest they are overmature since the Permian.

The temperature history of the modelled well section (Figure 55D) suggests that temperatures, apart from the Early Permian, did not reach above ~200°C. During the Permian thermal peak, temperatures of the basal section could have reached as high as 300°C.

For the Zeeland Formation this suggests that the temperatures, outside the Permian thermal peak, were for the most part of the geological history around 200°C. At present day, the Zeeland Formation has a modelled temperature of ~190°C.





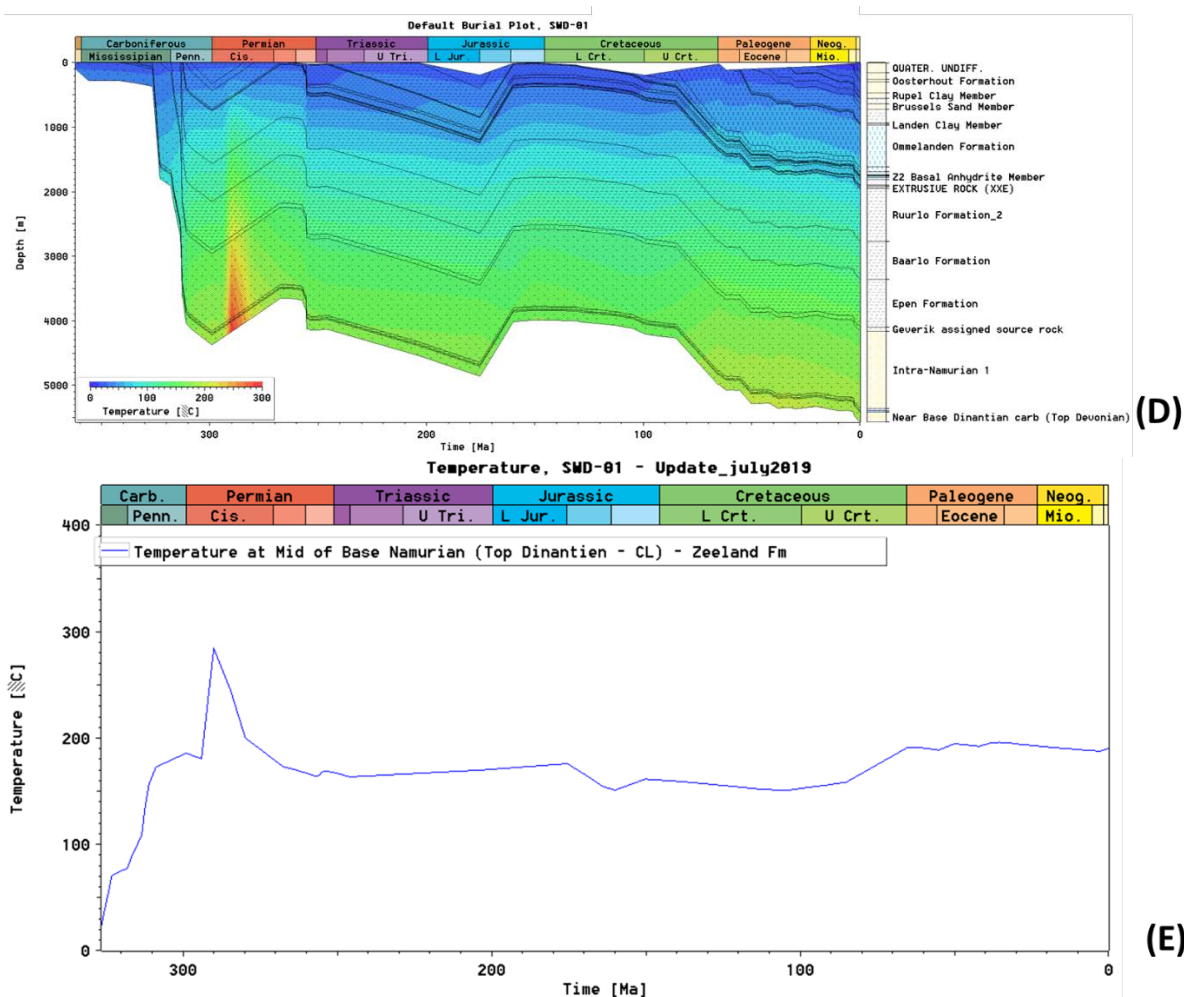


Figure 55: 1D basin model results for well SWD-01. [A]. Modelled present day maturity (%Ro) in well SWD-01 compared to measured Vitrinite reflectance (Vr%). [B] Burial history with the modelled maturity (%Ro). [C] Transformation Ratio (TR %) of the main source rocks in well SWD-01. [D] Modelled temperature history for the entire well section and [E] the modelled temperature evolution for the top of the Zeeland Formation.

### Well BAC-01

Well stratigraphy is based on the drilled section complemented with extractions from the regional TNO 3D model. The deepest part penetrated by the well section is the Limburg Group (2282 m MD). Deeper units until 5336 m and Carboniferous erosion estimates are extracted from the regional 3D TNO model.

Four erosion events are included in the model:

- Neogene event: 300 m in the Lower North Sea Group
- The Laramide event (Late Cretaceous): Total erosion of 1800 m.
- The Late Kimmerian event (Middle-Late Jurassic): Total erosion of 1900 m.
- The Saalian event (Late Carboniferous-Early Permian): Total erosion thickness of 1050 m.

Five vitrinite reflectance and four BHT measurements are available as maturity and temperature calibration data.

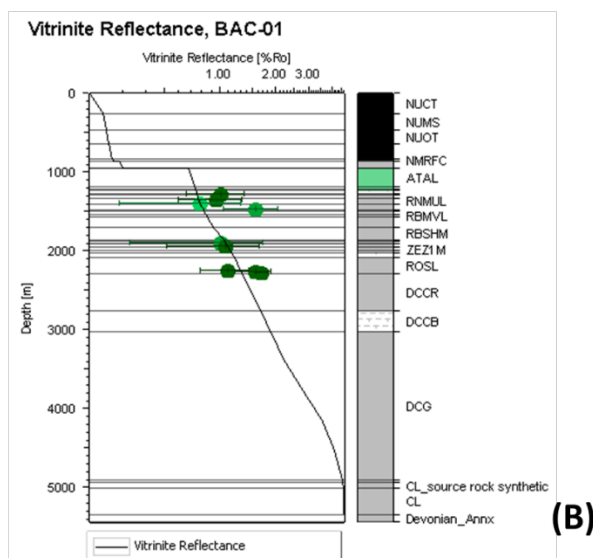
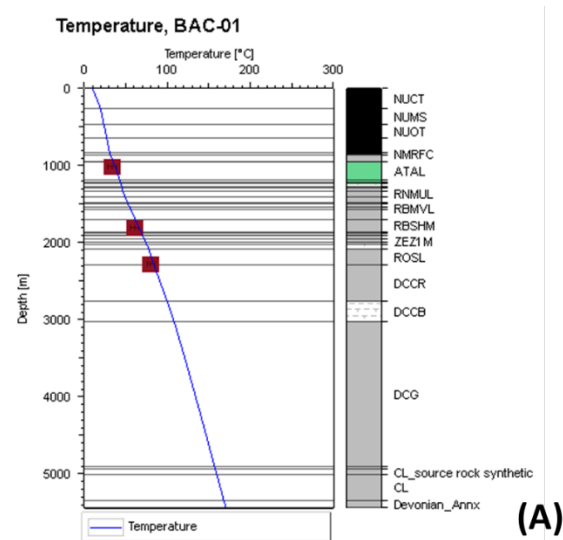
Main Westphalian source rocks in this well are identified as the Maurits (entirely eroded), Ruurlo (partially eroded) and the Baarlo Formations (Table 6). From the existing TNO

regional 3D model, the Geul Group (DCG, 1850 m thickness) and Epen Formation (DCGE, 35 m thickness) are considered; a Namurian source rock (Geverik Member) was not included in this model. For 1D basin modelling purposes and to test potential hydrocarbon generation, the thin DCGE considered as a Namurian source rock. From the Carboniferous Limestone Group (CL), the top 75 m has been assumed as a potential Dinantian source rock. Both source rocks may not be present, are here assumed to test possible hydrocarbon expulsion from the Dinantian and Limburg Group units.

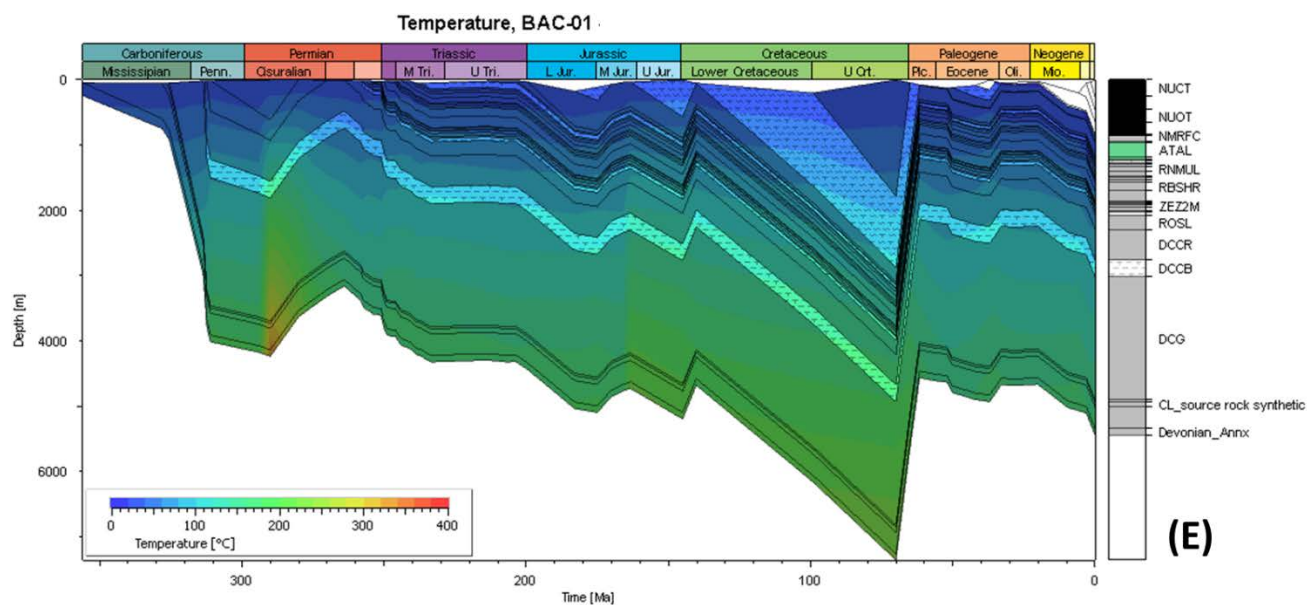
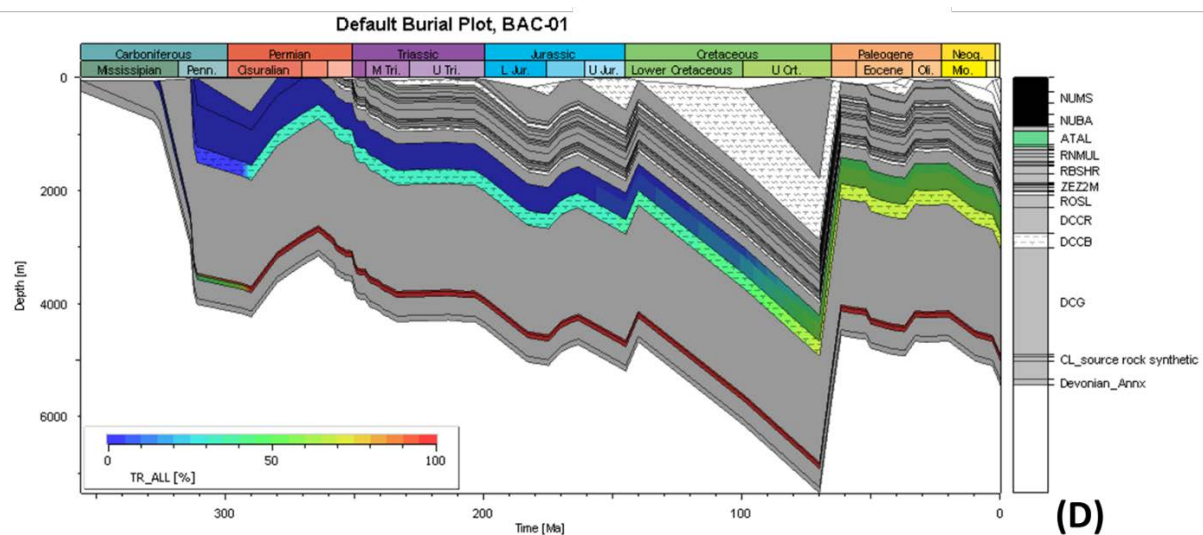
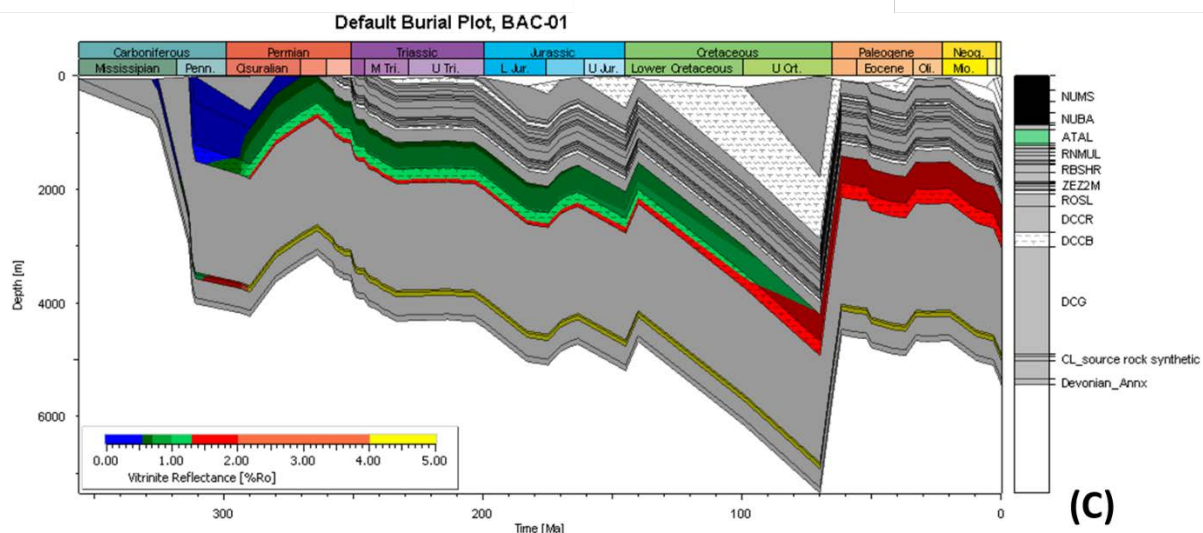
Modelled maturity suggests that the Westphalian source rocks reached an initial peak maturity in the Permian of  $R_o\%$  ~1.00 (oil window, Figure 56). Subsequent burial during the Late Cretaceous resulted in a maximum maturity around  $R_o\%$  ~1.80 (wet to dry gas window). Modelled TR data suggests that for the Ruurlo Formation only a small portion (<2%) of the organic matter may have been converted to hydrocarbons (likely mainly oil) during the Permian. For the Baarlo Formation, this amounts to 18-25%. The main peak of hydrocarbon generation (predominantly gas) for the Ruurlo and Baarlo Formations occurred during the Late Cretaceous, resulting in up to ~65% of all organic material converted.

The modelled maturity for the assumed Namurian DCGE layer and Dinantian CL layer suggests  $R_o$  3.00 – 4.50, suggesting it is overmature since the Permian. Modelled TR suggests that all of the organic matter (100%) has been converted to hydrocarbons in the Permian.

The temperature history of the modelled well section (Figure 56E) suggests that temperatures of the deep sections reached its maximum values in the Early Permian. For the middle of the Carboniferous Limestone (CL) unit, the modelled temperatures suggest that they were for the most part of the geological history around 200°C and the modelled present day temperature is ~160°C.









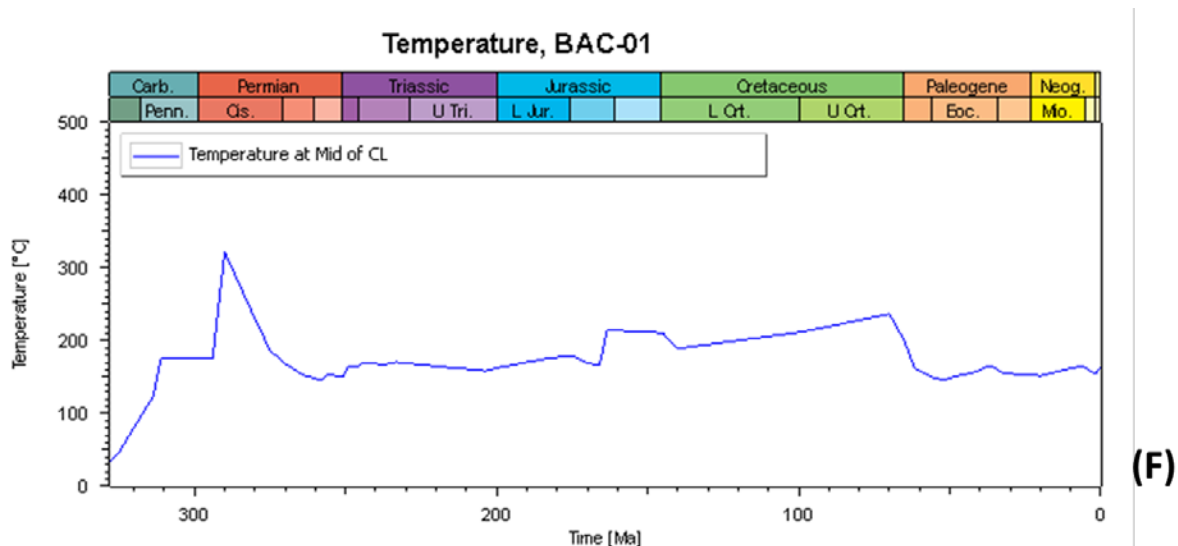


Figure 56: 1D basin model results for well BAC-01. [A] Present day modelled geothermal gradient versus well borehole temperature data. [B] Modelled present day maturity (%Ro) in well BAC-01 compared to measured Vitrinite reflectance (Vr%). [C] Burial history with the modelled maturity (%Ro). [D] Transformation Ratio (TR %) of the main source rocks in well BAC-01. [E] Modelled temperature history for the entire well section and [F] the modelled temperature evolution for the middle of the CL unit.

### Well EMO-01

Well stratigraphy is based on the drilled section. The deepest penetrated section is the Namurian Epen Formation (DCGE). The Lower Westphalian Baarlo Formation (DCCB) is also encountered in the well. These two Carboniferous formations are considered to be source rocks.

Three erosion events are included in the model:

- The Laramide event (Late Cretaceous): Total erosion of 50 m.
- The Late Kimmerian event (Middle-Late Jurassic): Total erosion of 650 m.
- The Saalian event (Late Carboniferous-Early Permian): Total erosion thickness of 800 m.

Four BHT and five vitrinite measurements are available for model calibration purpose.

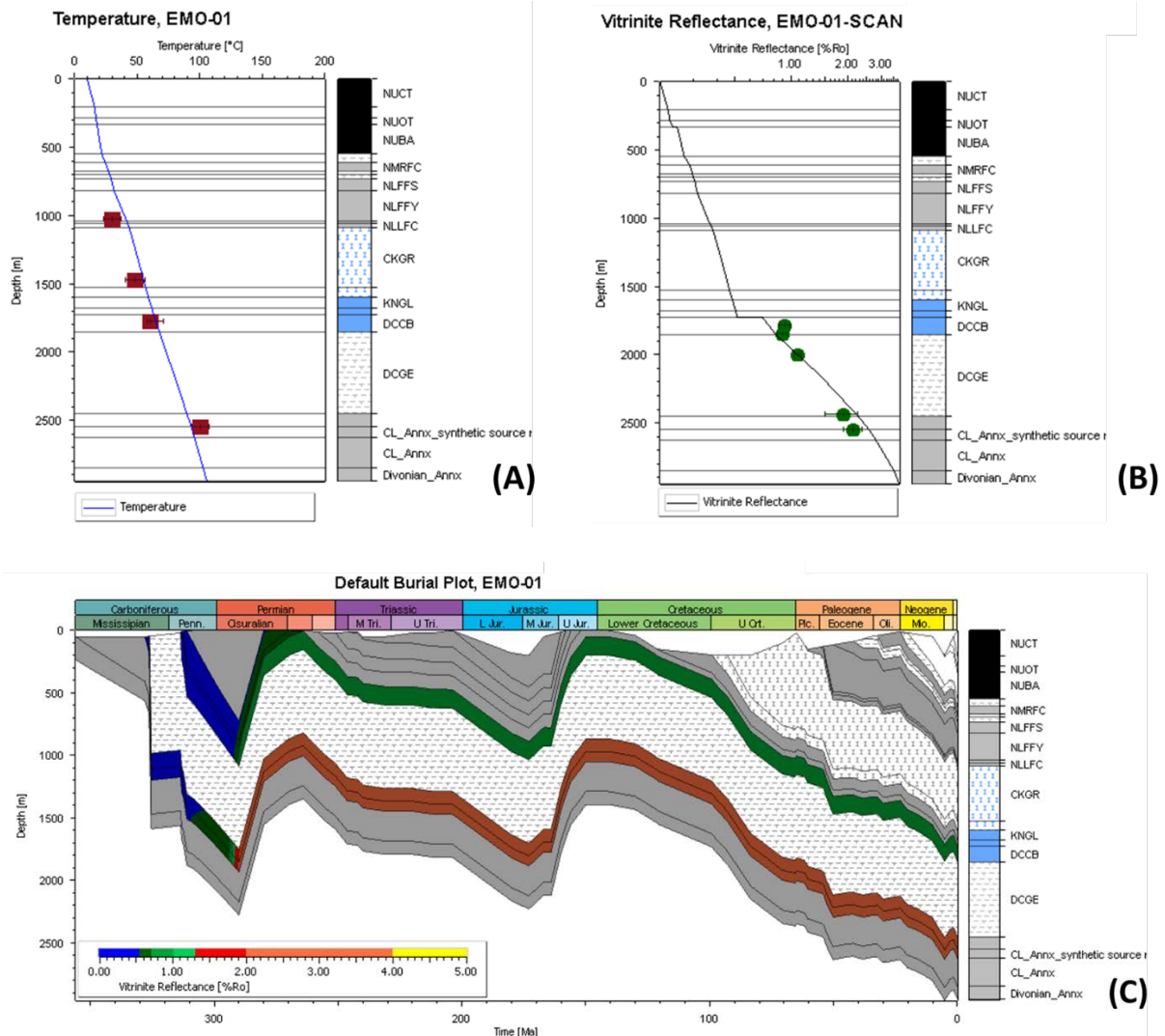
The main Westphalian source rocks in this well are the Maurits and Ruurlo (both eroded) and the Baarlo Formations (Table 6). Namurian source rock (Geverik Member) has not formally been identified in the drilled section and only the Epen Formation was identified (NLOG database). However, in the original well logs (NLOG database) argillaceous units have been observed. In order to test if hydrocarbons could have been expelled, the basal 96 m of the Epen Formation (total thickness 696 m) has been assigned as a source rock. To test a similar scenario, the top 75 m of the Carboniferous Limestone Group (CL), has been assigned as potential Dinantian source rock.

Modelled maturity suggests that the main phase of Westphalian source rocks maturation occurred during the Permian, when maturity reached Ro% ~0.75 (oil equivalent window, Figure 57). Subsequent post Cretaceous burial resulted in a modelled present-day maturity of Ro% 0.80. Modelled TR data show that only a small portion (<1%) of the organic matter in the Westphalian source rocks have been converted to hydrocarbons since the Permian. This would suggest that the Westphalian source rocks have remaining organic matter that at present day has the potential to expel hydrocarbons.

The modelled maturity for the assumed Namurian DCGE layer and Dinantian CL layer yielded %Ro 2.00 (Figure 57), suggesting it is in the dry gas (maybe still wet gas) equivalent window since the Permian. Post Cretaceous burial resulted in further maturation to Ro% 2.70 (end of dry gas window). Modelled TR suggests that nearly all of the organic matter (97%) has been converted to hydrocarbons in the Permian. At present day, less than 2% of the organic matter may still be converting to hydrocarbons.

The temperature history of the modelled well section (Figure 57D) suggests that, apart in the Early Permian, the temperatures for most of the history never reached above ~150°C. During the Permian thermal peak, temperatures of the basal section could have reached as high as 250°C.

For the Carboniferous Limestone Group (CL) unit, the modelled temperatures from the Triassic onward never were higher than around 120°C. At present day, the CL unit has a modelled temperature of ~100°C.



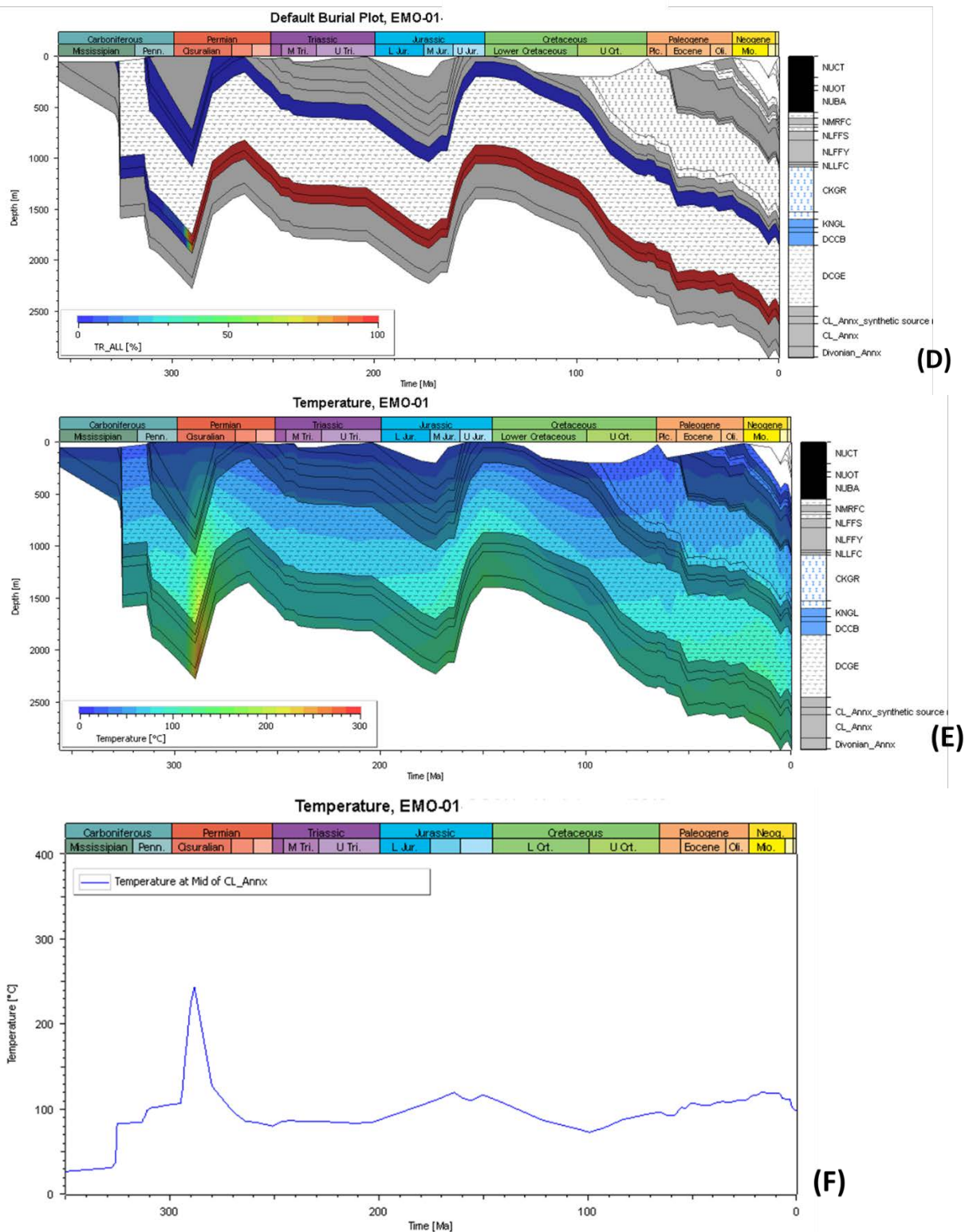


Figure 57: 1D basin model results for well EMO-01. [A] Present day modelled geothermal gradient versus well borehole temperature data. [B] Modelled present day maturity (%Ro) in well EMO-01 compared to measured Vitrinite reflectance (Vr%). [C] Burial history with the modelled maturity (%Ro). [D] Transformation Ratio (TR %) of the main source rocks in well EMO-01. [E] Modelled temperature history for the entire well section and [F] the modelled temperature evolution for the middle of the CL unit.

## Well NAG-01

Model well stratigraphy is based on the drilled section. The deepest penetrated section is the Namurian Epen Formation (DCGE) and the Lower Westphalian Baarlo (DCCB) and Ruurlo (DCCR) Formations (DCCB) are drilled in the well. These two Carboniferous formations are considered to be source rocks.

Four erosion events are included in the model:

- Savian event (Late Paleogene): total erosion thickness of 180 m.
- The Laramide event (Late Cretaceous): Total erosion of 50 m.
- The Late Kimmerian event (Middle-Late Jurassic): Total erosion of 1209 m.
- The Saalian event (Late Carboniferous-Early Permian): Total erosion thickness of 1265 m.

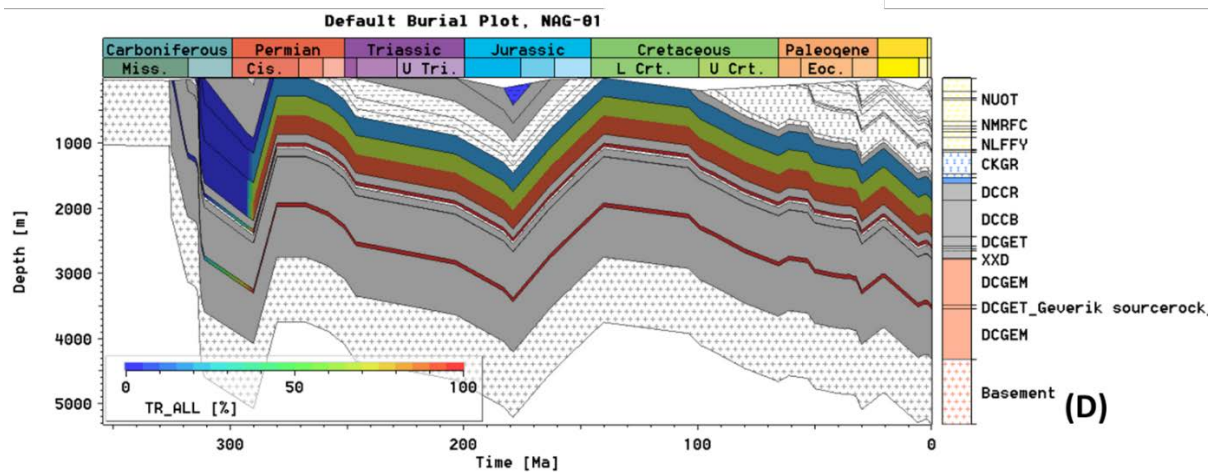
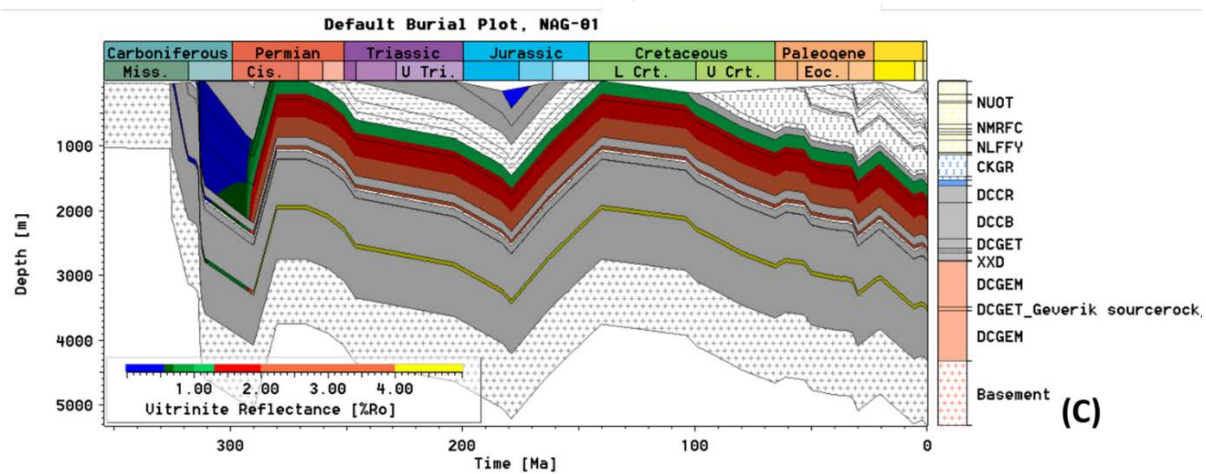
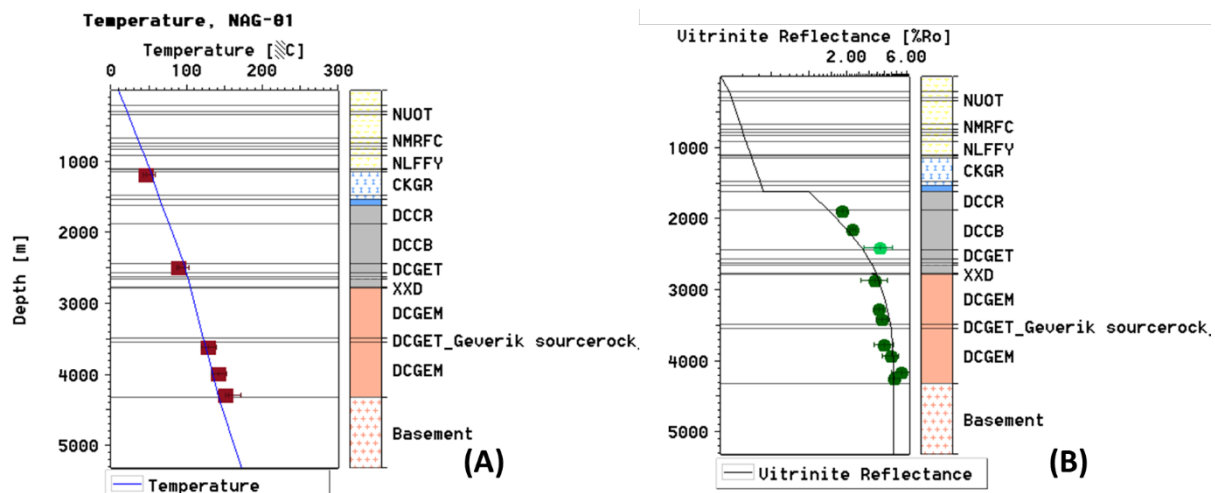
The main Westphalian source rocks in this well are the Maurits (eroded), Ruurlo and Baarlo Formations. A Namurian source rock (Geverik Member) was not encountered in the drilled section (available from NLOG database). In the original well description, argillaceous units have, however, been identified in the Upper Epen and Main Epen Members. To evaluate potential hydrocarbon generation from this section and for modelling purposes, parts of the Upper and Main Epen Members have been assigned as source rocks. Generally, the Geverik Member is stratigraphically positioned under the Main Epen Member, though given the thickness of the Main Epen Member in the drilled well section (1527 m), the assigned source rock has been placed in the middle of the Main Epen Member.

Modelled maturity suggests that the main phase of Westphalian source rocks maturation occurred during the Permian. For the eroded Maurits Formation maturity reached  $R_o\%$  ~0.60, whereas the Ruurlo Formation reached a maturity of 0.80 – 1.00, suggesting the latter is in the oil window (Figure 58). For the Baarlo Formation, modelled maturity ranges from  $R_o\%$  ~1.75 for the top of the formation tot  $R_o\%$  ~2.50 for the basal parts. At present-day, the modelled maturity suggests  $R_o\%$  1.21 (Ruurlo Fm) to 2.60 (Baarlo Fm). Modelled TR data show that the main phase of hydrocarbon generation occurred in the Permian. In the Ruurlo Fm, roughly 18 % of the organic matter may have been converted to hydrocarbons (likely oil) and at present day over 80% of organic material has not been converted. Modelled TR of the Baarlo Formation suggests that from the upper parts of this formation, roughly 60-70% of organic material has been converted. For the basal parts of the Baarlo Fm, modelled TR suggests that nearly 90% of organic material has been converted. For the Westphalian source rocks, the model suggests that they may contain variable amounts of organic material (~80 % in the Ruurlo Fm to 10 % in the basal Baarlo Fm) that is able of hydrocarbon generation at present day.

The modelled maturity for the two assumed (synthetic) layers mimicking the Namurian Geverik Member in the Main and Upper Epen Members yielded % $R_o$  3.00 and 4.50 respectively, suggesting that if source rocks are present (given the stratigraphic position of the Geverik Member it will likely be towards the deeper parts of the Epen Formation), they are overmature since the Permian (Figure 58). Modelled TR suggests that for both synthetic layers, main phase of hydrocarbon generation occurred in the Permian, with nearly 100% of organic material converted since.

The temperature history of the modelled well section (Figure 58E) suggests that high temperatures (> 200°C) were reached in the deepest sections during the Permian thermal peak,. In this well, no Dinantian units were identified, hence the temperature evolution of the Epen Formation is shown (Figure 58F). Modelled temperatures suggest that the Epen Formation never experienced temperatures in excess of 160°C and has a modelled present day temperature of ~140°C.





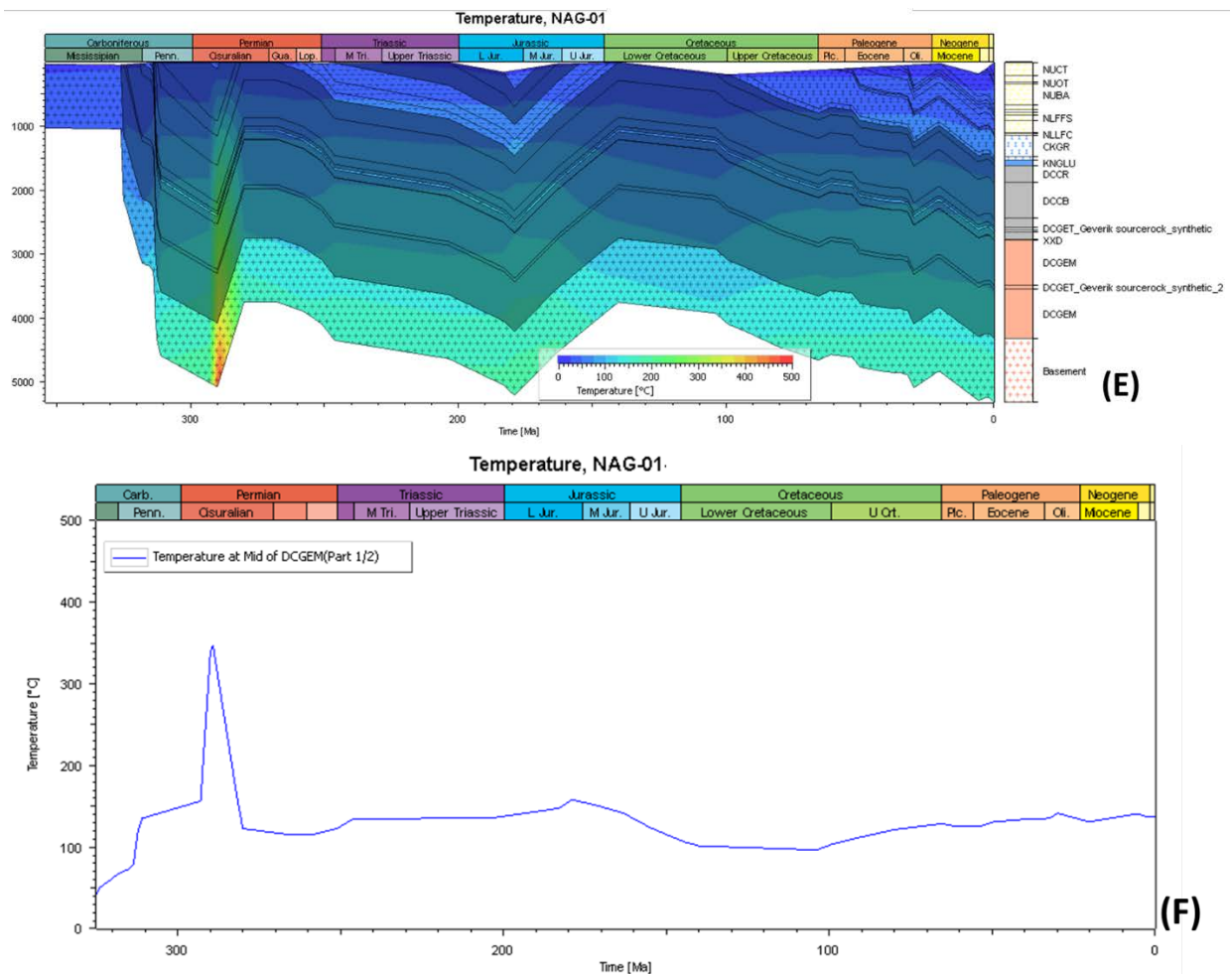


Figure 58: 1D basin model results for well NAG-01. [A] Present day modelled geothermal gradient versus well borehole temperature data. [B] Modelled present day maturity (%Ro) in well NAG-01 compared to measured Vitrinite reflectance (Vr%). [C] Burial history with the modelled maturity (%Ro). [D] Transformation Ratio (TR %) of the main source rocks in well NAG-01. [E] Modelled temperature history for the entire well section. [F] In absence of a Dinantian unit, the temperature evolution of the overlying Epen Formation is shown.

## Well Ext-1

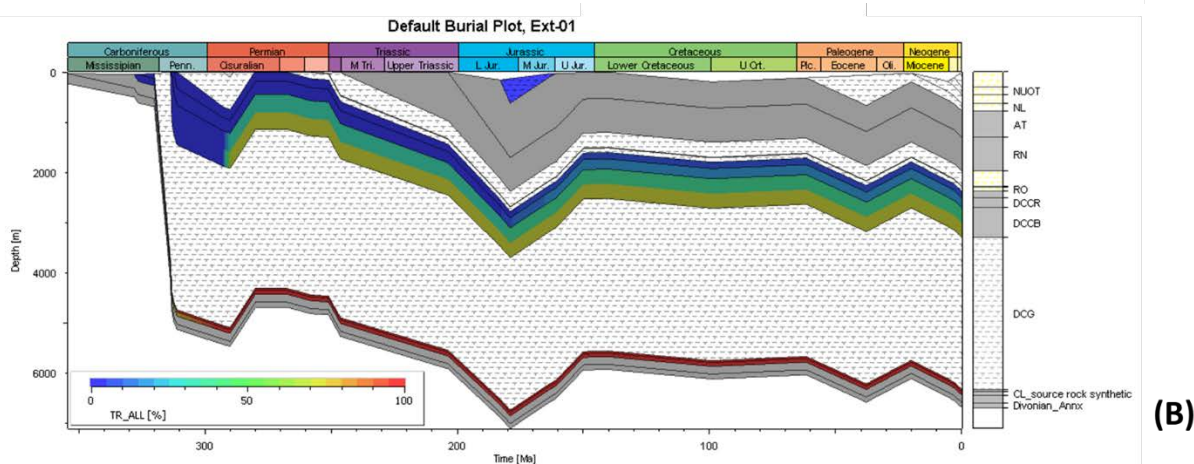
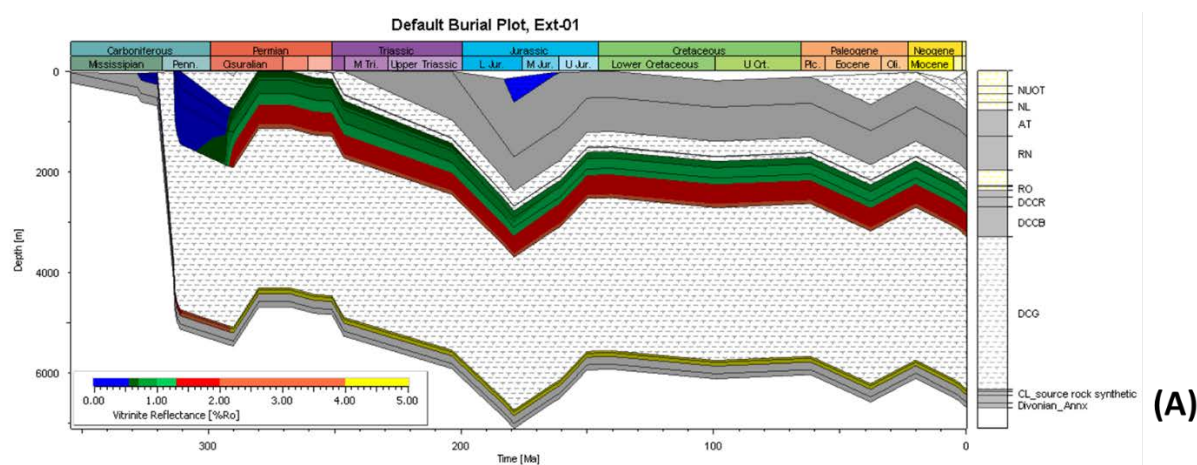
Well Ext-01 is a pseudo well extracted from thickness maps from the existing TNO 3D model complemented for the deepest parts with new horizons from the structural interpretation. The extraction is located to the south east of Utrecht (Figure 12). Base of the well is at ~6600 m in the pre-Upper Devonian “basement”.

Three erosion events are included in the model:

- Savian event (Late Paleogene): total erosion thickness of 365 m.
- The Late Kimmerian event (Middle-Late Jurassic): Total erosion of 1029 m.
- The Saalian event (Late Carboniferous-Early Permian): Total erosion thickness of 750 m.

Main Westphalian source rocks in this well are identified as the Maurits (partially eroded), Ruurlo and Baarlo Formations. The Geverik Member is considered the Namurian source rock. Dinantian source rocks are not well understood, though in order to assess if the carboniferous

Limestone Group (CL) could have expelled hydrocarbons if a source rock were to be present, a 75 m thick layer from the top of the CL was assigned as a synthetic source rock. Modelled maturity suggests that the main phase of Westphalian source rocks maturation occurred during the Permian. Modelled maturity in the partially eroded Maurits Formation reached Ro% 0.67 (oil window) to Ro% ~2.20 in the basal Baarlo Formation (Figure 59). Post-Permian subsidence was insufficient to further mature the Westphalian units. Modelled TR data show that the main phase of hydrocarbon generation was in the Permian. For the Maurits Formation, the model suggests that only a small portion (<1%) of the organic matter has been converted to hydrocarbons. For the Ruurlo Formation this increases to ~5%, whereas in the Baarlo Formation the modelled TR suggests that 42% (upper part of the formation) to 75% (basal part of the formation) has been converted. This would suggest that depending on the stratigraphic unit, the Westphalian source rocks may have remaining organic matter that at present day has the potential to expel hydrocarbons (oil or gas). The modelled maturity for the Namurian Geverik Member at the base of the DCG and the synthetic (assumed) Dinantian CL source rock yielded up to %Ro ~4.60 (Figure 59), in the Permian, suggesting that, if present, they are overmature. Modelled TR suggests that nearly all of the organic matter (100%) has been converted to hydrocarbons in the end of the Permian in both layers. Modelled temperature for the CL unit suggests that it never reached temperatures in excess of 230°C (with the exception during the early Permian thermal peak, when temperatures reached up to 400-450°C). Present day modelled temperatures at the mid-level of the CL unit are ~230°C.





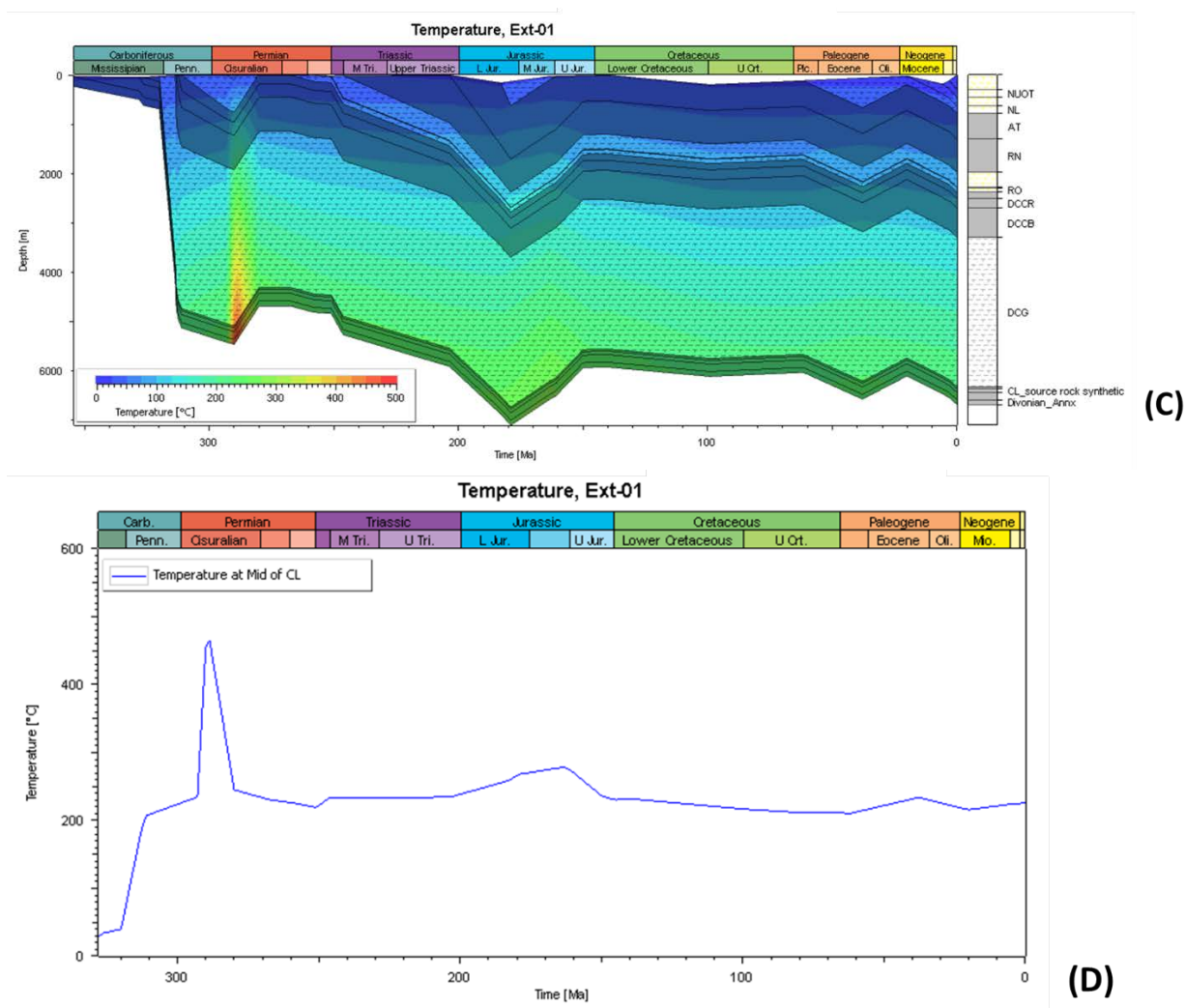


Figure 59: 1D basin model results for well Ext-01. [A] Burial history with the modelled maturity (%Ro). [B] Modelled Transformation Ratio (TR %) of the main source rocks. [C] Modelled temperature history for the entire well section and [D] the modelled temperature evolution for the middle of the CL unit.

## Well Ext-02

Well Ext-02 is a pseudo well extracted from thickness maps from the existing TNO 3D model complemented for the deepest parts with new horizons from the structural interpretation. The location of the extraction is to the east of Ede (Figure 12). Base of the pseudo well is at ~5100 m in the pre-Upper Devonian "basement".

Three erosion events are included in the model:

- Late Paleogene: total erosion thickness of 200 m.
- Jurassic/Triassic: Total erosion of 1340 m.
- The Saalian event (Late Carboniferous-Early Permian): Total erosion thickness of 911 m.

Main Westphalian source rocks in this well are identified as the Maurits (partially eroded), Ruurlo and Baarlo Formations (Table 6). The Geveik Member is considered the Namurian source rock. Dinantian source rocks are not well understood, though in order to assess if the

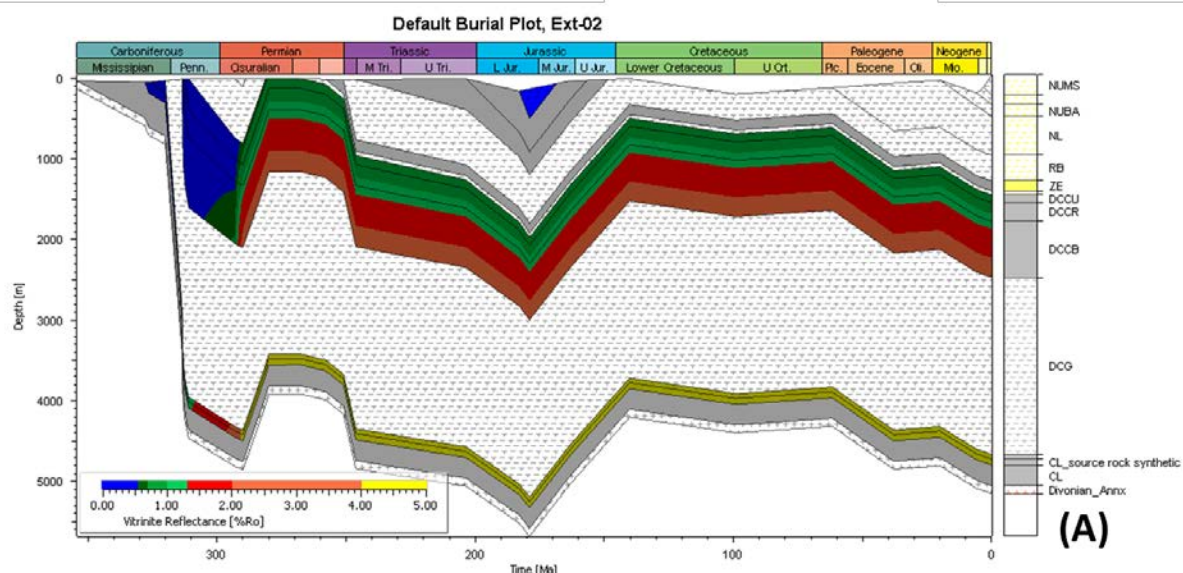


Carboniferous Limestone Group (CL) could have expelled hydrocarbons if a source rock were to be present, a 75 m thick layer from the top of the CL unit was assigned as a synthetic source rock.

Modelled maturity and TR for both the Westphalian, Namurian and Dinantian is similar to the model results for Ext-01. The main phase of Westphalian source rocks maturation occurred during the Permian. Modelled maturity in the Maurits Formation reached Ro% 0.80 (oil window) to Ro% ~1.10 in the Ruurlo Formation (56). The basal Baarlo Formation has the highest modelled maturity of the Westphalian source rocks, reaching Ro% 4.40. Modelled TR data show that the main phase of hydrocarbon generation was in the Permian. For the Maurits Formation, the model suggests that only a small portion (<1%) of the organic matter has been converted to hydrocarbons. For the Ruurlo Formation this increases to ~15%, whereas in the Baarlo Formation the modelled TR suggests that 58% (upper part of the formation) to 88% (basal part of the formation) has been converted. This would suggest that depending on the stratigraphic unit, the Westphalian source rocks may have remaining organic matter that at present day has the potential to expel hydrocarbons (oil or gas).

The modelled maturity for the Namur Geverik Member at the base of the DCG and the synthetic (assumed) Dinantian CL source rock yielded up to %Ro ~4.65 (Figure 60), in the Permian, suggesting that, if present, they are overmature. Modelled TR suggests that nearly all of the organic matter (100%) has been converted to hydrocarbons in the end of the Permian.

Modelled temperature for the CL unit suggests that it never reached temperatures in excess of 250°C. During the Early Permian however, the formation temperature reached up to 400-450°C, which can be attributed to the early Permian heat flow peak (Figure 60C and D). Present day modelled temperatures at the mid-level of the CL unit are ~170°C.



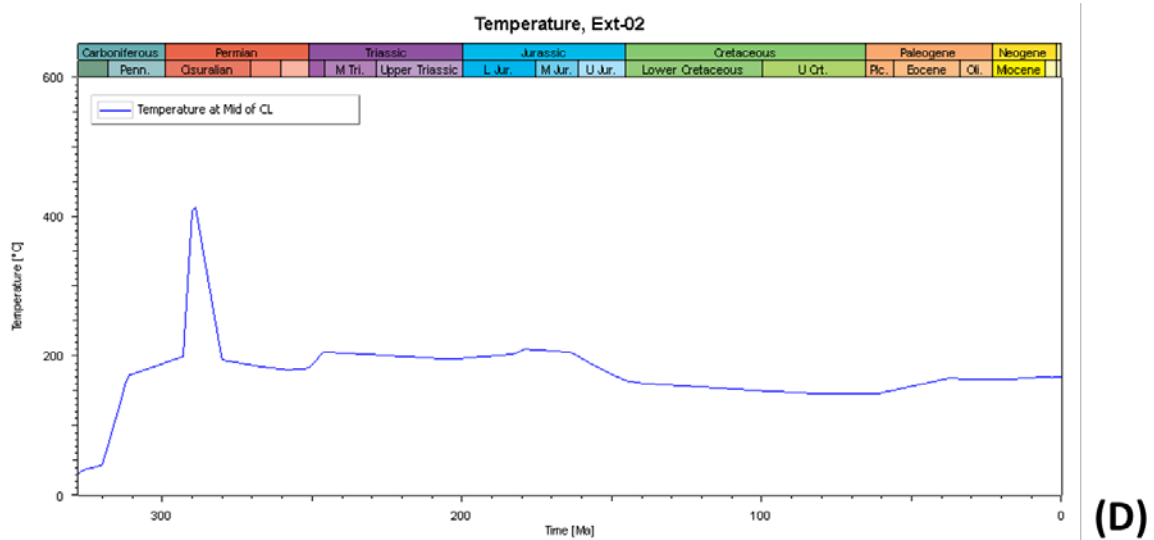
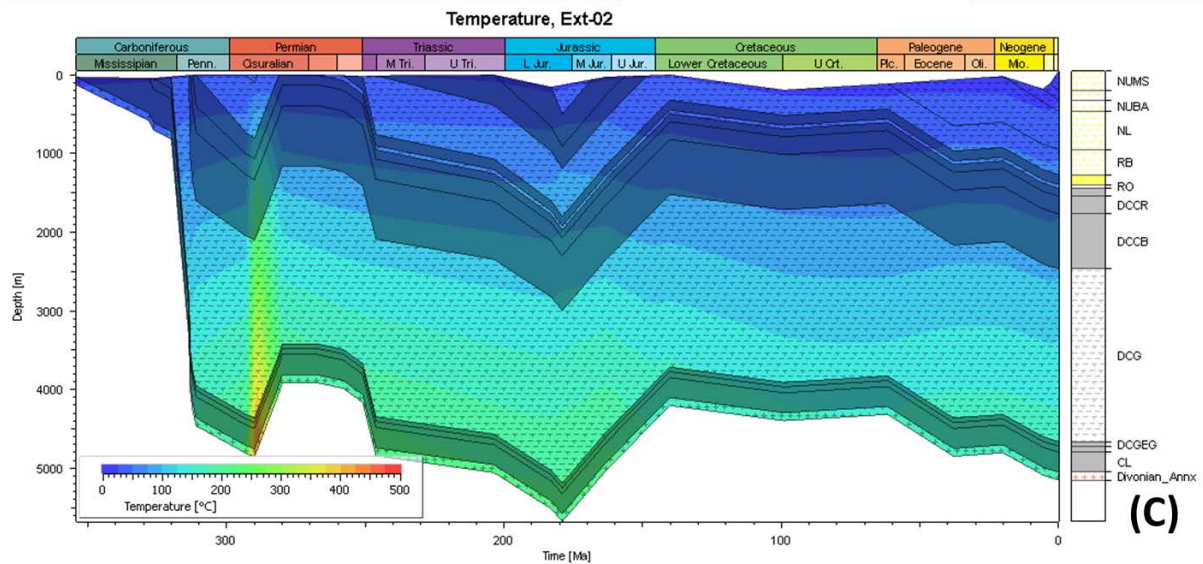
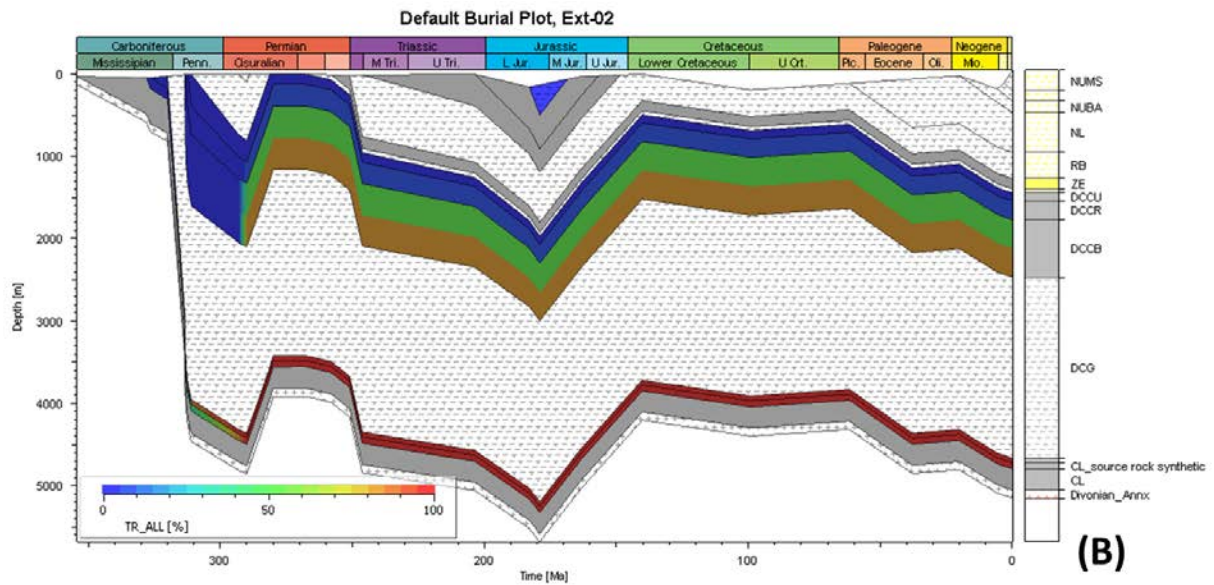


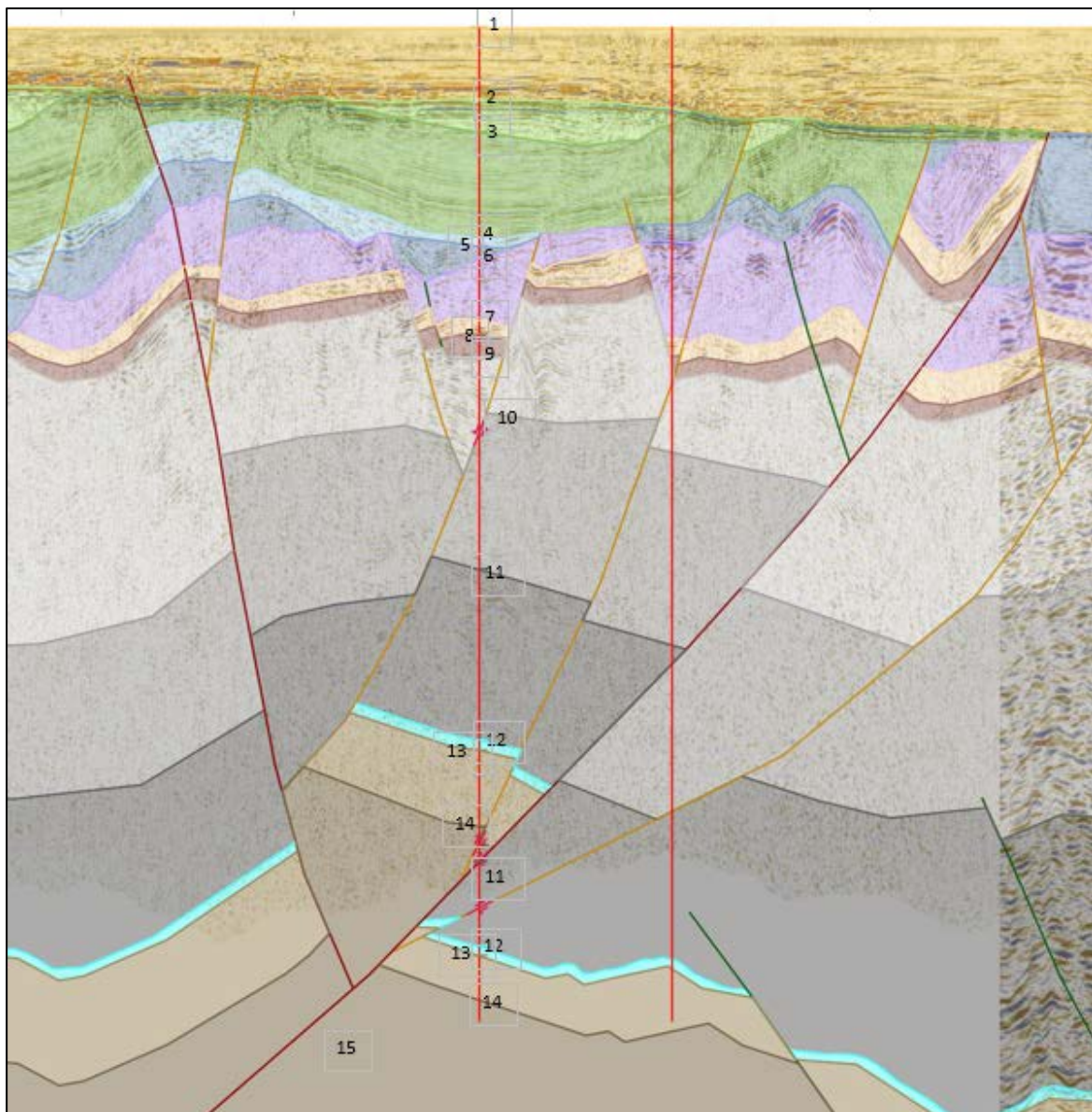
Figure 60: 1D basin model results for well Ext-02. [A] Burial history with the modelled maturity (%Ro). [B] Modelled Transformation Ratio (TR %) of the main source rocks. [C]



Modelled temperature history for the entire well section and [D] the modelled temperature evolution for the middle of the CL unit.

### Well Ext-3

Well Ext-03 is a pseudo well extracted from thickness maps derived from the new structural interpretation conducted in the structural restoration work package. The location of the extraction is along the Western Section just 7 km offshore IJmuiden (Figure 12). Depth horizons of the deepest levels are based on interpretations derived from gravity and magnetic data, as well as seismic data. Fault interpretations are derived from seismic interpretation carried out for the Western Section that was structurally restored. The interpretation of the geometry of this fault system is supported by another wells (JUT-01) that show repeated stratigraphic section. This well is located along the same structurally complex zone located between the West and Central Netherland Basin (Zandvoort Ridge to Peel Massbommel Complex). Ext-03 is in close proximity to well BAC-01, and is constructed through several fault blocks (Figure 61).



The temperature evolution for the CL units above and below the fault is shown in Figure 62C & D. Modelled present day temperature of the CL unit above the fault is 225°C.



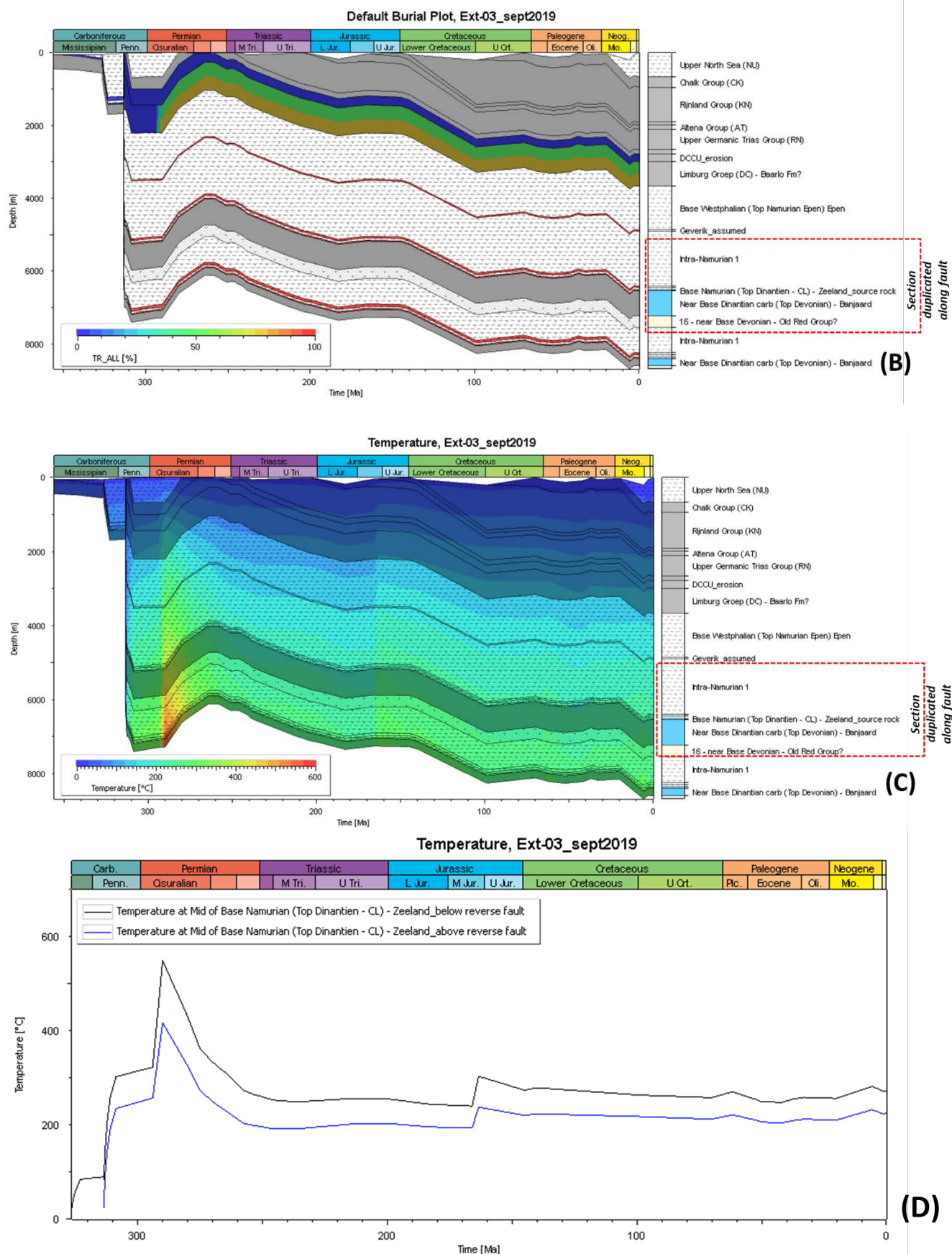


Figure 62: 1D basin model results for well Ext-03. [A] Burial history with the modelled maturity (%Ro). [B] Modelled Transformation Ratio (TR %) of the main source rocks. [C]

Modelled temperature history for the entire well section and [D] the modelled temperature evolution for the middle of the CL unit. Modelled temperature evolutions are shown for the CL unit above the fault (blue line) and below the fault (black line).

## Well AST-01-EXT

Well stratigraphy is based on the drilled section of well AST-01 complemented with extractions from the regional TNO 3D model and the new structural interpretation. The deepest part penetrated by the well section is the Lower Germanic Trias Group (RBSHN at 2664 m MD). Deeper units until the Top Westphalian ~4886 m depth and Mesozoic/Paleozoic erosion estimates are extracted from the regional 3D TNO model. The deepest section (Westphalian to Devonian at depth 5473 m) is based on the new structural interpretation. The erosion events included are:

- The Laramide event (Late Cretaceous): Total erosion of ~270 m.
- The Late Kimmerian event (Middle-Late Jurassic): Total erosion of 184 m.
- The Saalian event (Late Carboniferous-Early Permian): Total erosion thickness of 100 m.

No temperature or maturity calibration data are available for this well.

Main Westphalian source rocks in this well are identified as the Ruurlo (partially eroded) and the Baarlo Formations (Table 6). A Namurian source rock has not been identified in the drilled section or model extraction. The Top Namurian (50 m thickness at 5028 m depth) was identified from the new structural interpretation and for 1D basin modeling purposes assigned as the Namurian source rock.

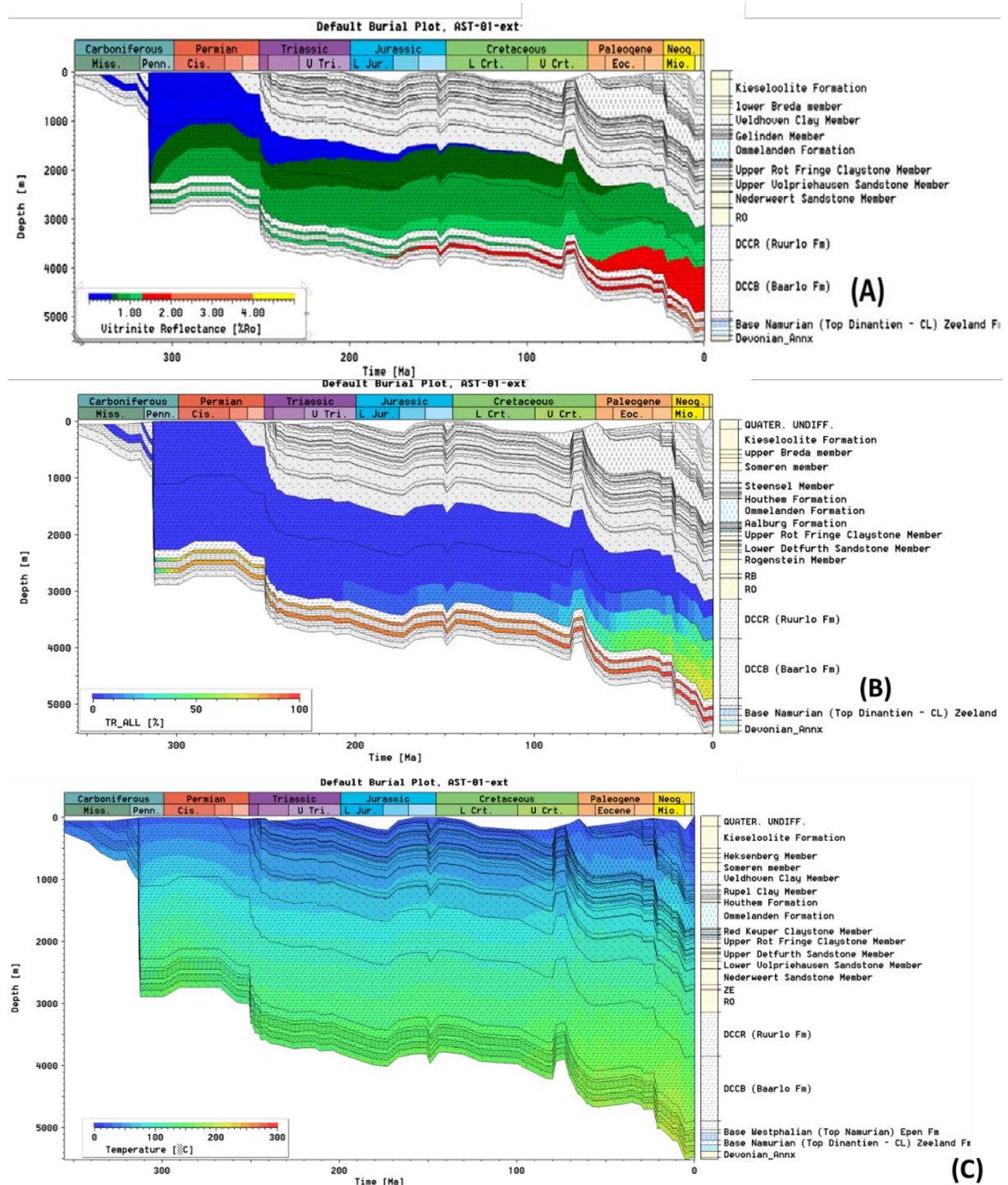
Potential Dinantian source rocks are simulated by assigning the basal 75 m of the Zeeland Formation (Base Namurian (Top Dinantien - CL) Zeeland Fm) as source rock.

Modelled results suggest that maturation of the Westphalian source rocks started post deposition and progressively increased towards present day (Figure 63). An initial maturation phase occurred in the Late Carboniferous – Permian during which maturity of the Ruurlo Formation reached Ro% ~0.50, whereas for the Baarlo Formation modelled vitrinite data suggests that top of the formation yielded Ro% ~0.5 to ~0.90 at the base of the formation (being in the oil window). From the Permian onwards, maturity of the Westphalian source rocks continued, reaching present day modelled vitrinite values of Ro% 0.85 (top) to 1.20 (base) of the Ruurlo Formation (oil window), and Ro% 1.20 (top) to ~2.00 (base) of the Baarlo Formation (wet as window, Figure 63). Modelled TR data show that the Ruurlo was not buried deep enough to generate hydrocarbons until at least the Oligocene, after which the modelled TR suggests that by present day up to 20% of the organic material may have been converted to hydrocarbons. For the Baarlo Formation, hydrocarbon generation may have initiated already in the Early Jurassic (Figure 63), with up to 72% of organic material converted at present day. Both Westphalian source rocks thus may contain variable amounts of organic matter (~80% in the Ruurlo to ~30% in the Baarlo Formations) that at present day may be expelling hydrocarbons.

The modelled maturity for the two assumed (synthetic) layers mimicking the Namurian Geverik Member and Dinantian source rocks show progressive maturity from Ro% 1 – 1.13 in the Permian to Ro% 2.20 – 2.30 at present day (dry gas window, Figure 63). Modelled TR data suggests that the Namurian source rock some 80-85% of organic matter has been converted to hydrocarbons in the Permian. At present day, only minor amounts (~3%) of unconverted organic matter remains and could be expelling hydrocarbons. For the Dinantian, modelled hydrocarbon expulsion initiated at the end of the Carboniferous, with a progressive

expulsion continuing to present day with some ~10% of non-converted organic matter remaining.

The temperature history of the modelled well section (Figure 63E) suggests that temperatures in the deepest sections never reached above ~230°C. Modelled temperatures in the middle of Zeeland Formation suggest a subtle increase, reflecting continuous burial. Modelled present day temperature at the mid-level of the Zeeland Formation is ~180°C.





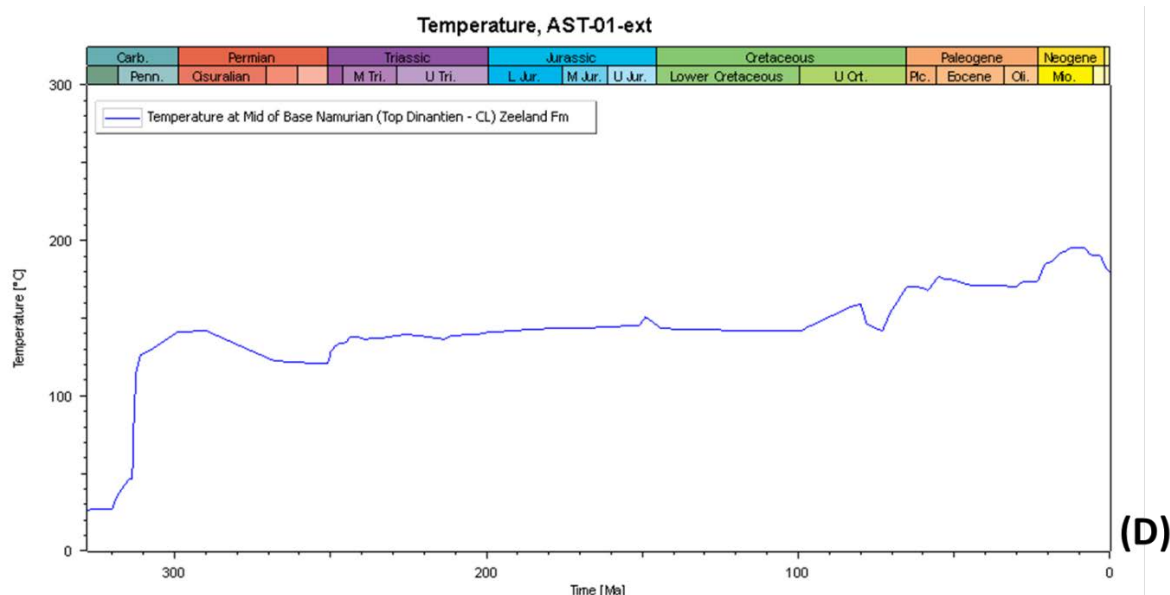


Figure 63: 1D basin model results for well AST-01-EXT. [A] Burial history with the modelled maturity (%Ro). [B] Modelled Transformation Ratio (TR %) of the main source rocks. [C] Modelled temperature history for the entire well section and [D] the modelled temperature evolution for the middle of the CL unit

### Well HVS-01

Well stratigraphy is based on the drilled section complemented with extractions from the regional TNO 3D model and the new structural interpretation. The deepest part penetrated by the well section is the Limburg Group (Ruurlo Formation). Deeper units until pre-Upper Devonian “basement”. (at ~6690 m depth) are derived from the new structural interpretation. The erosion events included are:

- The Laramide event (Late Cretaceous): Total erosion of 200 m.
- The Late Kimmerian event (Middle-Late Jurassic): Total erosion of ~530 m.
- Due to the presence of the youngest Westphalian stratigraphy (Strijen Formation) still preserved at the position of this well, the Saalian unconformity was not taken into account for this model.

Calibration data include vitrinite reflectance (31 measurements) and BHT (11 measurements) for this well.

Main Westphalian source rocks in this well are identified as the Maurits, Ruurlo and Baarlo Formations (Table 6). A Namurian source rock has not formally been identified in the drilled section or structural interpretation. The Top Namurian (50 m thickness at 6441 m depth) was interpreted from the new structural interpretation and for 1D basin modeling purposes assigned as the Namurian source rock.

To evaluate potential hydrocarbon generation from this section, Potential Dinantian source rocks are simulated by assigning the basal 30 m of the Zeeland Formation (Base Namurian (Top Dinantien - CL) Zeeland Fm) has been assigned as source rock.

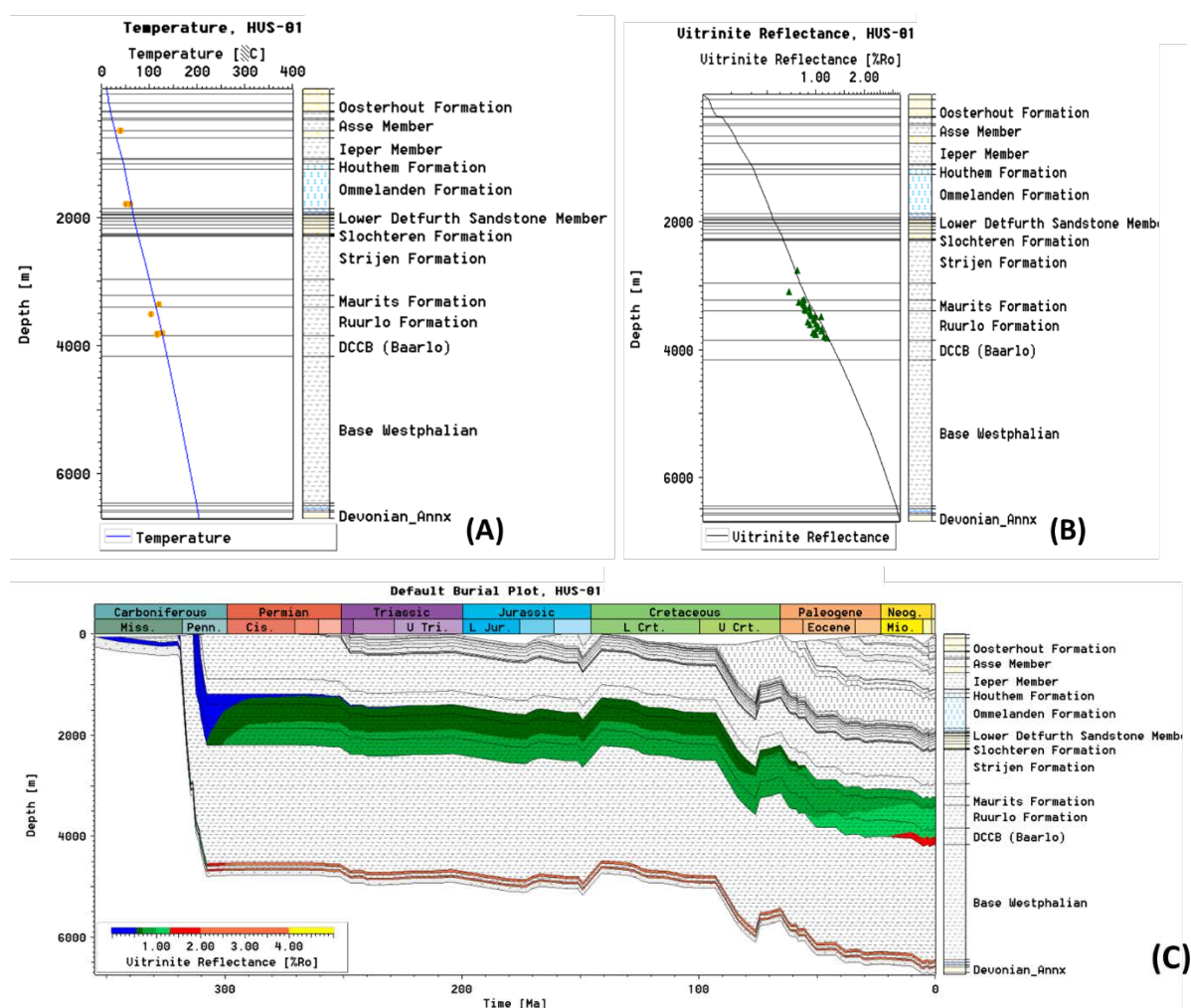
Model results suggest that following deposition, the Westphalian source rocks started to mature progressively until present day (Figure 64). Initial maturation occurred during the Late Carboniferous – Permian as shown by maximum modelled vitrinite data for the Maurits Formation (Ro% ~0.60), Ruurlo Formation (Ro% 0.71) and Baarlo Formation (Ro% ~0.84). Following a relatively stable period between the Permian – Cretaceous, subsidence continued



from the Late Cretaceous onward, resulting in progressive maturation into the late oil to wet gas window as suggested by modelled Ro% ~0.90 (Maurits Formation) to Ro% 1.35 (Baarlo Formation, Figure 64).

Modelled TR data suggest that hydrocarbon generation from the Westphalian source rocks did not start until the Late Cretaceous (Baarlo Formation) to Paleocene (Maurits Formation, Figure 64). Modelled TR data suggests that at present day, some 5% of the organic matter in the Maurits Formation to ~40% in the Baarlo Formation have been converted to hydrocarbons. The Westphalian units thus may have significant amounts of remaining organic matter from which hydrocarbons can be expelled.

The modelled maturity for the two assumed (synthetic) layers mimicking the Namurian Geverik Member and Dinantian source rocks show the main maturation phase in the Carboniferous – Permian, yielding modelled vitrinite of Ro% 2.60 – 2.70 respectively (dry gas window to overmature, Figure 64). Modelled TR data suggests that for both synthetic layers, virtually all (98 -99%) organic matter had been converted by the Late Permian. Modelled temperature for the middle of the Zeeland Formation suggest that following deposition of a thick Westphalian unit, the temperature rapidly increased in the Late Carboniferous related to burial and subsidence. From the Permian onward, the modelled temperature did not increase significantly and never reached temperatures in excess of ~220°C. The present day temperature in the Zeeland Formation is modelled at ~200°C.



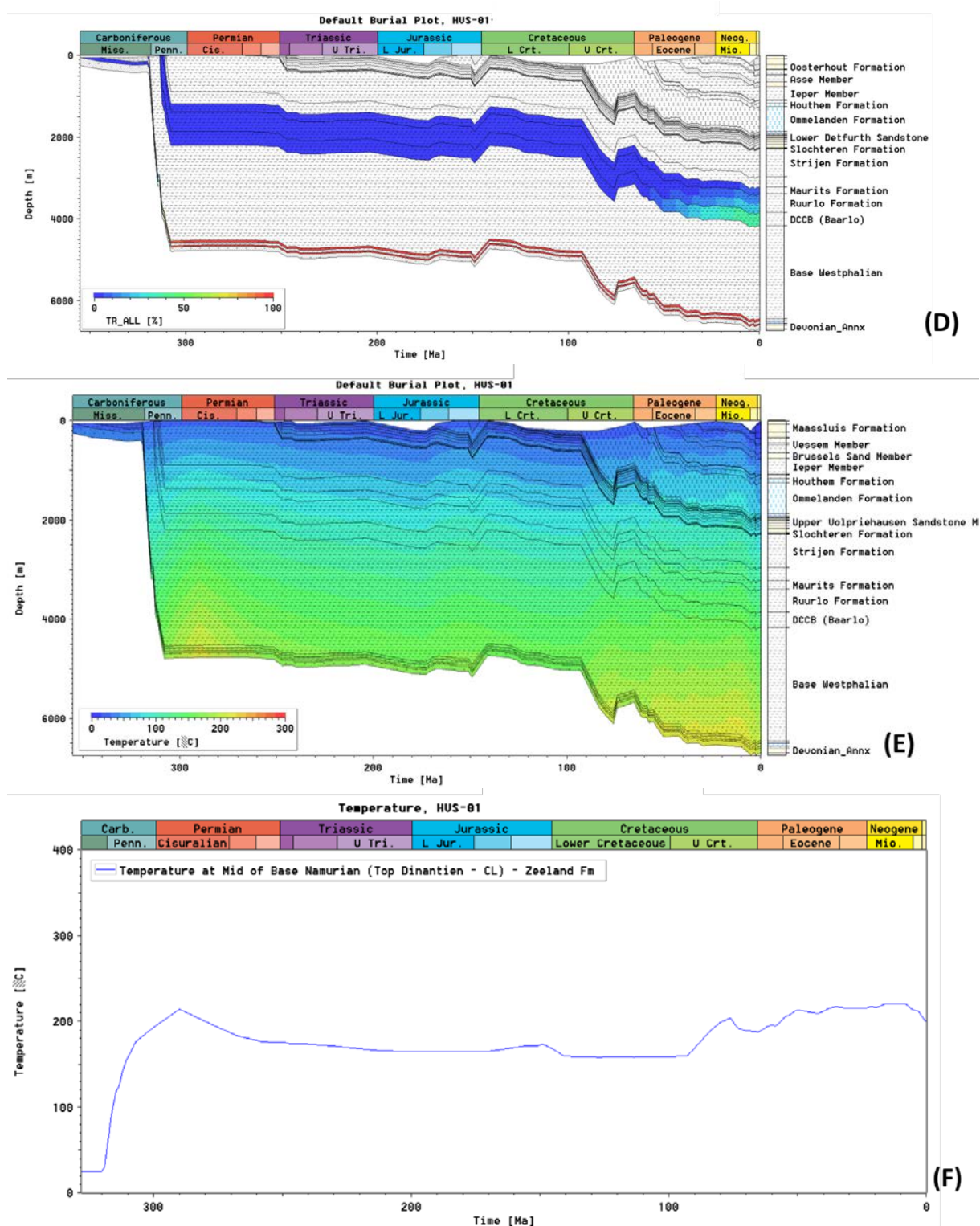


Figure 64: 1D basin model results for well HVS-01. [A] Present day modelled geothermal gradient versus well borehole temperature data. [B] Modelled present day maturity (%Ro) in well HVS-01 compared to measured Vitrinite reflectance (Vr%). [C] Burial history with the modelled maturity (%Ro). [D] Transformation Ratio (TR %) of the main source rocks. [E] Modelled temperature history for the entire well section and [F] the modelled temperature evolution for the middle of the CL unit Well HVS-01.

## London Brabant Massif/ Zeeland High area

Wells BHG-01, S02-02 and WDR-01 are located on the Zeeland High, along the northern flank of the London Brabant Massif (LBM). In all three wells the Carboniferous strata are directly overlain by Cretaceous Chalk deposits. The resulting ~200 My unconformity yields various questions for the 1D basin modeling:

- Was the LBM a stable block following the Carboniferous onto which no significant subsidence/deposition occurred until the Cretaceous Chalk?
- Have Permian to Early Cretaceous sediments been deposited onto the northern flanks of the LBM? If yes, what was the thickness of these deposits?
- If present, when were the Permian to Early Cretaceous sediments eroded, and did erosion occur in single or multiple phases?

To our knowledge, two apatite fission track (AFT) studies are available that could provide few insights in the time-temperature and exhumation (denudation) history of the LBM (Van den Haute and Vercoutere, 1990; Barbarand *et al.*, 2018). Both studies are located along the southern and central (Belgian) part of the LBM. Whether or not the results from both fission track studies can be translated directly to the northern Dutch flanks of the LBM is a matter of debate, but they provide the closest information on estimating the timing and amounts of erosion that have occurred between the latest Carboniferous and the overlying Cretaceous chalks.

AFT ages from Upper Ordovician igneous rocks outcropping along the southern margin of the Brabant Massif yield 184 – 143 Ma (Van den Haute and Vercoutere, 1990). Thermal modelling was not done by these authors, but it was suggested that the samples were never heated to temperatures higher than 100 °C (just below the partial annealing zone) and that a main, single cooling phase occurred from ~100 °C to surface temperatures between ~180 to 100 Ma (Van den Haute and Vercoutere, 1990).

Barbarand *et al.* (2018) collected samples from the Caledonian basement, Devonian and Carboniferous ash-beds and various Paleozoic and Mesozoic sandy facies (surface samples, and one well sample at 745 m depth) in the Ardennes and Brabant Massif. Resulting AFT data yielded ages between 260 to 140 Ma. Thermal modelling of selected samples suggest that the samples experienced two heating (burial) and cooling (exhumation) phases (Figure 65). Following Devonian-Carboniferous deposition, the samples were heated to temperatures > 120 °C roughly between 350 – 280 Ma, resulting in complete annealing of the fission tracks. This was followed by a first Jurassic cooling phase between ~260 – 220 Ma, when the samples were cooled to (near) surface temperatures. Depending on the assumed geological constraints (Jurassic and/or Cretaceous deposition), the samples experienced a second (minor) heating and cooling phase in the Late Jurassic-Cretaceous. In the second heating phase, initiating roughly 210 Ma, the samples reached temperatures of roughly 40-60 °C (maximum 80 °C) at around 180 Ma. This was followed by the second and final cooling phase from ~160 Ma to present day surface temperatures (Barbarand *et al.*, 2018).

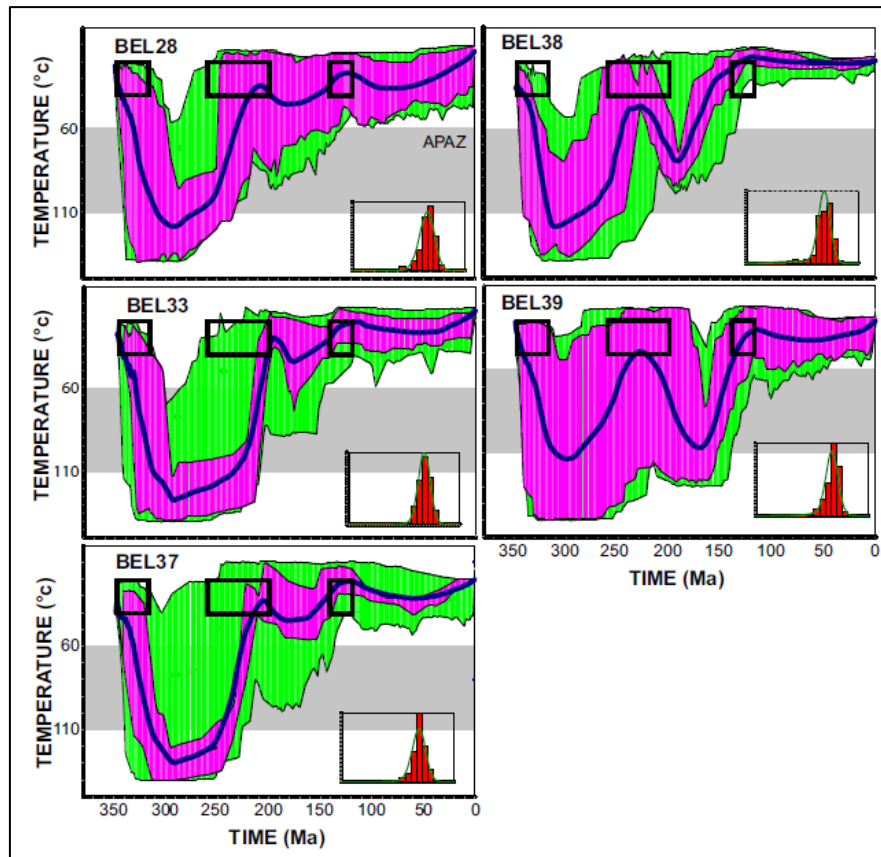


Figure 65: Apatite Fission Track (AFT) thermal models from which the subsidence/uplift history is derived for the 1D basin modelling of the London Brabant Massif wells. AFT data from the southern and central flanks of the Belgian Brabant Massif (Barbarand *et al.* 2018).

Three geological constraints were used in the thermal model (see Barbarand *et al.* 2018 for discussion on these constraints):

- Constraint A: Viséan age of the ash-beds;
- Constraint B: Near surface presence (20–40 °C) of the rocks during the Late Permian–Triassic after the post-Carboniferous inversion;
- Constraint C: Surface presence during the Early Cretaceous (140–120 Ma).

If only constraint A is used in the thermal models, effectively one single heating/cooling history is modelled. In the Carboniferous, samples were heated (buried) to >140 °C, and then cooled slowly in a near linear path to surface temperatures at present day. When using constraints, A and B, model results suggest Carboniferous heating followed by cooling to (near) surface temperatures in the Jurassic; post-Jurassic the rock samples hovered around the surface and were not buried significantly anymore. When constraints A, B and C are used, then the post Jurassic heating becomes more apparent (up to ~60 °C). Best-fit AFT thermal models were obtained when all three constraints were used (Barbarand *et al.* 2018).

Although the AFT provides some insights in the burial/exhumation history of the LBM, this mainly applies to the central/southern flanks of the LBM. It is possible that along the northern, Dutch flank of the LBM the cooling/exhumation history occurred (slightly) different compared to the south. Conducting a fission track study on available well data or on outcrops along the northern flank of the LBM may provide better insights in the erosion/exhumation history of the LBM. This could refine the 1D basin model studies conducted for the current BHG-01, S02-02 and WDR-01 wells.



Based on available AFT data, and integrating the results of the structural restoration work package, the following assumptions are made for the Carboniferous to Cretaceous unconformity for the 1D basin models for wells BHG-01, S02-02 and WDR-01:

- Cooling/heating trends in the AFT data from the southern flank of the LBM can roughly be translated to the northern flank;
- After the Carboniferous, a first phase of heating/burial occurred until ~280 Ma followed by a period of cooling/exhumation until ~220 Ma;
- A second, Jurassic heating/burial phase occurred from ~200 – 140 Ma;

The thickness/amount of erosion amount of the Permian-Jurassic sections are used to obtain a good fit between the calibration data (well temperature and VR data) and the modelled output data. Sensitivity tests have been conducted to understand the influence of the various heating/burial and cooling/exhumation phases but are not reported here.

## Well BHG-01

Well is based on the drilled section (available from NLOG website). The well penetrated the Banjaard Group (Bollen Claystone Formation, OBBS) at TD 2907 m. Carboniferous strata (Baarlo Formation) are unconformably overlain by the Cretaceous Ommelanden Formation (at 1398 m), resulting in an ~220My unconformity. In the Mesozoic section, several short hiatuses and erosion events were introduced mimicking the Kimmerian (Jurassic, 500 m of erosion) and Savian (Late Paleocene, 100m of erosion) events.

Source rock kinetics are assigned as per Table 6 for the Westphalian (Baarlo Fm) and Namurian (Epen Fm) rocks. In the drilled section however, only the Epen Formation was identified. Available GR logs however suggest a thick shale layer is present at the base of the Epen Formation. For the basin modelling exercise therefore, a 68m thick layer was introduced (Geverik\_ synthetic), which was assigned SR kinetics (Table 6). To evaluate if the Goeree and Beveland Members (Zeeland Formation) could expel hydrocarbons if thin source rocks were present, the lower parts of these members (31 m for Goeree Member and 43 m for the Beveland Member) were assigned as source rocks.

Three corrected borehole temperature calibration data are available. In total 10 VR datapoints are available for the Carboniferous and Devonian formations. For 8 of those data points, the Ro% was given (plus standard deviation); the %Ro min and %Ro\_max were calculated from the standard deviation. Two recently measured VR data points were included as well.

Below, the results are presented for the best-fit 1D basin model for well BHG-01. The subsidence and erosion events roughly follow the main trends derived from the apatite fission track data discussed above.

In order to fit the model data to the calibration data, two parameters were tested: the basal heat flow for the Abdul Fattah *et al.* (2012) model and the amount of Permian-Jurassic deposition/erosion. Varying heat flow and erosion data will affect both the temperature and maturity data. It was observed that varying (higher) heat flow values had a significant effect on the modelled temperatures. Our approach was to obtain good fit between the modelled and well temperature data using heat flow variations, and then adjust the amount of post Carboniferous erosion/deposition to fit the modelled VR data to the measured data.

Using the “initial” Abdul Fattah *et al.* (2012) heat flow model, the modelled temperature curve is underestimated compared to the well temperature calibration data. Heat flow was therefore increased in 5mW/m<sup>2</sup> steps to fit the model data to the well calibration data.

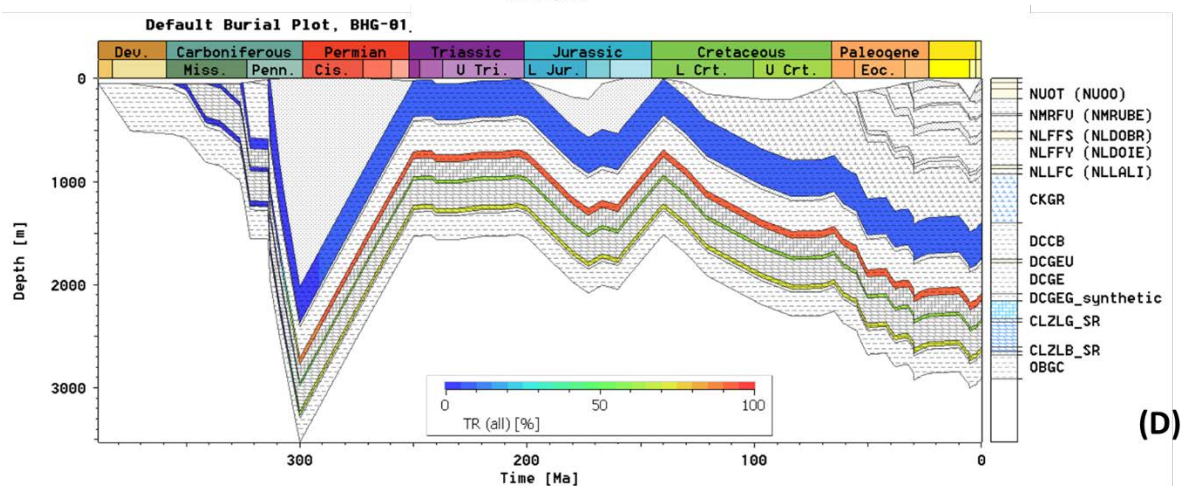
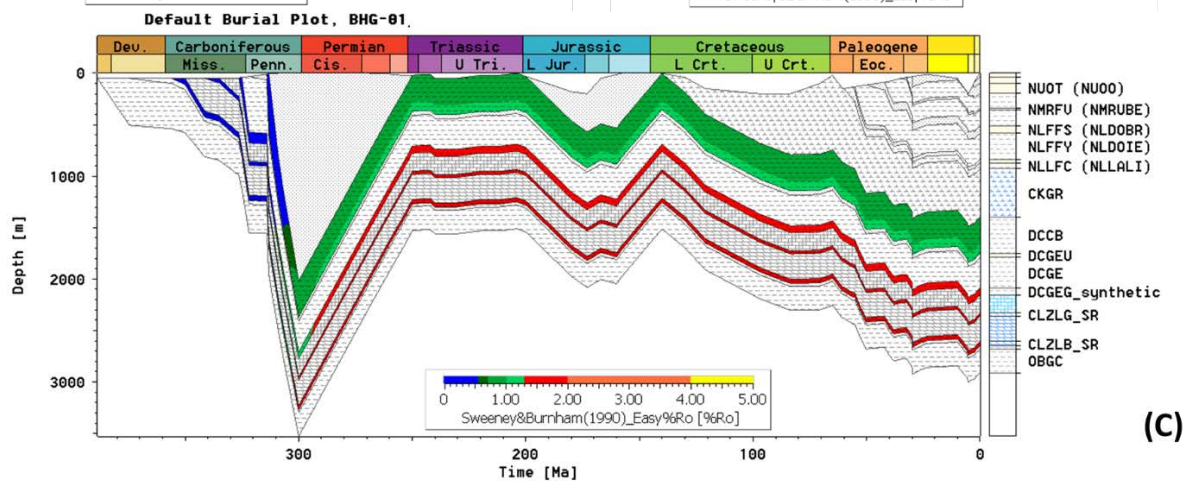
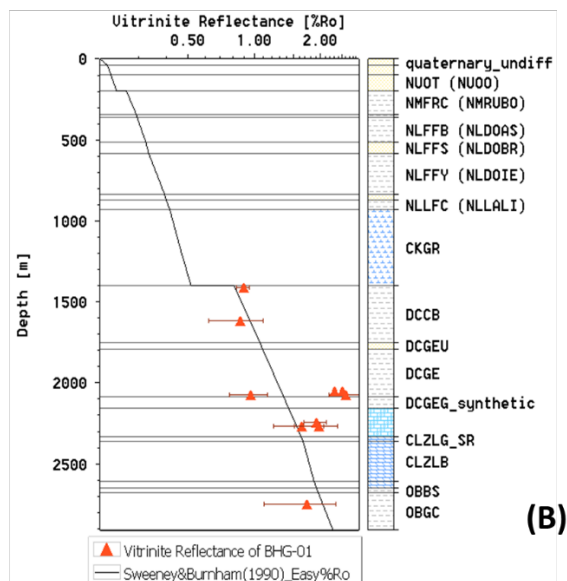
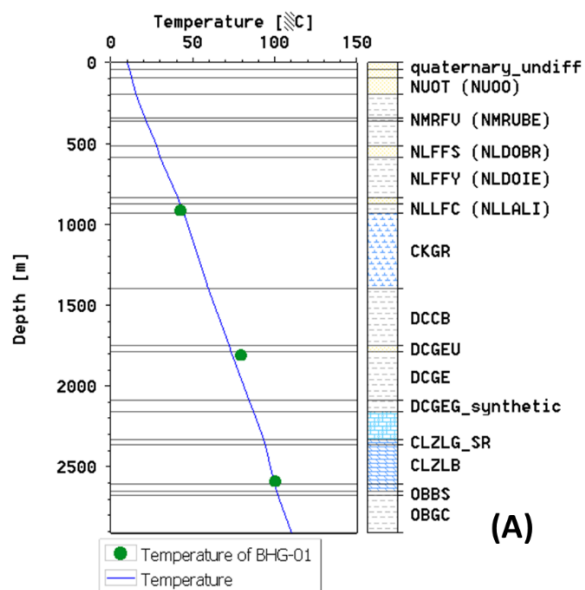
Figure 66 shows the best fit 1D basin model to the calibration data. To obtain this best fit,  $10\text{mW/m}^2$  was added to all heat flow data points of the Abdul Fattah *et al.* (2012) model. In order to fit the modelled data to the calibration VR data, some 2000 m of Late Carboniferous deposits are required (deposited until 300 Ma), which are subsequently eroded during the Permian-Jurassic. A second phase of Jurassic-Early Cretaceous subsidence requires some 500 m of sediments to be deposited prior to Cretaceous inversion and resulting erosion. None of the Jurassic-Early Cretaceous sediments are preserved, as Late Cretaceous chalk deposits of the Ommelanden Formation directly overlie the Carboniferous Baarlo Formation. Modelled maturity data suggests that the Westphalian source rock (Baarlo Fm) is in the oil to wet gas window (%Ro 0.7 – 1.00) since the onset of the Permian (Figure 66). Subsequent subsidence in the Late Jurassic-Early Cretaceous and Neogene was not sufficient to further mature the source rock. Modelled TR data suggests that at present day less than 10% of convertible organic matter in the Baarlo Formation has been converted to hydrocarbons, which occurred at the onset of the Permian (Figure 66).

At present day, part of the Baarlo Formation may still be in the oil window and because not all the organic material has been converted, it has the potential to expel some hydrocarbons. Modelled data suggest that at present day, the Baarlo Formation may be expelling hydrocarbons. Modelled data suggest that at present day, the Baarlo Formation may be expelling hydrocarbons (oil, possibly wet gas).

Model data for the Namurian source rock (assumed Geverik Member, Zeeland Formation) suggests that its maturity is in the wet to dry gas window, which was reached at the onset of the Permian (%Ro ~1.40). Modelled TR for the Namurian suggests that 90-95% of convertible organic matter has been converted to hydrocarbons. A small portion of the source rock may be able to expel (probably) gas at present day.

For the Dinantian units, the model predicts maturity values around %Ro 1.90 suggesting it is in the dry gas window from the Permian onwards (Figure 66). Modelled TR suggest that around 60 to 75% of organic matter is converted to hydrocarbons for the Goeree and Beveland Members respectively. At present day, these members may be expelling predominantly dry gas.

The temperature evolution of the Dinantian units is strongly linked to the postulated burial and uplift history. At the end of the Carboniferous strong subsidence resulted in a rapid increase in temperature of the Zeeland Formation units to a maximum of nearly  $200^\circ\text{C}$ . Rapid uplift and related erosion resulted in decreasing temperatures. From the Triassic onwards, a steadily but slow increasing temperature reflects the postulated slow subsidence of the Dinantian units. Modelled present day temperature for the Goeree and Beveland Members is  $\sim 100 - 110^\circ\text{C}$  (Figure 66 E & F).



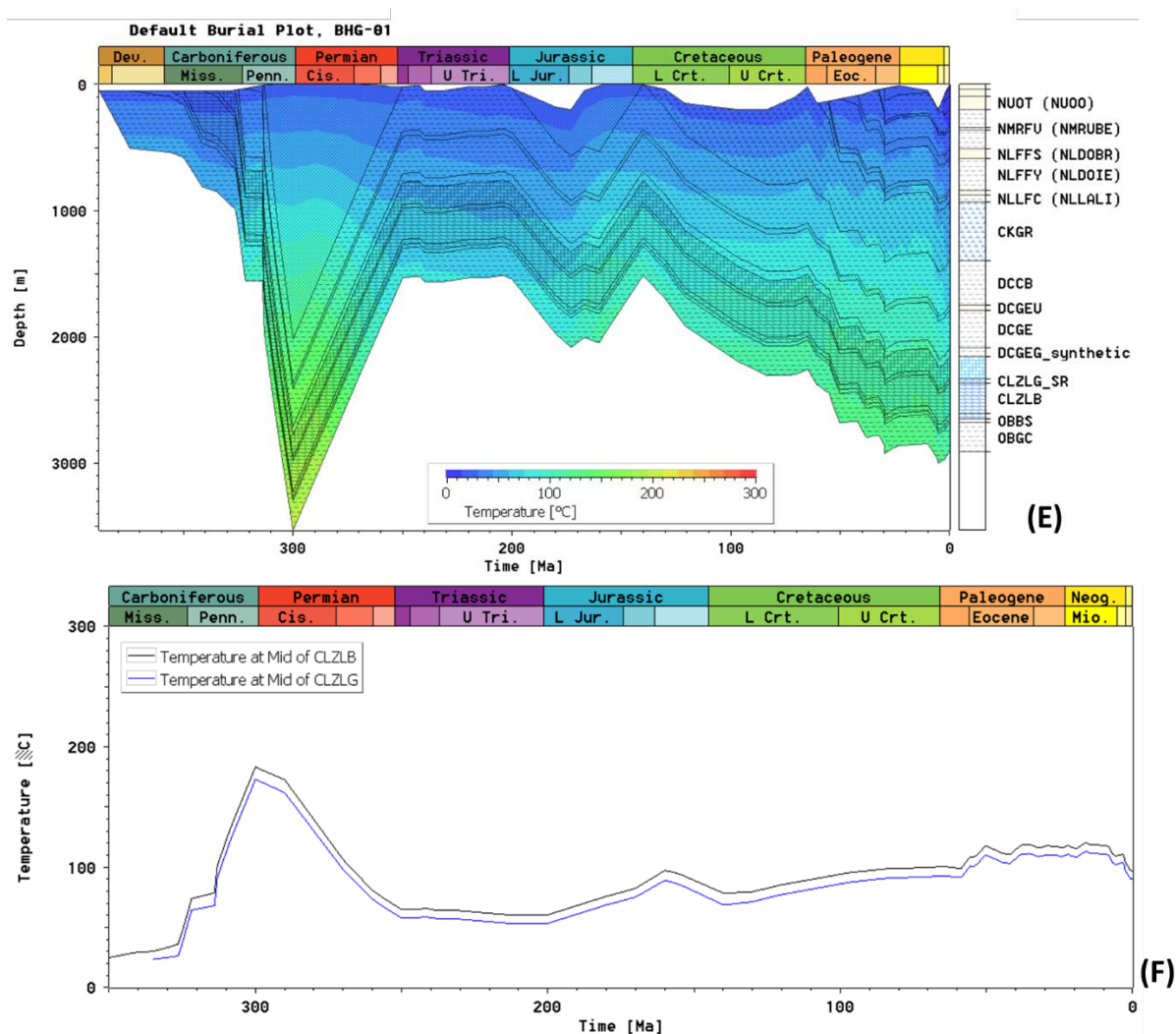


Figure 66: 1D basin model results for well BHG-01. [A] Present day modelled geothermal gradient versus well borehole temperature data. [B] Modelled present day maturity (%Ro) in well BHG-01 compared to measured Vitrinite reflectance (Vr%). [C] Burial history with the modelled maturity (%Ro). [D] Transformation Ratio (TR %) of the main source rocks. [E] Modelled temperature history for the entire well section and [F] the modelled temperature evolution for members of the Zeeland Formation: Goeree Member (blue line) and Beveland Member (black line).

## Well S02-02

Well is based on the drilled section (available from NLOG website). The well penetrated the Banjaard Group (Bollen Claystone Formation, OBBS) at TD 2878 m. Carboniferous strata (Ruurllo Formation) is unconformably overlain by the Cretaceous Ommelanden Formation (at 1336 m), resulting in an ~220My unconformity. As in BHG-01, several short hiatuses and erosion events were introduced in Mesozoic formations, mimicking the Late Kimmerian and Savian (Late Paleocene) events.

Source rock kinetics are assigned as per Table 6 for the Westphalian (Ruurllo & Baarlo Fms) and Namurian (Epen Fm) rocks. In the drilled section however, only the Epen Formation was identified (see NLOG website). Available GR logs however suggest a ~100m thick shale layer is present at the base of the Epen Formation. For the basin modelling exercise therefore,



a conservative 75 m thick layer was introduced (Geverik\_synthetic), which was assigned SR kinetics.

To evaluate if the Dinantian units (Goeree, Schouwen and Beveland Members) could expel hydrocarbons if thin source rocks were present, the lower parts of these members (31 m for Goeree Member, 72 m for the Schouwen Member and 43 m for the Beveland Member) were assigned as source rocks.

For the Dinantian units (Goeree, Schouwen and Beveland Members), source rock parameters were assigned to small portions of each member (15% of the original thickness, at the base of the member). Lithological composition was adopted from the Zeeland Formation and source rock parameters as per Table 6.

One static seabed temperature and three uncorrected borehole temperature data points are available. A 5°C temperature correction was applied to the later. A total of 23 VR measurements were available in both the Carboniferous and pre-Upper Devonian “basement”. (17 measurements) as well as the overlying Mesozoic formations (5 measurements). In the original well reports (NLOG website), low grey mean, and high grey mean %Ro data have been reported. These data were taken as min and max %Ro from which an average value was calculated. The min and max %Ro values were considered as the error bars. The quality of the Vr data from the Mesozoic section was questionable and therefore they were excluded from the model calibration procedures.

Owing to its proximity to well BHG-01, the same modelling approach was followed as outlined for well BHG-01. For well S02-02 the same adjusted heat flow model (+10 mW/m<sup>2</sup> to all data points) of Abdul Fattah *et al.* (2012) was taken as used to model well BHG-01.

Figure 67 shows the best fit modelled temperature data for well S02-02.

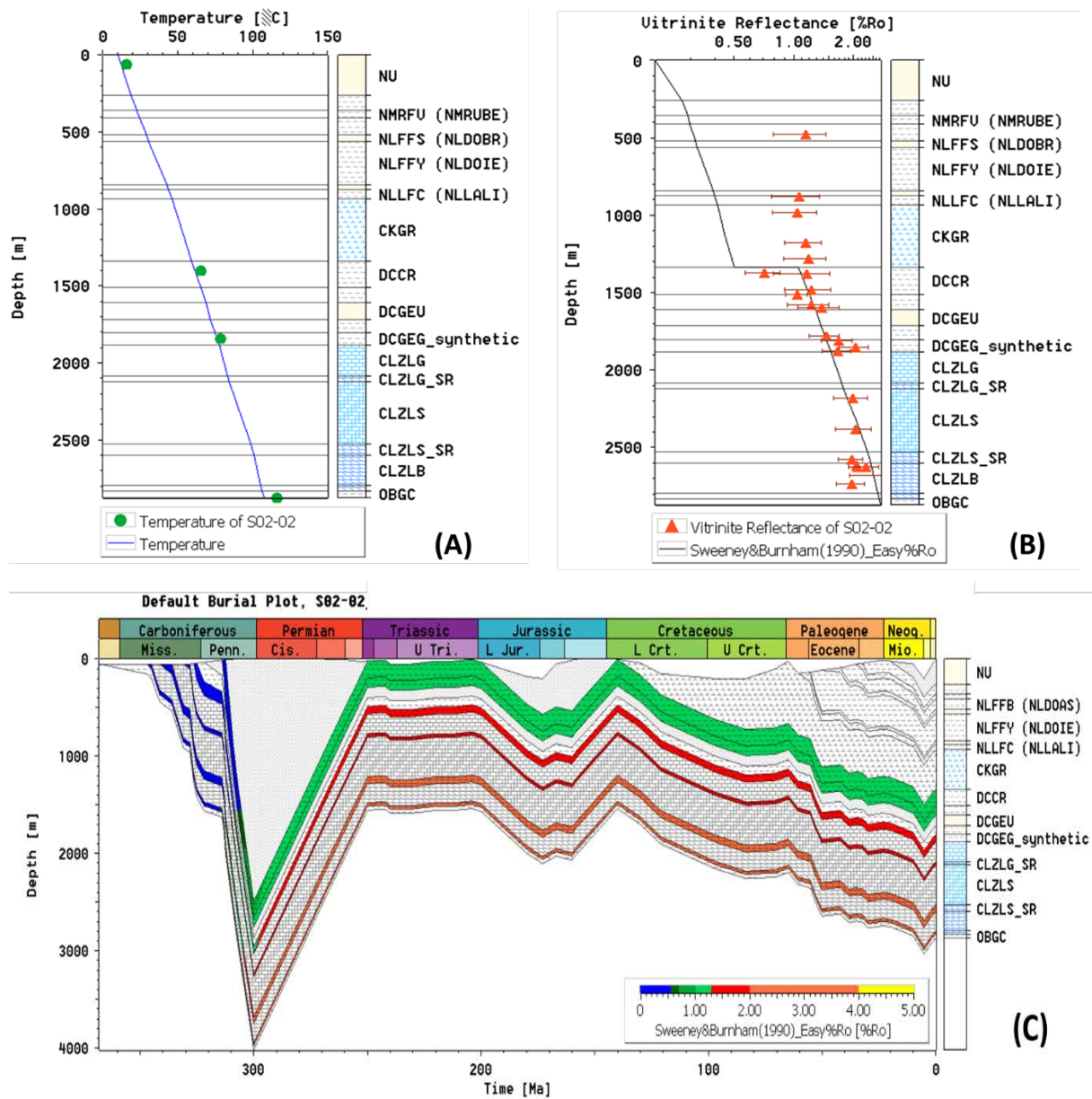
In order to fit the modelled data to the Calibration VR data (at least for the Carboniferous strata below 1300 m), some 2500 m of Late Carboniferous deposits are required (deposited until 300 Ma), which are subsequently eroded during the Permian-Jurassic. A second phase of Jurassic-Early Cretaceous subsidence requires some 500 of sediments to be deposited prior to Cretaceous inversion and erosion. None of the Jurassic-Early Cretaceous sediments are preserved, as Late Cretaceous chalk deposits of the Ommelanden Formation directly overly the Carboniferous Ruurlo Formation.

Modelled maturity data suggests that the Westphalian source rocks (Ruurlo and Baarlo formations) are in the oil to wet gas window (%Ro 1.0 – 1.25) since the onset of the Permian. Modelled TR data suggests that at present day some 20 - 30% of convertible organic matter in the Ruurlo and Baarlo Formations have been converted to hydrocarbons. Peak hydrocarbon generation occurred at the onset of the Permian (Figure 67).

Model data for the Namurian source rock (assumed Geverik Member, Epen Formation) suggests that its maturity is in the wet to dry gas window (Figure 67), which was reached at the onset of the Permian (%Ro ~1.5). Modelled TR for the Namurian suggests that 90-95% of convertible organic matter has been converted to hydrocarbons. A small portion of the organic matter in the source rock may be able to expel (probably) gas at present day.

Potential Dinantian source rocks (if present) would reach a modelled maturity of %Ro 2.00 – 3.00, suggesting it would be in the dry gas window to being overmature. For the Goeree source rocks, the modelled data suggests that some 50% of the organic matter is transferred to hydrocarbons, for the deeper Shouwen and Beveland Members, this is 90-100% (Figure 67). The temperature evolution of the Dinantian units is strongly linked to the postulated burial and uplift history. At the end of the Carboniferous strong subsidence resulted in a rapid increase in temperature to a maximum of nearly 200°C. Rapid uplift and related erosion resulted in decreasing temperatures. From the Triassic onwards, a steadily but slow increasing temperature reflects the postulated slow Mesozoic subsidence of the Dinantian units.

Modelled present day temperature for the Goeree, Schouwen and Beveland Members is ~90 – 105°C (Figure 67 E & F). Present day modelled temperature is ~105°C.



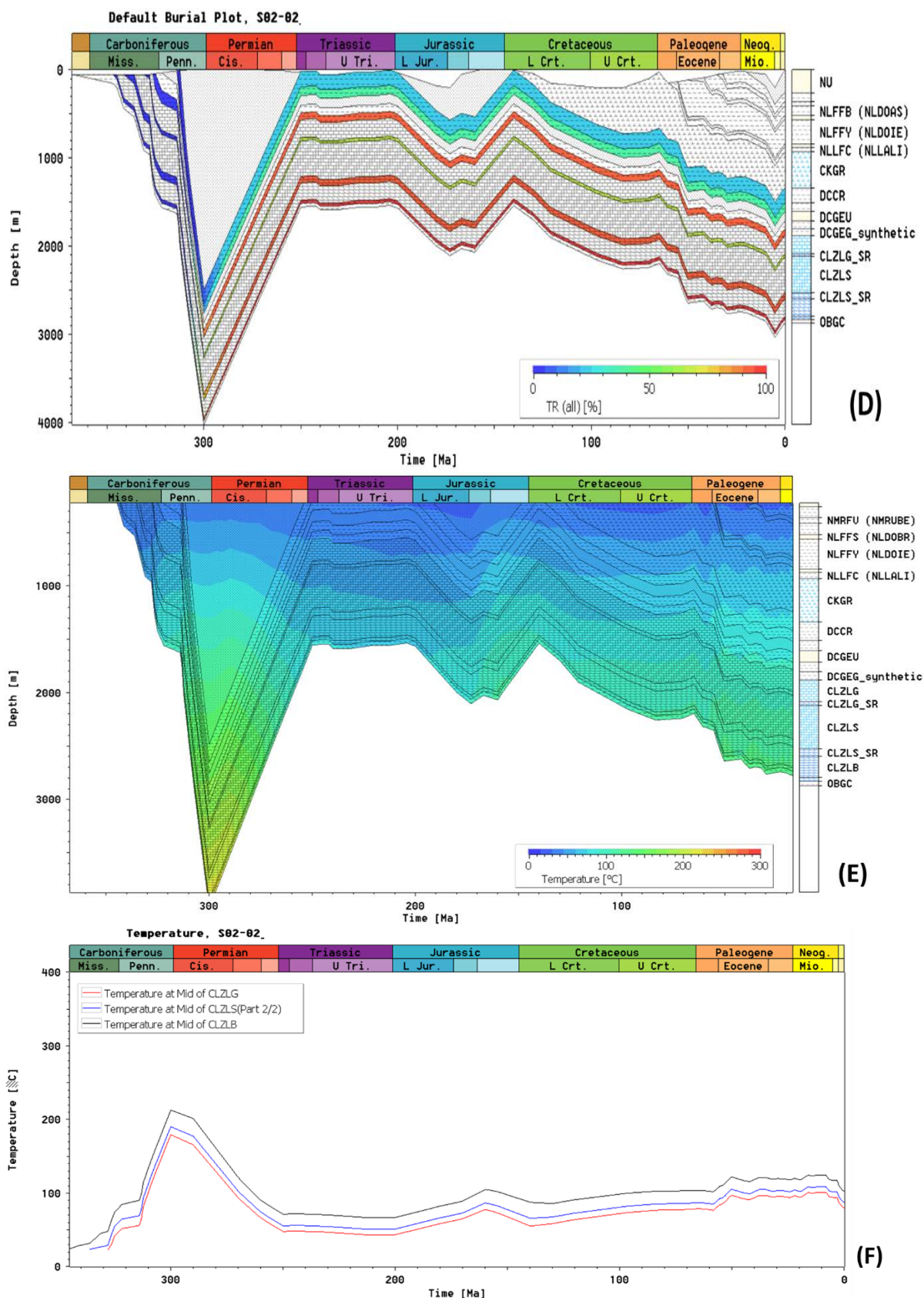


Figure 67: 1D basin model results for well S02-02. [A] Present day modelled geothermal gradient versus well borehole temperature data. [B] Modelled present day maturity (%Ro) in well S02-02 compared to measured Vitrinite reflectance (Vr%). [C] Burial history with the modelled maturity (%Ro). [D] Transformation Ratio (TR %) of the main source rocks. [E] Modelled temperature history for the entire well section and [F] the modelled temperature

evolution for members of the Zeeland Formation: Goeree Member (red line), Schouwen Member (blue line) and Beveland Member (black line).

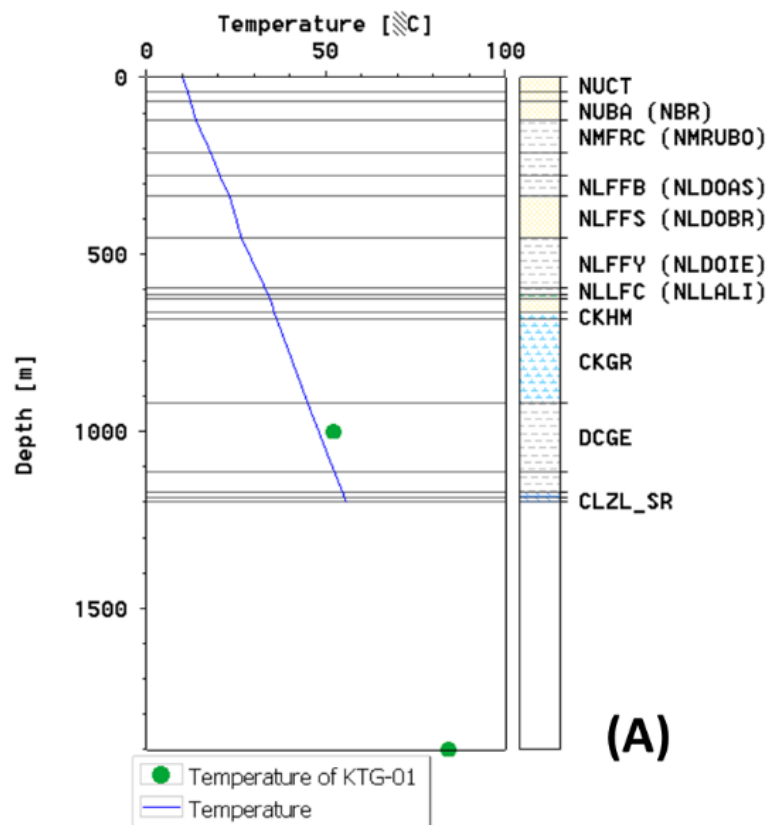
## Well WDR-01

The well is based on the drilled section (available from NLOG). The well penetrated the Dinantian Zeeland Formation to a TD 1205 m. Carboniferous strata (Epen Formation) is unconformably overlain by the Cretaceous Ommelanden Formation (at 919 m), resulting in an ~220My unconformity. As in BHG-01, several short hiatuses and erosion events were introduced in Mesozoic formations, the mimicking the Kimmerian (Jurassic) and Savian (Late Paleocene) events.

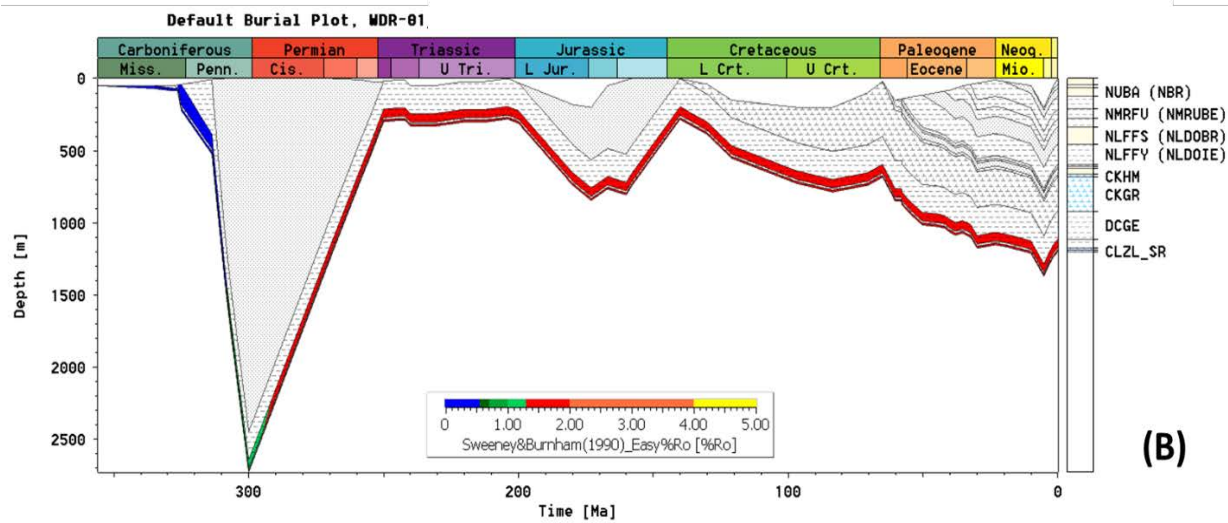
Potential source rocks of Carboniferous origin could be present in the Epen Formation. In the drilled section (see NLOG website) the Epen Formation was not further subdivided. However, in the initial well drilling report, an ~75 m thick shale layer was described just above the Dinantian Zeeland Formation. For the basin model for well WDR-01 this has been assumed and interpreted as the Geverik Member, therefore a conservative 60 m thick layer was introduced (Geverik\_synthetic) as a potential source rock and assigned kinetics as per Table 6. To evaluate if the also the Zeeland Formation could expel hydrocarbons if (thin) source rocks were present, the lower 14 m of the Zeeland Formation was assigned as source rocks. No borehole temperature (BHT) or VR data are available for well WDR-01. Owing to its proximity to well KTG-01, the BHT of this well has been used as calibration data for well WDR-01. Unlike for wells BHG-01 and S02-02, no VR data is available for WDR-01 to constrain the amount of required Permian erosion. Some 2500 m of Permian erosion therefor is assumed analogue to BHG-01.

To fit the model data to calibration data, the same modelling approach was followed as outlined for well BHG-01. Assuming that the BHT data of well KTG-01 can be used as a proxy for well WDR-01, 15mW/m<sup>2</sup> of heat flow data requires to be added to the “initial” Abdul Fattah *et al.* (2012) heat flow model, 5mW/m<sup>2</sup> more than in wells BHG-01 and S02-02. It is possible that the used BHT of KTG-01 is overestimating the temperature in WDR-01 and therefore should be taken cautiously for temperature calibration in WDR-01. Model data for both the Namurian and Dinantian source rocks (assumed Geverik Member in the Epen Formation and the Zeeland Formation synthetic source rock respectively) suggests that its maturity is in the wet to dry gas window (%Ro 1.30 – 1.40), reached during the Permian (Figure 68). Modelled TR for the Namurian source rock suggests that about 90% of its convertible organic matter has been converted to hydrocarbons in the Permian. A small portion of the source rock may be expelled as (probably) gas at present day. For the Dinantian source rock, some 50-60% of organic matter has been converted to hydrocarbons. Both the modelled VR and TR data depends strongly on the temperature calibration to well KTG-01 (and using a higher heat flow than in wells BHG-01 and S02-02). Therefore, the model results for well WDR-01 have less confidence than for wells BHG-01 and S02-02. The Dinantian temperature evolution is strongly linked to the postulated burial and uplift history. Post Carboniferous deposition, strong subsidence resulted in a rapid increase in temperature to a maximum of nearly 200°C. Rapid uplift and related erosion resulted in decreasing temperatures. From the Triassic onwards, the temperatures slowly increased but never exceeded ~75°C. Modelled present day temperature for the Zeeland Formation ~55°C (Figure 68 D & E).





(A)



(B)

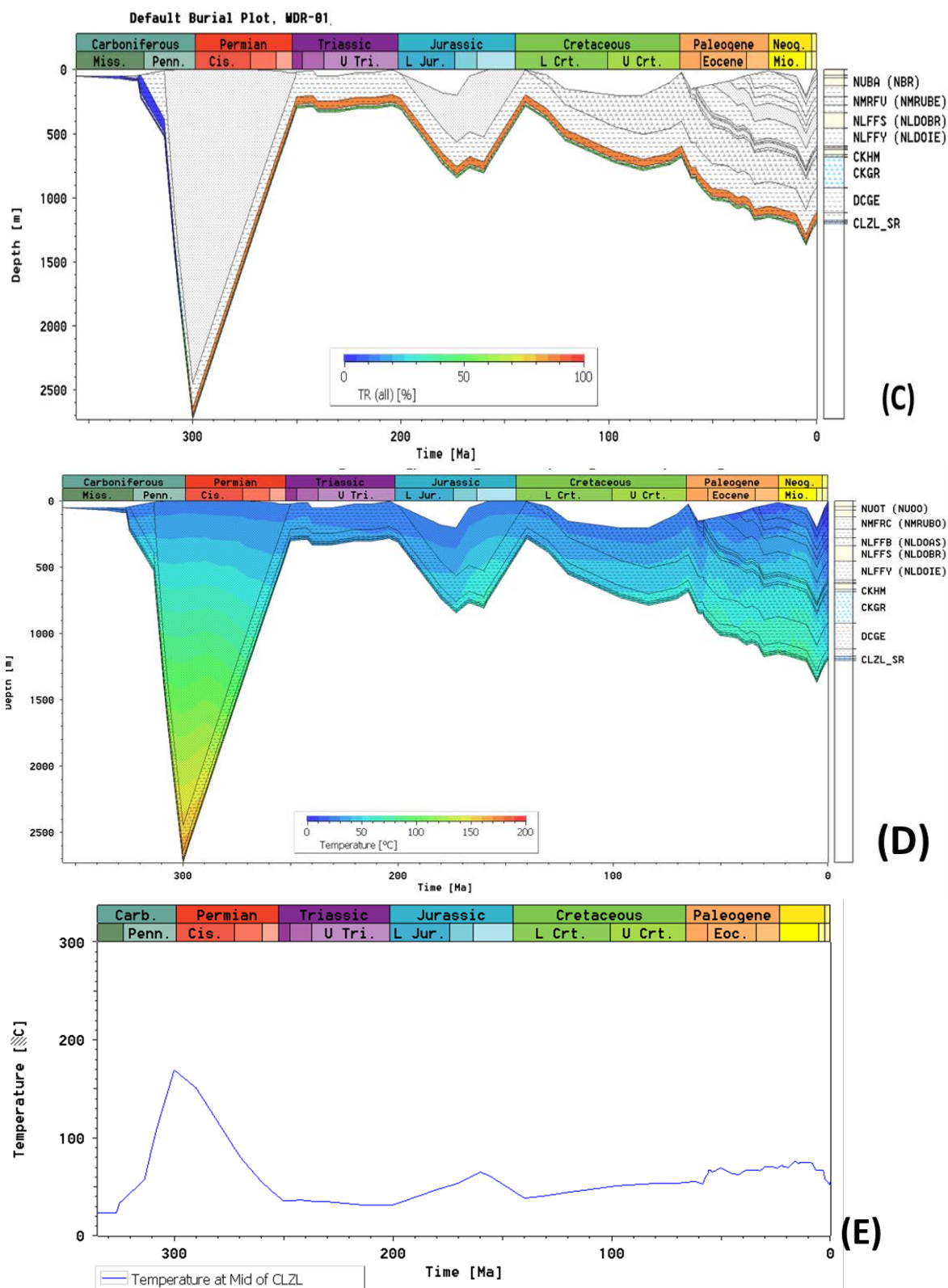


Figure 68: 1D basin model results for well WDR-01. [A] Present day modelled geothermal gradient versus well borehole temperature data. For WDR-01 no BHT data is available, the BHT of the nearby KTG-01 is used instead. [B] Burial history with the modelled maturity (%Ro). [C] Transformation Ratio (TR %) of the main source rocks. [D] Modelled temperature history for the entire well section and [F] the modelled temperature evolution for the Zeeland Formation.

## 8. Discussion and integration

The results from the 2D structural restoration and 1D maturity modelling are discussed in the section in relation to the burial history of the Dinantian carbonates.

### 8.1. 2D structural restorations

The 2D structural restorations show that the complex structural history of the Dutch onshore, that was heavily impacted by several phases of extension (Devonian/Silesian and Triassic/Jurassic) and contraction (Variscan and Alpine) since the Devonian, can be understood better by taking into account all data (well, VR, seismic) and knowledge available and integrating them into detailed structurally sound back stripped sections. It is important to notice that some important parameters such as the amount of stratigraphic thickness eroded at the base Permian and during the Jurassic are still difficult to fully comprehend. The information at hand and used in this project, from previous studies, from expert knowledge and from direct data (e.g. vitrinite reflectance data, seismic erosional patterns), make this study the most complete and integrated study regarding the structural evolution and burial history of the Dutch onshore. In the next chapter will be described the additional work that could help further decreasing the uncertainties.

The structural evolution of the Dutch onshore and the burial history of the Dinantian carbonates can be evaluated using the results of the restorations. An update structural evolution chart is presented in Appendix 5 and includes the main lessons learned from the two restorations and for specific structural elements present along the profiles.

A few faults were active during and prior to the deposition of the Dinantian Carbonate. These structures likely influenced the localization and growth histories of these carbonates platforms.

The two structural restorations clearly highlight the major kinematic differences between the dynamic southern basinal area (Roer Graben Valley, West Netherlands Basin and Central Netherlands Basin) and the more stable area further north (Noord-Holland Platform, Texel IJsselmeer High, Vlieland Basin and Friesland Platform). The southern area behaved as a mechanically weak zone with successive periods of significant uplift and subsidence, whilst the northern area is overall more stable and was subject to significant erosions (BPU and Mid-Cimmerian Unconformity). The reason for such a different mechanical behaviour is unknown, but a few possible options can be proposed: 1) the presence of mechanically strong geobodies along the northern edge of the CNB, such as intrusive magmatic bodies, 2) the early weakening of the northern edge of the CNB that focused subsequence structuration, or 3) the presence of an pre-existing deep crustal boundary, possibly associated with the Low Velocity Zone of Smit *et al.* (2016) that bound the limit between the Avalonia and Baltica plates further north.

Figures 69 and 70 shows the burial of the Dinantian through time from its original depth at the time of deposition/carbonate growth (light blue polygons) to its present-day position (light orange polygons) along the two restored sections. Figure 69 shows that in the southern part of the central section (ZH and OP) the Dinantian Carbonates were buried the deepest (4.5 to 6 km) during the Westphalian, while in the northern 2/3<sup>rd</sup> of the section, from the southern part of the PMC to the GP, the Dinantian was buried the deepest (5 to 8.5 km) during the Early Jurassic. It is also noticeable that the northern boundary fault of the CNB represent an

important limit in regards of the structural evolution of the Dutch sector and therefore of the Dinantian burial. Below are some of the key lessons learned from these burial graphs:

- The Dinantian reached its maximum burial depth at different time, depending on the its position with different structural elements. The average maximum burial and present depths are:
  - Zeeland High: 4.5 to 6,5 km deep during the Westphalian. Present day: 1 to 5 km deep.
  - West Netherlands Basin: 8 to 10 km deep during the Early, Late Cretaceous or present day. Present day 8-9 km deep.
  - Peel Massbommel Complex: 7 to 9 km deep at present or during the Lower Jurassic. Present day: 8 to 6 km deep.
  - Central Netherlands Basin: 6 to 11 km deep during the Lower Jurassic or Late Cretaceous. Present day: 5 to 10 km deep.
  - Noord-Holland Platform: 7 to 7,5 km deep during the present day, Westphalian or Early Jurassic. Present day: 7 km
  - Texel Ijsselmeer High: 5.5 to 8 km deep during the Westphalian or Lower Jurassic. Present day: 5 to 7,5 km.
  - Vlieland Basin: 6,5 to 8 km deep during the Westphalian. Early Jurassic or Late Cretaceous: Present day: 6 to 6,5 km deep
  - Friesland Platform: 5,5 to 7 km deep during the Westphalian or Lower Jurassic. Present day: 5 to 6 km deep.
  - Lauwerszee Trough: 6.5 to 9 km deep during the Lower Jurassic or present day. Present day: 6,5 to 9 km deep.
  - Groningen Platform: 5 to 8,5 km deep during the Early Jurassic or Late Cretaceous. Present day: 4.5 to 8,5 km deep.
- From the Early to Late Jurassic, all area except the West Netherlands Basin were uplifted by an average of 2 km due to a combination of uplift related to the Mid-North Sea doming and the uplift of the rift shoulder during the Jurassic rifting.
- Along the Central Section, the northern two third part of the Dutch onshore (from Peel-Massbommel Complex), reached maximum burial depths during the Early Jurassic.

Such results can allow to precisely estimate critical depth of burial and give additional information regarding the burial history of the Dinantian carbonates studied in the SCAN Dinantien Program (Mozafari *et al.*, 2019). Such results, combined with the fault kinematic results, can also give new insights on possible local fault reactivations, associated dolomitization, fracture characterisation and fluid flow dynamics. For further integration, such topic will be discussed with other SCAN Dinantian representatives of the other projects.



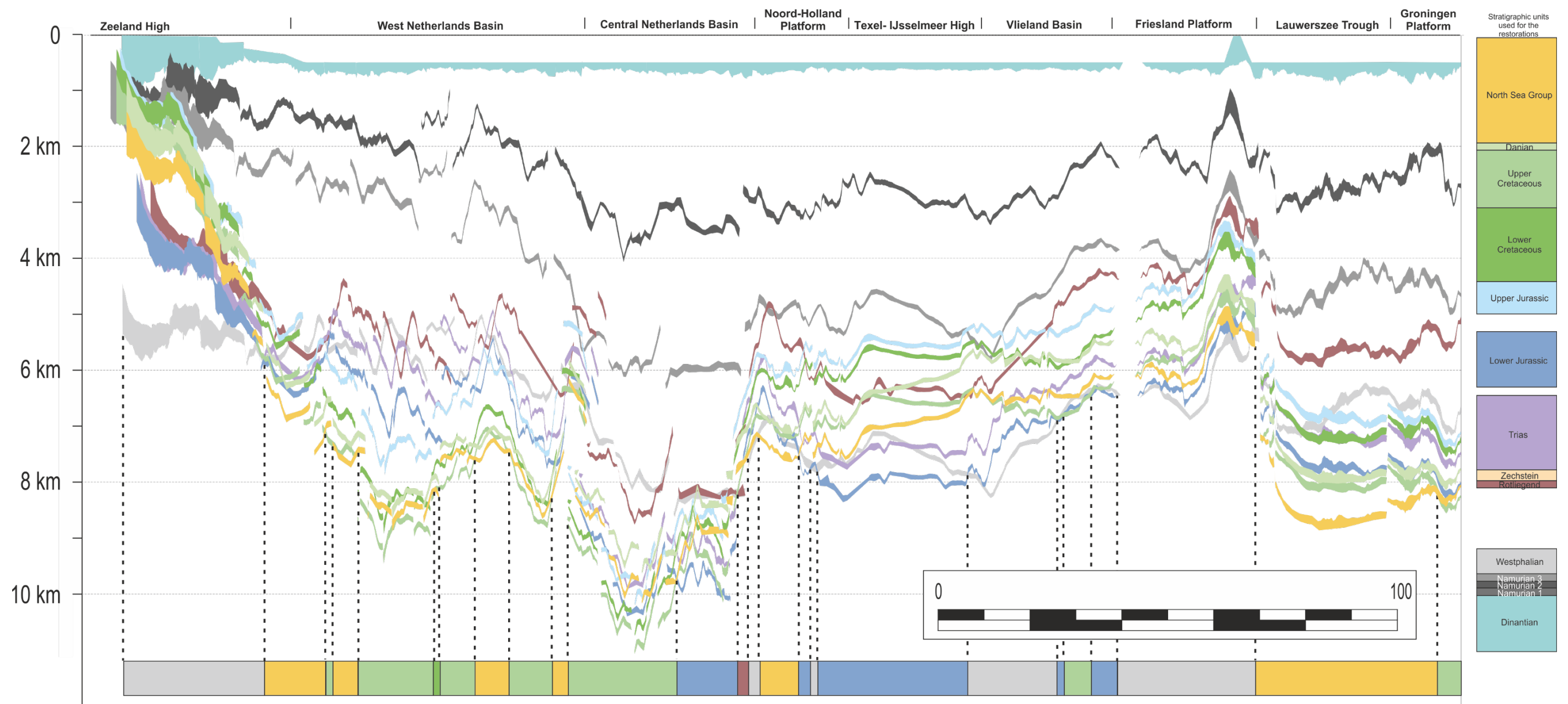


Figure 69: Dinantian summary burial graph for the Western Section. Coloured polygons represent the depth of the Dinantian carbonate at different time, based on the modelled depths obtained from the different time steps of the 2D structural restoration. The coloured row at the bottom of the figure represents the period at which the Dinantian was at its deepest position along this profile.

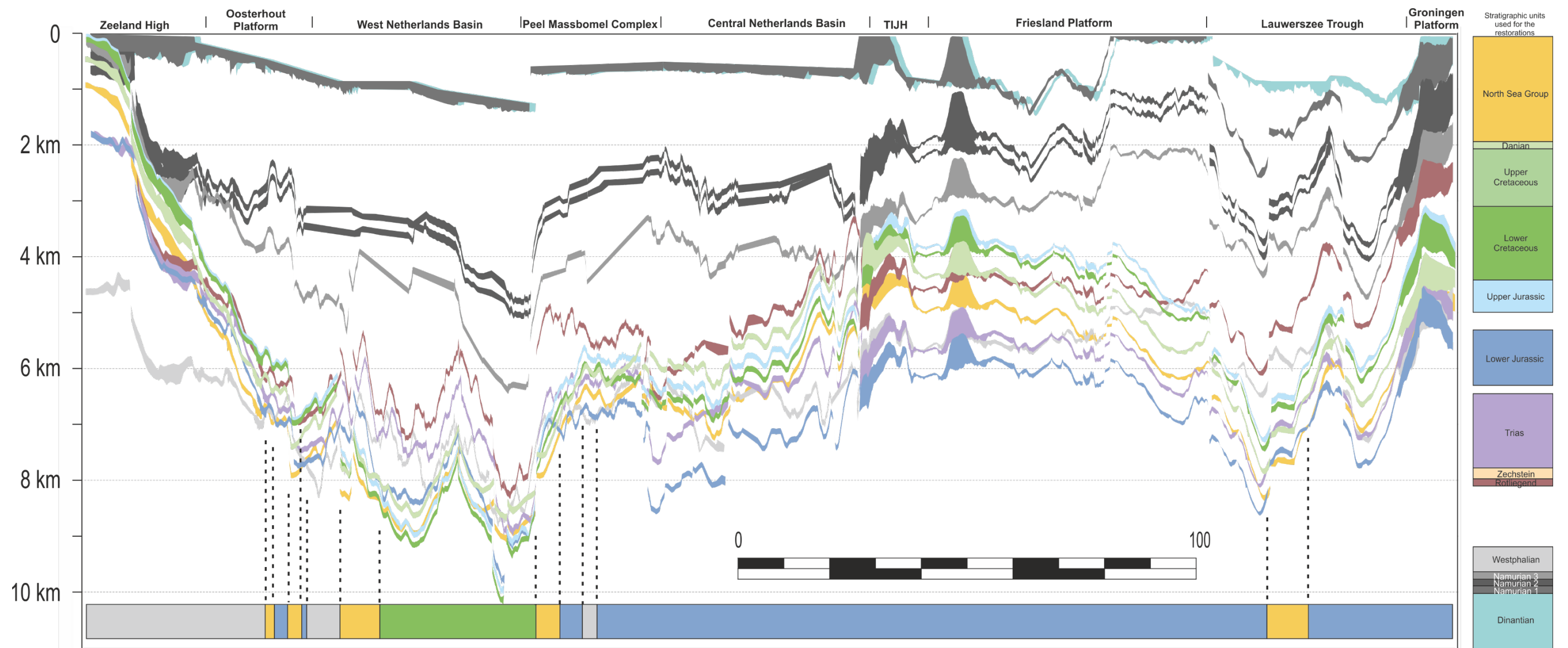


Figure 70: Dinantian summary burial graph for Central Section. Coloured polygons represent the depth of the Dinantian carbonate at different time, based on the modelled depths obtained from the different time steps of the 2D structural restoration. The coloured row at the bottom of the figure represents the period at which the Dinantian was at its deepest position along this profile.

## 8.2. 1D Basin Modelling

The main objectives of the 1D basin modelling work were to reconstruct and better understand the burial history (burial/uplift) of the Dinantian carbonates and provide predictions on the potential of Carboniferous source rocks to generate and expel hydrocarbons. In this section, we summarise the main outputs of the burial history reconstructions and integrate them with the structural reconstruction work.

For most of the modelled wells, the stratigraphy was based on the drilled well sections available from NLOG. Most wells terminated in the Mesozoic sections; only few wells encountered the Carboniferous and deeper strata. The new seismic interpretations of the Palaeozoic units conducted in WP 2.1.1 (seismic interpretation) and in the structural reconstruction proved instrumental in generating better 1D basin models of the deepest Carboniferous to Devonian intervals. This allowed us to better constrain the deep burial history of Dinantian units and model the maturity and hydrocarbon generation in potential Namurian to Dinantian source rocks.

In addition to aiding the maturity modelling of the Paleozoic units, the structural reconstructions provided independent constraints on one important uncertainty factor in the basin modelling: the amount of modelled erosion. In most of the studied wells, erosion amounts were derived from regional 3D TNO models and other independent constraints. Exception to this are the wells on the LBM, where the amounts of erosion (and deposition) are used to calibrate the modelled versus the measured maturity data.

Within the structural reconstruction framework, the various subsurface horizons are cross-balanced and reconstructed to their time of deposition. By doing so, also estimates on the amounts of erosion are made, providing an independent assessment of the erosion used in the 1D basin models. For most wells there appears to be good agreement in the order of magnitude of erosion modelled. For the LBM/ZH wells, where the assumed amounts of erosion and deposition are key factors in the basin modelling, the 1D basin models suggest around 2 – 2.5 km of Permian-Jurassic erosion. This appears to be in good agreement with the ~2-3 km of erosion derived from the structural reconstruction study. From the structural reconstruction, however, it is suggested that up to 4.5 km of burial must have occurred during the Westphalian. Compared to the 1D basin modelling results this is slightly overestimated as the 1D basin models suggest up to 3 km of burial. Further work on the burial and erosion history of the LBM would be required to better understanding the processes in play.

Figure 71 summarises the main phases of Westphalian source rock maturation and/or hydrocarbon generation. The various 1D basin models for the studied wells suggest that at some stage in the geological history, the source rocks have been matured sufficiently to reach the oil and/or gas window. For most wells, modelled data suggests that the initial, and main phase of Westphalian source rock maturation and hydrocarbon generation occurred during the Late Carboniferous – early Permian. For wells from the WNB (HVS-01 and AST-01-Ext), BAC-01 and SWD-01, modelled results suggest that this was followed by a later, second maturation phase in the Late Cretaceous to Neogene.

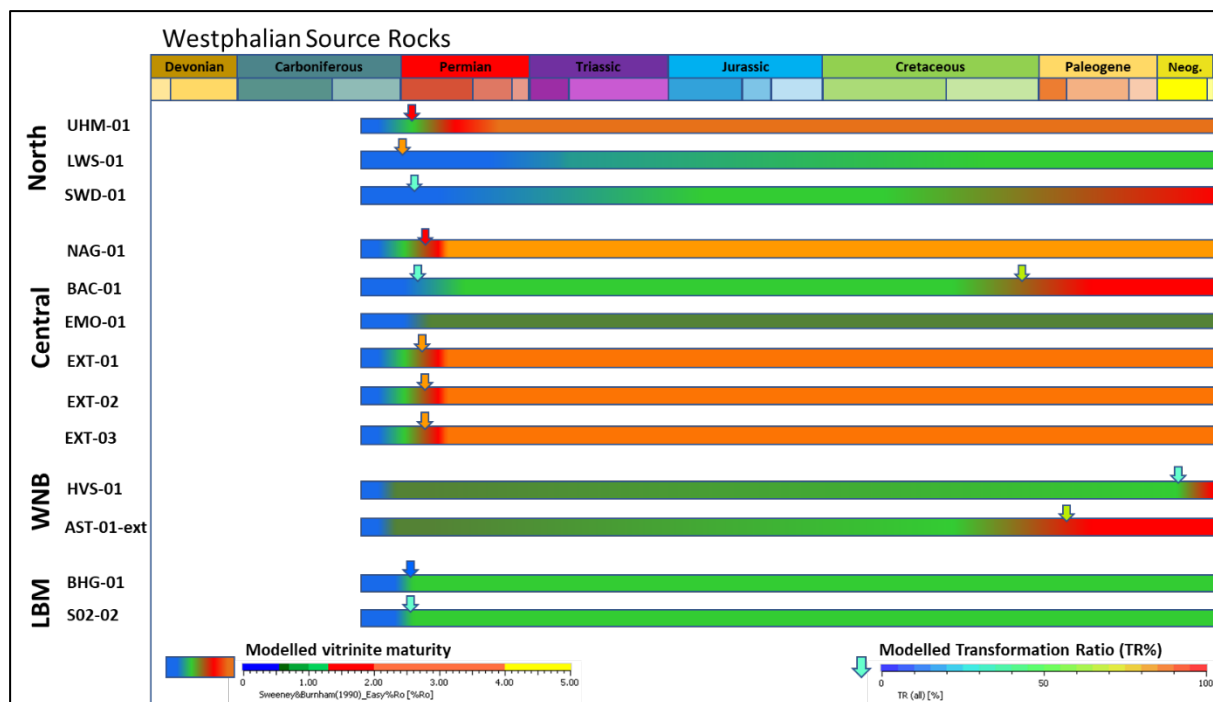


Figure 71: Summary of main phases of Westphalian source rock maturation and hydrocarbon generation. Average values for the Westphalian at well location is given. Coloured horizontal bars indicate for each well the modelled source rock vitrinite maturity (scale bar lower left). Arrows indicate the main phase of hydrocarbon generation, whereby the colour indicates the maximum modelled Transformation Ratio (scale bar lower right).

Modelled Transformation Ratio's (TR%, a proxy for the amount of organic material present in the source rocks that have been converted into hydrocarbons), suggest that for most Westphalian source rocks, at least half to all of the available organic material was converted into oil and/or gas. Main phase of oil/gas generation occurred in the Permian, with the exception of the wells in the WNB and BAC-01 which appear to have been generating hydrocarbons in the Late Cretaceous to Neogene.

1D basin model results for the potential Namurian and Dinantian source rocks suggest that in most wells, the source rocks are over mature since the Permian, and any hydrocarbon expulsion must have occurred prior.

Although the 1D basin models provide indications of the potential for hydrocarbon generation, it does not quantify volumes or reconstruct migration pathways. Hence, the fact that the 1D basin models suggest that hydrocarbons have been generated, does not mean that they are still in place. Conversely, this also does not mean that hydrocarbons will not be present. In order to understand the presence of hydrocarbons at the studied well locations, (local) detailed 3D basin models are required.

The 1D basin models are calibrated against independent measurements such as vitrinite and bore hole temperatures. For the LBM/ZH wells, sensitivity tests were conducted to constrain the heat flow required to attach the modelled data to the measured data. From these tests it was apparent that a higher than expected heat flow was needed for these wells. Similar observations were made in for example UHM-02, where (only) one vitrinite measurement indicated that a high heat flow was required in order to explain the high vitrinite measurement. . In the current study, we do not propose any specific explanations for the higher heat flow gradients. Further work is required to build on the observations obtained by the other SCAN Dinantien projects, and especially the petrophysical study of Carlson (2019).



## 9. Recommendations for future work

This project encapsulated numerous information from previous work, from other SCAN Dinantian Projects and from a variety of data types. This is a robust structural update on the Pre-Zechstein Dutch onshore structural evolution and adds valuable insights on this complex history.

However, this project, which was completed in four months, required to integrate information (e.g. horizon grids, faults) at “face value” without the time to remap or re-evaluate in 3D the local geological architecture. Below we propose a series of recommendations for future work that would add substantial knowledge in the future for de-risking the Dinantian carbonate geothermal play.

- Additional seismic mapping of Carboniferous horizons is required to better understand the structural evolution of the Dutch onshore and the burial history of the Dinantian carbonates. We believe that 2D regional mapping of three to four more horizons would allow to capture more precisely the Carboniferous architecture. We would propose to map at least two intra Namurian horizons and one to two intra-Westphalian horizons. In addition to the horizon mapping, 3D fault mapping of key Carboniferous structures would also allow to better understand the lateral variability along basin margins and structural highs and, therefore, better predict the lateral continuity (or not) of Dinantian Carbonates platforms along basin margins.
- Detail mapping and 3D kinematic analysis of the Dinantian pre- and syn-depositional faults should be undertaken to evaluate the known and potentially undiscovered carbonate platforms that are located on the footwall of these structures. Modern stratigraphic modeling that take into account the fault activity can also shed some lights on the location, growth and preservation of these carbonate depositional systems.
- The newly acquired, or soon to be acquired seismic data in the Dutch onshore should be used, in addition to the existing seismic database, to further validate the existing interpretation (Ten Veen *et al.*, 2019) and to map new horizons. With such a new geological model, a revision of the structural restorations produced in this project could be attempted as well as add other sections to be restored (e.g. a SSW-NNE trending section in the eastern part of the Netherlands).
- New biostratigraphic analysis of Paleozoic wells and outcrops in the Netherlands, Belgium and Germany is also required to decrease uncertainties in the presence and preservation of pre- and post- Dinantian strata. The Dutch Geological Survey is expected to carry out a new study in early 2020 on a series of wells located in the Dutch sector (CAL-GT-01 to -05, UHM-02, WSK-01, O18-01 and LTG-01) and in Belgium (Mol Geothermal wells). The new information should then be added to the knowledge base constructed from the SCAN Program and be presented as an addendum when completed.
- Shorter structural restoration sections with different orientation would also allow to better understand the lateral burial evolution of specific Dinantian carbonate platforms and allow to further de-risk those targets for future geothermal exploration. Figure 72 shows five restorations sections (green lines) that could add valuable knowledge on the evolution of the Dinantian carbonates and the Dinantian platforms and potential platform locations. Smaller scale restorations (20-50 km long) could also be valuable to test some ideas on specific sites, including consortia sites (Figure 12).

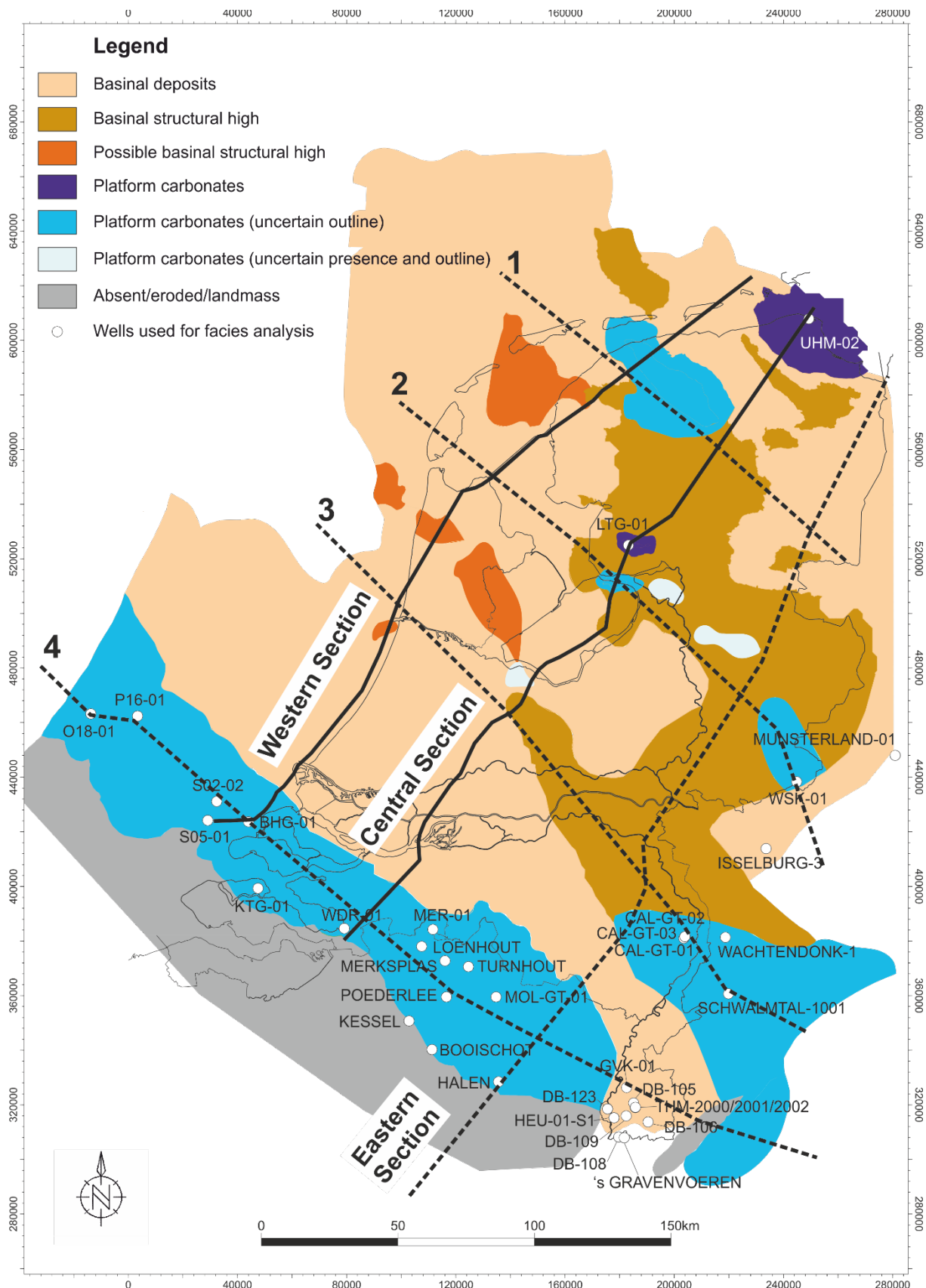


Figure 72: Location of proposed additional 2D structural restorations (black dashed lines) for follow up geothermal exploration research projects. Base map is the Moliniacian-Livian and Warnantian facies distribution map from Mozafari *et al.* (2019).

- From the 1D basin models it has been apparent that in certain wells, notably those on the LBM, but also in for example UHM-01, the heat flow required to match the modelled temperature and/or maturity data to the measured calibration data is significantly higher than what would be expected based on the regional heat flow models. Future work should investigate the reasons for the required higher heat flows as this may impact the (modelled) diagenetic events in the Dinantian carbonate rocks.
- Gain better understanding of the burial and uplift history of the Dutch segment of the LBM/ ZH. The large unconformity between the Carboniferous and Cretaceous units hampers understanding of a significant part of the Mesozoic geological evolution of the Zeeland High area. Low temperature thermochronological studies (e.g., apatite (U-Th)/He and or Fission Track) work should be conducted as part of this work.
- Additional geochronological analysis along the northern flank of the London Brabant Massif (Zeeland High, OP, Campine Basin, Limburg High) would also be valuable to better calibrate the evolution of the Paleozoic strata in this area.

## 10. References

- Abdul Fattah, R., Verweij, J.M., Ten Veen, J.H., 2012b. 4D Basin modelling of the Broad Fourteens Basin and offshore West Netherlands Basin; Erosion and heat flow reconstruction and its influence on temperature, maturity and hydrocarbon generation. TNO – Geological Survey of the Netherlands (Utrecht). Report number TNO 2012 R10670.
- Abdul Fattah, R., Verweij, J.M., Witmans, N., Ten Veen, J.H., 2012a. Reconstruction of burial history, temperature, source rock maturity and hydrocarbon generation for the NCP-2D area, Dutch Offshore. TNO – Geological Survey of the Netherlands (Utrecht). Report number TNO-034-UT-2010-0223.
- Abdul Fattah, R., Verweij, J.M., Witmans, N., Ten Veen, J.H., 2012. Reconstruction of burial history, temperature, source rock maturity and hydrocarbon generation in the northwestern Dutch offshore. *Netherlands Journal of Geosciences – Geologie en Mijnbouw*, 91(4), pp. 535-554.
- Baldschun, R., Jaritz, W. & Koch, W., 1977. Stratigraphy of the Upper Cretaceous in northwest Germany (Pompeckj Block). *Geologisches Jahrbuch A* 38 : 3-123
- Ballèvre, M., Bosse, V., Ducassou, C. and Pitra, P, 2009. Palaeozoic history of the Armorican Massif: Models for the tectonic evolution of the suture zones , *C. R. Geoscience* 341 (2009) 174–201
- Barbarand, J., Bour, I., Pagel, M., Quesnel, F., Delcambre, B., Dupuis, C., Yans, J., 2018. Post-Paleozoic evolution of the northern Ardennes Massif constrained by apatite fission-track thermochronology and geological data, *BSGF - Earth Sciences Bulletin* 189: 16.
- Besly, B.M., 1988a. Late Carboniferous sedimentation in northwest Europe: an introduction. In: Besly, B.M. & Kelling, G. (eds). *Sedimentation in a synorogenic basin complex: The Carboniferous of northwest Europe*. Blackie, Glasgow, 1-7.
- Besly, B.M., 1988b. Palaeogeographic implications of late Westphalian to early Permian red beds. Central England. In: Besly, B.M. & Kelling, G. (eds). *Sedimentation in a synorogenic basin complex: The Carboniferous of northwest Europe*. Blackie. Glasgow, 200-221.

- Betz, D., Führer, F., Greiner, G. & Plein, E., 1987. Evolution of the Lower Saxony Basin. *Tectonophysics*, 137: 127-170.
- Bonté, D., Abdul Fattah, R., Nelskamp, S., Cloetingh, S. Smit, S. & van Wees, J. D., subm. Quantifying the late- to post-Variscan pervasive heat flow, Central Netherlands, Southern Permian Basin
- Bouroullec, R., Verreussel, R., Geel, K., Munsterman, D., de Bruin, G., Zijp, M., Janssen, N., Milán, I., Boxem, T., 2015. Upper Jurassic Sandstones: Detailed sedimentary facies analyses, correlation and stratigraphic architectures of hydrocarbon bearing shoreface complexes in the Dutch offshore. TNO report, 270 pp.
- Bouroullec R., Verreussel, R., Boxem, T., de Bruin, G., Zijp, M., Kerstholt-Boegehold, S., Janssen, N., Munsterman, D., Karamitopoulos, P., Peeters, S., 2016. Understanding Jurassic Sands of the Complex Margins of the eastern part of the Terschelling Basin during the Upper Jurassic and Lowermost Cretaceous. TNO report 2016 R11341, 183pp.
- Bouroullec, R., Verreussel, R., Geel, C.R., De Bruin, G., Zijp, M., Kőrösi, D., Munsterman, D.K., Janssen, N.M.M., Kerstholt-Boegehold, S.J., 2018. Tectonostratigraphy of a rift basin affected by salt tectonics: synrift Middle-Jurassic-Lower Cretaceous Dutch Central Graben, Terschelling Basin and neighboring platforms, Dutch offshore. In *Geological Society, London, Special Publications (Vol. 469)*. Geological Society of London.
- Boxem, T.A.P., Veldkamp J.G. & van Wees J.D.A.M., 2016. Ultra-diepe geothermie: Overzicht, inzicht & to-do ondergrond, TNO 2016 R10803.
- Carlson, T. (2019). Petrophysical Report of the Dinantian Carbonates in the Dutch Subsurface (SCAN). Downloadable from: [https://www.nlog.nl/sites/default/files/2019-08/scan\\_dinantien\\_petrophysics\\_report.pdf](https://www.nlog.nl/sites/default/files/2019-08/scan_dinantien_petrophysics_report.pdf).
- Cartwright, J., Bouroullec, R., James, D., Johnson, H., 1998. Polycyclic motion history of some Gulf Coast growth faults from high-resolution displacement analysis *Geology*, 26, 9, 819-822.
- Corfield, S. M., Gawthorpe, R. L., Gage, M., Fraser, A. J. & Besly, B. M., 1996, Inversion tectonics of the Variscan foreland of the British Isles: *Journal of the Geological Society*, 153, 17-32.
- Debacker, T.N., 2001. Palaeozoic deformation of the Brabant Massif within eastern Avalonia: how, when and why? Unpublished Ph.D. thesis, Laboratorium voor Paleontologie, Universiteit Gent.
- Debacker, T.N., 2012. Folds and cleavage/fold relationships in the Brabant Massif, southeastern Anglo-Brabant Deformation Belt. *Geologica Belgica*, 15, 81–95.
- Debacker, T.N., Herbosch, A., Verniers, J. & Sintubin, M., 2004. Faults in the Asquempont area, southern Brabant Massif, Belgium. *Netherlands Journal of Geosciences/Geologie en Mijnbouw* 83, 49-65.
- Debacker, T.N., Sintubin, M. & Verniers, J., C.L., 2005. Timing and duration of the progressive deformation of the Brabant Massif, Belgium. *Geologica Belgica* 8, 20-34.
- Debacker, T.N., Broothaers, M., Deckers, J., Ferket, H., Lagrou, D., Matthijs, J., Rombaut, B & Williamson, P., in prep. Using gravity data for (sub-)regional mapping purposes (Campine Basin, Belgium)
- De Jager, J., 2007, Geological development, in Wong, T. E., Batjes, D. A. J., and de Jager, J., eds., *Geology of the Netherlands: Amsterdam, Royal Netherlands Academy of Arts and Sciences (KNAW)*, 5-26.
- De Jager, J. & Geluk, M.C., 2007. Petroleum geology. In: Wong, T.E., Batjes, D.A.J. and De Jager, J. (Eds): *Geology of the Netherlands. Royal Netherlands Academy of Arts and Sciences (Amsterdam)*: 241-264.



- De Vos, W., 1997. Influence of the granitic batholith of Flanders on Acadian and later deformation (Brabant Massif, Belgium). *Aardkundige Mededelingen* 8, 49-52.
- Deckers J., De Koninck R., Bos S., Broothaers M., Dirix K., Hambsch L., Lagrou, D., Lanckacker T., Matthijs, J., Rombaut B., Van Baelen K. & Van Haren T., 2019. Eindrapport Geologisch (G3D) en hydrogeologisch (H3D) 3D lagenmodel van Vlaanderen – versie 3. Studie uitgevoerd in opdracht van: VPO en VMM; 2018/RMA/R/1569
- Domeier, M., 2016. A plate tectonic scenario for the Iapetus and Rheic oceans: *Gondwana Research*, 36, 275-295.
- Dusar, M., Lagrou, D. 2007. Cretaceous flooding of the Brabant Massif and the lithostratigraphic characteristics of its chalk cover in northern Belgium. *Geologica Belgica* 10, 27-38.
- Dusar, M., Lagrou, D. & Debacker, T.N. 2015. Boven-Paleozoïcum tot Mesozoïcum. *Geologie van Vlaanderen*. (Borremans, M., Ed.). Academia Press, Gent., ISBN: 978 90 382 2433 6.
- Duin, E.J.T., Doornenbal, J.C., Rijkers, R.H.B., Verbeek, J.W. & Wong, T.E., 2006. Subsurface structure of the Netherlands; results of recent onshore and offshore mapping. *Netherlands Journal of Geosciences* 85 (4): 245-276.
- Everaerts, M., Poitevin, C., De Vos, W. & Sterpin, M., 1996. Integrated geophysical/geological modelling of the western Brabant Massif and structural implications. *Bulletin de la Société belge de Géologie* 105, 41-59.
- Fossen, H. & Dunlap, W.J., 1998. Timing and kinematics of Caledonian thrusting and extensional collapse, southern Norway: evidence from  $^{40}\text{Ar}/^{39}\text{Ar}$  thermochronology. *Journal of Structural Geology*, 20, 765–781
- Franke, W., 2000. The mid-European segment of the Variscides: tectonostratigraphic units, terrane boundaries and plate tectonic evolution. In: Franke, W., Altherr, R., Haak, V. and Oncken, O. (Eds): *Orogenic processes – Quantification and modelling in the Variscan Belt of central Europe*. Geological Society Special Publication (London) 179: 35-61.
- Fraser, A.J. & Gawthorpe, R.L., 1990. Tectono-stratigraphic development and hydrocarbon habitat of the Carboniferous in northern England. In: Hardman, R.F.P. and Brooks, J. (Eds): *Tectonic Events Responsible for Britain's Oil and Gas Reserves*. Geological Society Special Publication (London) 55: 49-86.
- Fraser, A. J. & Gawthorpe, R. L. 2003. An Atlas of Carboniferous Basin Evolution in Northern England. Geological Society Memoir no. 28. 79 pp.
- Gast, R.E., Dusar, M., Breitzkreuz, C., Gaupp, R., Schneider, J.W., Stemmerik, L., Geluk, M.C., Geisler, M., Kiersnowski, H., Glennie, K.W., Kabel, S. & Jones, N.S., 2010. Rotliegend. In: Doornenbal, J.C. and Stevenson, A.G. (editors): *Petroleum Geological Atlas of the Southern Permian Basin Area*. EAGE Publications b.v. (Houten): 101-121.
- Geluk, M., Dusar, M. & De Vos, W., 2007, Pre-Silesian, in Wong, T. E., Batjes, D. A. J., and de Jager, J., eds., *Geology of the Netherlands*: Amsterdam, Royal Netherlands Academy of Arts and Sciences (KNAW), 197-221.
- Geluk, M.C., 2007b. Triassic. In: Wong, T.E., Batjes, D.A.J. and de Jager (Eds): *Geology of the Netherlands*. Royal Netherlands Academy of Arts and Sciences (Amsterdam): 63-84.
- George, G.T., Berry, J.K., 1993. A new lithostratigraphy and depositional model for the Upper Rotliegend of the UK sector of the southern North Sea. In: North, C.P. & Prosser, D.J. (eds) *Characterization of Fluvial and Aeolian Reservoirs*. Geological Society, London, Special Publications, 73, 295-323.

- George, G.T., Berry, J.K., 1997. Permian (Upper rotliegend) synsedimentary tectonics, basin development and palaeogeography of the southern North Sea. In Geological Society, London, Special Publications (Vol. 123, pp. 31-61). Geological Society of London.
- Gibbs, A. D., 1983. Balanced cross-section construction from seismic sections in areas of extensional tectonics. *Journal of structural geology*, 5, 2, 153-160.
- Guterch, A., Wybraniec, S., Grad, M., Chadwick, R., Krawczyk, C., Ziegler, P., Thybo, H. & De Vos, W., 2010. Crustal structure and structural framework, *in* Doornenbal, H., and Stevenson, A., eds., *Petroleum Geological Atlas of the Southern Permian Basin Area: Houten*, EAGE, 11-23.
- Herngreen, G.F.W., Smit, R. & Wong, T.E., 1991. Stratigraphy and tectonics of the Vlieland basin, The Netherlands. In: Spencer, A.M. (Ed.): *Generation, accumulation and production of Europe's hydrocarbons*. Special Publication of the European Association of Petroleum Geoscientists 1: 175-192
- Holdsworth, R. E., Woodcock, N. H. & Strachan, R. A., 2012. Geological Framework of Britain and Ireland, in Woodcock, N., and Strachan, R., eds., *Geological History of Britain and Ireland*, Blackwell Publishing Ltd, 19-39.
- Hollywood, J.M. and Whorlow, C.V., 1993, January. Structural development and hydrocarbon occurrence of the Carboniferous in the UK Southern North Sea Basin. In Geological Society, London, *Petroleum Geology Conference series* (Vol. 4, pp. 689-696). Geological Society of London
- Keppie, J. D., Murphy, J. B., Nance, R. D. & Dostal, J., 2012. Mesoproterozoic Oaxaquia-type basement in peri-Gondwanan terranes of Mexico, the Appalachians, and Europe: TDM age constraints on extent and significance: *International Geology Review*, /54, 313-324.
- Kimpe, W.F.M., Bless, M.J.M., Bouckaert, J., Conil, R., Groessens, E., Meessen, J.P.M.Th., Poty, E., Streel, M., Thorez, J. & Vanguetstaine, M., 1978. Paleozoic deposits East of the Brabant Massif in Belgium and the Netherlands. *Meded. Rijks Geol. Dienst* 30, 37-103.
- Kombrink, H., Leever, K. A., Van Wees, J.-D., Van Bergen, F., David, P. & Wong, T. E., 2008. Late Carboniferous foreland basin formation and Early Carboniferous stretching in Northwestern Europe: inferences from quantitative subsidence analyses in the Netherlands: *Basin Research*, 20, 377-395.
- Kombrink, H., Besly, B.M., Collinson, J.D., Den Hartog Jager, D.G., Drozdowski, G., Duser, M., Hoth, P., Pagnier, H.J.M., Stemmerik, L., Waksmundzka, M.I. & Wrede, V., 2010. Carboniferous. *In*: Doornenbal, J.C. and Stevenson, A.G. (editors): *Petroleum Geological Atlas of the Southern Permian Basin Area*. EAGE Publications b.v. (Houten): 81-99.
- Kombrink, H., Doornenbal, J.C., Duin, E.J.T., Den Dulk, M., Van Gessel, S.F., Ten Veen, J.H. & Witmans, N., 2012. The geological structure of the Netherlands Continental Shelf; results of a detailed mapping project. *Neth. J. Geosci.* 91 (4), 403-418.
- Landes, M., Prodehl, C., Hauser, F., Jacob, A. W. B. & Vermeulen, N. J., 2000. VARNET-96: influence of the Variscan and Caledonian orogenies on crustal structure in SW Ireland: *Geophysical Journal International*, 140, 660-676.
- Leeder, M., R., 1988. Recent developments in Carboniferous geology: a critical review with implications for the British Isles and N.W Europe. *Proceedings of the geologists' Association*, 99, 73-100.
- Leeder, M. R. & Hardman, M., 1990. Carboniferous geology of the Southern North Sea Basin and controls on hydrocarbon prospectivity, in Hardman, R. F. P., and Brooks, J., eds., *Tectonic Events Responsible for Britain's Oil and Gas Reserve*, Volume 55, Geological Society, London, Special Publications, 87-105.

- Legrand, R., 1967. Ronquières, documents géologiques. Mémoires pour servir à l'Explication des Cartes géologiques et minières de la Belgique 6, 1-60.
- Legrand, R., 1968. Le Massif du Brabant. Mémoires pour servir à l'Explication des Cartes géologiques et minières de la Belgique 9, 1-148.
- Lott, G.K., Wong, T.E., Dusar, M., Andsbjerg, J., Mönnig, E., Feldman-Olszewska, A. & Verreussel, R.M.C.H., 2010. Jurassic. In : Doornenbal, J.C. and Stevenson, A.G. (editors) : Petroleum Geological Atlas of the Southern Permian Basin Area. EAGE Publications b.v. (Houten): 175-193
- Maguire, P., England, R., and Hardwick, A., 2011, LISPB DELTA, a lithospheric seismic profile in Britain: analysis and interpretation of the Wales and southern England section: *Journal of the Geological Society*, 168, 61-82.
- Mazur, S., Scheck-Wenderoth, M., 2005. Constraints on the tectonic evolution of the Central European Basin System revealed by seismic reflection profiles from Northern Germany. *Netherlands Journal of Geosciences – Geologie en Mijnbouw* 84-4, 389-401.
- McCann, T., 2008. Carboniferous. In: McCann, T. (ed.). *The Geology of Central Europe*. Geological Society, London, 1-20.
- Michon, L., Van Balen, R.T., Merle, O., Pagnier, H., 2003. The Cenozoic evolution of the Roer Valley Rift system integrated at a European scale. *Tectonophysics*, 367, 101-126.
- Mijnlieff, H., 2002. Top Pre-Permian distribution map & some thematic regional geologic maps of the Netherlands , ICCP, 2002.
- Mozafari, M., Gutteridge, P., Riva, A., Geel, C. R., Garland, J. and Dewit, J. (2019). Facies analysis and diagenetic evolution of the Dinantian carbonates in the Dutch subsurface (SCAN). Downloadable from [www.nlog.nl](http://www.nlog.nl) .
- McKerrow, W.S., 1988. Wenlock to Givetian deformation in the British Isles and the Canadian Appalachians. In: Harris, A.L. and Fettes, D.J. (Eds): *The Caledonian-Appalachian Orogen*. Geological Society Special Publication (London) 38: 437-448.
- Muchez, Ph., Viaene, W., Wolf, M., Bouckaert, J., 1987. Sedimentology, coalification pattern and paleogeography of the Campine-Brabant Basin during the Visean. *Geologie en Mijnbouw*, 66: 313-326.
- Muchez, Ph. & Langenaeker, V., 1993. Middle Devonian to Dinantian sedimentation in the Campine Basin (northern Belgium): its relation to Variscan tectonism. *Spec. Publ. Int. Ass. Sediment.* 20, 171-181.
- Mutterlose, J. & Bornemann, A., 2000. Distribution and facies patterns of Lower Cretaceous sediments in northern Germany: a review. *Cretaceous Research*, 21, 733-759.
- Nalpas, T., Le Douaran, S., Brun, J.-P., Unternehr, P., Richert, J.-P., 1995. Inversion of the Broad Fourteens basin (offshore Netherlands), a small-scale model investigation. *Sedimentary Geology*, 95, 237-250
- Nederlandse Aardolie Maatschappij B.V. and Rijks Geologische Dienst (NAM & RDG), 1980: *Stratigraphic Nomenclator of The Netherlands – Kon. Ned. Geol. Mijnbouwk. Gen. Verh.* 32, 77 pp
- Nelskamp, S., 2011. Structural evolution, temperature and maturity of sedimentary rocks in the Netherlands. PhD thesis, Rheinisch-Westfälische Technische Hochschule Aachen (Aachen), 175. NITG, 1999.
- Nelskamp, S., Goldberg, T., Houben, S., Geel, K., Wasch, L., Verreussel, R., Boxem, T., 2015. Improved sweet spot identification and smart development using integrated reservoir characterisation (Phase 2). TNO report 2015 R10740.
- Oncken, O., Plesch, A., Weber, J., Ricken, W. & Schrader, S., 2000. Passive margin detachment during arc-continent collision (Central European Variscides). In: Franke, W., Altherr, R., Haak, V. and Oncken, O. (Eds): *Orogenic processes – Quantification*

- and modelling in the Variscan Belt of central Europe. Geological Society Special Publication (London) 179: 199-216.
- Patijn, R.J.H., 1963. Het Carboon in de ondergrond van Nederland en de oorsprong van het Massief van Brabant. *Geologie en Mijnbouw* 42, 341-349.
- Pharaoh, T.C., 1999. Palaeozoic terranes and their lithospheric boundaries within the Trans-European Suture Zone (TESZ): a review. *Tectonophysics* 314, 17-41.
- Pharaoh, T.C., Dusar, M., Geluk, M.C., Kockel, F., Krawczyk, C.M., Krzywiec, P., Scheck-Wenderoth, M., Thybo, H., Vejbæk, O.V. & Van Wees, J.D., 2010. Tectonic evolution. In: Doornenbal, J.C. and Stevenson, A.G. (editors): *Petroleum Geological Atlas of the Southern Permian Basin Area*. EAGE Publications b.v. (Houten): 25-57.
- Poty, E. & Delculée, S., 2011. Interaction between eustasy and block-faulting in the Carboniferous of the Visé – Maastricht area (Belgium, The Netherlands). *Z. dt. Ges. Geowiss.* 162, 117-126.
- Poty, E., 2016. The Dinantian (Mississippian) succession of southern Belgium and surrounding areas: stratigraphy improvement and inferred climate reconstruction. *Geologica Belgica* 19, 177-200.
- Reijmer, J.J.G., ten Veen, J.H., Jaarsma, B. & Boots, R., 2017. Seismic stratigraphy of Dinantian carbonates in the southern Netherlands and northern Belgium Netherlands *Journal of Geosciences, Geologie en Mijnbouw*, 96-4, 353-379.
- Rijkers, R.H.B. & Geluk, M.C., 1996. Sedimentary and structural history of the Texel-Dsselmeer High, The Netherlands. In: Rondeel, H.E., Batjes, D.A.J. & Nieuwenhuizen, W.H. (eds): *Geology of gas and oil under the Netherlands*. Kluwer (Dordrecht): 265-281.
- Schroot, B.M., De Haan, H.B., 2003. New insights into structural interpretation and modelling. In Geological Society, London, Special Publications (Vol. 212, pp. 23-37). Geological Society of London.
- Schoot, B.M., van Bergen, F., Abbink, O.A., David, P., van Eijs, R., Veld, H., 2006. Hydrocarbon potential of the Per-Westphalian in the Netherlands on- and offshore – report of the PETROPLAY project. TNO report NITG 05-155-C.
- Sclater, J. G., and P. A. F. Christie, 1980, Continental stretching: An explanation of the Post-Mid-Cretaceous subsidence of the central North Sea Basin: *Journal of Geophysical Research: Solid Earth*, v. 85, p. 3711-3739.
- Sintubin, M., 1999. Arcuate fold and cleavage patterns in the south-eastern part of the Anglo-Brabant Fold Belt (Belgium): tectonic implications. *Tectonophysics* 309, 81-97.
- Sintubin, M. & Everaerts, M., 2002. A compressional wedge model for the Lower Palaeozoic Anglo-Brabant Belt (Belgium) based on potential field data. In: Winchester, J., Verniers, J. & Pharaoh, T. (eds.) *Palaeozoic Amalgamation of Central Europe*. Geological Society, London, Special Publications 201, 327-343.
- Smit, J., van Wees, J.-D. & Cloetingh, S., 2016. The Thor suture zone: From subduction to intraplate basin setting: *Geology*, 44, 707-710.
- Smit, J., van Wees, J.-D. & Cloetingh, S., 2018. Early Carboniferous extension in East Avalonia: 350 My record of lithospheric memory: *Marine and Petroleum Geology*, 92, 1010-1027.
- Szulczewski, M., Bełka, Z. & Skompski, S., 1996. The drowning of a carbonate platform: an example from the Devonian-Carboniferous of the southwestern Holy Cross Mountains, Poland. *Sedimentary Geology* 106: 21-49.
- Ter Borgh, M. M., Jaarsma, B. & Rosendaal, E. A., 2018. Structural development of the northern Dutch offshore: Paleozoic to present, in Monaghan, A. A., Underhill, J. R., Hewett, A. J. & Marshall, J. E. A. Eds., *Paleozoic Plays of NW Europe.*, Volume 471: London, Geological Society, London, Special Publications.



- Ten Veen, J.H., de Haan, H.B., de Bruin, G., Holleman, N., Schöler, W. (2019). Seismic Interpretation and Depth Conversion of the Dinantian carbonates in the Dutch subsurface (SCAN). Downloadable from [www.nlog.nl](http://www.nlog.nl)
- Torsvik, T. H. & Cocks, L. R. M., 2013. Gondwana from top to base in space and time: *Gondwana Research*, 24, 999-1030.
- Underhill, J.R. & Partington, M.A., 1993. Jurassic thermal doming and deflation in the North Sea: implications of the sequence stratigraphic evidence. *Petroleum Geology*, 337-345.
- Vandenberghe, N., De Craen, N. & Beerten, K., 2014. Geological framework of the Campine Basin Geological setting, tectonics, sedimentary sequences. Studiecentrum voor Kernenergie. External Report 262: 1–113.
- Vandewijngaerde, W., Piessens, K., Duser, M., Bertier, P., Krooss, B.M., Littke, R. & Swennen R., 2016, Investigations on the shale oil and gas potential of Westphalian mudstone successions in the Campine Basin, NE Belgium (well KB174): Palaeoenvironmental and palaeogeographical controls, *Geologica Belgica*, 19/3-4: 225-235.
- Van Adrichem Boogaert, H.A. & Burger, W.F.J., 1983. The development of the Zechstein in the Netherlands. *Geologie en Mijnbouw*.
- Van Adrichem Boogaert, H.A. & Kouwe, W.F.P., 1993. Stratigraphic nomenclature of the Netherlands, revision and update by RGD and NOGPA. *Mededelingen Rijks Geologische Dienst* 50: 1-40.
- Van Bergen, M.J., Sissingh, W., 2007. Magmatism in the Netherlands: expression of the north-west European rifting history. In Th.E. Wong, D.A.J. Batjes & J. de Jager (Eds.), *Geology of the Netherlands* (pp. 197-221) (354 p.). royal Netherlands Academy of Arts and Sciences.
- Van Buggenum, J.M., den Hartog Jager, D.G., 2007. Silesian. In: *Geology of the Netherlands*. Edited by Th.E. Wong, D.A.J. Batjes & J. de Jager Royal Netherlands Academy of Arts and Sciences: 43–62.
- Van Den Haute, P. & Vercoutere, C., 1989. Apatite fission-track evidence for a Mesozoic uplift of the Brabant Massif: preliminary results. *Annales de la Société Géologique de Belgique* 112(2), 443-452.
- Van Wees, J.-D., Stephenson, R.A., Ziegler, P.A., Bayer, U., McCann, T., Dadlez, R., Gaupp, R., Narkiewicz, M., Bitzberg, F., Scheck, M., 2000. On the origin of the Southern Permian basin, Central Europe. *Marine and Petroleum Geology* 17: 4359.
- Van Wees, J.-D., van Bergen, F., David, P., Nepveu, M., Beekman, F., Cloetingh, S. and Bonte, D., 2009, Probabilistic tectonic heat flow modeling for basin maturation: Assessment method and applications, *Marine and Petroleum Geology* 26, 536–551
- Van Wijhe, D.H., 1987a. Structural evolution of inverted basins in the Dutch offshore. *Tectonophysics* 137: 171-219.
- Vercoutere, C., van den Haute, P., 1993. Post-Paleozoic cooling and uplift of the Brabant Massif as revealed by apatite fission track analysis. *Geological Magazine*, 130, 639-646.
- Verniers, J., Pharaoh, T.C., André, L., Debacker, T., De Vos, W., Everaerts, M., Herbosch, A., Samuelsson, J., Sintubin, M. & Vecoli, M., 2002. The Cambrian to mid Devonian basin development and deformation history of Eastern Avalonia, east of the Midlands Microcraton: new data and a review. In: Winchester, J.A., Pharaoh, T.C. and Verniers, J. (Eds): *Palaeozoic Amalgamation of Central Europe*. Geological Society Special Publication (London) 201: 47-93.
- Verweij, J.M. & Simmelink, H.J., 2002 Geodynamic and hydrodynamic evolution of the Broad Fourteens Basin (The Netherlands) in relation to its petroleum systems. *Marine and Petroleum Geology* 19: 339-359.

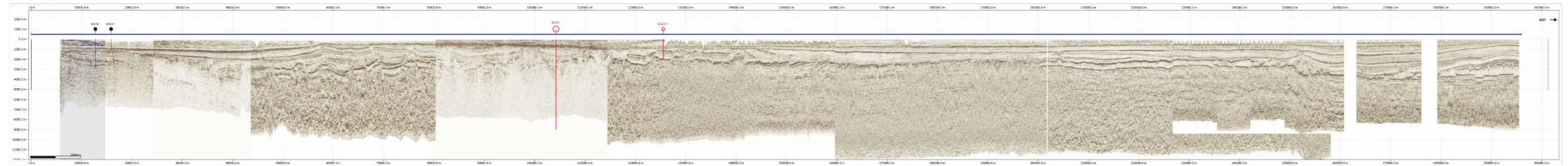
- Woodcock, N. H., 2012. The Cambrian and Earliest Ordovician Quiescent Margin of Gondwana, in Woodcock, N. H., and Strachan, R., eds., Geological History of Britain and Ireland, John Wiley & Sons, Ltd, 150-161.
- Yudistira, T., Paulssen, H. & Trampert, J., 2017. The crustal structure beneath The Netherlands derived from ambient seismic noise: Tectonophysics, 721, 361-371
- Ziegler, P.A., 1989. Evolution of Laurussia – a study in Late Palaeozoic plate tectonics. Kluwer Academic Publishers (Dordrecht, Boston, London): 102 pp..
- Ziegler, P. A., 1990. Geological Atlas of Western and Central Europe, Bath, Shell Int. Pet. Mij., distributed by Geol. Soc. Publ. House, pp. 238
- Zijerveld, L., Stephenson, R., Cloetingh, S., Duin, E. & Van den Berg, M.W., 1992. Subsidence analysis and modelling of the Roer Valley Graben (SE Netherland). Tectonophysics 208, 159– 171.
- Zwart, H. & Dornsiepen, U., 1978. The tectonic framework of central and western Europe: Geol. Mijnbouw, 57, 627-654.

## 11. Appendices

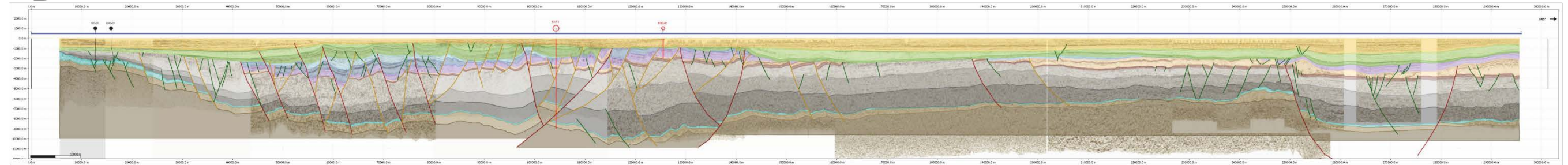


## Western Section

A



B

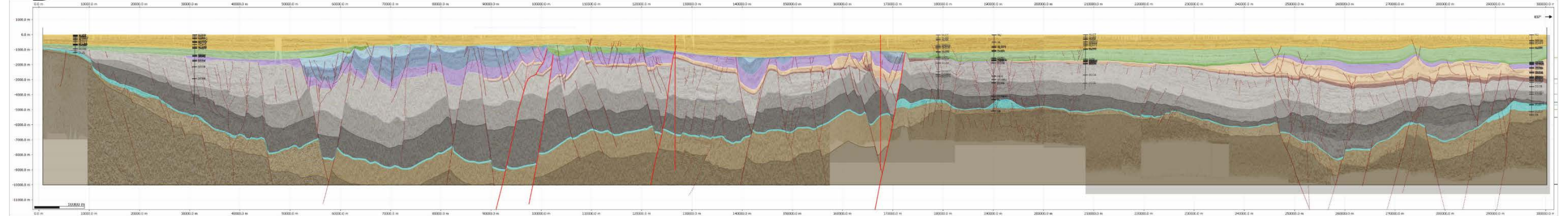


## Central Section

C

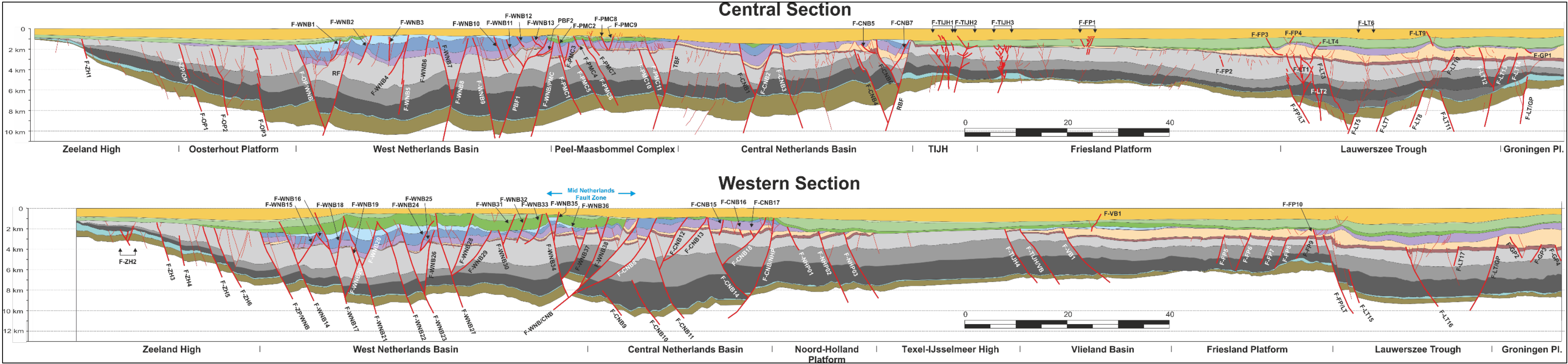


D



Appendix 1A: Present-Day uninterpreted (A and C) and interpreted (B and D) depth migrated sections used for the 2D structural restorations. See Figures 12 and 23 for location.





Appendix 1B: Present-Day interpreted depth migrated sections used for the restoration. See location map in Figures 12 and 23.

Period	Age (Ma)	Major tectonic phase	Major unconformity	London-Brabant Massif	Zeeland High	Limburg High	Oosterhout Platform	Roer Valley Graben	West Netherlands Basin	IJmuiden Platform	Broad Fourteens Basin	Peel-Massbommel Complex	Zandvoort Ridge	Central Netherlands Basin	Noord-Holland Platform	Texel-IJsselmeer High	Vlieland Basin	Friesland Platform	Daftsen High	Lower Saxony Basin	Lauwerszee Trough	Groningen Platform	
				LBM	ZH	LH	OP	RVG	WNB	IJP	BFB	PMC	ZR	CNB	NHP	TIJH	VB	FP	DH	LSB	LT	GH	
Neogene	0-23	<ul style="list-style-type: none"><li>Savian pulse (end-Oligocene / Early Miocene) followed by thermal subsidence</li></ul>	<ul style="list-style-type: none"><li>Savian U/C at base of Upper North Sea Group</li></ul>	<ul style="list-style-type: none"><li>Subsidence and sedimentation</li></ul>				<ul style="list-style-type: none"><li>Subsidence and sedimentation</li></ul>	<ul style="list-style-type: none"><li>Savian pulse seen in the WNB but little elsewhere in the Netherlands (20).</li></ul>		<ul style="list-style-type: none"><li>Savian inversion not seen (20)</li></ul>					<ul style="list-style-type: none"><li>Subsidence and sedimentation</li></ul>							
Late Cretaceous and Paleogene	23-100	<ul style="list-style-type: none"><li>Pyrenean pulse (end-Eocene) caused by broad uplift</li><li>Laramide pulse (mid-Paleocene) mark the end of the Chalk deposition.</li><li>Sub-Hercynian pulse during the Campanian</li></ul>	<ul style="list-style-type: none"><li>Pyrenean U/C at the base of the Middle North Sea Group.</li><li>Laramide at the base of the Lower North Sea Group.</li><li>Sub-Hercynian U/C is an intra Chalk Group U/C</li></ul>	<ul style="list-style-type: none"><li>Overstepped and overlapped by Upper Cretaceous sediments, but was later partly denuded (18, 19)</li></ul>	<ul style="list-style-type: none"><li>Onlap (18)</li></ul>			<ul style="list-style-type: none"><li>Less inversion than the WNB and CNB</li><li>Multiple phases of inversion between Late Cretaceous and Early Cenozoic (36)</li><li>Inversion resulted in reverse reactivation of pre-existing faults forming prominent ridges of flower structures on dominantly west-north-west and north-north-west trends with a dextral displacement (18)</li></ul>	<ul style="list-style-type: none"><li>Mildly to strongly inverted (1)</li><li>Erosion (6)</li><li>Chalk eroded in the south-eastern part (1)</li><li>Pre-existing faults reactivated with flower (transpressional) structure observed (6)</li><li>Thinning of the Upper Chalk from the SE (6)</li><li>Dextral displacement along main faults due to E-W Late Cimmerian extension transitioning to N-S compression in Late Cretaceous Early Cenozoic.</li><li>Inversion resulted in reverse reactivation of pre-existing faults forming prominent ridges of flower structures on dominantly west-north-west and north-north-west trends with a dextral displacement (18)</li></ul>		<ul style="list-style-type: none"><li>Strongly inverted (1) during both Laramide and Pyrenean pulses.</li><li>Up to 300 m of uplift (38)</li><li>Erosion (6)</li><li>Chalk Group removed (1)</li><li>Structural style different than WNB and CNB due to the presence of Zechstein salt</li><li>NW-SE anticline growth (8).</li><li>Some of the reactivated faults observed down to the Carboniferous (17)</li></ul>	<ul style="list-style-type: none"><li>Subsidence (6)</li><li>Peel Boundary Fault to the south has up to 1000 m of post-inversion throw (20)</li></ul>	<ul style="list-style-type: none"><li>Subsidence with thick Chalk deposited (18)</li></ul>	<ul style="list-style-type: none"><li>Strongly inverted (4)</li><li>Erosion, locally down to the Triassic (6)</li></ul>		<ul style="list-style-type: none"><li>Sedimentation</li></ul>				<ul style="list-style-type: none"><li>Up to 8 km of shortening occurred along listric thrust planes that can be traced into the lower crust (18).</li><li>Strongly inverted (4)</li><li>Inversion largely ceased after the Late Cretaceous and earliest Cenozoic (20, 30)</li><li>Erosion</li><li>Some thick Chalk in rim synclines along salt structures (33)</li></ul>	<ul style="list-style-type: none"><li>Increased thickness of Paleogene</li><li>Maps at the Cretaceous and Cenozoic levels indicate that both north-north-west and east-north-east-trending faults were reactivated during the Cenozoic (20)</li></ul>		
Early Cretaceous (except Ryazanian)	100-140	<ul style="list-style-type: none"><li>Post rifting thermal subsidence</li><li>Cimmerian pulses</li><li>E-W extension</li></ul>	<ul style="list-style-type: none"><li>Late Cimmerian U/C (30) locally seen at the base of the Rijnland Group related to lithosphere-scale deformations combined with an earliest Cretaceous eustatic sea-level lowstand. Most distinctive in the basin margins and on the platform areas.</li></ul>	<ul style="list-style-type: none"><li>Sedimentation (6) and onlap (18)</li><li>Widespread karstification of the Dinantian carbonates). Exact timing often difficult to tell in the Campine Basin (42)</li></ul>	<ul style="list-style-type: none"><li>Missing (1)</li></ul>	<ul style="list-style-type: none"><li>Eroded</li></ul>		<ul style="list-style-type: none"><li>Missing</li></ul>	<ul style="list-style-type: none"><li>Post rift strain onlap on the basin margins</li></ul>		<ul style="list-style-type: none"><li>Locally eroded (1)</li></ul>	<ul style="list-style-type: none"><li>Late-Cimmerian uplift leading to erosion of most of the Middle Jurassic to Permian cover, locally down to the Westphalian</li></ul>								<ul style="list-style-type: none"><li>Deep-seated intrusions inferred beneath the Lower Saxony Basin may have been emplaced during the Aptian (30, 31).</li><li>Subsidence with non-marine (Wealden) deposition during the Berriasian (32)</li></ul>	<ul style="list-style-type: none"><li>Increased thickness</li></ul>		
Late Jurassic to Early Cretaceous (Ryazanian)	140-165	<ul style="list-style-type: none"><li>Mid- to late-Cimmerian rifting phases</li><li>Major rifting</li></ul>	<ul style="list-style-type: none"><li>The basal Mid-Cimmerian U/C is Bajocian age</li></ul>	<ul style="list-style-type: none"><li>Thins and onlaps on the LBM then thicken to the south to 700 m (Wessex-Weald Basin and Boulonnais) (7, 27)</li><li>Mid-Cimmerian phase, which removed 3000 m of its post-Caledonian cover including the Lower Jurassic (39)</li><li>Fission-track data suggest that a thickness of 3000 m of overburden was removed (16, 47, 48)</li><li>Possible faulting in the Campine Basin with faults mainly oriented NNW-SSE and NW-SE trending but also NNE-SSW structures can be recognised in gravity data (45, 46)</li></ul>				<ul style="list-style-type: none"><li>Strongly subsiding in a similar manner than the DCG.</li><li>Orientation probably controlled by pre-existing structures (6)</li><li>Transensional reactivation of pre-existing basement structures (18)</li><li>Subsidence was controlled by the reactivation of the main Variscan faults (36)</li></ul>	<ul style="list-style-type: none"><li>Orientation probably controlled by pre-existing structures (6)</li><li>Syn-rift classics of the Delfland Subgroup in half grabens</li><li>Dextral displacement along main faults</li><li>Transensional reactivation of pre-existing basement structures (18)</li></ul>		<ul style="list-style-type: none"><li>Likely connected to the Dutch Central Graben (1)</li><li>Subside rapidly during Kimmeridgian (18_</li></ul>		<ul style="list-style-type: none"><li>Important wrench-induced feature separating the West and Central Netherlands basins (18)</li></ul>	<ul style="list-style-type: none"><li>Only patches of Jurassic preserved but could have had a wider distribution (1)</li><li>Orientation probably controlled by pre-existing structures (6)</li><li>Transensional reactivation of pre-existing basement structures (18)</li><li>Subside rapidly during Kimmeridgian (18_</li></ul>	<ul style="list-style-type: none"><li>Main erosion (1)</li><li>Uplifted (6)</li></ul>	<ul style="list-style-type: none"><li>Depocenter with connection to the Terschelling Basin (7)</li><li>Transensional reactivation of pre-existing basement structures (18)</li><li>Mafic volcanism with volcanoclastics (27)</li></ul>	<ul style="list-style-type: none"><li>Uplift and Erosion, down to the Triassic and Zechstein levels (1)</li><li>No faulting (18)</li></ul>		<ul style="list-style-type: none"><li>Extension</li><li>Transensional reactivation of pre-existing basement structures (18)</li></ul>	<ul style="list-style-type: none"><li>Absent (5)</li><li>The high is largely shaped by the late Cimmerian tectonic phase during the Jurassic (25)</li></ul>			
Early to Middle Jurassic	165-198	<ul style="list-style-type: none"><li>North Sea doming start at end of Aalenian until Bathonian due to mantle plume on the lithosphere (7, 30, 40)</li></ul>	<ul style="list-style-type: none"><li></li></ul>	<ul style="list-style-type: none"><li>Uplifted with erosion of Triassic to Upper Carboniferous (18).</li></ul>				<ul style="list-style-type: none"><li>Quiescence</li></ul>	<ul style="list-style-type: none"><li>Normal faulting (6)</li></ul>		<ul style="list-style-type: none"><li>Normal faulting (6)</li></ul>		<ul style="list-style-type: none"><li>Quiescence</li></ul>	<ul style="list-style-type: none"><li>Quiescence</li></ul>		<ul style="list-style-type: none"><li>Missing (6)</li><li>Eroded locally down to the Westphalian (18)</li></ul>	<ul style="list-style-type: none"><li>Quiescence</li></ul>	<ul style="list-style-type: none"><li>Quiescence</li></ul>	<ul style="list-style-type: none"><li>W-NW faulting (29)</li><li>Transensional subsidence and internal differentiation into elongated horst and graben features (29)</li></ul>	<ul style="list-style-type: none"><li>Quiescence</li></ul>			
Triassic	198-252	<ul style="list-style-type: none"><li>Initiation of rifting</li><li>Early Cimmerian phase</li><li>Hardegesen pulse and a few less prominent pulses (pre-Volpriehausen, pre-Derfurth and intra-Solling)</li></ul>	<ul style="list-style-type: none"><li>Early-Cimmerian U/C is base Rhaetian in age.</li><li>Mostly seen along the SPB margins and are attributed to intraplate stresses operating on a lithospheric scale (41; 30).</li><li>Hardegesen U/C at the base of the Solling Formation</li></ul>	<ul style="list-style-type: none"><li>Low subsidence rate with 50 m of Lower Muschelkalk deposited (14).</li><li>Source of sediment for the RVB and WNB during lower Triassic (18)</li></ul>				<ul style="list-style-type: none"><li>Differential subsidence (14)</li><li>Differential subsidence ceased at the end of the Early Triassic and restart during Rot time (14)</li></ul>	<ul style="list-style-type: none"><li>Some growth faulting along the southern margin</li><li>Subsidence shifts northward</li><li>Differential subsidence ceased at the end of the Early Triassic (14)</li></ul>		<ul style="list-style-type: none"><li>Minor faulting (1, 2, 3)</li><li>Differential subsidence ceased at the end of the Early Triassic (14)</li></ul>			<ul style="list-style-type: none"><li>Heavily faulted (1)</li></ul>			<ul style="list-style-type: none"><li>Moderate subsidence</li></ul>	<ul style="list-style-type: none"><li>Up to 800 m in the east (1)</li></ul>					
Permian	252-298	<ul style="list-style-type: none"><li>Saalian phase</li></ul>	<ul style="list-style-type: none"><li>Base Permian U/C (BPU) and intra-Permian Saalian U/C</li></ul>	<ul style="list-style-type: none"><li>During the Mid and Late Permian, the sedimentation gradually extended to the LBM.</li><li>A source for Rotliegend in the North Sea (18)</li></ul>				<ul style="list-style-type: none"><li>Existed during the Paleozoic (1)</li><li>Thermal subsidence with minor faulting (37)</li></ul>	<ul style="list-style-type: none"><li>Devoided of Zechstein salt (6)</li><li>Fault controlled Rotliegend deposition (100 aeolian sand along the northern bounding fault (12)</li></ul>		<ul style="list-style-type: none"><li>Minor faulting (1, 2, 3)</li><li>Differential subsidence (12)</li></ul>	<ul style="list-style-type: none"><li>Thermal subsidence with minor faulting (37)</li></ul>		<ul style="list-style-type: none"><li>Differential subsidence (12)</li><li>Half Graben and pull-apart basin with up to 250 m of offset (12)</li></ul>		<ul style="list-style-type: none"><li>Strongly uplifted during the early Permian (6, 26)</li><li>Synsedimentary faulting (12)</li><li>Sand source area (13)</li><li>High poorly defined</li><li>Controlled Rotliegend alluvial fan systems around the high</li></ul>				<ul style="list-style-type: none"><li>Increased thickness of Rotliegend</li><li>Faulting with thickness variation up to 25 m</li></ul>			
Stephanian-Westphalian	298-312	<ul style="list-style-type: none"><li>Variscan phase with compression starting during the Asturian (Westphalian D) and early Stephanian</li></ul>	<ul style="list-style-type: none"><li></li></ul>	<ul style="list-style-type: none"><li>Passive thermal cooling that had started during the Namurian continues (23)</li><li>Western part of the LBM : Uplift and sourcing to the north (24), while Belgium part had a thick Westphalian cover due to subsidence.</li><li>Possible faulting in the Campine Basin with faults mainly oriented NNW-SSE and NW-SE trending but also NNE-SSW structures can be recognised in gravity data (45, 46)</li><li>Faillie Bordière's and Leut fault (eastern part of the LBM) active (45, 46)</li></ul>	<ul style="list-style-type: none"><li>Parasitic compaction-related faults that formed above the massive and rigid Dinantian carbonate fault blocks (35)</li></ul>	<ul style="list-style-type: none"><li>5.4 km of Namurian/Westphalian may have been removed (11)</li></ul>							<ul style="list-style-type: none"><li>Subsidence not the main driving force but rather the alternation of overthrust loading and relaxation in the Variscan thrust belt to the south. (10)</li></ul>										
Namurian	312-325		<ul style="list-style-type: none"><li></li></ul>	<ul style="list-style-type: none"><li>Uniform flexural subsidence</li><li>Marine and lacustrine sediments</li><li>Regional unconformity related to sea level lowstand (22)</li></ul>	<ul style="list-style-type: none"><li>Progressive onlap onto the LBM</li></ul>																<ul style="list-style-type: none"><li>Structural high originated during the Carboniferous (25)</li></ul>		
Viséan and Tournaisian (Dinantian)	325-358	<ul style="list-style-type: none"><li>Bretonian phase at the Devonian-Carboniferous boundary</li></ul>		<ul style="list-style-type: none"><li>Emersion and karstification at the end of Viséan with associated (fracture controlled) porosity (42)</li><li>Uplift of the WSW-ENE trending Boeze – Val Dieu Ridge (eastern part of the LBM) during Late Tournaisian (42, 43, 44).</li><li>Faillie Bordière's and Leut Fault (eastern part of the LBM) may have been active (45)</li></ul>	<ul style="list-style-type: none"><li>Small extensional (half-graben) basins that are related to long-lived faults that have been active since at least the Devonian (34)</li><li>The platform boundaries occasionally associated with faults with small throw. These faults may have played an important role in determining the location of these sedimentary facies transitions (35)A large extensional fault near well S02-01 has a half-graben geometry and accommodates significant throw (35)</li></ul>																		

Appendix 2 (previous page): Summary chart of the structural evolution of the 19 recognized structural elements identified in the study area. See list and description of each elements above. Numbers in the table refer to specific publication (listed below). (1) Kombrink *et al.* (2012); (2) Hooper *et al.* (1995); (3) Verweij & Simmelink (2002); (4) Nelskamp (2011); (5) Van Adrichem Boogaert & Kouwe (1993); (6) De Jager (2007); (7) Bouroullec *et al.* (2018); (8) Nalpas *et al.* (1995); (9) Geluk *et al.* (2007); (10) Van Buggenum & de Hartog Jager (2017); (11) Veld *et al.* (1996); (12) Geluk (2007); (13) Van Adrichem Boogaert & Burgers (1983); (14) Geluk (2007b); (15) Legrand (1968); (16) Van den Haute & Vercoutere (1990); (17) Schroot & De Haan (2003); (18) Pharaoh, *et al.* (2010); (19) Duser & Lagrou (2007); (20) De Jager (2007); (21) Kombrink *et al.* (2010); (22) McCann *et al.* (2008a, 2010); (23) Fraser & Gawthorpe (1990); (24) Besly (1988); (25) Gast *et al.* (2010); (26) George & Berry (1993, 1997); (27) Lott *et al.* (2010); (28) Van Bergen & Sissingh (2007); (29) Mazur & Scheck-Wenderoth (2005); (30) Ziegler (1990a); (31) Betz *et al.* (1987); (32) Mutterlose & Bornemann (2000); (33) Baldschuhn *et al.* (1977); (34) Muchez *et al.* (1987); (35) Reijmer *et al.* (2017); (36) Michon *et al.* (2003); (37) Zijerveld *et al.* (1992); (38) Van Wijhe (1987a); (39) Vercoutere & Van den Haute (1993); (40) Underhill & Partington (1993); (41) Cloetingh (1986); (42) Duser *et al.* (2015); (43) Poty and Delculée (2011); (44) Poty (2016); (45) Debacker *et al.* (in prep); (46) Deckers *et al.* (2019); (47) Patijn (1963); (48) Barbarand *et al.* (2018)

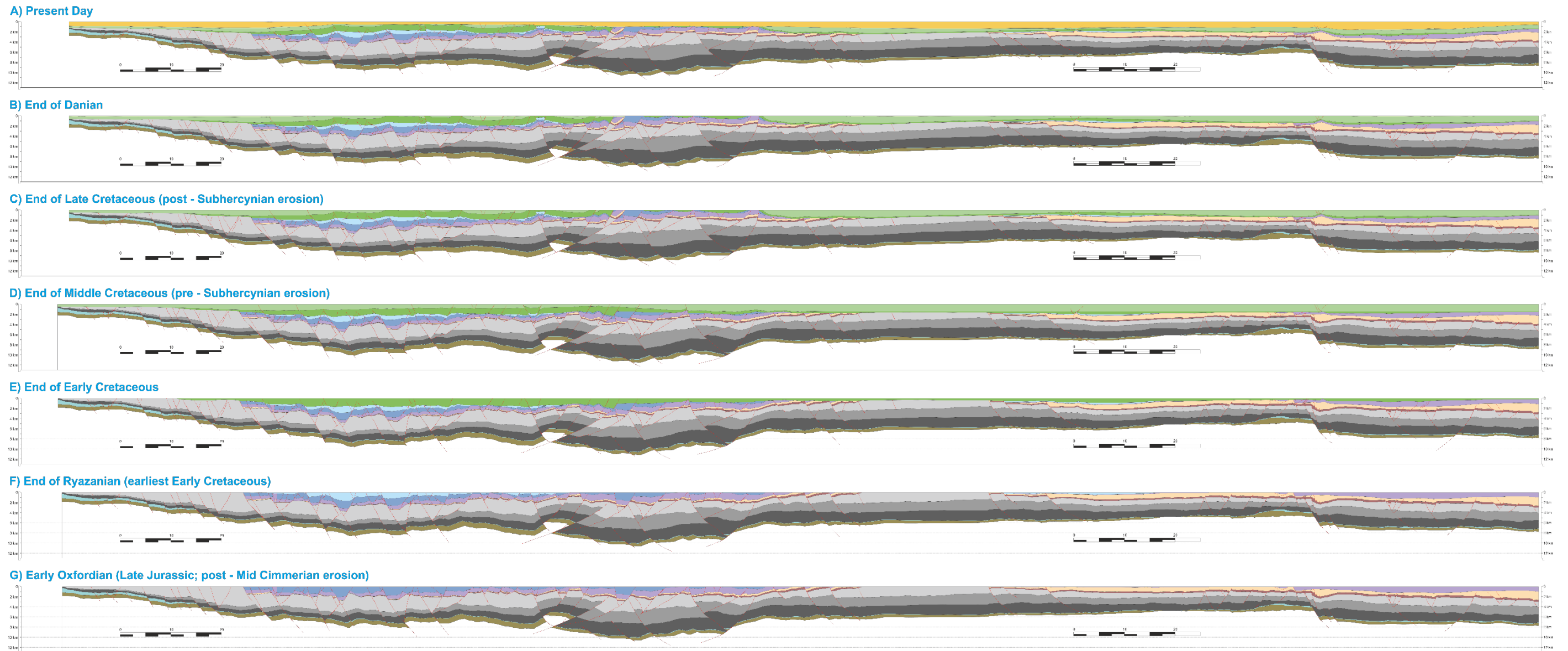
[illegible]

Appendix 3A: Western Section fault throw values for each time steps. Values are for vertical throw and are in meters. Red box highlight the reverse motions.

[illegible]

Appendix 3B: Central Section fault throw values for each time steps. Values are for vertical throw and are in meters. Red boxes highlight the reverse motions.

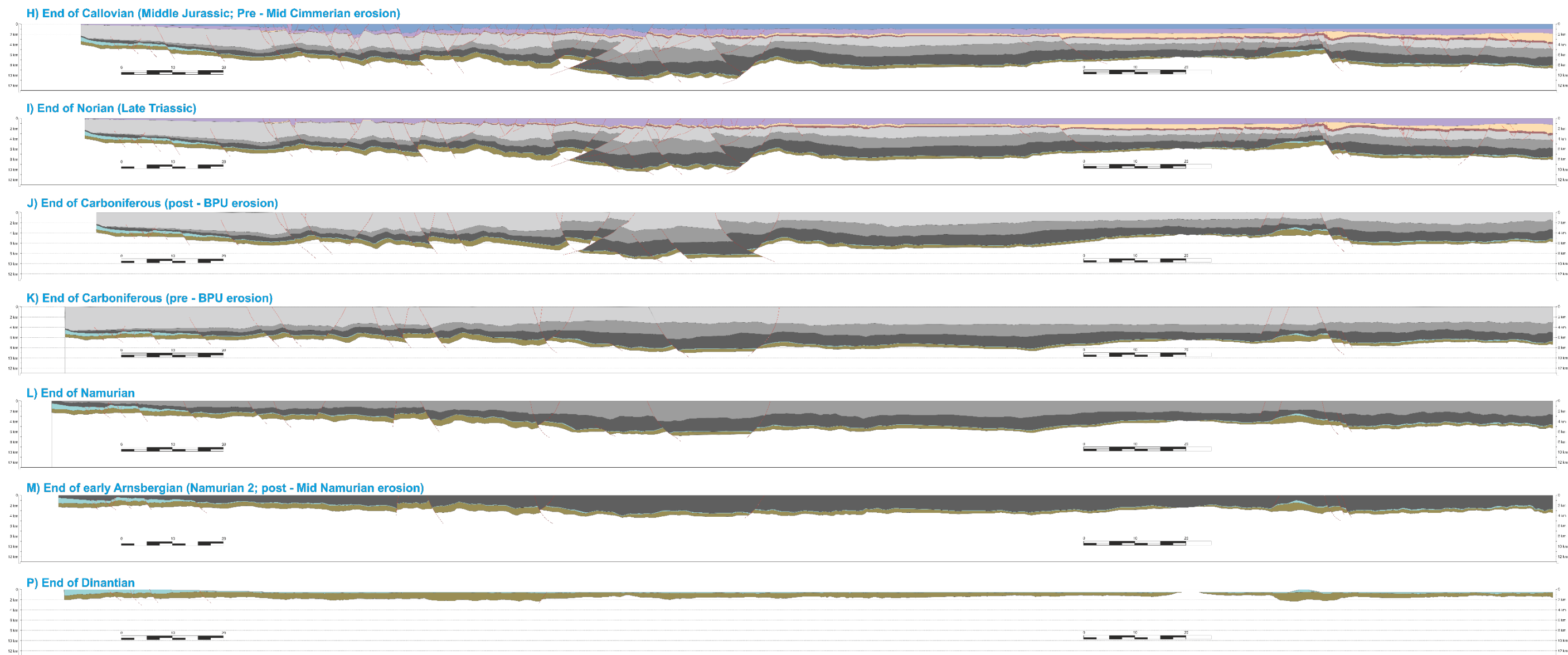
## Structural Restoration: Western Section (1/2)



Appendix 4A: Structural restoration of the Western Section at one to one scale (part 1). Note that the period with the largest amount of contraction measured along this section occurred 1) during the Middle Cretaceous to Present Day, with 0,7% (2.4 km) contraction ; and 2) during the Westphalian with 2.9 % (8.5 km) contraction. The maximum amount of extension occurred during 1) the Namurian with 0.8 % (2.5 km) of extension, and 2) during the Triassic to early Cretaceous with 2% (6 km) of extension.

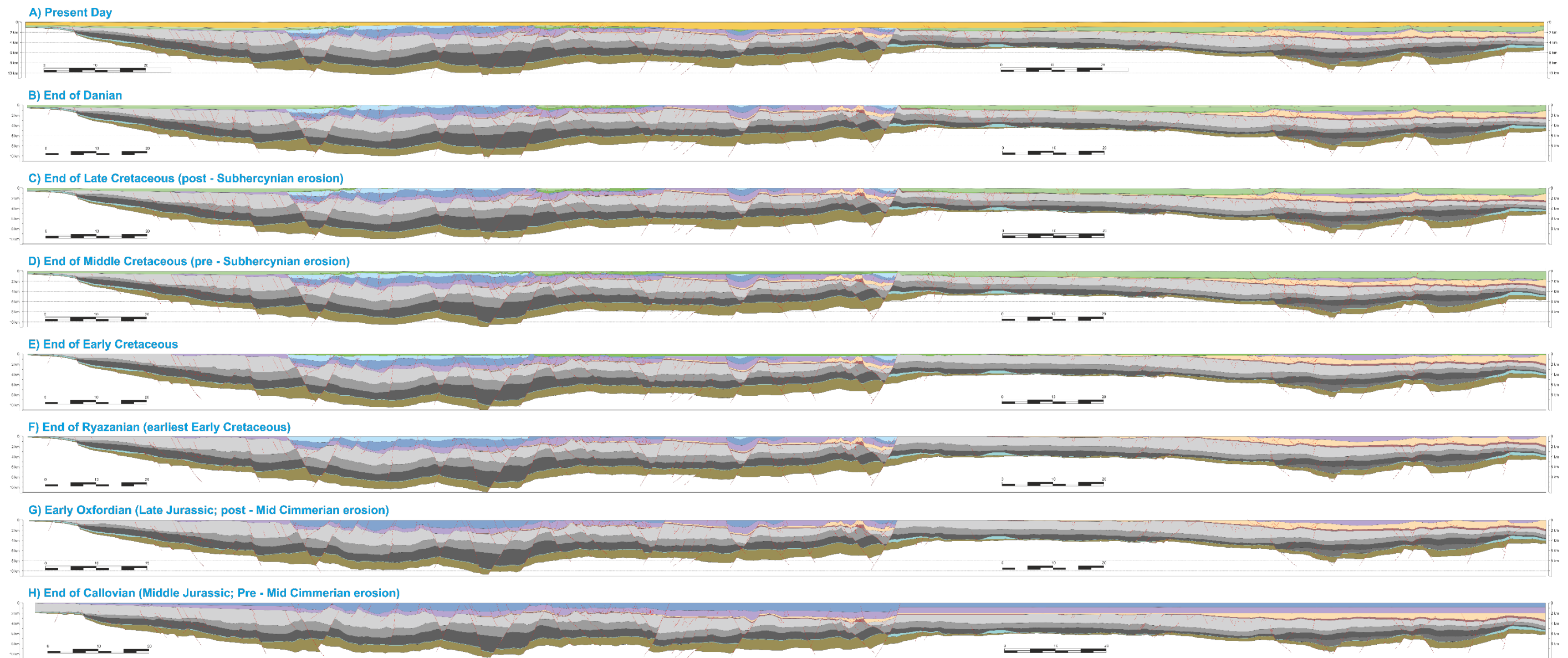


# Structural Restoration: Western Section (2/2)



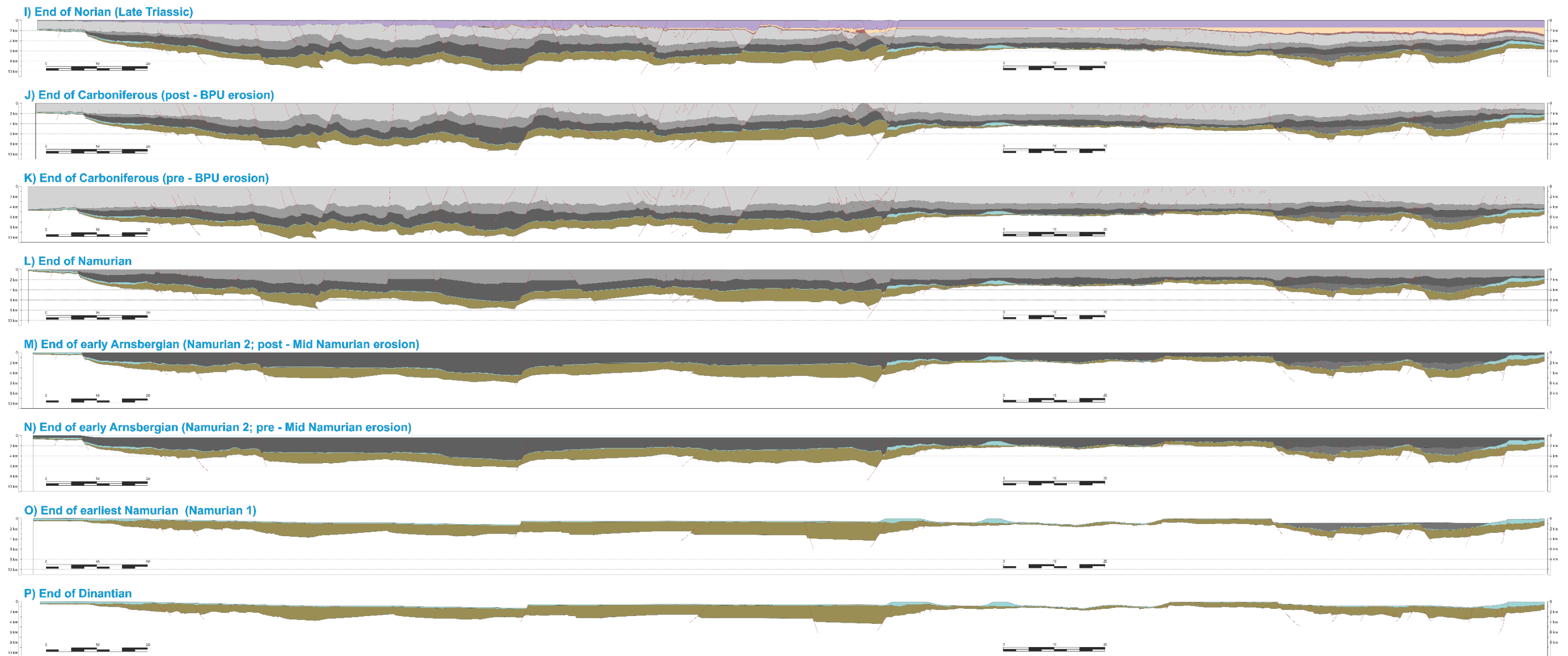
Appendix 4A: Structural restoration of the Western Section at one to one scale (part 2)

## Structural Restoration: Central Section (1/2)



Appendix 4B: Structural restoration of the Central Section at one to one scale (part 1).

## Structural Restoration: Central Section (2/2)



Appendix 4B: Structural restoration of the Central Section at one to one scale (part 2). Note that the period with the largest amount of extension measured along this section is limited and occurred during the Namurian with 0.7% of extension (2.5 km).



Period	Age (Ma)	Major tectonic phase	Major unconformity	London-Brabant Massif	Zeeland High	Limburg High	Oosterhout Platform	Roer Valley Graben	West Netherlands Basin	IJmuiden Platform	Broad Fourteens Basin	Peel-Massbommel Complex	Zandvoort Ridge	Central Netherlands Basin	Noord-Holland Platform	Texel-IJsselmeer High	Vlieland Basin	Friesland Platform	Daftsen High	Lower Saxony Basin	Lauwerszee Trough	Groningen Platform
				LBM	ZH	LH	OP	RVG	WNB	IJP	BFB	PMC	ZR	CNB	NHP	TIJH	VB	FP	DH	LSB	LT	GH
Neogene	0-23	<ul style="list-style-type: none"><li>Savian pulse (end-Oligocene / Early Miocene) followed by thermal subsidence</li></ul>	<ul style="list-style-type: none"><li>Savian UC at base of Upper North Sea Group</li></ul>	<ul style="list-style-type: none"><li>Subsidence and sedimentation</li></ul>				<ul style="list-style-type: none"><li>Subsidence and sedimentation</li></ul>	<ul style="list-style-type: none"><li>Savian pulse seen in the WNB but little elsewhere in the Netherlands (20).</li></ul>		<ul style="list-style-type: none"><li>Savian inversion not seen (20)</li></ul>			<ul style="list-style-type: none"><li>One normal fault active with 80 m of offset</li></ul>	<ul style="list-style-type: none"><li>Subsidence and sedimentation</li><li>A strike slip structures (flower structures) active</li><li>One normal fault active with 80 m of offset</li></ul>	<ul style="list-style-type: none"><li>Subsidence and sedimentation</li><li>Several strike slip structures (flower structures) active</li></ul>	<ul style="list-style-type: none"><li>One normal fault active with 100 m of offset.</li></ul>			<ul style="list-style-type: none"><li>Up to 8 km of shortening occurred along listric thrust planes that can be traced into the lower crust (18).</li><li>Strongly inverted (4)</li><li>Inversion largely ceased after the Late Cretaceous and earliest Cenozoic (20, 30)</li><li>Erosion</li><li>Some thick Chalk in rim synclines along salt structures (33)</li></ul>	<ul style="list-style-type: none"><li>Increased thickness of Palaeogene</li><li>Major at the Cretaceous and Cenozoic levels indicate that both north-west and east-north-east-trending faults were reactivated during the Cenozoic (20)</li><li>Several strike slip structures (flower structures) active</li></ul>	
Late Cretaceous and Palaeogene	23-100	<ul style="list-style-type: none"><li>Pyrenean pulse (end-Eocene) caused by broad uplift</li><li>Laramide pulse (mid-Palaeocene) mark the end of the Chalk deposition.</li><li>Sub-Hercynian pulse during the Campanian</li></ul>	<ul style="list-style-type: none"><li>Pyrenean UC at the base of the Middle North Sea Group</li><li>Laramide at the base of the Lower North Sea Group</li><li>Sub-Hercynian UC is an intra Chalk Group UC</li></ul>	<ul style="list-style-type: none"><li>Overstepped and overlapped by Upper Cretaceous sediments, but was later partly denuded (18, 19)</li></ul>	<ul style="list-style-type: none"><li>Onlap (18)</li></ul>			<ul style="list-style-type: none"><li>Less inversion than the WNB and CNB</li><li>Multiple phases of inversion between Late Cretaceous and Early Cenozoic (36)</li><li>Inversion resulted in reverse reactivation of pre-existing faults forming prominent ridges of flower structures on dominantly west-north-west and north-north-west trends with a dextral displacement (18)</li></ul>	<ul style="list-style-type: none"><li>Mildly to strongly inverted (1)</li><li>Erosion (6)</li><li>Chalk eroded in the south-eastern part of the WNB</li><li>Pre-existing faults reactivated with flower (transpositional) structures observed (6)</li><li>Thinning of the Upper Chalk from the SE (6)</li><li>Dextral displacement along main faults due to E-W Late Cimmerian extension transitioning to N-S compression in Late Cretaceous Early Cenozoic.</li><li>Inversion resulted in reverse reactivation of pre-existing faults forming prominent ridges of flower structures on dominantly west-north-west and north-north-west trends with a dextral displacement (18)</li><li>One reverse fault active during Danian</li><li>Reverse and normal fault active, with up to 630 m and 850 m of reverse motion and 210 m of normal motion.</li><li>Central part of the WNB uplifted by up to 600 m and 850 m.</li><li>Compartmentalization of the uplifted zone 1 the southern part of the WNB and in smaller zones in the central and northern part of the WNB.</li></ul>		<ul style="list-style-type: none"><li>Strongly inverted (1) during both Laramide and Pyrenean pulses.</li><li>Up to 380 m of uplift (38)</li><li>Erosion (6)</li><li>Chalk Group removed (1)</li><li>Structural style different than WNB and CNB due to the presence of Zechstein salt</li><li>NW-SE anticline growth (8).</li><li>Some of the reactivated faults observed down to the Carboniferous (17)</li></ul>	<ul style="list-style-type: none"><li>Subsidence (6)</li><li>Peel Boundary Fault to the south has up to 1000 m of post-inversion throw (20)</li><li>Normal and reverse faulting during the Danian with up to 60 m of reverse motion and 280 m of normal motion.</li><li>Both normal and reverse faults active. Normal faults with maximum offset of 280 m. Reverse fault with maximum offset of 350 m</li></ul>	<ul style="list-style-type: none"><li>Subsidence with thick Chalk deposited (18)</li></ul>	<ul style="list-style-type: none"><li>Strongly inverted (4)</li><li>Erosion, locally down to the Triassic (6)</li><li>Minor normal faulting with up to 100 m of offset</li><li>A few active faults with reverse motion between 25 and 800 m of offset (Raalte Boundary Faults), as well as normal faults with up to 210 m of offset.</li><li>CNB uplifted by up to 250 m</li><li>Up to 1.7 km of reverse motion on the bounding fault between the NHP and the CNB (fault F- CNB/CNP)</li></ul>	<ul style="list-style-type: none"><li>Southern part of NHP is uplifted by 1.3 km CNB</li><li>Up to 1 km of reverse motion on the bounding fault between the NHP and the CNB (fault F- CNB/CNP)</li></ul>	<ul style="list-style-type: none"><li>Uplifted during Danian and Chalk time from 700 m on the margin to 1.30 km of erosion in the central part of the VB.</li><li>One reverse fault with 120 m of vertical offset.</li></ul>	<ul style="list-style-type: none"><li>Minor normal and reverse faulting in the north.</li><li>Uplifted during Danian and Chalk time, with 700 m erosion.</li></ul>		<ul style="list-style-type: none"><li>Deep-seated intrusions inferred beneath the Lower Saxony Basin may have been emplaced during the Aptian (30, 31).</li><li>Subsidence with non-marine (Wealden) deposition during the Berriasian (32)</li></ul>	<ul style="list-style-type: none"><li>Increased thickness</li><li>Several strike slip structures (flower structures) present and active during the Cretaceous.</li></ul>		
Early Cretaceous (except Ryazanian)	100-140	<ul style="list-style-type: none"><li>Post rifting thermal subsidence</li><li>Cimmerian pulses</li><li>E-W extension</li></ul>	<ul style="list-style-type: none"><li>Late Cimmerian UC (30) locally seen at the base of the Rijland Group related to lithosphere-scale deformations combined with an earliest Cretaceous eustatic sea-level lowstand. Most distinctive in the basin margins and on the platform areas.</li></ul>	<ul style="list-style-type: none"><li>Sedimentation (6) and onlap (18)</li><li>Widespread karstification of the Dinantian carbonates). Exact timing often difficult to tell in the Campine Basin (42)</li></ul>	<ul style="list-style-type: none"><li>Missing (1)</li></ul>	<ul style="list-style-type: none"><li>Eroded</li></ul>	<ul style="list-style-type: none"><li>Strike-slip structure active</li></ul>	<ul style="list-style-type: none"><li>Missing</li></ul>	<ul style="list-style-type: none"><li>Post rift strata onlap on the basin margins</li><li>Normal faulting, with offset up to 210 and 400 m.</li></ul>		<ul style="list-style-type: none"><li>Locally eroded (1)</li></ul>	<ul style="list-style-type: none"><li>Late-Cimmerian uplift leading to erosion of most of the Middle Jurassic to Permian cover, locally down to the Westphalian</li><li>Both normal and reverse faults active. Normal faults with maximum offset of 280 m. Reverse fault with maximum offset of 90 m</li></ul>	<ul style="list-style-type: none"><li>Normal faulting, with offset up to 210 m</li></ul>	<ul style="list-style-type: none"><li>Several strike slip structures (flower structures) active</li></ul>		<ul style="list-style-type: none"><li>Minor normal faulting</li></ul>		<ul style="list-style-type: none"><li>Deep-seated intrusions inferred beneath the Lower Saxony Basin may have been emplaced during the Aptian (30, 31).</li><li>Subsidence with non-marine (Wealden) deposition during the Berriasian (32)</li></ul>	<ul style="list-style-type: none"><li>Increased thickness</li><li>Several strike slip structures (flower structures) present and active during the Cretaceous.</li></ul>			
Late Jurassic to Early Cretaceous (Ryazanian)	140-165	<ul style="list-style-type: none"><li>Mid-to late-Cimmerian rifting phases</li><li>Major rifting</li></ul>	<ul style="list-style-type: none"><li>The basal Mid-Cimmerian UC is Bajocian age</li></ul>	<ul style="list-style-type: none"><li>This and onlaps on the LBM then thicken to the south to 700 m (Weesse-Weald Basin and Boeltonaai) (7, 27)</li><li>Mid-Cimmerian phase, which removed 3000 m of its post-Caledonian cover including the Lower Jurassic (39)</li><li>Fission-track data suggest that a thickness of 3000 m of overburden was removed (16, 47, 48).</li><li>Possible faulting in the Campine Basin with faults mainly oriented NNW-SSE and NW-SE trending but also NNE-SSW structures can be recognised in gravity data (45, 46).</li></ul>			<ul style="list-style-type: none"><li>Normal faulting with up to 300 m of offset</li><li>Mid Cimmerian: 700 to 900 m of Triassic to Lower Jurassic eroded</li></ul>	<ul style="list-style-type: none"><li>Strongly subsiding in a similar manner than the DCG.</li><li>Orientation probably controlled by pre-existing structures (6)</li><li>Transsectional reactivation of pre-existing basement structures (18)</li><li>Subsidence was controlled by the reactivation of the main Variscan faults (36)</li></ul>	<ul style="list-style-type: none"><li>Orientation probably controlled by the Dutch Central Graben (1)</li><li>Syn-tilt clastics of the Delfland Subgroup in half grabens</li><li>Dextral displacement along main faults</li><li>Transsectional reactivation of pre-existing basement structures (18)</li><li>Most faults observed were active as normal faults, with up to 850 m and 1.6 km of offset on the southern bounding fault.</li></ul>	<ul style="list-style-type: none"><li>Likely connected to the Dutch Central Graben (1)</li><li>Subside rapidly during Kimmeridgian (18)</li></ul>	<ul style="list-style-type: none"><li>Only a few normal faults active, with maximum offset of 210 m</li><li>Mid Cimmerian: Up to 600 m of Triassic and Lower Jurassic eroded</li></ul>	<ul style="list-style-type: none"><li>Important wrench-induced feature separating the West and Central Netherlands basins (18)</li></ul>	<ul style="list-style-type: none"><li>Only patches of Jurassic preserved but could have had a wider distribution (1)</li><li>Orientation probably controlled by pre-existing structures (6)</li><li>Transsectional reactivation of pre-existing basement structures (18)</li><li>Subside rapidly during Kimmeridgian (18)</li><li>All interpreted faults active as normal faults, with up to 730 m and 1.3 km of offset</li><li>Mid Cimmerian: Up to 2.1 km of Triassic to Lower Jurassic eroded</li><li>Mid Cimmerian: Up to 1 km of Lower Triassic eroded.</li></ul>	<ul style="list-style-type: none"><li>Mid Cimmerian: 400 m of Lower Jurassic to Triassic eroded in the south of the NHP and up to 2.7 km of Lower Jurassic to Westphalian eroded in the north.</li><li>Up to 500 m of fault normal offset</li></ul>	<ul style="list-style-type: none"><li>Main erosion (1)</li><li>Uplifted (6)</li><li>Mid Cimmerian: 2.3 km of Westphalian, Permian, Triassic and Jurassic eroded.</li><li>Up to 500 m of fault normal offset</li><li>Mid Cimmerian: 2 km of Westphalian, Permian, Triassic and Lower Jurassic eroded.</li></ul>	<ul style="list-style-type: none"><li>Depocenter with connection to the Terschelling Basin (7)</li><li>Transsectional reactivation of pre-existing basement structures (18)</li><li>Mafic volcanism with volcanoclastics (27)</li><li>Mid Cimmerian: 1.7 km of Triassic and Lower Jurassic eroded.</li></ul>	<ul style="list-style-type: none"><li>Uplift and Erosion, down to the Triassic and Zechstein levels (1)</li><li>No faulting (18)</li><li>Mid Cimmerian: 2.1 km of Westphalian, Permian, Triassic and Jurassic eroded</li><li>Mid Cimmerian: 1.8 to 2.1 km of Permian, Triassic and Jurassic eroded</li></ul>		<ul style="list-style-type: none"><li>Extension</li><li>Transsectional reactivation of pre-existing basement structures (18)</li></ul>	<ul style="list-style-type: none"><li>Mid Cimmerian: 900 m to 2 km of Triassic and Jurassic eroded.</li><li>Mid Cimmerian: 800 m of Triassic and Lower Jurassic eroded.</li></ul>	<ul style="list-style-type: none"><li>Absent (5)</li><li>The high is largely shaped by the late Cimmerian tectonic phase during the Jurassic (25).</li><li>Mid Cimmerian: 800 m of Triassic and Lower Jurassic eroded.</li></ul>	
Early to Middle Jurassic	165-198	<ul style="list-style-type: none"><li>North Sea doming start at end of Aalenian until Bathonian due to mantle plume on the lithosphere (7, 30, 40)</li></ul>		<ul style="list-style-type: none"><li>Uplifted with erosion of Triassic to Upper Carboniferous (18).</li></ul>				<ul style="list-style-type: none"><li>Quiescence</li></ul>	<ul style="list-style-type: none"><li>Normal faulting (6)</li><li>Most faults observed were active as normal faults, with up to 1 km and 1.3 km of offset.</li></ul>		<ul style="list-style-type: none"><li>Normal faulting (6)</li></ul>	<ul style="list-style-type: none"><li>Several normal faults active, with up to 2 m of offset</li></ul>	<ul style="list-style-type: none"><li>Quiescence</li></ul>	<ul style="list-style-type: none"><li>Quiescence</li><li>A few normal faults active with up to 250 m of offset</li><li>No fault active on the Western Section</li></ul>		<ul style="list-style-type: none"><li>Missing (6) Eroded locally down to the Westphalian (18)</li></ul>	<ul style="list-style-type: none"><li>Quiescence</li></ul>	<ul style="list-style-type: none"><li>Quiescence</li></ul>	<ul style="list-style-type: none"><li>W-NW faulting (29)</li><li>Transsectional subsidence and internal differentiation into elongated horst and graben features (29)</li></ul>	<ul style="list-style-type: none"><li>Quiescence</li></ul>		
Triassic	198-252	<ul style="list-style-type: none"><li>Initiation of rifting</li><li>Early Cimmerian phase</li><li>Hardegeen pulse and a few less prominent pulses (pre-Volgprishausen, pre-Dierluth and intra-Solling)</li></ul>	<ul style="list-style-type: none"><li>Early-Cimmerian UC is base Rhaetian in age.</li><li>Mostly seen along the SPB margins and are attributed to intraplate stresses operating on a lithospheric scale (41; 30).</li><li>Hardegeen UC at the base of the Soling Formation</li></ul>	<ul style="list-style-type: none"><li>Low subsidence rate with 50 m of Lower Muschelkalk deposited (14).</li><li>Source of sediment for the RVB and WNB during lower Triassic (18)</li></ul>				<ul style="list-style-type: none"><li>Differential subsidence (14)</li><li>Differential subsidence ceased at the end of the Early Triassic and restart during Rot time (14)</li></ul>	<ul style="list-style-type: none"><li>Some growth faulting along the southern margin</li><li>Subsidence shifts northward</li><li>Differential subsidence ceased at the end of the Early Triassic (14)</li><li>The northern part of the WNB has several normal faults active, with up to 700 m of offset.</li><li>Several normal faults active, with up to 1000 m of offset in the southern part of the WNB.</li></ul>	<ul style="list-style-type: none"><li>Minor faulting (1, 2, 3)</li><li>Differential subsidence ceased at the end of the Early Triassic (14)</li></ul>	<ul style="list-style-type: none"><li>Several normal faults active, with up to 610 m of offset.</li></ul>		<ul style="list-style-type: none"><li>Heavily faulted (1)</li><li>Most faults active as normal faults with up to 1.2 km of growth</li><li>Only one normal fault active with 100 m of offset</li></ul>			<ul style="list-style-type: none"><li>Moderate subsidence</li></ul>	<ul style="list-style-type: none"><li>Up to 800 m tick in the east (1)</li><li>One normal fault active with 270 m of offset</li></ul>					
Permian	252-298	<ul style="list-style-type: none"><li>Saalian phase</li></ul>	<ul style="list-style-type: none"><li>Base Permian UC (BPU) and intra-Permian Saalian UC</li></ul>	<ul style="list-style-type: none"><li>During the Mid and Late Permian, the sedimentation gradually extended to the LBM.</li><li>A source for Rotliegend in the North Sea (18)</li></ul>	<ul style="list-style-type: none"><li>BPU: 1.5 to 2.4 km of Westphalian eroded.</li><li>BPU: 1 to 2 km of Westphalian eroded</li></ul>		<ul style="list-style-type: none"><li>BPU: 800 to 1.6 km of Westphalian eroded</li></ul>	<ul style="list-style-type: none"><li>Existed during the Palaeozoic (1)</li><li>Thermal subsidence with minor faulting (37)</li></ul>	<ul style="list-style-type: none"><li>Devoided of Zechstein salt (6)</li><li>Fault controlled Rotliegend deposition (100 m-dian sand along the northern bounding fault (12)</li><li>A few normal faults active during or prior to Rotliegend deposition. Up to 310 m of offset.</li><li>BPU: 100 to 150 m of Westphalian eroded</li><li>BPU: 1.1 to 2.1 km of Westphalian eroded</li><li>BPU: Up to 1400 m of Westphalian eroded</li></ul>	<ul style="list-style-type: none"><li>Minor faulting (1, 2, 3)</li><li>Differential subsidence (12)</li></ul>	<ul style="list-style-type: none"><li>Thermal subsidence with minor faulting (37)</li><li>One normal fault active during or prior to the deposition of the Rotliegend, with up to 100 m of offset</li><li>BPU: 1.1 to 2.1 km of Westphalian eroded</li></ul>		<ul style="list-style-type: none"><li>Differential subsidence (12)</li><li>Half Graben and pull-apart basin with up to 250 m of offset (12)</li><li>One reverse fault active during or prior to the deposition of the Rotliegend, with up to 100 m of offset</li><li>BPU: Up to 1.3 km and 1.4 km of Westphalian eroded. Locally even up to 2.8 km in the northern part of the CNB</li></ul>	<ul style="list-style-type: none"><li>BPU: Up to 1.7 km of Westphalian eroded.</li></ul>	<ul style="list-style-type: none"><li>Strongly uplifted during the early Permian (6, 26)</li><li>Synsedimentary faulting (12)</li><li>Sand source area (13)</li><li>High poorly defined</li><li>Controlled Rotliegend alluvial fan systems around the high</li><li>One normal fault active with 220 m of offset</li><li>BPU: 1.6 km of Westphalian eroded</li><li>BPU: 1.5 km of Westphalian eroded.</li></ul>	<ul style="list-style-type: none"><li>BPU: 1.7 km to 2.3 km of Westphalian eroded</li></ul>	<ul style="list-style-type: none"><li>BPU: up to 1.3 of Westphalian eroded</li><li>BPU: Between 2 and 2.4 km of Westphalian eroded</li></ul>		<ul style="list-style-type: none"><li>Increased thickness of Rotliegend</li><li>Faulting with thickness variation up to 25 m</li><li>One strike slip structure possibly active during the Permian</li><li>Some normal faulting with up to 320 m of offset</li><li>BPU: 800 m to 2.5 km of Westphalian eroded.</li><li>BPU: 700 m to 1.7 km of Westphalian eroded</li></ul>	<ul style="list-style-type: none"><li>BPU: 2.5 km of Westphalian eroded</li><li>BPU: 800 m to 1.2 km of Westphalian eroded</li></ul>		
Stephanian-Westphalian	298-312	<ul style="list-style-type: none"><li>Variscan phase with compression starting during the Arturian (Westphalian D) and early Stephanian</li></ul>		<ul style="list-style-type: none"><li>Passive thermal cooling that had started during the Namurian continues (23)</li><li>Western part of the LBM: Uplift and sourcing to the north (24), while Belgium part had a thick Westphalian cover due to subsidence.</li><li>Possible faulting in the Campine Basin with faults mainly oriented NNW-SSE and NW-SE trending but also NNE-SSW structures can be recognised in gravity data (45, 46)</li><li>Faults Brediere's and Leut fault (eastern part of the LBM) active (45, 46)</li></ul>	<ul style="list-style-type: none"><li>Parasitic compaction-related faults that formed above the massive and rigid Dinantian carbonate fault blocks (35)</li><li>Normal faulting with up to 180 m of normal offset.</li><li>Normal faulting with up to 150 m of normal offset.</li><li>4.2 to 4 km of burial during the Westphalian, prior to the BPU.</li><li>4.6 to 3.7 km of burial during the Westphalian, prior to the BPU.</li></ul>	<ul style="list-style-type: none"><li>5.4 km of Namurian Westphalian may have been removed (11)</li></ul>		<ul style="list-style-type: none"><li>Numerous faults active, all with normal offset, up to 1.35 km</li><li>Numerous faults active, all with normal offset, up to 900 m and reverse offset up to 1.8 km (fault F- WNB34)</li></ul>		<ul style="list-style-type: none"><li>Normal fault movement with up to 720 m of offset</li></ul>	<ul style="list-style-type: none"><li>Subsidence not the main driving force but rather the alternation of overthrust loading and relaxation in the Variscan thrust belt to the south. (16)</li></ul>										<ul style="list-style-type: none"><li>Some normal faulting with up to 380 m of offset</li></ul>	
Namurian	312-325			<ul style="list-style-type: none"><li>Uniform flexural subsidence</li><li>Marine and lacustrine sediments</li><li>Regional unconformity related to sea level lowstand (22)</li></ul>	<ul style="list-style-type: none"><li>Progressive onlap onto the LBM</li><li>Normal faulting with up to 740 m of normal offset.</li><li>Normal faulting with up to 600 m of normal offset.</li><li>300 m of erosion during mid-Namurian relative sea level drop.</li></ul>	<ul style="list-style-type: none"><li>Normal faulting with up to 70 m of offset</li></ul>		<ul style="list-style-type: none"><li>Five faults with normal growth identified, up to 1 km of offset in the basin centre and up to 2 km on the northern bounding fault.</li><li>Namurian thickens from 2.7 km in the southern part of the WNB to 6 km in the northern part of the WNB</li><li>Several normal faults active with up to 2 km of vertical offset on fault F- WNB27</li></ul>		<ul style="list-style-type: none"><li>Late Namurian normal fault movement with up to 820 m of offset</li></ul>	<ul style="list-style-type: none"><li>1.8 km of normal faulting on the southern boundary fault (Raalte Boundary Fault). Several other faults also active with up to 1.7 km and 2.2 km of offset.</li><li>1.4 km of normal offset on the fault that separate the CNB from the WNB.</li><li>Decompressed Namurian is 6 km thick in the CNB.</li></ul>	<ul style="list-style-type: none"><li>Decompressed Namurian is 5 km thick in the NHP.</li></ul>	<ul style="list-style-type: none"><li>Decompressed Namurian is up to 5.8 km thick in the TIJH.</li></ul>			<ul style="list-style-type: none"><li>Nagde Carbonate Platform formed on the southern side of the TIJH</li><li>Paleo water depth up to 800 m toward the north.</li><li>No proven carbonate platform on the Western Section</li></ul>	<ul style="list-style-type: none"><li>Paleo water depth from 820 in the south to 1.6 km in the north 800 m toward the middle of the FP.</li><li>A carbonate platform (Fryslan Platform) with up to 750 m of topography present in the southern part of FP.</li><li>A structural high (or a combined carbonate platform/structural high) present in the northern part of FP.</li><li>Possible carbonate platform in the northern part of FP</li></ul>	<ul style="list-style-type: none"><li>Some normal faulting with up to 1 km of offset. The northern bounding fault has 510 m of offset.</li><li>Paleo water depth 400 m in the south of L.T. deepening northward to 1.3 km.</li></ul>		<ul style="list-style-type: none"><li>Numerous normal fault active with up to 1.5 km of offset on the northern bounding fault.</li><li>Older basin fill in the trough.</li><li>Paleo water depth of 900 m during the early part of the Namurian and decreasing in later stage due to the trough being fill up</li></ul>	<ul style="list-style-type: none"><li>Structural high originated during the Carboniferous (25)</li></ul>	
Viséan and Tournaisian (Dinantian)	325-358	<ul style="list-style-type: none"><li>Bretonian phase at the Devonian-Carboniferous boundary</li></ul>		<ul style="list-style-type: none"><li>Erosion and karstification at the end of Viséan with associated (fracture controlled) porosity (42)</li><li>Uplift of the WSW-ESE trending Boose - Val Dieu Ridge (eastern part of the LBM) during Late Tournaisian (42, 43, 44).</li><li>Faults Brediere's and Leut Fault (eastern part of the LBM) may have been active (45)</li><li>No observed faulting during the Dinantian.</li><li>Interpreted transition from ramp carbonate to slope and deep-water (&gt;500 m) carbonates</li></ul>	<ul style="list-style-type: none"><li>Small extensional (half-graben) basins that are related to long-lived faults that have been active since at least the Devonian (34)</li><li>The platform boundaries occasionally associated with faults with small throw. These faults may have played an important role in determining the location of these sedimentary facies transitions (35)</li><li>A large extensional fault near well S02-01 has a half-graben geometry and accommodates significant throw (35)</li><li>No observed faulting during the Dinantian.</li><li>Interpreted transition from ramp carbonate to slope and deep-water (&gt;500 m) carbonates</li></ul>	<ul style="list-style-type: none"><li>Normal faulting with up to 250 m of offset</li></ul>	<ul style="list-style-type: none"><li>650 m of normal fault growth on the southern boundary fault between the WNB and the PMC.</li><li>Paleo water depth estimated at 1.3 km in the southern part of the area</li><li>Paleo water depth estimated at 600-700 m</li></ul>	<ul style="list-style-type: none"><li>Paleo water depth estimated at 400 m in the southern part of the area</li></ul>	<ul style="list-style-type: none"><li>1.8 km of normal faulting on the southern side of the TIJH</li><li>Paleo water depth up to 800 m toward the north.</li><li>No proven carbonate platform on the Western Section</li></ul>	<ul style="list-style-type: none"><li>Nagde Carbonate Platform formed on the southern side of the TIJH</li><li>Paleo water depth up to 800 m toward the north.</li><li>No proven carbonate platform on the Western Section</li></ul>	<ul style="list-style-type: none"><li>Paleo water depth from 820 in the south to 1.6 km in the north 800 m toward the middle of the FP.</li><li>A carbonate platform (Fryslan Platform) with up to 750 m of topography present in the southern part of FP.</li><li>A structural high (or a combined carbonate platform/structural high) present in the northern part of FP.</li><li>Possible carbonate platform in the northern part of FP</li></ul>	<ul style="list-style-type: none"><li>Some normal faulting with up to 1 km of offset. The northern bounding fault has 510 m of offset.</li><li>Paleo water depth 400 m in the south of L.T. deepening northward to 1.3 km.</li></ul>										



Appendix 5 (previous page): Updated summary chart of the structural evolution of the 19 recognized structural elements identified in the study area. See list and description of each elements above. The text in black refers to the information gather prior to this study. The text in dark green refers to the lessons learned from the restoration of the Western Section, while dark blue refers to the lessons learned from the restoration of the Central restoration. Numbers in the table refer to specific publication (listed below). (1) Kombrink *et al.* (2012); (2) Hooper *et al.* (1995); (3) Verweij & Simmelink (2002); (4) Nelskamp (2011); (5) Van Adrichem Boogaert & Kouwe (1993); (6) De Jager (2007); (7) Bouroullec *et al.* (2018); (8) Nalpas *et al.* (1995); (9) Geluk *et al.* (2007); (10) Van Buggenum & de Hartog Jager (2017); (11) Veld *et al.* (1996); (12) Geluk (2007); (13) Van Adrichem Boogaert & Burgers (1983); (14) Geluk (2007b); (15) Legrand (1968); (16) Van den Haute & Vercoutere (1990); (17) Schroot & De Haan (2003); (18) Pharaoh, *et al.* (2010); (19) Duser & Lagrou (2007); (20) De Jager (2007); (21) Kombrink *et al.* (2010); (22) McCann *et al.* (2008a, 2010); (23) Fraser & Gawthorpe (1990); (24) Besly (1988); (25) Gast *et al.* (2010); (26) George & Berry (1993, 1997); (27) Loot *et al.* (2010); (28) Van Bergen & Sissingh (2007); (29) Mazur & Scheck-Wenderoth (2005); (30) Ziegler (1990a); (31) Betz *et al.* (1987); (32) Mutterlose & Bornemann (2000); (33) Baldschuhn *et al.* (1977); (34) Muchez *et al.* (1987); (35) Reijmer *et al.* (2017); (36) Michon *et al.* (2003); (37) Zijerveld *et al.* (1992); (38) Van Wijhe (1987a); (39) Vercoutere & Van den Haute (1993); (40) Underhill & Partington (1993); (41) Cloetingh (1986); (42) Duser *et al.* (2015); (43) Poty and Delculée (2011); (44) Poty (2016); (45) Debacker *et alet al.* (in prep); (46) Deckers *et al.* (2019); (47) Patijn (1963); (48) Barbarand *et al.* (2018

# Onderzoek in de ondergrond voor aardwarmte